ISSN 0236-2945 / e-ISSN 2541-9935

LIGHT & ENGINEERING

Volume 28, Number 2, 2020

Editorial of Journal
"Light & Engineering" (Svetotekhnika), Moscow

The purpose and content of «Light & Engineering» is to develop the science of light within the framework of ray, photometric concepts and the application of results for a comfortable light environment, as well as for visual and non-visual light technologies, including medicine. The light engineering science is a field of science and technology and its subject is the development of methods for generation and spatial redistribution of optical radiation, as well as its conversion to other forms of energy and use for various purposes.

The scope of journal includes articles in the following areas:

- Sources of light;
- Light field theory;
- Photometry, colorimetry and radiometry of optical radiation;
- Visual and non-visual effects of radiation on humans;
- Control and regulation devices for light sources;
- Light devices, their design and production technology;
- Light devices for the efficient distribution and transportation of the light energy: hollow light guides, optical fibers;
- Lighting and irradiation installations;
- Light signaling and light communication;
- Light remote sensing;
- Mathematical modelling of light devices and installations;
- Energy savings in light installation;
- Innovative light design solutions;
- Photobiology, including problems of using light in medicine;
- Disinfection of premises, drinking water and smell elimination by UV radiation technology;
- Light transfer in the ocean, space and other mediums;
- Light and engineering marketing;
- Legal providing and regulation of energy effective lighting;
- Light conversion to other forms of energy;
- Standardization in field of lighting;
- Light in art and architecture design;
- Education in field of light and engineering.

Journal “Light & Engineering” had been founded by Prof. Julian B. Aizenberg in 1993

LIGHT & ENGINEERING

СВЕТО ТЕХНИКА

Editorial of Journal “Light & Engineering/Svetotekhnika”

Moscow, 2019

Editorial Office:

Russia, VNISI, Rooms 327 and 334
106 Prospekt Mira, Moscow 129626

Tel: +7.495.682.26.54
Tel./Fax: +7.495.682.58.46
E-mail: lights-nr@inbox.ru
http://www.l-e-journal.com

Scientific Editors:

Sergei G. Ashurkov
Alexander Yu. Basov
Eugene I. Rozovsky
Raisa I. Stolyarevskaya
Art and CAD Editor
Andrei M. Bogdanov
Style Editor
Marsha D. Vinogradova

Light & Engineering" is an international scientific Journal subscribed to by readers in many different countries. It is the English edition of the journal "Svetotekhnika" the oldest scientific publication in Russia, established in 1932.

Establishing the English edition "Light and Engineering" in 1993 allowed Russian illumination science to be presented the colleagues abroad. It attracted the attention of experts and a new generation of scientists from different countries to Russian domestic achievements in light and engineering science. It also introduced the results of international research and their industrial application on the Russian lighting market.

The scope of our publication is to present the most current results of fundamental research in the field of illumination science. This includes theoretical bases of light source development, physiological optics, lighting technology, photometry, colorimetry, radiometry and metrology, visual perception, health and hazard, energy efficiency, semiconductor sources of light and many others related directions. The journal also aims to cover the application illumination science in technology of light sources, lighting devices, lighting installations, control systems, standards, lighting art and design, and so on.

"Light & Engineering" is well known by its brand and design in the field of light and illumination. Each annual volume has six issues, with about 80–120 pages per issue. Each paper is reviewed by recognized world experts.

CONTENTS

VOLUME 28 **NUMBER 2** **2020**

LIGHT & ENGINEERING

Light & Engineering
Vol. 28, No. 2, pp. 4–16, 2020
https://doi.org/10.33383/2020-001
Svetotekhnika #3, 2020

LIGHTING PUBLIC SPACES: NEW TRENDS AND FUTURE EVOLUTIONS

Roger Narboni

Lighting Designer CONCEPTO
roger.narboni@concepto.fr

ABSTRACT

The article is devoted to the history and prospects of the development of outdoor lighting in public spaces with new opportunities of rapidly developing lighting technologies and trends in architecture and architectural lighting, taking into account environmental problems.

Keywords: nocturnal scene, lighting designer, night geographer, tonality of light, lighting pole, lighting mast, trees up-lighting, landscape lighting, LED, smart phone, smart luminous column, light projection (image), lighting effect deconstruction, luminous lounge, autonomous light objects, phosphorescence, bioluminescence, light materials, mastery of darkness, luminous city

1. BIRTH AND ADVENT OF PUBLIC LIGHTING

In the first decades after the end of the Second World War, lighting the public spaces was only about lighting the roadways so that motorists could see clearly at night and detect obstacles or pedestrians, because at that time the cars headlights were very poorly performing.

Initially, in the Middle Ages, the lighting, that was not yet called public, was first concentrated near the places of power (the castle), before then extending to the bourgeois neighbourhoods. The appearance of gas lanterns, incandescent lamps at the end of the 19th century, and then discharge lamps, helped to democratize public lighting by multiplying its presence, even in the poorest urban areas. More recently, around the 1970s, it expanded to the entire cities territory and to suburban roads.

At the very beginning of the public spaces lighting, long before the advent of the civilization of the automobile and the urban development that resulted from it, the night safety of walking, the protection of property and people were at the origin of the birth and then of the development of public lighting and these subjects persist and remain very current in all public debates on urban lighting, its creation as well as its renewal.

When after the Second World War, the number of vehicles in the city began to increase steadily, continuously and significantly, the issue of the motorists vision appeared and started to greatly influence the functionalist design of public lighting installations, which is still visible today in the vast majority of cities in the world and which is still the one that is mostly implemented by city engineers in the megalopolises under development.

These functional lighting necessities have led to the methodical installation of lighting poles located at the edge of the roadway, and regularly spaced according to their height, to reach the sacrosanct and abstract uniformity of illuminance but routinely prescribed by lighting engineers. From these principles and doctrines were born all the daytime and nighttime images of the streets and all the current pointillist night landscapes of the cities. Only the tonalities of light, linked to the successive technological evolutions of the sources, have modified at the margin these starry nocturnal scenes.

The roadways, lined or not with sidewalks, were illuminated on a regular and continuous basis by lu-

Fig. 1. Tramway line, Grenoble, France (Attica, architects, Roger Narboni, CONCEPTO, lighting design)

minaires fixed on poles of height proportionate to the width of the track and positioned at the edge of the roadway (in a single-sided or bilateral way). When the roadway was lined with trees, a pedestrian lighting system (pedestrian pole or pedestrian luminaire attached to the mast at mid-height and directed towards the sidewalk) was sometimes added. In dense cities, when the built fronts were continuous or when the sidewalks were too narrow, the luminaires intended to light the roadways were fixed directly on the facade (on one or on both sides of the street) at a height also proportionate to the width of the road (Fig.1).

More exceptionally, a pedestrian mall, an alley in a park or a river bank, were illuminated specifically by smaller pedestrian lighting poles (usually between 3m to 5m high) arranged just as regularly. The light temperature of the public lighting depended on the technological evolution of lamps (incandescent lamps in 1879, mercury vapour lamps in 1931, fluorescent tubes in 1938, halogen lamps in 1958, high-pressure sodium lamps in 1962, metal halide lamps in 1964), and for a very long time technicians did not differentiate the lighting of pedestrian spaces or that of roads.

With the emergence of high-pressure sodium lamps, a new and very technical lighting doctrine was born from the supposed properties of night vision (different from central to peripheral vision), which promoted an orange-coloured lighting on the roadway (high-pressure sodium lamps) and a cold white side pedestrian lighting (mercury vapour lamps) to improve the perception and contrast of motorists behind its wheel. This doctrine prevailed over all Parisian public lighting until the mid-1990s.

It was towards the end of the 80s, with the introduction of the first white sodium lamps (2500 K CCT) and later the metal halide lamps with ceramic burner (3000 K CCT), when avenues and then streets from the lighting for pedestrian up to the road lighting are getting benefit with an unique tone from facade to facade. With the arrival of the power LEDs in the early 2010s, public lighting is gradually undergoing to a real revolution.

The level of illuminance of public spaces has always increased over time until the first lighting standards appeared (the European standards were published in 2005). The first public gas lights struggled to illuminate the streets due to the optical inefficiency of the lanterns. At the time of reconstruction after the Second World War, an average light level of 5 lx on a road could surprise observers by its high intensity. A few decades later and until the application of European standards for public lighting (followed by the establishment of relatively similar standards by other continents, taking into account the coordination work carried out by the International Lighting Commission – CIE – founded in 1913), it was frequently requested for any lighting project average illuminance levels of 30 lx to 35 lx on roadways and between 10 lx to 20 lx on sidewalks.

This increase in light levels in the city was of course due to technological changes in the sources and optics of the fixtures, but also in response to the supposed expectations of the inhabitants who have always thought wrongly (encouraged by the lobby in the lighting sector) that more intense lighting contributed to the reduction of night-time insecurity and improved road safety. This demagogic response has never taken into account the specificity of our night vision (mesopic and scotopic visions), the need for contrasts in the nocturnal perception, and the time it takes for the eye to adapt to lighting changes.

Fig. 2. Cours des 50 Otages in Nantes, France,1991 (Italo Rota & Bruno Fortier architects, Roger Narboni, CONCEPTO, lighting design, photo copyright Philippe Ruault)

Fig. 3. City centre of Niort, France, 1992 (Roger Narboni, CONCEPTO, lighting design)

The European standards negotiated between the North European countries, more appreciative of low light levels in the city than the southern European countries, have fortunately helped to reduce the light levels applicable for city lanes thanks to policies reduction in vehicle speed and better consideration of night-time uses, particularly in the second part of the night (the light levels recommended in the standards are in fact related to the speed and density of vehicles, the presence or not of different types of users, and the light environment).

On the other hand, and until very recently (with rare exceptions initiated in the late 1980s and early 1990s in France, thanks to the nascent profession of lighting designers specializing in urban lighting), the way to illuminate public space has hardly changed since the origins of public lighting. Lighting systems are invariably installed on facades or more rarely suspended between them, and since the appearance of gas lighting and then electricity attached to supports of different heights installed at the edge of the roadway, which can easily be seen when walking in all the cities of the world but also, unfortunately, in all the new neighbourhoods which are under studying as well as under construction.

2. THE FIRST ATTEMPTS TO ILLUMINATE PEDESTRIAN SPACES DIFFERENTLY

The design of the public lighting was conditioned by existing fixtures and lamps on the market. The so-called road fixtures were composed of a special-shaped optic adapted to the lamp and intended to illuminate a roadway much longer than wide. For a long time, these same luminaires, possibly smaller in size and equipped with a lower-powered lamp (and a different light tone) were used for lighting pedestrian spaces. Gradually, optics of shapes more suited to pedestrian spaces have been appeared (revolution optics, symmetrical or asymmetrical). In France, in the early 1990s, the first pedestrian lighting poles with indirect lighting and light columns inspired by those and existing from the 1950s arrived to create new, more comfortable luminous ambiances for pedestrians, Fig.2.

A few years later, projectors originally intended for the monuments lighting were tested to illuminate large pedestrian-dominated spaces. These large projectors were also attached to the surrounding facades, Fig.3. In the mid-1990s, with the development of new optics adapted to the metal halide lamps, lighting designers had the idea of setting up several architectural projectors on large dedicated masts (from 8 m to 14 m height) installed in large squares under redevelopment (in the centre or around the space) to create a more spatial and enveloping lighting that freed itself from the sacrosanct axial regularity and uniformity of illuminance. This type of lighting allowed the number of small masts in space to limit and, thus, to release the views of many verticals at day and night. It also offered the advantage of the certain modularity (by modifying the orientation and setting of the projectors on site according to particular events), although in practice few modifications were made or attempted once the installation approved.

The appearance of the first coloured metal halide lamps or the addition of colour filters also al-

Fig. 4. Sables d'Olonne waterfront, France, 2008–2013 (Gerard Lancereau, architect, Jacqueline Osty & Associates, landscape architects, Roger Narboni & Virginie Nicolas, CONCEPTO, lighting design)

Fig. 5. Harbor district, Pantin, France (Jacqueline Osty & Associates, landscape architects, Roger Narboni, CONCEPTO, lighting design)

lowed the first tests of coloured lighting in the public space.

The lighting tools for public spaces then diversified with the integration of light effects into objects or benches, Fig.4, mainly at the time using outdoor devices, equipped with white or coloured fluorescent tubes. The ground lighting with fixtures equipped with coloured LEDs or compact fluorescent lamps, which appeared in the early 1990s, have multiplied the possibilities of nocturnal composition of a space, regardless of its size. They were used to draw light paths or to signal a dedicated route or an itinerary (tramway lines, cycle's path, or dedicated pedestrians alley).

The up-lighting of trees and landscaping that of fountains were also important elements of the lighting schemes at the time. Finally, we must also mention the development of architectural lighting, illuminations of facades located around a public space in order to create lighted vertical plans that were fully involved in the light composition and in the three-dimensional nocturnal perception of the illuminated space.

3. LIGHTING UP PUBLIC SPACES TODAY

The public spaces lighting design has changed radically in recent years, although these new approaches remain very marginal on a global scale. The lighting of public spaces has evolved, on the one hand, because the project management teams in charge of the development or redevelopment, under the impetus of public or private contractors, are increasingly using lighting designers since the tendering or competition phase, on the other hand, because the ways of appropriation of nocturnal public spaces have also evolved with new expectations of users but also because the LEDs revolution (which today represents 100 % of the lighting projects sources) has allowed lighting designers to greater creativity and new approaches.

This new design of public lighting spaces is in line with the current designs of development projects that have gradually adapted to the transformation of cities and which are now and primarily concerned with public transport and soft mobility modes at the expense of cars (fortunately for the light designer, thus released from high levels of illuminance and uniformity recommended for roadways). The willingness and growing demand of a large number of elected officials for more nature in the city as well as for development projects more respectful of the environment and biodiversity also influences new urban lighting projects.

The project management teams were able to respond to these new demands by integrating more systematically, in addition to the usual urban architects, landscape architects and engineers, lighting designers (who are more in charge of the nocturnal aspects of the public spaces and not only their simple lighting), but also and according to the projects, ecologists, designers, artists, sociologists and even sometimes philosophers or night geographers, Fig.5.

As a result, the lighting design of public spaces has become more complex.

Fig. 6.Vallée aux Loups Park, Chatenay Malabry, France (Jacqueline Osty & Associates, landscape architects, Roger Narboni, CONCEPTO, lighting design)

Fig. 7.Al Azaiba Park, Muscat, Oman (Jacqueline Osty & Associates, landscape architects, Roger Narboni, CONCEPTO, lighting design)

It must now, of course, respond to technical, normative, energy, environmental and budgetary constraints, but at the same time it must create attractive and varied luminous ambiances, propose new uses and new night readings of public spaces. It also wants to encourage the interactivity of pedestrians.

The job of lighting designer has, therefore, also gradually evolved to meet all these new challenges and the public spaces lighting is now completely renewed.

3.1. Pedestrian Lighting Poles with LEDs

The design of pedestrian lighting poles has grown enormously over the past decade, thanks to the many possibilities offered by LEDs in terms of range of light effects and dedicated optics, the decline of the energy consumption, the miniaturization of sources as well as the multiplication of decorative lightings integrations. Unfortunately, we sometimes see drifts where the whimsical design of the pedestrian lighting pole becomes the only conceptual objective at the expense of the creation of pedestrian luminous ambiances.

These new models of lighting poles, bearing luminous decorative elements and accessories, nevertheless allow public spaces to animate differently and offer to pedestrians and city dwellers more contemporary approaches to urban lighting and more varied visions of night spaces, Figs. 6,7.

Fig. 8. Epars square, Chartres, France (Reichen & Robert, architects, Jacqueline Osty & Associates, landscape architects, Roger Narboni, CONCEPTO, lighting design)

3.2. Smart Luminous Columns

The desire to minimize the number of masts in public space, as well as the desire to group different lighting possibilities or needs on the same mast (functional, decorative, architectural, signage) led to the creation of cylindrical modular luminous columns to arrange these various lighting functions at different heights.

In addition, cities have expressed the idea of installing loudspeakers, video surveillance cameras, sockets for luminous decorations and, if possible, television management, presence detection or sensor systems.

Thus, were born and developed in almost all lighting fixtures and supports manufacturers these modular luminous columns so-called smart, beginnings to the announced deployment of "smart lighting". They also offer electric charging sockets (e.g. smartphones, self-service bicycles or scooters).

Fig. 9. Flaubert Garden, Grenoble, France (Jacqueline Osty & Associates, landscape architects, Roger Narboni, CONCEPTO, lighting design)

Fig. 10. Cultural centre Garden, Saint-Lo, France (Urbanica, architects, Virginie Nicolas, CONCEPTO, lighting design)

These luminous columns smart or not allow the night space to structure and offer several light effects and thus several potentials of light compositions.

3.3. The High Lighting Masts

In the same spirit, spatial lighting from numerous orientated architectural projectors fixed at different heights on high masts was developed. These masts are increasingly drawn, decorated with luminous faults, double skins and light graphics (permitted by the use of LEDs) which makes them visible from afar in the perspectives to architecture and sign the night image of the large pedestrian squares, Fig.8.

Given the desire of a growing number of Western countries to minimize light pollution and preserve night-time biodiversity in the city, a majority of elected officials have banned the up-lighting of trees from ground recessed fixtures (although this practice had spread significantly in some French and foreign cities in the late 1990s).

The high lighting masts now offer again to the lighting designers the only possibility of down-lighting the trees so as not to disturb animal species with the help of dedicated projectors equipped with LEDs sources which light spectrum has been based on the needs of nocturnal biodiversity to be preserved, Fig. 9.

3.4. Coloured Lights

Coloured LEDs and tuneable white LEDs have also allowed the use and development of coloured or tinted lights in an increasing number of public spaces' lighting, even if the range of colours offered by manufacturers has been limited in recent years. They struggle to come up with hybrid LEDs engines composed at the client request of a mix of different colours, capable of satisfying the lighting designer creativity.

The coloured light in the public static or dynamic space is increasingly accepted by city dwellers, even if some residents still resist, out of nostalgia for the ancient orange atmospheres supposedly more romantic when in reality they de-qualify the illuminated nocturnal space by their very poor colour rendering index, Fig. 10.

Coloured light can transform the space, create a special ambiance encourage city dwellers to stop to look differently at a place, a garden or a statue.

On the other hand, interactivity with passers-by, the possibility given to pedestrians to choose their own colour and their colourful atmospheres is not yet on the agenda, nor encouraged by the technical services of the cities.

3.5. Projection of Images or Videos

The use of still images or videos projected onto the surrounding ground surfaces, objects, trees or facades is increasingly integrated into the lighting project of certain public spaces. The reliability and robustness of LEDs outdoor lighting fixtures capable of projecting on the ground realistic or highly graphic slides of good light quality, allows these new approaches, although much remains to be done among manufacturers to offer small projectors that can be attached discreetly to masts or nearby facades.

Fig. 11.Harbor district, Pantin, France (Jacqueline Osty & Associates, landscape architects, Roger Narboni, CONCEPTO, lighting design)

Light projections create a world of signs, symbols and graphics, clearly legible, which pleasantly complement the use of light effects alone. The projected images have a strong evocative power because they generate visual emotions, they envelop and immerse the spectators in a poetic light setting or refer them to cultural references that light alone cannot necessarily create, Fig.11.

The projected images are also capable of structuring the ground space or the facades, thanks to their density and positioning. Finally, this projection technique offers the advantage of being able to regularly change the sets or patterns projected and thus to significantly and regularly modify the night space created, Fig.12.

3.6. Ground Textures and Deconstruction of Lighting Effects

More recently, lighting designers have expressed in their public space lighting project a desire for non-homogeneity, contrast and a will for textures, and deconstruction of effects created by LEDs on the ground or on the surrounding walls, using specially designed filters or refractors.

Fig. 13. Saint-Charles Church square, Lille, France (Atelier Jours, Landscape architects, ON, lighting design)

Fig. 12. Interlude, Valenciennes, France (Roger Narboni & Fanny Guerard, CONCEPTO, lighting design)

The pointillist frame of LEDs in projectors or lighting fixtures, which manufacturers strive to erase to obtain a homogeneous light beam and uniform illuminance, is deliberately decomposed to recreate a mesh on the illuminated surface of more or less blurred light points or effects of textures that will sign the illuminated public space and allow for a more unusual nocturnal composition, Fig. 13. In

Fig. 14. Paris Saclay campus, France (Michel Desvigne, landscape architects, Roger Narboni & Fanny Guerard, CONCEPTO, lighting design)

Fig. 15. Queen Elizabeth Olympic Park, London, UK (James Corner Field Operations, Landscape Architects, MAKE, architects, Speirs + Major, lighting design, Michael Grubb Studio, Executive Lighting Designer, Photo James Newton)

some cases, the refractor filter can be set on site to focus or defocus the desired light effect. In the case of using a mixed LEDs in the device (white tones or different colours), defocusing allows us to create surprising mixed textures and colourful graphics, Fig.14.

3.7. Special or Custom Products

Technological innovation does not necessarily precede the creative desires of lighting designers who want to illuminate public spaces. It is therefore often they who, depending on their project, will solicit new technologies or stimulate new and innovative approaches from manufacturers that will then lead to ranges of devices or accessories that will be integrated into the catalogues. The development of special products by lighting designers and the "customization" of existing devices are also frequently convened for large-scale projects.

At the same time, the incorporation of lighting and lighting effects into outdoor furniture, structures or landscaped elements designed by architects, landscape architects or designers has become more systematic, which has enlarged in a way the panoply of lighting tools available to lighting designers and therefore the diversity of night images created for public spaces. In addition, differentiated computing management of the various LEDs sources and the development of complex dynamic scenarios are also now an integral part of the practice of lighting designers when developing original lighting public spaces, Figs.15, 16.

Fig. 16. Shakespeare's New Place, Stratford-upon-Avon, UK (Timothy O'Brien RDI and Chris Wise RDI, joint Artistic Directors and Co-Designers, Speirs + Major, lighting design, Photo James Newton)

3.8. Luminous Lounges

The idea of imagining luminous lounges, inspired by the desire to recreate a cosy and welcoming interior image in the outdoor public space deemed harder, was initially confined to positioning a pedestrian lighting pole, more or less decorative, near a bench, thus changing the nocturnal image of the small demarcated space, Fig. 17.

Fig. 17. Central station square, Poitiers, France (Antoine Grumbach & Associates, architects, Roger Narboni & Virginie Nicolas, CONCEPTO, lighting design, Photo Xavier Boymond)

Fig.18. Extimity – Lounge lighting – Copyright Roger Narboni & Technilum

Gradually, a real form of living room, more complex and structured, was thought by the designers and set up in some large public spaces to accommodate passers-by or allow them a break in their daytime and nocturnal journey. The light is used to signal this reception space at night and to transform its night image into a break with the surrounding public lighting (through the use of light effects, lighting types or different colours).

More recently, modular and three-dimensional dedicated structures have been designed to serve as both a lighting or lighting effects support, but also a day and night climate shelter, complemented by a whole range of possible functions and services: charging smart phone and laptop, speaker to play music, allowing passers-by to change the light mood, etc.

This next generation of luminous lounges also allow us to create virtual volumes of light and delineate a night space and a light atmosphere localized in three-dimensions, Fig.18. They are the beginnings of luminous, more complex, connected, and interactive spaces that are set to develop in the city of tomorrow.

4. AND TOMORROW

For several years now, in most of the world dense cities, new urban policies have been put in place to reduce the car's space and the speed of vehicles in the city, and to redistribute the public space gained to promote public transport, soft modes and pedestrians. These, major urban, developments should encourage us to revolutionize the way we think about the public spaces' lighting in the city.

The expectation is, therefore, high among all lighting players regarding the development and maturity of the so-called smart lighting. Beyond the real-time adaptation of lighting in public spaces (in terms of light levels and light tones) according to the needs and presence of users, the expected television management of light fixtures and the knowledge of equipment and energy consumption, the smart lighting, the dense mesh of its supports in the public space will gradually become major players in the development of digital uses in the city.

The lighting mast will also become a support of information (traffic, environmental, climatic, tourist), from sensors, light signals and user-friendly interfaces.

Coupled with applications for users' smart phones, new digital services will be able to be offered using the mesh of public lighting: sound infor-

Fig. 19. Portable lanterns, Chengdu Jincheng Greenway, Sichuan, China (CONCEPTO & Winlux lighting, lighting design, computer rendering copyright, Floriane Deleglise, CONCEPTO)

mation, video, city map, tourist or commercial information, ambient temperature, air quality, traffic density, availability of nearby parking spaces.

The LED engines of the luminaires designed to illuminate public spaces, already able to modify on demand the tone of light emitted, will evolve in the near future to take into account in a more systematic way the necessary and imperative preservation of biodiversity at night. This will require builders to provide specific LEDs spectra adapted to the fauna and flora present or to come to the proposed site.

5. IN A MORE DISTANT FUTURE

5.1. A Nocturnal City Dedicated to City Dwellers

The planned scarcity of passenger cars or their absence in the longer term, the gradual disappearance of the lanes used to them will transform the design of the public space to propose pedestrian continuous plateaus from façade to façade, which will no longer need lined-up and regularly spaced lighting pole to illuminate a now defunct roadway. Thus, the city will become again and gradually devolved and dedicated to city dwellers as it was before the invention of the automobile.

The offer of public lighting poles, once they become obsolete, will have to transform and evolve into a range of modular lighting structures capable of creating immaterial luminous volumes and different types of night spaces with various dimensions.

Another urban lighting, different forms of lighting with diverse functions are, therefore, to be invented to respond to these future morphological evolutions of public space. The new lighting systems will allow the city to be illuminated differently, not only to see clearly and to move as it has been the case since the birth of public lighting, but to generate invitations, stopovers, cuts, enlargements that will definitely break with the regularity and rectitude of the public lighting mesh of yesteryear.

These user-friendly spaces and light volumes, capable of providing climate shelter, will also be designed to be dedicated to the well-being of city dwellers (anti-stress environments, taking into account biological rhythms, light therapy, chromo therapy and dark-therapy), to foster dialogues and encounters in the public space. They will generate nocturnal places, immaterial volumes, able to transform and shape the nearby light environment and to interact visually with the surrounding space by highlighting it, delimiting it, cutting it, to multiply the possible uses and associated services.

Fig. 20.Personal halos, 2053, the future of urban lighting exhibition (Roger Narboni, curator, computer rendering copyright, Noémie Riou, CONCEPTO*)*

They will also offer to passers-by the opportunity and freedom to drive and choose their luminous atmospheres from the cocktails of proposed compositions (intensities, colours, light sequences, types of lighting, distribution in space, effects, volumes, etc.).

In the long run, it is a real democratization of the public spaces' lighting that can be offered to users so that they regain control over their nocturnal environment as well as the luminous ambiances they desire, and finally free themselves from the control of technicians and operators of the lighting sector who have always decided, studied and designed functionally the lighting of the world's cities without real contradiction or citizen debate.

5.2. Autonomous Light Objects

While walking around today with a smart phone has become a no-brainer for city dwellers around the world, while this object that became familiar did not exist thirty years ago and its use became democratized in the late 1990s, the nocturnal urban set will gradually change in the future with the appearance of autonomous portable lanterns that will give users the opportunity to control their near-night environment according to their needs and wishes.

Indeed, even if smart phones are already equipped with a lighting system that allows clear to see at night in the absence of lighting, this one is rudimentary and does not allow the creation of real luminous ambiance, Fig.19. And the headlamps used for night trips in the dark (especially by joggers and

Fig. 21. Silhouette, 2053, the future of urban lighting exhibition (Roger Narboni, curator, computer rendering copyright, Loeïza Cabaret, CONCEPTO)

night hikers) are also very simple and unfriendly because they dazzle passers-by.

The creation of autonomous and rechargeable portable light objects, their voluntary networking, will allow passers-by to reconstruct a collective light space, or even illuminate on demand an element of architecture or landscape. These self-contained portable lanterns could be thought of as current economic models of bikes, scooters or electric cars in open access and temporary rental.

The street lighting will no longer be public but shared and could only work in the presence of users.

5.3. Accessories and Bright Clothing

Light emitting clothing and light accessories integrated into shoes, roller skates or skateboards, for example, made possible by the development and miniaturization of LEDs, batteries and their autonomy, personalize urban dwellers that are passionate about innovation and give them the first forms of nocturnal autonomy, Fig.20.

These panoplies will develop to offer night users, luminous jewellery, adornments, dressing elements allowing them to be seen in obscure urban public spaces, parks or natural spaces of very low light level, but also the ability to diffuse a soft light capable of illuminating their intimate space, Fig.21.

The recent appearance of civilian drones, remotely piloted or programmed to follow a person, and the first experiments to use them as lighting carriers, let us portend a future where the creation of luminous ambiances, the lighting of public spaces, landscapes and architectural sites, can also be made in three dimensions from the surrounding space and not just from the ground or from low-rise masts. These new flying light objects will quickly integrate into the range of lighting designers (they already allow them to create stage and event lighting) to multiply the possibilities offered to night users.

Thus, it is easy to imagine that in the future, the initial function of public lighting, which was to allow to see and be seen, will be gradually contradicted by the freedom given to city dwellers to decide when and how their near night space must and can be illuminated.

This revolutionary transformation of urban lighting into active urban light can pave the way for a rediscovery of darkness in the city and experimentation with sharing and pooling urban darkness.

5.4. Phosphorescence and Bioluminescence

Research on phosphorescent materials capable of being integrated into ground arrangements, prospective studies on the controlled use of genetically modified bioluminescent bacteria, increased understanding of the phenomenon of bioluminescence of

Fig. 22. Bioluminescence, 2053, the future of urban lighting exhibition (Roger Narboni, curator, computer rendering copyright, Noémie Riou, CONCEPTO)

certain plants and animals, augurs a new revolution in non-energy-consuming urban lighting, which will automatically adapt in real time to new urban uses (analysis of ambient light and urban form, users' flows and density, lighting needs, temporalities) and which will be ordered at the request of city dwellers.

These futuristic light sources with qualities and potentials still unimaginable today will lead to the creation of new nocturnal landscapes, natural or urban, totally in tune and in symbiosis with the environment as with the new irreversible trend of re-naturation of cities, Fig.22.

5.5. The Advent of Luminous Architecture

Since the birth of public lighting in the middle ages, public spaces, i.e. the voids in the city, have always been illuminated, especially at the beginning from lanterns fixed on the surrounding facades.

Historical, modern or contemporary architectures (the city's solids that line the hollows) are sometimes illuminated, decorated with lights or sometimes decorated with signs or light advertisements, but these lighting systems linked to the buildings almost never participate in the lighting of the public spaces, including in the lower strata of the city, close to the pedestrian. Public lighting, including in normative and regulatory terms, therefore, remains totally indifferent to the illuminated or uninhibited architectures it encounters.

With the evolutions in the morphology of cities that can be imagined in the future, the new relationship to be instituted between private and public developments, the role that built fronts could now play in the city, new forms of architecture that could increasingly incorporating structures deployed over the public space, the lighting pole, which today clutter the streets, will certainly disappear to make way for light emitting surfaces, light materials fixed on walls, integrated directly into facades, structures, sub-sides of infrastructure, floors to illuminate the adjoining public space or located below without unnecessarily occupying it.

The building materials of the grounds and facades will become luminous at night to ensure this new perception of the night space.

The advent of light materials for floors and walls will profoundly change the design of the architectures. The relationships Architecture / Urban Space / Light always thought according to the only natural light will be transformed. The architecture will no longer be conceived as today only according to its solar orientation (and the possible contributions of natural light) but also according to its potential nocturnal role in the lighting of adjoining public spaces, resulting in an inevitable transformation, from the illuminated city to the luminous city.

Fig. 23. City of Lille's dark infrastructure (Roger Narboni, CONCEPTO, lighting design, computer rendering copyright, Loeïza Cabaret, CONCEPTO)

This luminous city in the making will gradually establish for city dwellers a different relationship to the public space who will be accustomed to rubbing shoulders with luminous public transport and pedestrians dressed in lighted costumes or carrying their own lights.

5.6. A Development and a Mastery of Darkness

Since the early 2010s, new lighting strategies coupled with the study and development of dark infrastructures have been initiated on the one hand to reduce the electricity consumption of cities and on the other hand to control light pollution and to best preserve biodiversity at night, Fig.23.

It is in this way that plans for the preservation of darkness were born, capable of being spread over the whole of a city or a large territory in addition to and in support of the green and blue infrastructures.

This subtractive, dark-based approach was initially studied by theorizing the respective roles that public lighting and darkness can and should play in the city, in response to the demands of locals who had clearly expressed, at the time of workshops and nocturnal exploratory marches, their observation of too much lighting in the city and their desire to preserve darkness especially in the great natural spaces.

The dark infrastructure then allowed defining and delineating areas of geographical and temporal darkness, partial or temporary, their links and their

crossings. Once adopted by the elected representatives, it is available in all development projects located on or near the great natural spaces in order to carry out an in-depth reflection on the preservation of ordinary nocturnal biodiversity in relation to the photo-pollution.

When darkness is no longer systematically synonymous of irrational fears or feelings of insecurity, new urban scenarios could be imagined in response to energy crises, the global will to fight climate change and reduce air pollution, in order to experience a rediscovery of the night in the city and the invention of new ways of illuminating that respect the darkness.

The development of environmental mesh, green belts around major metropolises, will play a leading role in changing the nightscape in and around the city. The areas of darkness will gradually expand to contain and delineate at night the luminous islands formed by the megalopolises. These new large dark territories will allow the human eye to develop and rediscover new nocturnal visual abilities, which will encourage city dwellers to mentally and psychologically rehabilitate themselves to wandering in the dark night.

The gradual abandonment of systematic, continuous and ubiquitous public lighting will pave the way for night learning and new therapies based on the pleasure of being and moving in deep darkness.

The urban night, which has always represented 50 % of a city time, with the corollary transformation of the public spaces lighting, will become a specific territory to be explored in order to better respond to urban changes and lifestyles evolutions of city dwellers which will sure surprise us in a not-so-distant future.

Roger Narboni,
the world-renowned French lighting designer, visual artist and electronic engineer, President of CONCEPTO studio, founded in 1988, has realized more than 200 landscape, urban, heritage and architectural lightings. In 1987, he launched a new discipline called Light Urbanism. Since then, he has realised more than 140 lighting master plans in France and abroad

Light & Engineering
Vol. 28, No. 2, pp. 17–27, 2020

https://doi.org/10.333.83/2019–066
Svetotekhnika #5, 2019, pp. 76–83

STAGE IN THE SPOTLIGHT AND PARADOXES OF THE PROFESSION: ARTIST, LIGHT, THEATRE

Elena A. Zaeva-Burdonskaya[1] and Yuri V. Nazarov[2]

[1] Moscow State Stroganov Academy of Design and Applied Arts (S.G. Stroganov MGHPA)
[2] National Design Institute, Moscow
E-mail: lenartt@gmail.com

Light is a worldview
Federico Fellini

ABSTRACT

Nowadays, the lighting designer is becoming one of the leading figures in forming of the concept of theatrical scene design. Lighting technologies with great potential of illumination, colour and graphic capabilities allowed the profession to occupy the leading positions in the space of any object. Today's orientation of the whole visual culture to staginess alongside with avant-garde inventions of stage designers in the early 20th century have formed the main artistic trends of this art. Nowadays, the modernistic findings of the past are supplemented by innovative multimedia technologies. Visual techniques worked out in stage shows have seriously affected the people's attitude towards the stage space. They have made theatrical performance very dynamic by using lighting and media effects, sufficiently widened the scope of visual and expressive abilities of an artist.

The new paradigm of light as an active tool of form-making allowed modelling the space by means of lighting technologies. Stage light has become a form possessing great emotional power inseparably associated with the dramatic composition of performance. At the same time, the goal of a lighting designer cooperating with theatre designers and costume designers should permanently lead the audience to *catharsis* and innovative light engineering techniques play a great role in it.

Naturally, such innovations in theatre art made it necessary to correct the programmes of training of universal specialists required in this area. Professional education of a theatre lighting designer, apart from knowledge of technology and basics of scenography, requires serious artistic training.

The methodological experience obtained in scenography training of future designers in the Environment Design sub-department of S.G. Stroganov MGHPA may provide an example of new design approaches to solving of comprehensive problems of scenography. Design training techniques used in the sub-department include the method of environmental approach, the method of script modelling using a virtual design model and the method of conceptual design.

Key words: light designer, light design, scenography, design training, conceptual design, script modelling, catharsis, building of the stage space

1. INTRODUCTION

1.1. Basics of the Contemporary Trends in Theatrical Lighting

"The ramp goes out – there is no theatre any longer," M. Bulgakov used to say. The light is the basis of a theatrical performance as it is built in the structure of scenography as one of the key players. Expression of a theatrical performance is influenced by

its synthetic nature. The architectural, artistic, dramatic, dramaturgic and musical model of a performance comes to life in a visual plot played on the basis of a light script. There is an aphorism by one of the today's most sought-after theatrical designers A. Melnik: "A lighting designer should listen with own eyes".

The newest trends of the contemporary synthetic theatrical performance were founded back in the last quarter of the 19th century by R. Wagner in his version of "national drama". On the basis of the national epic, dramaturgy of the great composer's operas united music, visual and applied arts, decoration landscape and light. Technical achievements and stylistic mobility of art nouveau established new genres of colour music (A. Skryabin, M. Čiurlionis). V. Meyerhold synthesised scenography with avant-garde futuristic solutions in the field of graphic design which is rooted in mass culture. By means of light projection, the director introduced text images of mottoes, slogans, eye-catching names of episodes, advertisements, etc. in performances [1].

In the art deco era, alongside with search for interdisciplinary synthesis, a reverse process is notable: a theatrical performance itself becomes a force initiating innovative processes in light design and other types of visual art. Such processes appeared due to global reorientation of culture from "figurativeness" to "expression", its refocusing from literature to spectacles on the cusp of the 19th and the 20th centuries. "…To the least extent, our epoch is being verbal… in the 20th century we are facing the "echo" of the forms of communication created at the early stages of the human history. Today, expression of these forms is concentrated in visual communication." [2].

The project of interior lighting developed for French oceanic liners SS Paris and SS Normandie (1930's) also obeyed the laws of scenography. According to the René Lalique's idea, shining jewellery of the visitors of the ship restaurant and flaring light columns should blind the guests and demonstrate the luxury and beauty of the interior (architects Patout and Pacon) turning it into "the newest version of the Versailles mirror hall." [3].

New capabilities allowed economically feasible methods to use for industrial production of pressed glass. Substantially, a new sphere of architectural glass industry was established, with its high thickness, transparency, shine and mat surface sometimes engraved. Mysticism of the visions of illuminated pressed embossed glass in the Lalique's interior decorations formed the dramaturgy with tension similar to that of a liturgy in the St. Matthew's church known as the Glass Church in Millbrook (Jersey Island in the Channel Islands).

Theatricalised game with the interior space originated new forms and types of artificial lighting: lighting cornices made of pressed glass panels with quarter round cross-section and a cast ornament on the outer curve. For the first time, cast forms of glass used for suspended ceiling lamps and chandeliers (designed by R. Lalique) created unusual stray light with the ceiling acting as a reflector. The electric light created an effect of two levels on the ceiling lamp – the reliefs of the decoration and the background (as continuation of the game with the space and the spectator). According to art critic Gabriel Mourey (1865–1943), "It is commercial art, greatly thought-out and clear, which allows us to use a really modern and lively feeling in decoration… and in arrangement and decoration of public buildings such as… dance halls, shops, banks, theatres, concert halls, etc. It definitely bears the sign of our complex civilisation eager for elegance, originality, comfort and luxury." [3].

1.2. Factor of Innovative Technologies in Light Scenography

Theatre is distinct from other synthetic arts due to the great power of tradition. "Pursuits and discoveries of theatre designers of the beginning of the 20th century, had defined the development of the world's performance art for many years to come. Modern technologies just develop the directions founded decades ago." [4]. One of them is the experimental field of light scenography which keeps enriching itself by lots of innovations originated by the digital era.

Dramatic change of paradigms in the lighting art turned it from a supplement to objective and spatial environment into a real tool for form-making and artistic modelling. Such terms as "light plastics", "light form" and "light environment" (N.I. Shchepetkov) appeared as self-consistent design formats capable to cover the whole stage space. Such conceptual setting resulted from the stage-by-stage development of the field of activity of a light designer proposed by the English researcher Christopher Cuttle "…to identify the main themes that have di-

rected the objectives of the lighting profession. It is proposed that the objective of the first stage was provision of uniform illumination over a horizontal plane, and that of the second stage has been to provide illuminance suited to human need, based on visual performance. This brings us up to the current era, and… That the second stage has failed to achieve its objective… Familiar notions of lighting effectiveness and efficiency are turned upside down, and an entirely different way of thinking about interior lighting design is revealed… The essential difference is a switch from assessing light incident on planes to assessing *light arriving at the eye*. Such change in thinking may be seen as a precursor for the third stage of the lighting profession" [5] which takes a spectator's emotional state into account.

In the 21st century, theatre has changed the nature of visual perception of a performance even as compared this to thirty years ago. Today's consumer fed-up with excessively dynamic media flow often lacks emotions and psychological tension in an environment formed by a conventional light plot. We cannot imagine ourselves beyond the elements of a show which brought additional elements of dynamics to theatre. Of course, they include video mapping in the form of *2D* and *3D* projections (semi-transparent curtains, smoke, water flow, etc. act as a screen). Laser installations, holographic sculptures, art objects based on light and colour dynamics, etc., which are gradually being introduced in stage dramaturgy, may also be included in this list. Television projections and special concert light effects are pro-actively embedded in stage performance. Their goal is to efficiently affect emotions of the audience, to emphasise accents, to express director's remarks. However, suggestive nature of light embodied "in unpredictable dynamics of light flows affecting nerve centres of human body hides lots of mysterious and non-studied mechanisms which are intended to provide the hypnotism so required by theatre in different portions." [6]. Given the powerful psychological effect of light on a spectator's state of mind, it is necessary to use correct approach and to be very careful when arranging the light stage space.

Illusory space often becomes an analogue of romantic "expression of inexpressible" which is finally within an artist's control. Friedrich Schiller noted that "…everything that our souls feel in the form of vague and unclear senses is provided to us by theatre in loud words and bright visions with astonishing power." [7]. In the Human Voice one-woman performance (Helicon Opera, designed by R. Protasov, directed by D. Bertman, 2019), at the moment of the highest emotional tension the microphone on stage begins to shine brightly during the aria performed by T. Gverdtsiteli symbolising the singer's "soul light" (equality of light and reason is recognised since the Enlightenment).

In The Government Inspector (Alexandrinsky Theatre, director V. Fokin, designer A. Borovsky), in order to create phantasmagoric, amplified, grotesque plots and to solve the visual space of Saint Petersburg capable to "twist, sevurity, destroy", I. Epelbaum from the Shadow theatre was invited, and planar decorations acted as the screen surface [8].

Opinion of a reputed director M. Zakharov confirms artistic priority of such effects. The maitre admits that "…light should serve as a catalyst of acting processes and even the detonator of possible emotional explosion leading to *catharsis*, the shock…, for which people burdened by modern information still keep going to theatres. Fancifully developed light plot in a talented scenography uniting with actors' inspiration on the same energy basis forms an integral whole." [6]. Answering the question about the future role of video projections in design of opera and dramatic performance and whether the projectors will replace traditional decorations, E. Roller, light designer of the Zurich Opera House *(known for his innovative light engineering approaches in performances – author's note)* was confident: "Everything depends on the director's ideas and scenography solutions. But I don't think that projection technologies will fully replace theatrical decorations." [9].

1.3. Aspects of Theatre Light Designer Training

It is obvious that further development of dualistic artistic and technical light plot of a performance has two dimensions. The first one is using of the wider technical and technological innovations which are infinite in terms of possibilities. The second one is involvement of artistic imagination formation of which is due in no small part to the training programme of a future specialist. This is the nature of the universality phenomenon of the profession of theatre light designer which is still a result of random choice for many specialists.

In fact, schools of theatre arts train their students as technician artists, however, the programme is full of theoretical disciplines detriment of practical ones. This situation is common not only for theatre light designers but for light designers in general. M.A. Kanatenko and O.M. Mikhailov note in their work [10] that "…today's students who have been trained much better and are more all-round than their peers were 50 years ago still have to start at the same point as their fathers and grandfathers…".

Due to its conservatism and medieval structure, theatre has kept the guild principle of transfer of skills from a master to an apprentice. Due to the fact that "there is no education [in the profession], a feeling of a school is very important… Funny as it is, there is no normal theatre light design school." [11]. The roles of a "master" and an "apprentice" make theatre related to the methodology of artistic education where, similar to theatre, the mission of a mentor keeps defining the quality of professional knowledge and skills of a student actualising author's, free and creative attitude to the work material. Thanks to emotional and artistic potential, we still consider interesting the performances by the great theatre designers: E. Gansburg, a light designer (A. Bryantsev Youth Theatre, Lensoviet Theatre, BDT, Alexandrinsky Theatre); O. Sheintsis, chief scenographer, and M. Babenko, a light designer with Lenkom Theatre (Juno and Avos, The Memorial Prayer); D. Borovsky who cooperated with directors of the Moscow Art Theatre, Maly Theatre, Taganka Theatre, Sovremennik Theatre, etc. "The power of his scenography… drafts and sketches… the performance itself… transformations of space, colour, light, interaction of the decoration and the music" [12] certainly give evidence of an artist's synthetic talent. Not coincidentally, the academic tradition of the classics of stylistic allusions can be seen in works by D. Borovsky (The Gambler opera by Prokofiev) where "architectural sources from the High Remus to Art Nouveau are edited by a constructivist." [12].

In his Stage Lighting Lessons, Neil Fraser, the director of Technical Training with the Royal Academy of Dramatic Art, London, listing the results to be achieved by means of stage lighting, emphasised, among others, "the feeling of the stage and overcoming by special effects". He focused on innovative and artistic approaches to design: "…test your ideas practically, try something new, explore and create learn from painters to use light and build composition of your picture. The works by Rembrandt, Caravaggio or David Hockney may serve as good examples." [13]. The master's programme of the famous *Parsons School of Design* (New York), the world's leader in the spheres of theatrical, architectural, interior and exhibition lighting as well as design and manufacturing of equipment, offers "interdisciplinary variants of learning allowing students to develop deep technical and aesthetic understanding of interrelations between light, architecture and interior design" [14].

1.4. Design Training

Let us try to consider the main principles of theatrical light application and related artistic capabilities as exemplified by the training projects of the Environment Design sub-department of S.G. Stroganov MGHPA. In 1906, in his Handbook for a Dramatic Actor, K.S. Stanislavski wrote: "There is no and there is not should be neither a study guide not a grammar of dramatic art. As soon as it becomes possible to fit our art into narrow, dull and straight-lined framework of a grammar or a study guide, we'll have to admit that our art no more exists." [15]. All these make the way to an experiment performed in scenography training projects much more complex. The selected methods of design are justified by necessity to make creative searches totally free, to keep respect for position of an author, by aspiration for stimulation of artistic processes when considering fundamental compositional and artistic and visual laws of stage space building.

2. METHOD OF STUDY

The main principle of a theatre designer is possibility to talk only about creative principles but not about abstractive universal methods of formation of stage lighting space. In each case, this will be its own approach to design selected basically within the dependence on the artistic challenges of a performance. However, in any case, the artistic and humanitarian component is the priority of the design approach.

2.1. Environment Approach Method

The environment approach, the analogue of the system approach, has become the basis for analysis and development of scenography projects cre-

ated as part of design training in the Environment Design sub-department. It is based on the most important concept adopted by design together with the post-modernism paradigm back in 1970's. The context always implies the dialogue of two components (*according to M.M. Bakhtin*): "text-context", or "object" and its contextual "background". Basically, the environment approach includes the more complex system of "designed environment" as the main component which is the basis for synthesis of arts and use of expressive means contained in it. Light is contained in the "text" of scenography as an integral giving the true life to a performance.

2.2. Method of Script Modelling with Building of a Virtual Design Model

As part of the environment approach, the method of script modelling is formed which contains "… methodology aiming at active use of designer's intuition and reflection, by virtue of which, a designer may initiate introduction of innovative form-making processes into a designer environment. Uniting of script modelling methods may serve as the groundwork for creation of such design methodology." (V.F. Sidorenko [16]). A script is allowing to plan the work with an object stage by stage, in accordance with the goal and challenges, forming the most optimal parameters of an environment affected by a large number of factors (which also include the synthetic theatrical performance).

The design method of script modelling is similar to space theatrecalization techniques. This deliberate creation of "successful" points of perception implies frame by frame showing up of sights (stage settings) forming a spectator's environment perception with consideration of role positions of "environment explorers", distribution of script axes, stage settings, introduction of "intrigue", etc. [17]. A script provides naturally stable lighting environment with visual dynamics. Visualisation of immaterial virtual light objects and visions, changes of visual light frames have exclusively author's emotional and creative foundation. It's no coincidence that the profession of a light director is similar to the profession of light designer. Use of multimedia techniques of light arrangement on stage reflected in engineering, directing and artistic components has opened a gate for interactivity of the stage space and its dynamic filling, active effects of light visions, including as part of the psychological dialogue between an actor and a spectator. Digital modelling has made it easier to build volumetric and spatial analogue models facilitating the work with light plot with consideration of different "points of view".

2.3. Conceptual Design Method

The principle of conceptual design is based on humanitarian approach to environment design, with human always acting as a starting point. In many cases, the concept of a light project may interfere with the common environment scenario but most frequently goes beyond the storyline dealing with artistic and technical aspects, design technologies and visual effects. The concept involves the project of light arrangement of stage environment from elaboration of ideological strategy (as a result of pre-design analysis) and definition of the system of design approaches to creation of a visual work model of a light environment, i.e. the visible image of a future object. Legitimacy of selection of conceptual approach to light design of a performance is confirmed by priority of artistic component in the work of a light designer. Due to introduction of innovative lighting technologies in scenography, light designers have been pretending to a right to form the light image of a stage space more actively. The established procedure of work with a lighting project including setting up a problem, origination of an idea and creation of art images provides an evident analogy with academic art which possesses a wide potential of design capabilities for creation of a light scenario.

3. RESULTS

All of the training projects are distinctive with their conceptual basis. Design technology prioritises the visual artistic component of scenography including development of the structure of subsequent shift of performance stage settings, design of volumetric-and-spatial and planar decorations (if any), *3D* visualisation of the stage space, development of costumes, and preparation of advertising materials.

3.1. Metaphor of Light

Modern technologies allow us to interpret familiar and already classic stories in a new manner. De-

Fig.1. Design concept of a performance based on Hans Christian Andersen's Snow White (Design project, 5th year of education, specialist programme. Author: Yu.A. Malyutenko. Educators: Prof. E.I. Ruzova and Prof. E.A. Zaeva-Burdonskaya, 2009)

veloping traditional scenography directions founded in the past, light technologies are allowing to create bright and dynamic light images providing the decoration with a nature of a "speaking" object. *Metaphor of Light* embeds in the script texture, manifesting itself not so much at the form level as at the sense level.

In the scenography project of the famous fairy tale The Snow Queen by Hans Christian Andersen (Fig. 1), light becomes a metaphor of bluish white ice acquiring an image of moving semi-transparent figure and modular decorations. By means of a video projection, an illusion of show fall and a blizzard is created, giant roses "grow" and frost winter trees appear on a transparent net screen. The light "lightens" the Moon in the sky, illuminates the windows, etc. An advantage of the project is minimum amount of decorations with high compositional variability in changing of the episodes. The stage space is built with consideration of maximum freedom of movement provided for the actors.

Capabilities to create projects integrating innovative multimedia digital content into the system of traditional plastic form-making of stage and projects based on light technologies appeared on the cusp of the 20th and 21st centuries. A number of technological methods may be united in one performance, which partially resembles the environment of variety shows with their goals to create a complex and fairy image – "expression of inexpressible". By means of laser projection, a whirlwind accompanying appearing of a genie out of a lamp is created, projection technologies are allowing to make characters "fly" on a magic carpet, to build the walls of a mirage town, etc. Directed light beams of a fountain supplement illuminated semi-transparent screens of the decorations of a sultan's palace interior (Fig. 2).

Light not just creates the forms and visions of a theatrical environment but also arranges the space, emphasises plans, provides the stage "box" with a feeling of infinity, depth and dynamics.

Fig. 2. Design project of the Aladdin performance based on the Aladdin and the Wonderful Lamp (Design project, 5th year of education, specialist programme. Author: E. Shonia Educators: Prof. E.A. Zaeva-Burdonskaya, prof. E.I. Ruzova, 2009)

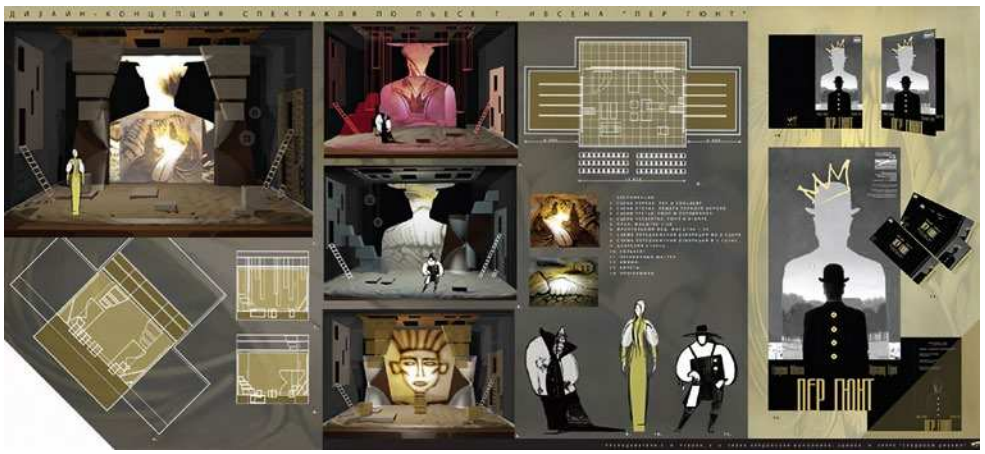

Fig. 3. Design project of a performance based on Peer Gynt play by H. Ibsen (Design project, 5th year of education, specialist programme. Author: N. Zykova. Educators: Prof. E.I. Ruzova and prof. E.A. Zaeva-Burdonskaya, 2009)

Constant projection on a stage background becomes the main technique supporting the kinetics of a performance. For the duration of a performance, the process of creation of pictures for a specific act of a performance using sand animation is being demonstrated. Smartness of Henrik Ibsen's dramaturgy is metaphorically reproduced through transience and fluctuation of flowing sand particles, the colour palette of light on the picture plane. All the sand pictures demonstrated in the project were made by the student (Fig. 3).

A project based on a famous tragedy by A.S. Pushkin is designed for performance in the Mimics and Gesture Theatre (Moscow). The performance is intended for deaf spectators, which defines the distinctions of visual arrangement of scenes (Fig. 4). Dramatic dance, plastic movements of actors are forming the basis of the "text" of a play are accompanied by video projections in the style of shadow shows. Selection of black and white silhouette light images and red light of projectors (the image metaphors of blood and poisoned wine) increases the mystical dramatic effect of the stage. Reflective surface of deformed floor multiplies the blood-red and white light flows and LED strips of improvised "columns" imitate the infinite depth in the space of black box of the stage.

3.2. Performance in Reflection

W. Shakespeare's classic is immortal, which makes it a constant source of inspiration. The fol-

Fig. 4. Design concept of a performance based on Mozart and Salieri by A.S. Pushkin (Design project, 5th year of education, specialist programme. Author: E. Baimova. Educators: Prof. E.I. Ruzova and prof. E.A. Zaeva-Burdonskaya, 2009)

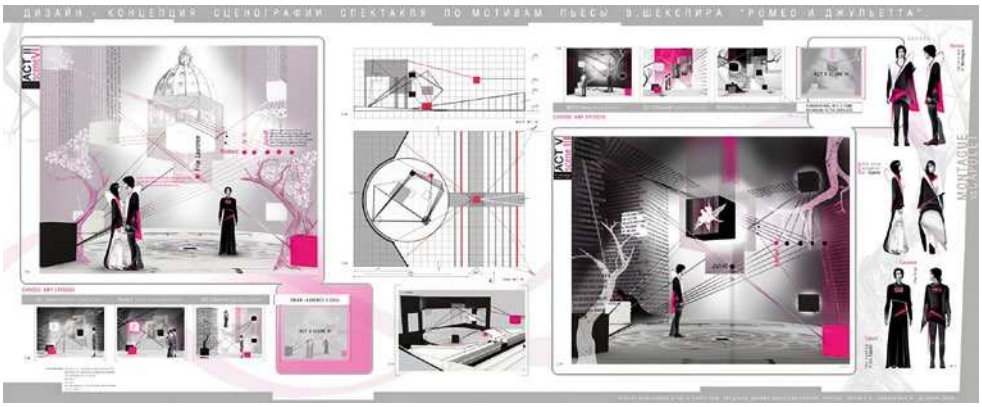

Fig. 5. Design concept of scenography for a performance based on Romeo and Juliette by W. Shakespeare (Design project, 5th year of education, specialist programme. Author: O. Simatova. Educators: Prof. E.A. Zaeva-Burdonskaya, prof. E.I. Ruzova, 2006)

lowing quote is given in the *Light* journal "…there are stories which embody the capability to expand the horizons of customary approaches to stage production and not just to present a familiar story to the audience but to create a startling unity of music and decorations. In Hamlet-machine opera by W. Rihm, Shakespeare's well-known play turns into grotesque, the drama breaks into fragments, which provides actors with a large space for interpretations." [9]. In the Zurich Opera House's performance described by the journal, high-definition *Christie Boxer 4K30* projectors were used.

In the interpretation of the Romeo and Juliette project (Fig. 5), the love theme sounds like a super-temporal model of the great human drama expressed by the theatre designer by means of high technologies.

The projections not only build separate pictures providing the whole space of the stage for actors by enhance emotional space of the performance. The

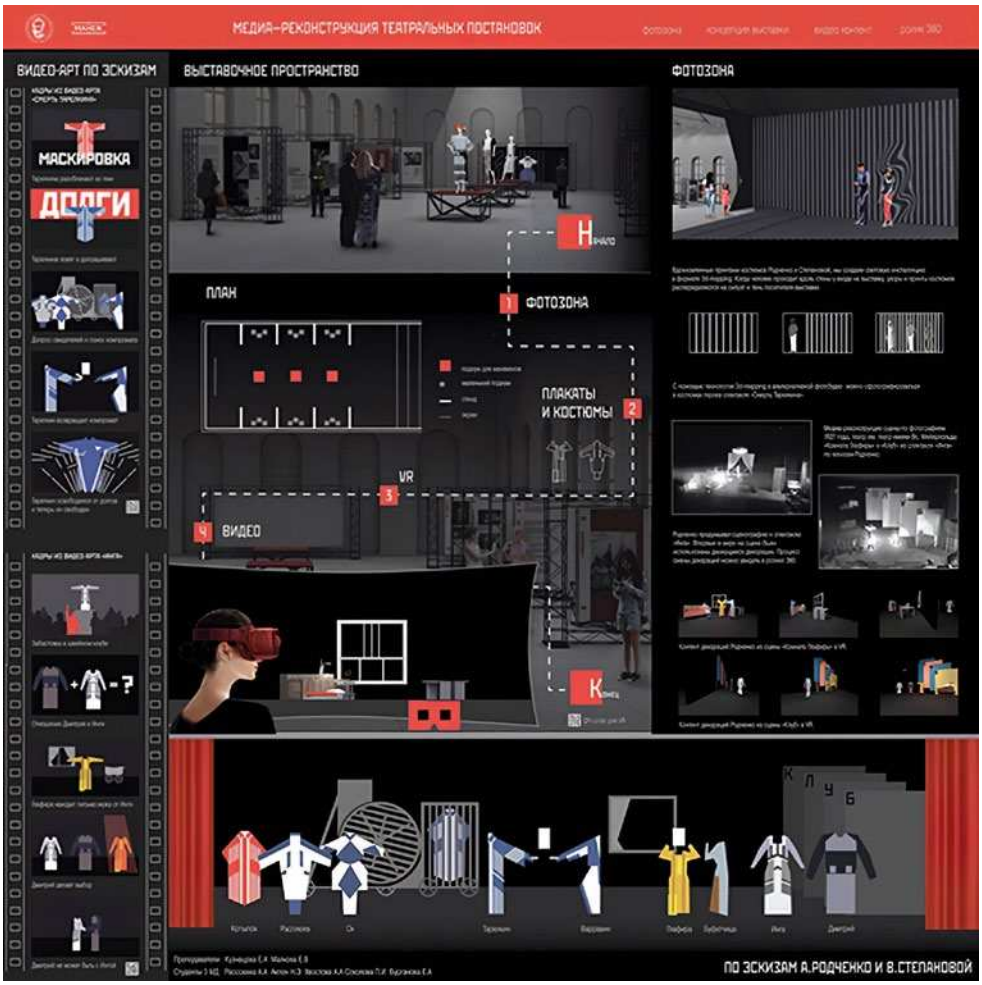

Fig. 6. Project of media reconstruction of costumes for Inga and The Death of Tarelkin based on sketches by Rodchenko and Stepanova (Design project, 3rd year of education, bachelor's programme. Authors: N.E. Akgyun, A.A. Rassokhina, E.I. Burganova P.A. Sokolova, A.A. Khvostova. Educators: senior lecturer E.A. Kuznetsova, E.V. Malkova, 2019)

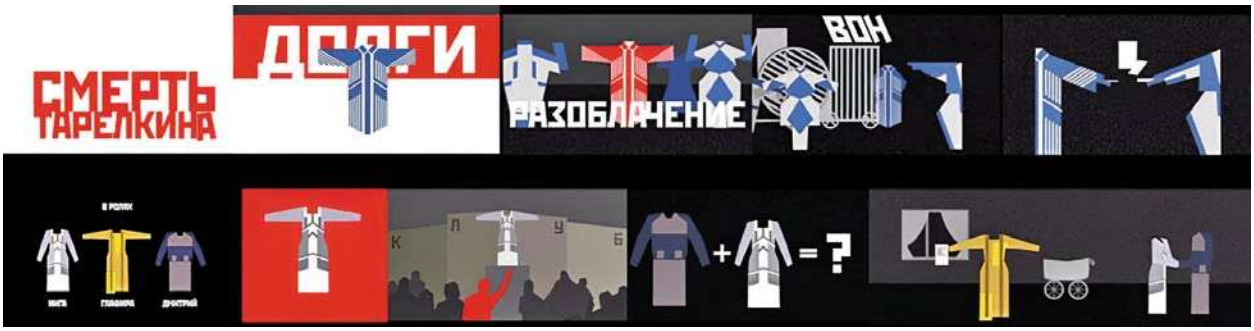

Fig. 7. Photo-script of the video reconstruction of plots for The Death of Tarelkin and Inga performances (Project of media reconstruction of costumes for Inga and The Death of Tarelkin based on sketches by Rodchenko and Stepanova design project, 3rd year of education, bachelor's programme. Authors: N.E. Akgyun, A.A. Rassokhina, E.I. Burganova P.A. Sokolova, A.A. Khvostova. Educators: senior lecturer E.A. Kuznetsova, E.V. Malkova, 2019)

magic of light illusions introduces the events of the Italian Renaissance time into the new value system formed by the era of mass media, the Internet and social media. Visualisation of the project is the mix of advertising materials of the performance taken from the website of the theatre. Such approach makes the nature of the work with the subject itself completely different. A new approach to scenography appears – through the lens of a screen, with a system of information provision, by means of infographics, etc.

3.3. Media Reconstruction of a Performance

The new Multimedia profile of the Environment Design sub-department has expanded the boundaries of innovations in stage space dismissive of traditional plastic form-making techniques. The format of an experiment tightly related to avant-garde art is constantly present in creative searches of the "Stroganovka" students in the 21st century. All of this was available for visitors of the AVANT-GARDE–THEATRE–FASHION2019 exhibition commemorating the 100th anniversary of constructivism which had been held in the Moscow Maly Manezh Exhibition Hall in October, 2019 (the project curator is the president of the Fashion Magic foundation N.B. Kozlova). The exhibition included archive materials from personal collections of the family of A. Rodchenko[1]: costume sketches for Inga and the Death of Tarelkin performances made by A. Rodchenko and V. Stepanova.

Looking for the ways of revolutionary renewal of theatre, the innovator directors of the early 20th century addressed futurist artists. Nowadays, the digital revolution has modified famous works by great designers of the past and presented them in a "filmed" multimedia format. The project reconstruction of the performance is made in the *video art* format. Brief content of the play is told by performance of "actors", the original thinking process of authors in the course of the drafting work is reproduced through the aesthetics of theatre costumes. The video sequence enters the wider space of media exhibition: with an interactive photo zone in the form of *3D mapping* textures from the scene of the performance (the prison bars on the stage stylised in elements of Tarelkin's costume); in the form of the hall with posters and mannequins in original theatrical costumes; with fragments of performance decorations in virtual reality (*VR*) in 360° format ("Artist's Dreams"), Figs. 6 and 7.

The format of media reconstruction has discovered the new method of work with theatrical subjects. The interactive script is based on versions of forms familiar from sketches of historical exhibits. A modern spectator who is rather distant from the intrigue our compatriots were concerned with in the 1920's gradually indulges in the environment of unfamiliar collisions by means of familiar technical devices. This technique allows people to accept and feel the unique tension of artistic passion which originated the great Constructivism era which has become the starting point of the world's design and still defines the creative search of the students of today's "Stroganovka" to a large extent.

[1] The original materials, namely the sketches of costume for Inga and Death of Tarelkin, were kindly procured by A. Rodchenko's grand-son, professor, Doctor of Art Studies, A.N. Lavrentiev, Pro-Rector for Research with S.G. Stroganov MGHPA.

4. DISCUSSION AND CONCLUSIONS

Light and digital technologies have become the basis for revolutionary changes in theatre since the late 20th century. The widest range of capabilities which came with the era of media art embodied in the search for new scenography forms sometimes strikes the principles of theatre replacing them with surrogate shows. K.S. Stanislavski said: "If theatre had been just an entertaining show, it would probably not have been worth making such efforts. But theatre is the art of reflecting life." [18].

Design training is becoming a field for experiments and development of new expressive means of scenography. Unlimited students' ideas find solutions of traditional subjects in inversive and sometimes paradox design solutions. Dramaturgical material itself leads a designer who sometimes does not even have special knowledge of theories and practices of scenography. "There are frequent cases when light, image, or performance are created either intuitively or contrary to all canons. That is where the paradox of art lies within… One can accidentally… direct a great performance not even being a director." [4].

In the wide area of technologies originated from the digital revolution, light design entered theatre scenography with confidence. The new model of theatre lighting forms its own concept, its system of visual values where actors and audience perceiving the performance remain the initial parameters stabilizing multimedia innovations on stage. A director's or theatre designer's vision takes the visual capabilities of new technologies into account from the beginning. Artists begin to think with light forms. The term *lighting thinking* is used to identify design using human as a starting point of a problem. Light is created around him and he is the centre of gravity [19].

The experience of scenography training as exemplified by the Environment Design sub-department of S.G. Stroganov MGHPA has shown that application of multimedia has been increasing in project methodology selection and has led the further deviation from property system of space arrangement. This is witnessed by scenography works created in the Environment Design sub-department over the recent years, which do not comprise volumetric-and-spatial modelling but save the genre uniqueness of performance. Natural background and design culture acquired during training are kept and developed thanks to comprehensive academic art training.

To a large extent, light designers are swift learners, and such specialty remains at the stage of establishment due to unilateralism of professional training methodology. Still dominant, canonical guild system of learning and sharing of experience from master to apprentice will be probably enriched by methods elaborated in the course of training of environment designers and multimedia. Use of new design techniques of *3D* visualisation, building of work models of images and scenes of a performance, creation of digital photo-scripts, etc. may become an important stage of work with dramatic art by theatre designers and light designers. Relevant design models will allow us to "play" the technological effects in advance and to determine their necessity and possibility to be embodied cost-effectively.

REFERENCES

1. URL: https://www.krugosvet.ru/enc/kultura_i_obrazovanie/teatr_i_kino/SVET_TEATRALNI.hml (date of reference: 01.08.2019).

2. Social and Psycological Problems of Scientific and Technological Progress [Sotsyalno-psikhologicheskiye problemy nauchno-tekhnicheskogo progressa] / Eds. B.D. Parygin. Leningrad: Nauka, 1982, 169 p.

3. Bayer P., Waller M. The Art of René Lalique// London: Eagle, 2002,186 p.

4. Melnik, A.V. Theatrical and Concert Lighting. Performance Video [Teatralno-knotsertnoye postanovochnoye osveshcheniye. Postanovochnoye video]. (2018 edition). URL: https://lightsoundnews.ru/a-melnik-teatralno-kontsertnoe-postanovochnoe-osveshhenie-osnovy-postanovochnogo-video/ (date of reference: 01.08.2019).

5. Cuttle C. Towards the third stage of the lighting profession// Lighting Research and Technology, March 2010, Vol. 42, #1, pp.73–93. DOI: 10.1177/1477153509104013.

6. Zakharov, M. Light is Ideology. On Scenography and Oleg Sheyntsis [Svet – eto mirovozzreniye. O Stsenografii i Olege Sheyntsise]. URL: http://www.l-teatr.ru/directors/oleg-sheyntsis/47/ (date of reference: 01.08.2019).

7. URL: https://antrio.ru/iogann-fridrih-shiller-citaty/ (date of reference: 01.08.2019).

8. Beryozkin, V. Aleksandr Borovsky. Theatre Matters [Aleksandr Borovsky. Voprosy teatra] / PROSCAENIUM. Moscow, 2010, pp. 69–92.

9. Music Becomes Visible in Zurich Opera House [V Tsyurikhskom opernom teatre muzyka stanovitsya zrimoy]. Light. Sound. News. 2018, Vol. 3, #56, pp. 24–25.

10. Kanatenko, M.A., Mikhailov, O.M. The Light Engineering Discipline in State Universities and Educational Standard [Distsyplina "Svetotekhnika" v gosudarstvennykh universitetakh i obrazovatelnom standarte]. Saint Petersburg. URL: http://lightonline.ru/svet/articles/discipline_svetotehnika_v_obrazovanii.html (date of reference: 01.08.2019).

11. URL: http://ptj.spb.ru/archive/29/face-to-face-29/svet-eto-dyxanie-sceny/ (date of reference: 01.08.2019).

12. Mikhailova, A. Borovsky in Opera [Borovskiy v opere], 2007. URL: http://timetable.theatre.ru/theatre-653/perf-22866/ (date of reference: 01.08.2019).

13. Fraser N. The light fantastic. The Lessons of Stage Lighting. Part 1. Introduction. URL: sistema-stage.ru / brand_news/neil-fraser-light-lessons-01 (date of reference: 01.08.2019).

14. URL: https://www.subjectart.ru/universities/parsons_school_of_design/ (date of reference: 01.08.2019).

15. Stanislavski, K.S. An Actor Prepares [Rabota aktyora nad soboy]. URL: https://www.psyoffice.ru/9/stank01/txt17.html (date of reference: 01.08.2019).

16. Kuznetsova, G.N. Principles of Interaction of Structural Form-making and Visual Ecology in Environment Design [Printsipy vzaimodeystviya strukturnogo formoobrazovaniya i vizualnoy ekologii v sredovom dizaine] / Abstract of thesis of Candidate of Art Studies. Moscow: 2011[2].

17. Yung, I.S. Implementation of the Method of Script Modelling of Urban Public Environment: Problems of Theory and History of Ukrainian Architecture [Realizatsiya metoda stsenarnogo modelirovaniya gorodskogo prostranstva: Problemy teorii i istorii arkhitektury Ukrainy], 2013, # 13, pp. 241–247.

18. URL: https://www.kritika24.ru/page.php?id=43880 (date of reference: 01.08.2019).

19. Skarlatou A.-Z. Light Effects in the Design Process. Bartlett Faculty of the Built Environment, University College London, in candidacy for the Degree of Doctorate of Philosophy, Department of Architecture. London July 2010, 270. URL: http://discovery.ucl.ac.uk/1211391/1/1211391.pdf (date of reference 01.08.2019).

[2] The method of script modelling is detailed in the article "Concept of Script Modelling", see collection: "Theoretical and Methodological Problems of Artistic Constructing of Complex Objects" [Teoreticheskiye i metodicheskiye problemy khudozhestvennogo konstruirovaniya kompleksnykh obyektov]. Moscow, 1979. (Transactions of VNIITE. Ser. Technical Aesthetics: issue 22, pp. 137–148.)

Elena A. Zaeva-Burdonskaya,
Prof., Ph.D. of Arts. In 1987, she graduated from Moscow Higher College of Art and Industry (former Stroganov College). At present, she is an Acting Head of the Environment Design sub-department of S.G. Stroganov MGHPA, Member of the Designers Union and the Artists Union of Russia, and Winner of the Moscow Award

***Yuri Vladimirovich Nazarov*,**
Prof., Dr. of Arts. In 1972, he graduated from Moscow Higher College of Art and Industry (former Stroganov College). At present, he is a Rector of the National Design Institute, Corresponding member of the Russian Academy of Arts. Honorary President of the Union of Designers of Russia

Light & Engineering
Vol. 28, No. 2, pp. 28–37, 2020

https://doi.org/10.33383/2019–052
Svetotekhnika #6, 2019, pp.58–66

USER LIGHTING PREFERENCES BASED ON NAVIGATION AND SPACE QUALITY IN VIRTUAL EXHIBITION ENVIRONMENTS

Aslıhan Çevik[1], Tuğçe Kazanasmaz, and Hasan Engin Duran

Izmir Institute of Technology, Turkey
[1]Email: aslihancevik@iyte.edu.tr

ABSTRACT

Just as any other interior environment, lighting of exhibition spaces must be examined to enhance its visual quality and comfort. In this study, user behaviour, perception and impressions are analyzed for more comprehensive understanding by including subjective reasoning. Due to the chaotic progress and contradictory choices in exhibition lighting, daylight is mostly avoided while the role of users and relation between quantitative and qualitative parameters are often neglected. A series of sample exhibition spaces illuminated either artificially or by daylight are modelled virtually in Lumion software to be evaluated in a three-step questionnaire. A total of 90 participants are selected from three different professions (architects, visitors, artists), their reaction like movement, preference and impressions are gathered via questionnaire while moving through the model. The study aims to find out the role of lighting type in exhibition navigation and its relation with non-lighting parameters using statistical analysis methods. Results show that natural light is preferred more in sculpture exhibition while artificial light is preferred in painting exhibition. Movement towards daylight increases in transition areas and towards the end of the exhibition. A significant difference in navigation choices are found between professions, architects preferred to move towards more natural light while artists preferred artificial light.

Keywords: museum and gallery lighting, exhibition, navigation, artificial light, daylight

1. INTRODUCTION

Exhibiting is possible with light. A complex combination of various quantitative and qualitative aspects should be regarded in lighting design for exhibition spaces. Lighting choices heavily influence the whole experience by altering display quality, atmosphere and the perception of displayed objects. Space and object characteristics also have an impact on lighting strategy and perception [1]. This makes every exhibition lighting design a unique work. In addition, importance of lighting factors changes in each work. Due to the uniqueness, a chaotic approach is commonly acknowledged among many galleries and museums' staff [2]. Although, fundamental choices of this approach can be traced by understanding lighting choices of the staff and their relation between mentioned aspects like exhibition type and light source.

Exhibiting is a collaborative process though priorities and intentions of lighting choices may change between different professions. For conservation-based jobs, preservation is the primary concern while indoor space quality is for architects and artistic expression is for the artists [2, 3]. A consensus has to be made to balance these concerns among different professions by following guidelines and principles. Although there are some guidelines, lighting designers or curators set their own principles and style over time by using trial and error method in practice [4,5]. This causes miscommunication which is considered as an impairing problem among associated professions. Even the target, visitor's perception and expectations are also ignored which

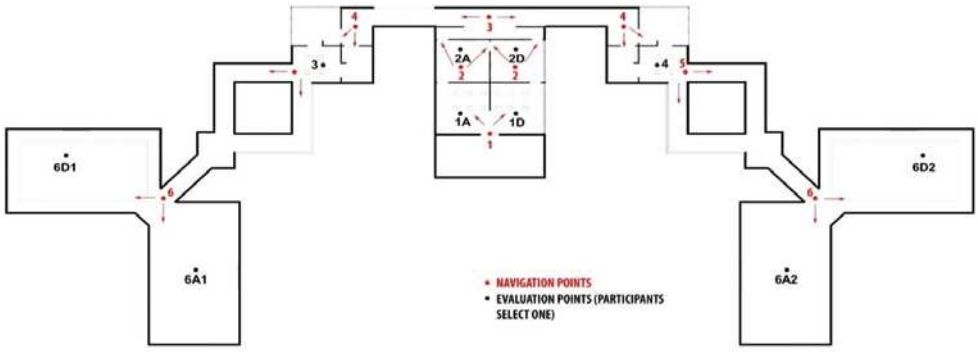

Fig.1. Plan of the exhibition space

can be useful to design more interactive and relatable lighting design. Additionally, the amount of undocumented knowledge increases which are needed for the understanding and the development of lighting design in exhibition [2].

Daylight is another ongoing controversial topic. Daylight is avoided, mainly because of preservation concerns such as amount of UV radiation. While the degree of deteriorating effects may vary with the material type, sunlight damages material regardless. As for visual comfort and quality, direct daylight and glare are not approved in any condition. Daylight controlling is considered as too much work and risk due to its dynamic behaviour and amount [6, 7]. On the other hand, avoidance of daylight in exhibition areas isn't a negligible matter since improvements in energy efficiency are expected regardless of building type. Despite the negative and unresponsive attitude in the field, there are many studies on the advantages of daylight in terms of visual quality, visitor satisfaction and sustainability with various proposals of design solutions [8]. Besides, the form of exhibition space and every exhibition type reacts with light differently and strengths of daylight must be detected under different conditions.

Psychological effect of light is needed to be examined especially in exhibition navigation. Illuminated area attracts attention and people tend to move towards it [9]. Most of the time, visitors determine a single direction route to tour exhibition area effectively though light can be used to monitor movement impulsively. Although there is no comprehensive research about it, studies about retail lighting can be referenced [10]. Similar to retail lighting, exhibitions have focus and relief points in order to not exhaust visitors with constant attention. Therefore, lighting shouldn't be monotonous and constantly dense. Dividing exhibition into parts with transition areas like foyers, corridors and circulation areas which lit differently is a common way to achieve it [1, 8]. Daylight can be useful to break the maze effect and to guide the visitor. Characteristics of daylight, visual connection to surroundings and revelation of form can create the in-and-out dynamism [11]. Relation between different light zones should be planned carefully. Mainly focusing on the mentioned aspects above, the aim of this study is to understand lighting choices in exhibitions from multiple points of views. The impact of lighting type and many other exhibition parameters like space and type on user preference are examined.

2. METHOD

2.1. Virtual Model

A series of virtual exhibition rooms are needed to figure out effecting conditions in participant's lighting preference by their orientation in exhibition. A model was prepared in ArchiCAD software (Fig. 1). Exhibition spaces were planned to generate 6 steps of exhibition types (evaluation points in black: 1A, 1D, 2A, 2D, 3, 4, 6A, 6D) and transition zones. Transition areas like corridors were used to locate navigation points (in red: 1, 2, 3, 4, 5, 6), where participants choose one room to continue with. Except the type of the light source, identical exhibition spaces were placed next to each other as a choice to see distinctive results in each step.

After designing process, the model was imported into real-time visualization software Lumion 6.0 to navigate through the model. Sculptures and paintings were added into the model also in this process. Spotlights were mounted to illuminate determined areas (labelled with "A") artificially while clear sunlight was adjusted in daylight areas (labelled with "D"). In exhibition space 6D, ceiling material was illuminated to generate skylight effect. All spot-

Table 1. Classification of the Evaluated Rooms

Exhibition Spaces	Space Dimensions	Exhibition Type	Light Source
1A	Medium	Sculpture	Artificial
1D			Daylight
2A		Painting	Artificial
2D			Daylight
3	Small	Sculpture	Both
4			
6A	Large	Both	Artificial
6D			Daylight

lights had the same colour temperature, brightness and beam angle (Table 1, Fig.2).

2.2. Questionnaire

A three-step questionnaire was prepared. In the first step, participants are navigated regarding which way they would like to continue (Fig.3). On these 6 navigation points, they are asked to move towards either day or artificially lit of the same exhibition area by stating their choice as "right" or "left". After that, the questionnaire data was entered as choices 1 and 2 for artificial and natural light respectively.

In the second step, participants select their favourite exhibition space and answer Likert scale questions based on 11 criteria for this area, giving values between 1 and 5 (Fig. 4). In the first Likert-scale question, recognition of light source is asked to see the visual fidelity of the Lumion software. In the questions between 2 and 9, participants are asked to evaluate both displaying and the space of the exhibition. Since human perception is deceiving when evaluating colour temperature [6], question 10 was put deliberately to find a relation between room and light parameters on colour temperature perception. Question 11 is put to measure the level of preference of evaluated spaces. In the final step, participants asked to pick 3 important questions to assess lighting from the second step (questions 1–11).

A total of 90 people around Izmir participated in the questionnaire. Three main occupation groups were determined as participants: 30 architects (including architecture students), 30 artists (sculptors, painters and curators) and 30 visitors (other occupations). Participants were divided into these groups to understand priorities and reasoning in lighting preference in each group. Since the progress of questionnaire is highly individual and interactive due to the choices and controlling of the virtual environment; participants joined the questionnaire one-by-one. Questionnaire has been done within 3-month period; lighting conditions of the questionnaire environment are included as variables along with personal information and possible visual im-

Fig.2. Evaluated Exhibition's Spaces

Fig. 3. A view from navigation points

Navigation Points		1	2	3	4	5	6
RIGHT		□	□	□	□	□	□
LEFT		□	□	□	□	□	□
Selected Exhibition Area: ____		1	2	3	4	5	
Lighting Type	1-natural	□	□	□	□	□	artificial
Displaying of the pieces	2-desegregated	□	□	□	□	□	integrated
Quality of the space	3-distinct	□	□	□	□	□	vague
	4-dim	□	□	□	□	□	bright
	5-dull	□	□	□	□	□	catchy
	6-tense	□	□	□	□	□	relax
	7-harsh	□	□	□	□	□	soft
	8-discomfort	□	□	□	□	□	comfort
	9-imbalanced	□	□	□	□	□	uniform
10-How pleasant is colour temperature? (circle the option)		Too warm □	Warm □	Fine □	Cold □	Too Cold □	
11- Overall visual quality of the space?		Very Bad □	Bad □	Fine □	Good □	Very Good □	

Fig.4. Questionnaire step 1 and 2

pairments. 59 women and 31 men participated while 33 % of them are between the ages 17–25, 37 % are between the ages 26–35 and 30 % are between the ages 36 and 75.

2.3. Statistical Analysis

OLS (ordinary least square), ANOVA, T-test and linear regression methods are used to analyze the gathered data (Fig.5). For the first part of the questionnaire, ANOVA is used to find whether there is a meaningful relation between light source type and navigation choices. In the following, the choices of the three occupation groups are analyzed separately.

The second part of the questionnaire is analyzed in two different methods and their results are compared. For T-test, five pairs are formed to simplify the differences of these spaces as one. OLS method is used to figure out the relevance of determined criteria in different exhibition conditions. Each criterion's relevance is analyzed in evaluated rooms (Table 1) excluding the results of exhibition spaces of 3 and 4 in order to use OLS method correctly. The relevance of each criterion is analyzed in dual comparisons of the rooms via T-test. Similar results in other analyses are mentioned in Discussion and Conclusion section.

Table 2. Means and Standard Deviations of Each Step in Exhibition Spaces and ANOVA Result (P-value)

Steps	1		2		3		4		5		6		ANOVA
Choices	M	S	M	S	M	S	M	S	M	S	M	S	P-Value
All groups	1.49	0.50	1.44	0.50	1.64	0.48	1.56	0.50	1.70	0.46	1.57	0.50	0.005*
Architects	1.50	0.51	1.43	0.50	1.67	0.48	1.67	0.48	1.73	0.45	1.57	0.50	0.15
Visitors	1.57	0.50	1.50	0.51	1.70	0.47	1.53	0.51	1.77	0.43	1.57	0.50	0.238
Artists	1.40	0.50	1.40	0.50	1.57	0.50	1.47	0.51	1.60	0.50	1.57	0.50	0.448

3. RESULTS

3.1. Navigation

Difference in navigation choices are observed in each step (Table 2 and Fig. 4). In Fig. 4, four means (all groups, architects, visitors, artists) of navigation choices are shown vertically. Movement towards daylight in means increase upwards while movement towards artificial light increases downwards. In Table 2, if mean value is closer to 1, artificial light tendency is more while from number 1.5 towards 2, natural light tendency increases. Participants preferred to move towards artificial light with 51 %, 56 %, 36 %, 44 %, 30 %, and 43 % respectively in 6 steps. In analysis of variance for all participants, there is a significant difference of light choices in each navigation point (p=0,005). When it's analyzed separately, occupation groups tend to prefer a single lighting type. Except point 2, architects preferred day lit areas. Visitors moved towards daylight in all points. On the contrary, artists moved towards artificial light except point 6 while movement towards daylight in transition areas is also lower in this group.

Although there are differences in preferring light source in exhibitions rooms (steps 1, 2, 4 and 6), participants distinctively preferred daylight in transition areas (3 and 5). Results indicate that, participants are almost divided into half in first steps.

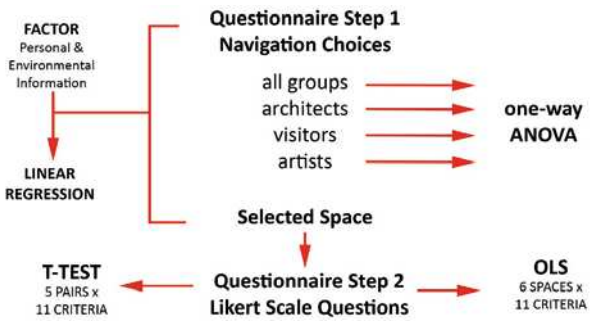

Fig.5. Statistical analysis diagram

Non-lighting factors like space and display positioning should be noted. Additionally, some participants stated that they kept certain orientation (right or left) when touring exhibitions to see everything. Regardless of all these, the tendency to move towards daylight increases when approaching the end of the exhibition. This can be interpreted as the fatigue by focusing exhibited objects or the different opening type in 6D space. Artificial light is mostly used to abstract the space around the displayed object to attract the visitor which consumes the visitor's focus after a while [1,12]. Focusing has to be relieved to keep the attention. When the orientation is examined room by room, results show noticeable differences in exhibition types (Table 2). Participants tend to move towards artificially lit room more when the pieces are paintings rather than sculpture (steps 1 and 2).

3.2. Selected Spaces, Significant Factors and Importance of Questions

Results show that, participant's most selected space is 6D with 29 %, other spaces are shown in Table 1. The main difference of this space from other spaces is that the opening type which is skylight. The second most selected place is 2D which is again another day lit space. This contradicts the relations between daylight – sculpture and artificial light – painting in other results. On the other hand, selection alone isn't enough to understand preference, catchiness must be eliminated. To integrate "selection" and level of "preference", selection percentages are compared with the ratings to questions 11 (Table 4). Even though, its selection percentage is 11 %, 6A is the highest rated space (Fig.7).

Linear regression model is applied to understand the impact of all variables in all selection-based answers like navigation. Personal information and environmental variables are entered as numbers for factors. For example, three age groups are deter-

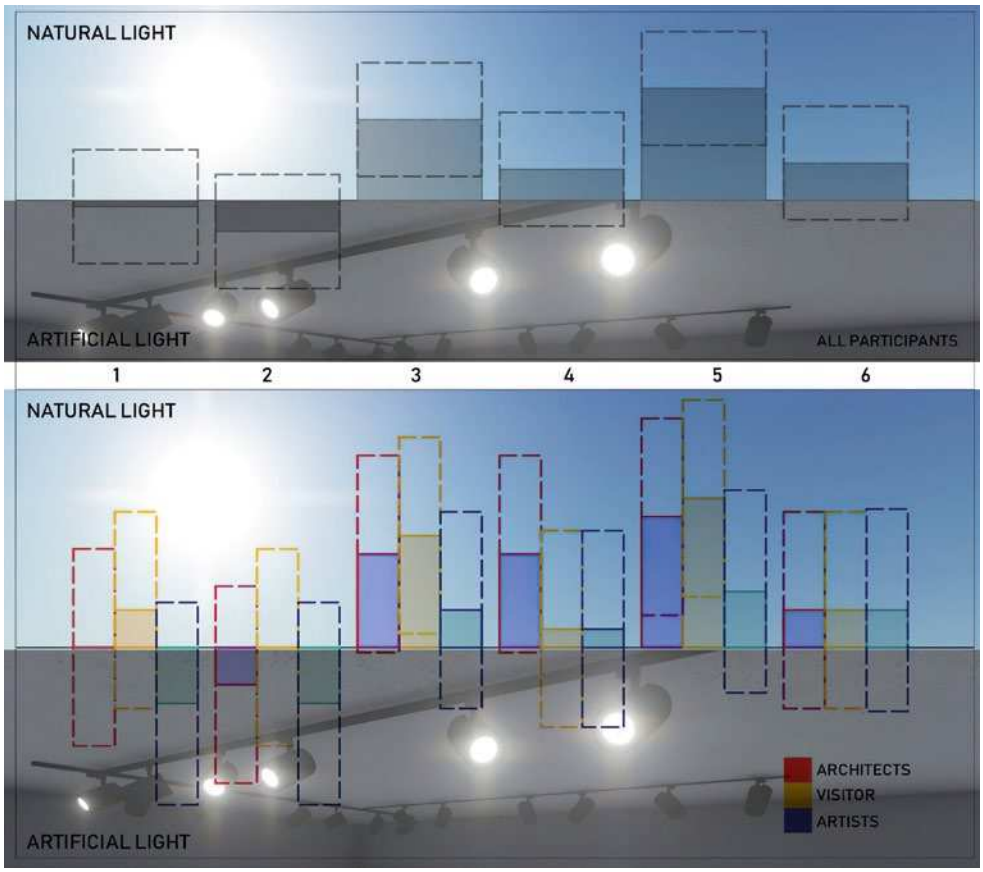

Fig.6. Lighting preference in each navigation point

mined and labelled as 1, 2 and 3. Results show that, age is a determining factor in the first navigation choice, moving towards either 1A or 2A. On the second and third navigation choices, gender is important. As needed, environmental or visual factors don't have significant impact on choices.

At the end of the questionnaire, participants are asked to pick three important criteria/questions to understand their awareness on the role and impact of lighting. As the most important criterion in lighting, the light source type (artificial/natural) (1) was picked 47 times while brightness (4) and colour temperature (10) are picked 35 and 36 times respectively. Relaxing (6), visual quality (11), uniformity (9) and comfort (8) are picked 26, 28, 24 and 20 times respectively. The least picked criteria are listed as integration (2) with 15 times, vagueness (3) with 10 times, catchiness (5) with 14 times and softness (7) with 15 times.

3.3. Dual Comparisons of the Spaces (T-test)

To understand and detect the impact of the space and exhibition factors, dual comparisons are made by using T-test. For analysis, five paired spaces are determined with the responses given to 11 different criteria. These spaces are paired deliberately to have single difference such as light source type or exhibition type, while rest of them stayed identical. Significance values in the Table 3 are analyzed with the mean values in Table 4. For the change in light source, 1A-1D, 2A-2D, 6A and 6D pairs are made while 1A-2A and 1D-2D pairs are made for the change in exhibition type.

In pair 1A-1D, same sculptures are exhibited. In the T-test, four questions showed significant results. In question 1, software's visual fidelity is tested to be successful as the distinction of light source is easily addressed by the participants with significance value of 0.0013. As for the harsh-

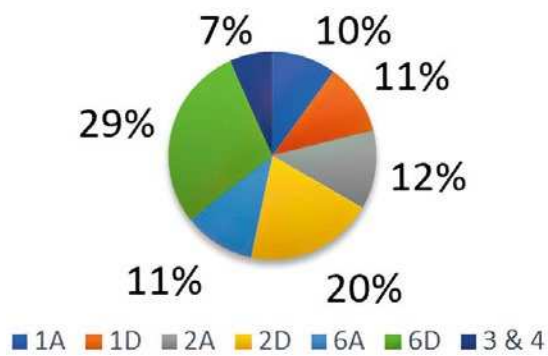

Fig.7. Percentage of Selected Space

Table 3. T-test Results for Pair of Spaces

SPACE PAIRS / CRITERIA	1	2	3	4	5
	1A-1D	2A-2D	1A-2A	1D-2D	6A-6D
1 – Natural / Artificial	0.0013	0.0001	0.1872	0.1375	0.0001
2 – Desegregated / Integrated	0.4841	0.0155	0.2378	**0.0888**	0.0020
3 – Vague / Distinct	0.1518	0.0489	0.4079	0.3305	0.4648
4 – Dim/ Bright	0.4445	0.0925	0.2672	**0.0492**	0.4738
5 – Dull / Catchy	0.3676	0.3484	0.3169	0.3551	0.2660
6 – Tense / Relax	0.1194	0.2781	**0.0170**	0.0391	0.1062
7 – Harsh/ Soft	0.0142	0.4580	0.0019	0.1904	0.3102
8 – Discomfort / Comfort	0.0426	0.3078	0.0040	0.0806	0.1885
9 – Imbalanced / Uniform	0.3488	0.3432	0.0865	0.2246	0.2079
10 – Color of Light	0.1136	0.0555	0.2930	0.3115	0.4907
11 – Visual Quality	0.0398	0.4055	**0.0531**	0.2836	0.1491

ness-softness scale in question 7, day lit exhibition is significantly found softer (p=0.0142). Spotlights create coarser shadows when compared to daylight on 3D objects. Linked to the question 7, day lit exhibition is found visually more comfortable (p=0.0426). Less contrast and soft shadows are perceived more comfortable as found in many other studies. Lastly, day lit sculpture exhibition is rated 0.7 point higher in terms of visual quality, preference (p=0.0398).

Same painting exhibition with different light sources are examined in pair 2A-2D. Five questions show significant results in the T-test. Just like in pair 1, participants addressed the light source successfully (p=0.0001). Artificially lit painting space is perceived more integrated (p= 0.0155). Balanced contrast areas are achieved with spotlights. Equally highlighting paintings abstracts the rest of the space which is perceived as a visual rhythm. Supporting the results of question 3, artificially lit painting space is found more distinct which again can be explained as the spotlights create more focusing points (p=0.0489). Despite of the similar illuminance levels with pair 1, day lit painting space is perceived brighter in pair 2 (p=0.0925). Lastly, artificially lit space is found significantly colder in terms of light colour (p=0.0555).

In the third pairing, sculpture exhibition 1A and painting exhibition 2A which are both illuminated by artificial lighting are compared. Five questions show significant results. The meaningful difference on light source type is not found since both spaces have the same lighting type. Painting exhibition is perceived 1.20 point more relaxing compared to sculpture exhibition (p=0.0170). Same significant difference is found in the comparison (1D and 2D) of same spaces in daylight. Regardless of light type, proportion of exhibited object in a space is the determining factor for this criterion. Paralleling to this, painting exhibition is found softer (p=0.0019) and visually more comfortable (p=0.0040). Shadows in artificially illuminated sculpture exhibition is coarser compared to same day lit space or painting exhibition, just like in the pair 1A and 1D. Additionally, painting exhibition is perceived more balanced (p=0.0865). In these four criteria, painting exhibition is rated "positive" and lastly higher in visual quality (p=0.0531).

In the fourth pairing, sculpture exhibition 1D and painting exhibition 2D which are both illuminated by daylight are compared. Sculpture exhibition is found more integrated (p=0.0888). Different from painting exhibition, shadows in sculpture exhibition form a composition. In question 4, painting exhibition is perceived brighter despite having the same illuminance level (p=0.0492). Painting exhibition enables light to radiate more with less shadow. Related to this, painting exhibition is found

Table 4. Mean and Standard Deviation Values for Spaces of Each Between 1–5 Criterions

SPACES /CRITERIA		1A	1D	2A	2D	3&4	6A	6D
1 –Natural / Artificial	Mean	4.00	1.90	3.45	1.44	2.50	4.10	2.19
	Std. Dev.	1.41	1.10	1.21	0.86	0.84	1.10	1.23
2 –Desegregated / Integrated	Mean	3.78	3.80	4.18	3.22	3.67	4.60	3.46
	Std. Dev.	1.39	0.92	0.98	1.26	1.03	0.70	1.50
3 –Vague / Distinct	Mean	4.67	4.30	4.73	4.11	3.50	4.00	4.04
	Std. Dev.	0.50	0.95	0.65	1.28	1.05	1.15	1.15
4 – Dim/ Bright	Mean	3.67	3.60	3.91	4.33	3.67	3.60	3.58
	Std. Dev.	0.87	1.17	0.83	0.77	1.21	0.84	1.14
5 –Dull / Catchy	Mean	3.56	3.70	3.73	3.83	4.00	4.10	3.85
	Std. Dev.	0.88	0.95	0.65	0.79	0.89	0.99	1.26
6 – Tense / Relax	Mean	2.78	3.50	4.09	4.33	3.00	2.80	2.23
	Std. Dev.	1.30	1.27	1.22	0.69	1.67	1.14	1.31
7 – Harsh/ Soft	Mean	2.11	3.40	3.82	3.78	3.33	2.90	3.08
	Std. Dev.	1.17	1.17	1.08	0.81	1.03	0.74	1.35
8 –Discomfort / Comfort	Mean	3.44	4.20	4.55	4.67	3.17	4.20	3.77
	Std. Dev.	0.88	0.92	0.69	0.49	1.33	1.32	1.14
9 –Imbalanced / Uniform	Mean	3.78	4.00	4.45	4.33	3.17	4.10	3.69
	Std. Dev.	1.20	1.25	0.82	0.69	1.17	1.37	1.12
10 – Colour of Light	Mean	3.22	2.70	3.00	2.56	2.83	3.30	3.31
	Std. Dev.	0.97	0.82	0.77	0.51	0.75	0.95	0.62
11 – Visual Quality	Mean	3.33	4.10	4.00	3.94	3.33	4.20	3.81
	Std. Dev.	1.00	0.74	0.63	0.54	0.82	1.03	0.80

more relaxing (p=0.0391) and visually comfortable (p=0.0806).

Finally, identical exhibition spaces 6A and 6D which have different light source are compared. In question 1, visual accuracy of the software is again found successful since the light types are different (p=0.0001). Artificially illuminated space is perceived more integrated (p=0.0020). It can be interpreted with the rhythm formed by focal lighting and the shadows.

3.4. Analysis of Impressions on Spaces (OLS)

Apart from T-test, the relation of exhibition space parameters and criteria/questions are analyzed with OLS (Table 5). Third criterion, vague-distinct, is found significant in artificially illuminated spaces 1A and 2A. In exhibition space 6A, this criterion isn't significant because both exhibition types are included and the space gets bigger. Painting exhibitions 2A and 2D are found significantly relaxing when compared to other spaces. Day lit 2D space is found even more relaxing. There is a significant relation between harshness criteria and exhibition space 1A since the space is both artificially illuminated and sculptures are exhibited which cause coarser shadows. Same criteria are found equally significant in painting exhibition illuminated by both artificial light and daylight (2A and 2D). Except the spaces 1A and 6D, comfort criteria are found relative in all spaces. Paralleling with the relaxing criteria, painting exhibitions 2A and 2D are perceived visually comforting. Daylight is perceived more comforting in sculpture exhibition significantly while in other exhibition spaces too. Uniformity criterion is found significant in painting exhibitions. Artificial light is found more balanced due to focal lighting. Lastly, 6A is significantly rat-

Table 5. OLS Results Showing Significant Dependence between Exhibition Space and Criteria

	1A	1D	2A	2D	6A	6D
2 – Desegregated / Integrated	0.865	0.835	0.413	0.446	0.146	0.714
3 – Vague / Distinct	0.039	0.146	0.025	0.223	0.362	0.263
4 – Dim/ Bright	1.000	0.897	0.631	0.157	0.897	0.842
5 – Dull / Catchy	0.397	0.559	0.589	0.722	0.845	0.732
6 – Tense / Relax	0.726	0.421	0.077	0.021	0.747	0.160
7 – Harsh/ Soft	0.040	0.908	0.391	0.398	0.345	0.611
8 – Discomfort / Comfort	0.592	0.044	0.007	0.002	0.044	0.177
9 – Imbalanced / Uniform	0.283	0.136	0.020	0.024	0.096	0.283
10 – Color of Light	0.317	0.725	0.655	0.424	0.221	0.157
11 – Visual Quality	1.000	0.061	0.097	0.101	0.035	0.184

ed the highest. Following, daylight in sculpture exhibition and artificial light in painting exhibition are significantly found successful.

4. DISCUSSION AND CONCLUSION

In this study, a questionnaire is applied to understand the relation between space, exhibition and user parameters in exhibition lighting. Virtual model is used to find out the effect of light type in navigation. Since exhibiting involves multiple disciplines, participants are selected equally from architects, visitors and artists to see difference in preference. Answers to the questionnaire are analyzed with multiple methods. Similar results are found from different methods.

In navigation, daylight is preferred in transition zones. Similarly, tendency to move towards daylight increases when approaching to the end of exhibition. There are different navigation choices in occupation groups. Architects preferred more daylight while artists preferred artificial light. Day lit exhibition space 6D is the most selected space while 6A is found visually more successful both in T-test and OLS methods. The relation between "preference", "visual quality" and "catchiness" can be examined in the further studies. Additionally, the most important lighting criteria when evaluate lighting is determined as light source by the participants.

Similar results are found in the second step of the questionnaire with the methods T-test and OLS. Firstly, Lumion software is found successful in visual accuracy in every condition. Daylight is perceived softer in T-test, visually more comfortable in both methods. Artificial light is evaluated over spotlights. Since spotlights are usually focused, the composition of bright and dim areas is perceived significantly integrated and balanced. Sculpture exhibition is found more integrated and better. Another difference in exhibition types is the usage of space and the amount of shadows. In both methods, painting exhibition is perceived relaxing, bright, soft and visually comfortable due to less space usage and less shadows. Apart from exhibition and space parameters, a relation is found between visual comfort and uniformity criteria.

REFERENCES

1. Cuttle, C. Light for Art's Sake Lighting for Artworks and Museum Displays (1st ed.). Oxford: Butterworth-Heinemann, 2007.

2. Garside, D., Curran, K., Korenberg, C., MacDonald, L., Teunissen, K., & Robson, S. How is museum lighting selected? An insight into current practice in UK museums// Journal of the Institute of Conservation, 2017, Vol.40, #1, pp.3–14.

3. Ajmat, R., Sandoval, J., Arana Sema, F., O'Donell, B., Gor, S., & Alonso, H. Lighting design in museums: Exhibition vs. preservation// WIT Transactions on the Built Environment, 2011, # 118, pp. 195–206.

4. Druzik, J. R., & Eshoj, B. Museum lighting: its past and future development. Museum Microclimates, 2007, pp. 51–56.

5. Kesner, C.W. Analysis of the museum lighting environment// Journal of Interior Design, 1997, Vol. 23, #2, pp. 28–41.

6. Thomson, G. The Museum Environment. Butterworths-Heinemann (2nd ed.). London, 1986.

7. Cannon-Brookes, S. Daylighting galleries: performance criteria// Lighting Research and Technology, 2000, Vol.32, #3, pp. 161–168.

8. Kim, C. S., & Chung, S.J. Daylighting simulation as an architectural design process in museums installed with top-lights// Building and Environment, 2011, Vol.46, #1, pp. 210–222.

9. Blake, S., Hall, J., & Sissel, S. Using Lighting to Enhance Wayfinding, 2010.

10. Şener Yılmaz, F. (2018). Human factors in retail lighting design: an experimental subjective evaluation for sales areas//Architectural Science Review, 2010, Vol.61, #3, pp.156–170.

11. Fördergemeinschaft Gutes Licht. Good Lighting for Museums, Galleries and Exhibitions// In Information on Lighting Applications, Frankfurt: Fördergemeinschaft Gutes Licht, 2007, p.48.

12. Haans, A. The Natural Preference in People's Appraisal of Light// Journal of Environmental Psychology, 2014, #39, pp. 51–61.

Aslıhan Çevik,
Res. Asst. She is currently working on her master thesis in İzmir Institute of Technology. She holds Architecture undergraduate degree from Yeditepe University. Her research topics are architectural lighting, and building physics; at present, she is a Research Assistant in İzmir Institute of Technology, Turkey

Tuğçe Kazanasmaz,
Prof. Dr., held a Doctor of Philosophy in Building Science from Middle East Technical University (METU). She has 19 years academic experience in architectural lighting, building physics and energy efficient design. At present, she is a Professor in the Department of Architecture in İzmir Institute of Technology, Turkey

Hasan Engin Duran, Assoc. Prof. Dr., held a Doctor of Philosophy in Economics from University of Venice. He has 14 years academic experience in regional growth, development, convergence and income inequalities, statistical analysis and research methods. At present, he is an Associate Professor in the Department of City and Regional Planning Department in İzmir Institute of Technology, Turkey

Light & Engineering
Vol. 28, No. 2, pp. 38–46, 2020

https://doi.org/10.33383/2019–054
Svetotekhnika #6, 2019, pp. 45–51

THE STATE OF MUSEUM LIGHTING IN RUSSIA[1]

Alexandra A. Bartseva[1], George V. Boos[2], Anatoly Sh. Chernyak[1], Alyona B. Kuznetsova[1], and Eugene I. Rozovsky[1]

[1] VNISI LLC, Moscow
[2]NIU MPEI, Moscow
E-mail: bartseva@vnisi.ru

ABSTRACT

The article contains the results of analysis of answers of 90 museums of the Russian Federation to questions regarding lighting of these museums as well as the results of inspection and measurement of lighting parameters (average exhibit illuminance, correlated colour temperature, colour rendering index, and luminance distribution) conducted in 7 museums and 1 conservation centre. It is found that museum lighting in the Russian Federation generally complies with the applicable requirements and recommendations and requires fundamental changes only in few cases. Many museums already use light emitting diodes (LEDs) as light sources and are ready to cross over to LED lighting completely. In the meantime, museums (primarily small ones) consider lack of regulations in the sphere of museum lighting one of the major problems.

Keywords: museum lighting in Russia, illuminance, correlated colour temperature, general colour rendering index, museum lighting standards

1. INTRODUCTION

In early 2018, the Ministry of Culture of the Russian Federation initiated the study aiming at development of up-to-date museum lighting requirements which museum employees may adhere to in their work [1]. One of the research directions of this study was to obtain a complete picture of the current state of museum lighting based on the results of polling and selective monitoring of lighting parameters in a number of museums of Moscow and Saint Petersburg.

2. POLLING RESULTS

In order to obtain a complete picture of the actual state of museum lighting in the Russian Federation, S.I. Vavilov VNISI, in cooperation with the Ministry of Culture of the Russian Federation, the State Hermitage, the State Tretyakov Gallery, and the State Conservation Research Institute (GosNIIR) developed a questionnaire, which was distributed among 168 museums of the Russian Federation of different levels, from state to regional.

The questionnaire contained 13 questions regarding different aspects of lighting of museum exhibits answered by 90 out of 168 museums (54 %), which allowed us to form the following picture of the state of museum lighting in the Russian Federation.

Question 1: General museum information

Most museums have no light engineers in employment and their duties are primarily performed by electricians not educated in the sphere of light engineering and even they are employed only by 53 % of the museums, which answered the questions.

Question 2: Exhibits

In some museums, collections are categorised by regions and peoples, and exhibits are not divided in terms of light stability in storage premises and exhi-

[1] Based on the report at the 29th CIE Quadrennial Session, June 14–22, 2019, Washington DC, USA.

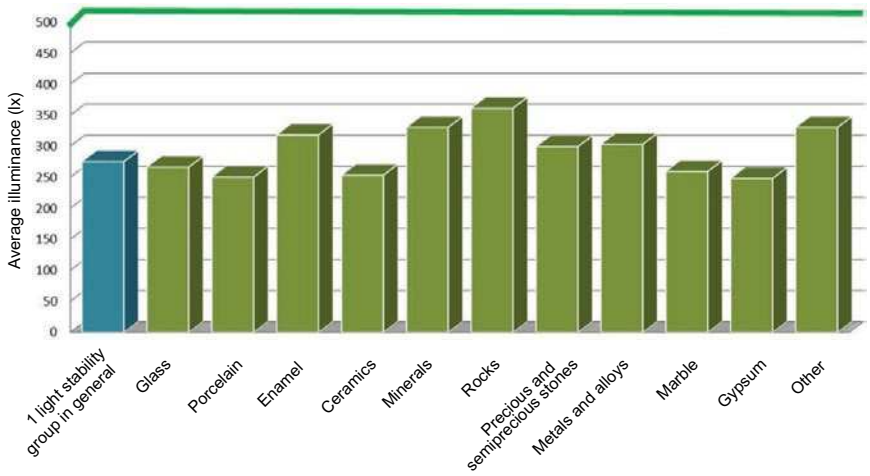

Fig. 1. Illuminance values for materials of the 1st light stability group averaged over all responding museums (according to the CIE recommendations [4], for the group 1 materials, illuminance levels are not limited, and green line stands for maximum acceptable value of illuminance according to Russian recommendations (500 lx) [2, 3])

bition halls, so in all premises where the exhibits are located, the integrated storage mode is maintained. This gives rise for the problem of correct maintenance of lighting mode for exhibits stored on the basis of the thematic and chronological principle.

Question 3: Applied light sources

For general lighting of exhibition halls, depositories and restoration workshops, museums use primarily fluorescent lamps (FL), compact fluorescent lamps (CFL) and warm white light-emitting diodes (LED) with correlated colour temperature (T_{cc}) of (2700–3200) K, and for accent lighting of exhibits, tungsten halogen lamps (THL), FL, white LED (T_{cc} equal to (3200–4200) K) and CFL are used. In museum depositories, mostly white (T_{cc} are in range (3200–4200) K) FL are used for general lighting and LED, CFL, or FL are used for accent lighting (Table 1, 2). In the case of quantitative indicators of introduction of LED lighting in museum practice, to a varying degree, LED light sources are already applied for general and accent lighting by 77 % and 61 % of polled museums respectively. The same holds for restoration workshops and depositories. At the same time, there are almost no exhibition premises without natural lighting, which is dangerous for works of art with poor light stability. As regards adjustment of light-engineering characteristics of accent and general lighting, it is essentially limited by adjustment of luminous flux values of light sources, i.e. varying of light source power and approximately 32 % of museums cannot afford even this. Just several museums use individual controls at bodies of lighting devices, *Bluetooth* adjustment, etc.

Question 4: Maintained illuminance level of artificial lighting

The respondents provided the data on the maintained levels of exhibit illuminance in accordance with the classification of exhibit light stability adopted in the Russian Federation [2, 3] which consists of three groups:

– Group 1 (low-sensitive (high light stability), which approximately corresponds to group I in accordance with CIE157:2004 [4]);

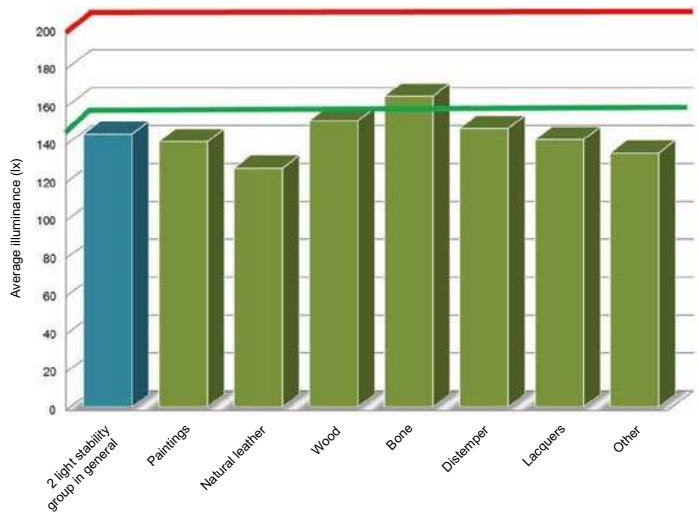

Fig. 2. Illuminance values for materials of the 2nd light stability group averaged over all responding museums (red line stands for the maximum acceptable illuminance value (200 lx) in accordance with the CIE recommendations [3] for materials of this group, green line stands for maximum acceptable value of illuminance according to Russian recommendations (150 lx) [2, 3])

Table 1. Types of Light Sources Used by the Museums for General Lighting, % of the Number of Responding Museums

Type of light source	Type of premises		
	Exhibit halls	Museum repositories	Restoration workshops
Daylighting	46	31	37
IL	18	14	10
THL	23	3	3
FL	54	56	43
CFL	49	30	18
LED	77	42	32
MHL	8	3	3

Table 2.Types of Light Sources Used by the Museums for Accent Lighting,% of the Number of Responding Museums

Type of light source	Type of premises		
	Exhibit halls	Museum repositories	Restoration workshops
IL	2	2	7
THL	33	3	7
FL	18	3	12
CFL	18	1	17
LED	61	6	14
MHL	9	0	2

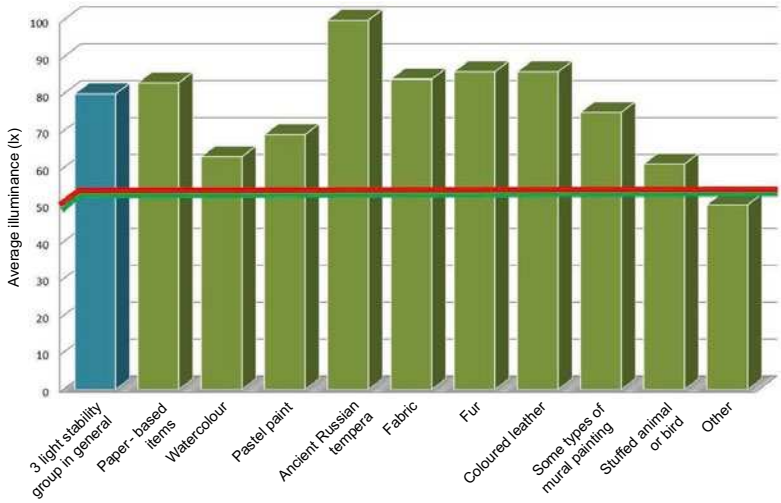

Fig. 3. Illuminance values for materials of the 3rd light stability group averaged over all responding museums (red line stands for the maximum acceptable illuminance value (50 lx) in accordance with the CIE recommendations [4] for materials of this group, green line stands for maximum acceptable value of illuminance according to Russian recommendations (also 50 lx) [2, 3])

– Group 2 (medium-sensitive (medium light stability), which approximately corresponds to group II in accordance with CIE157:2004 [4]);

– Group 3 (hypersensitive (low light stability), which approximately corresponds to group III in accordance with CIE157:2004 [4]).

In the context of this classification, it follows from the museums' answers that, for exhibits of light-stability groups 1 and 2, the recommendations regarding maximum acceptable illuminance levels applicable currently in Russia are complied with in most cases whereas the international requirements which are less strict in the case of the 2nd materials group are complied with almost in all cases. As regards exhibits of the 3rd light-stability group, just one half of the museums comply with the requirements (Tables 3–5, Figs. 1–3).

Questions 5 and 6: Exhibition hall background (walls) tonality and background illuminance (as compared to exhibit illuminance)

Table 3. Number of Museums Maintaining the Specified Value of Illuminance (% of General Number of the Museums Answering the Relevant Questions) and Average Value of Illuminance (lx) For Materials of the Light Stability Group Number1

Illuminance, lx*	0–100	100–200	200–300	300–400	400–500	> 500
Group 1 in general: Number of museums,%	19	27	21	9	23	1

* Illuminance averaged over all exhibits of group 1 is 275 lx.

Table 4. Number of Museums Maintaining the Specified Value of Illuminance (% of General Number of the Museums Answering the Relevant Questions) and Average Value of Illuminance (lx) for Materials of the Light Stability Group Number 2

Illuminance, lx*	0–100	100–150	150–200	200–300	>300	0–150**	0–200***
Group 2 in general: Number of museums,%	32	40	24	4	–	72	96

* Illuminance averaged over all exhibits of group 2 is 144 lx.
** Acceptable illuminance as per the recommendations applicable in Russia (<150 lx) [2, 3].
*** Applicable illuminance as per international recommendations (<200 lx) [4].

There are medium, light and dark background tonalities encountered in the museums, but medium or light and, to the less extent, dark background tonalities are preferred by the museums (Table 6). As regards preferences of the relation between illuminance of background and exhibits, background illuminance is primarily equal or less than exhibit illuminance and museums consider background with illuminance less than or approximately equal to illuminance of exhibits preferable (Table 7).

Question 7: What methods of daylight illuminance regulation and protection are used in the museum?

Museums use most of existing methods including curtains, louvres and protective glazing.

Question 8: Applied lighting control devices

Illuminance monitoring is conducted primarily by means of illuminance meters and, unfortunately, only 34 % of the monitored museums are equipped with them. Irradiance meters, colorimeters, and spectroradiometers are possessed only by 4 %, 3 % and 2 % of museums respectively and only one museum is equipped by a central lighting monitoring system. With that, it is noted that non-availability of necessary calibrated devices is caused by underfunding.

Question 9: What regulatory and/or recommendation documents do you use for arrangement of lighting in your museum? Please assess their practical utility for your work on a 1–10 scale

Analysis of answers to this question showed that museums primarily are keeping using the guideline issued by GosNIIR in 1995 [5] (38 % of museums) and already void Order of the Ministry of Culture of the Russian Federation dated on December 8, 2009 [6] (33 % of museums). On a scale of 1–10, practical utility of these documents was assessed as 9.3 and 8.3 respectively.

Question 10: Do the existing requirements to maximum acceptable illuminance levels provide adequate perception and preservation of exhibits in your opinion?

This question was designed to find out whether the museums consider that the existing requirements to maximum acceptable illuminance levels provide adequate perception and preservation of exhibits in exhibition halls, restoration workshops and depositories. As it follows from the data presented in Fig. 4–6, the most of the polled museums consider that the existing requirements to maximum acceptable illuminance levels provide adequate perception and preservation of exhibits in exhibition halls, restoration workshops, and depositories. However, about a half of the respondents were either undecid-

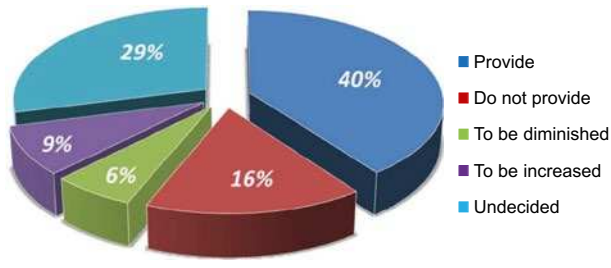

Fig. 4. Museum answers to question 10 of the questionnaire (adequacy of lighting requirements) as regards exhibition halls

Table 5. Number of Museums Maintaining the Specified Value of Illuminance (% of General Number of the Museums Answering the Relevant Questions) and Average Value of Illuminance (lx) for Materials of the Light Stability Group Number 1

Illuminance, lx*	0–50**	50–75	75–100	100–150	150–200	>200
Group 3 in general: Number of museums,%	51	16	16	9	6	2

* Illuminance averaged over all exhibits of group 1 is 80 lx.
** Acceptable illuminance as per the recommendations applicable in Russia and the international recommendations (<50 lx) [2–4].

Table 6. Preferred Tonality of Background (% of the Total Number of Museums (90) Answered Question 6 of the Questionnaire)

	Very light	Light	Medium	Dark	Very dark
Current	7	33	38	19	3
Preferable*	2	22	28	11	2

* 35 % of the museums were undecided

Table 7. Preferred Relation between Background Illumination and Exhibit Illumination (% of the Total Number of Museums (90) Answered Question 7 of the Questionnaire)

	Much less	Less	Roughly the same	Higher	Much higher
Current*	5	25	27	–	–
Preferable**	6	18	13	1	–

* 43 % of the museums were undecided to name the current relation
** 62 % of the museums were undecided to name the preferred relation

ed or gave negative answers, which suggests that it is necessary to make amendments to the applicable requirements.

Question 11: What would you like to change in lighting of your museum?

This question implied feedback by the museums regarding possible changes of lighting. As a result, it turned out that:

- 40 % museums would like to replace conventional artificial light sources for general and accent lighting in exhibition halls with LEDs. Linear LED light sources with individually selected chromaticity and high luminous efficacy are also required;
- 11 % of the responding museums would like to remove natural lighting in exhibition halls;
- 30 % of the museums would like to replace artificial light sources for general lighting of depositories with LED;
- 18 % of the museums would like to replace artificial light sources for accent lighting of depositories with LED;
- About 4 % of the responding museums would like to remove natural lighting in depositories;
- 26 % of the museums would like to replace artificial light sources for general lighting of restoration workshops with LED;

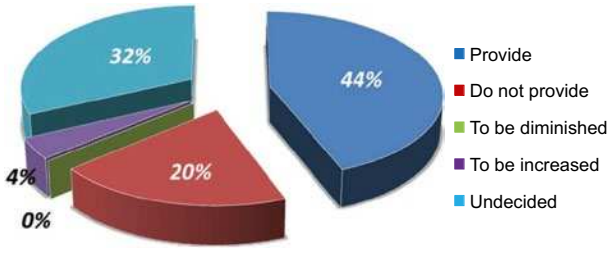

Fig. 5. Museum answers to question 10 of the questionnaire (adequacy of lighting requirements) as regards museum depositories

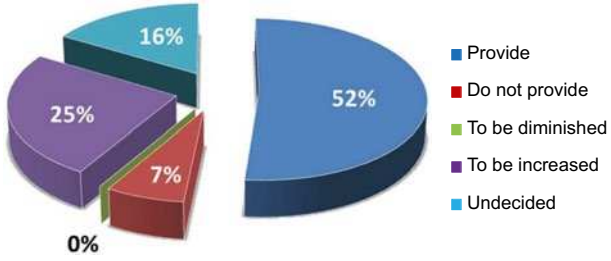

Fig. 6. Museum answers to question 10 of the questionnaire (adequacy of lighting requirements) as regards restoration workshops

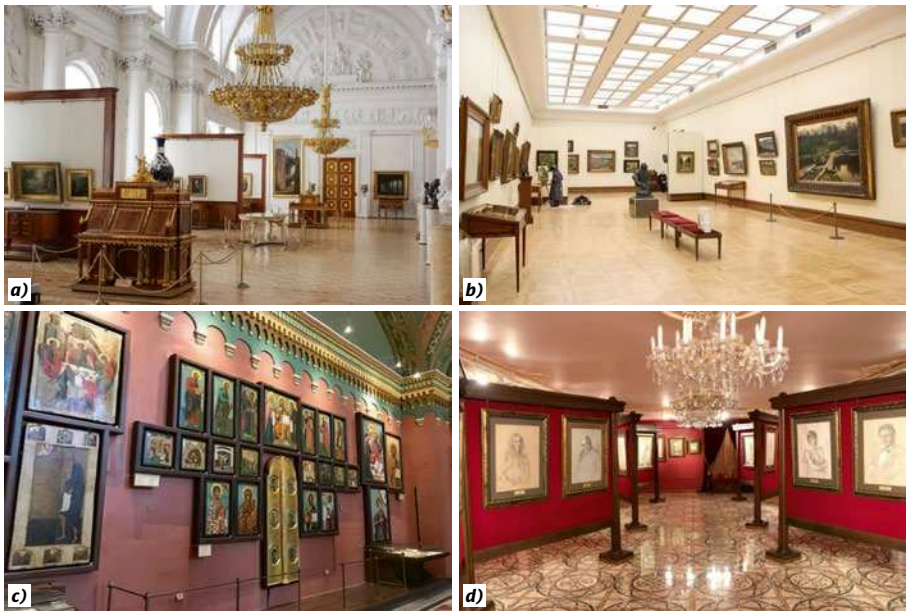

Fig. 7. Lighting of the halls of the State Hermitage (a), the State Tretyakov Gallery (b), the State Museum of History (c), and the Alexander Shilov Gallery (d)

• 19 % of the museums would like to replace artificial light sources for accent lighting of restoration workshops with LED;

• About 1 % of the responding museums would like to remove natural lighting in restoration workshops.

Question 12: Assess necessity of development of the following regulatory documents for monitoring and provision of preservation conditions for displayed and stored exhibits

It follows from the answers to this question, that the museum community is interested in development of a number of documents containing general requirements to museum lighting standardisation. These are:

• Standard, Museum lighting. General requirements;

• Standard, Museum lighting. Light and engineering characteristics measurement methods;

• Museum light sources and lighting devices selection recommendations.

Question 13: Your wishes as to standardisation of museum exhibits lighting

The next suggestions follow from the answers on this question:

• Start formulating standards or recommendations for standardisation of museum lighting with a uniform system of measurement of light and engineering (photometric) characteristics and criteria of selection of necessary cutting-edge equipment;

• Conduct experimental studies to obtain objective data for justification of exhibit illuminance standards;

• Standardise not only illuminance, but also annual luminous exposure for different materials;

• Organise a lighting standardisation workshop for heads of conservation.

3. MEASUREMENT RESULTS

In order to clarify the picture of the current state of museum lighting in the Russian Federation, we inspected lighting systems and measured their characteristics in the State Hermitage, the State Museum of History, the Museum of the 1812 French Invasion, the State Tretyakov Gallery, the Pushkin State Museum of Fine Arts, the Alexander Shilov Gallery as well in the Church of St. Nicholas in Tolmachi, which is the museum church and house church being a part of the Tretyakov Gallery and in the Academician I.E. Grabar All-Russian Art Restoration Research Centre[2]. In the course of this work, the following parameters were measured:

• Illuminance on exhibit surfaces and in halls including semi-cylindrical illuminance;

• Correlated colour temperature;

• General colour rendering index of the used light sources;

• Luminance distribution over a viewer's field of view.

Measurements of the listed parameters were performed by means of, respectively, Ekosfera illuminance meter by EcoLight, Russia,

[2] Preliminary results of these studies were published in [7]. – authors' note.

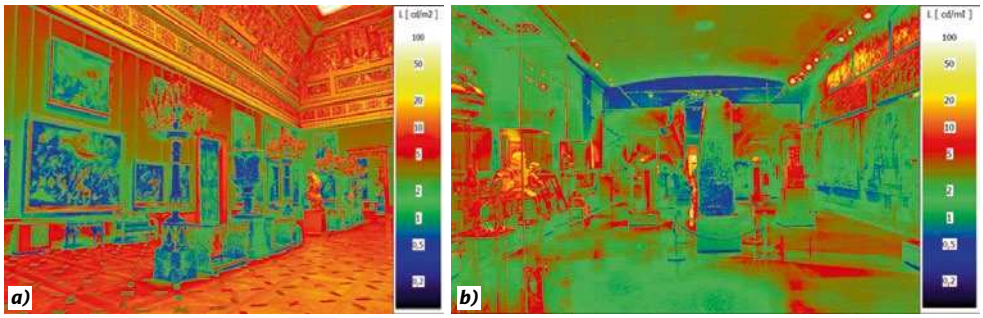

Fig. 8. Pseudo-colour luminance distribution in halls of the State Hermitage (a) and the Pushkin State Museum of Fine Arts (b)

and *LMT Pocket Lux 2* illuminance meter by *LMT*, Germany, *UPRtek MK350S* spectrophotometer by *United Power Research Technology Corporation*, Taiwan, and *LMK mobile advanced* luminance meter by *LMK*, Germany. At the initial stage, apart from measurement of photometric parameters, heating of works of art under effect of incident radiation, i.e. temperature distribution over picture surface was measured by means of *Testo 882* thermal camera by *Testo*, Germany, as well as the level of UV radiation, which was measured by means of TKA-AVS UV radiometer by TKA, Russia. At later stages, these measurements were not made due to negligible difference between temperature on picture surfaces and ambient temperature, and negligible, as compared to maximum allowed values [8], level of UV radiation reached by protective film on windows, and correct selection of artificial light sources.

The museums in which the survey was carried out differ significantly in the interiors for exhibiting the works of art (mainly paintings and graphics) and, accordingly, in their lighting systems. For instance, while the Hermitage is a complex of palace premises with remarkable architecture and decorations and is, therefore, a work of art in itself, a most valuable exhibit requiring quality interior lighting, the Tretyakov gallery, the Museum of History, and the Alexander Shilov Gallery are designed for demonstration of paintings and graphics and natural lighting is substantially limited or non-available there (Fig. 7).

As a result of the study, it was found that majority of lighting devices in the museums is based on tungsten halogen lamps and linear and compact fluorescent lamps following. At the same time, there is a trend of transition to LED-based luminaires. For instance, in the Hermitage, the leader in advancement of lighting systems, such devices are already installed over 15,000 (25 %) lighting points.

The measurement results showed that values of average illuminance on museum exhibits do not exceed recommended levels in the most museums and general luminance distribution is arranged rather well (Fig. 8). At the same time, in the Tretyakov Gallery, illuminance of certain areas of some pic-

Fig. 9. Lighting of the iconostasis of the Church of St. Nicholas in Tolmachi: Photograph (a) and pseudo-colour luminance distribution (b)

Fig. 10. Preservation specialist worktable lighting (a) and general lighting of restoration premises (b) of the Academician I.E. Grabar All-Russian Art Restoration Research Centre

tures is exceeded due to non-uniformity of lighting, whereas some pictures are insufficiently lighted in the Hermitage and the Museum of History. In the French Invasion Museum, where only LEDs are used for lighting, local areas with exceeding lighting of exhibits were found as well as cases of significant, up to thirty-fold, luminance variations. In the Pushkin Museum of Fine Arts, lighting of exhibits fully complies with the requirements although the level of illuminance was intentionally set higher in some cases for better perception of pictures by viewers.

It is worth noting that diversity of museum collections often makes lighting arrangement more difficult. For instance, in hall No. 223 of the Hermitage, there are two cases with different levels of lighting standing in front of each other one of which contains glass and bronze exhibits (with low light sensitivity) and the other one contains laceworks (hypersensitive exhibits with standard illuminance not exceeding 50 lx).

The values of correlated colour temperature of artificial lighting in the museums did not exceed (4000–4200) K, whereas the values of general colour rendering index usually exceeded 90.

Only lighting of the Church of St. Nicholas in Tolmachi, premises with high ceilings and not darkened windows without UV radiation protective film, is out of the generally favourable picture. Artificial lighting of interior, some icons and the iconostasis is performed by means of spotlights with 500 W THL and during daytime, in conditions of simultaneous effect of natural and artificial light, the level of lighting of icons is excessive and veiling reflections are formed (Fig. 9). Currently, reconstruction of lighting is being started in the church with transition to LEDs among others.

In the restoration premises of the Academician I.E. Grabar All-Russian Art Restoration Research Centre and the State Hermitage, natural light is widely used for more accurate demonstration of colours and perception of museum exhibits being preserved. For works with items with different levels of light stability, the restoration centre uses different types of lighting devices with different light sources including LEDs, by means of which lighting necessary for precision works and comfortable for conservation specialists is formed (Fig. 10). During works with paintings, illuminance levels do not exceed (300–400) lx.

4. CONCLUSION

The results of the studies demonstrated that museum lighting in the Russian Federation generally complies with the applicable requirements and recommendations and requires fundamental changes only in few cases. Many museums already use light emitting diodes as light sources and are ready to cross over to LED lighting completely. In the meantime, museums (primarily small ones) consider lack of regulations in the sphere of museum lighting as the major problem. In order to solve this problem and simplification of the process of museum transition to LED lighting, VNISI LLC has started developing a series of two standards and two preliminary standards in the sphere of LED museum lighting with financial support of the Rosnano Infrastructure and Educational Programmes Foundation. Moreover, in cooperation with the Ministry of Culture of the Russian Federation, it is planned to conduct studies of the effect of correlated colour temperature and the level of LED lighting on perception of museum exhibits and the effect of chromaticity of

LED lighting on aging of museum exhibits which will allow us to increase the framework for standardisation of museum lighting.

ACKNOWLEDGEMENT

This work was conducted with financial support rendered by the Ministry of Culture of the Russian Federation as part of the State Contract No. 436–01.1–41/05–18 dated on 18.05.2018.

REFERENCES

1. Shakhparunyantz, A.G., Rozovsky, E.I., Chernyak, A. Sh., Fedorishchev, P.A. LED in Museums: New Capabilities and Challenges [Svetodiody v muzeyakh: novyiye vozmozhnosti i problemy // Svetotekhnika, 2018, Special Issue Light in the Museum, pp. 36–39.

2. Museum Design Recommendations. [Rekomendatsii po proektirovaniyu muzeev]. B.S. Mezentsev TsNIIEP. Moscow: Stroyizdat, 1988.

3. Recommendations for Design of Artificial Lighting in Museums, Galleries and Exhibition Halls Rekomendatsii po proektirovaniyu iskusstvennogo osvashcheniya muzeev, kartinnykh galerei i vystavochnykh zalov.] Moscow: F.B. Yakubovsky VNIPI Tyazhpromelectroproekt, 1992.

4. CIE157:2004 "Control of Damage to Museum Objects by Optical Radiation".

5. Museum Storage of Art Treasures [Muzeinoye khraneniye khudozhestvennykh tsennostei]. Practical guidelines. Moscow: State Research Institute of Restoration, 1995, 17 p.

6. Order of the Ministry of Culture of the Russian Federation No. 842 of December 8, 2009 "On approval of uniform rules of organization, accounting, preservation and use of museum pieces and museum collections in the museums of the Russian Federation", cancelled by the Order No. 116 of 11.03.2010.

7. Chernyak Anatoly Sh., Kuznetsova Alyona B., and Bartseva Alexandra A. Measurement of Illumination Parameters of the Halls and Exhibited Items of the State Hermitage and the State Tretyakov Gallery// Light & Engineering Journal, Vol. 27, #4, pp. 66–72.

8. Sergei S. Bayev, Vladimir N. Kuzmin, and Konstantin A. Tomsky Research of Optical Radiation Impact on Materials of Museum Exhibits and Requirements to Measurement Devices// Light & Engineering Journal, Vol. 27, #4, pp. 73–80.

George V. Boos,
Ph.D., graduated from MPEI in 1986, President and Member of Directors Board of BL Group, Head of the chair "Light and Engineering" NIU MPEI. He is a Laureate of the State Prize of the Russian Federation (for the Moscow architectural illumination), Chairman of the Editorial Board of the "Svetotekhnika" and "Light & Engineering" Journals, Member of the Russian Academy of Natural Sciences

Eugene I. Rozovsky,
Ph.D. in Techinical Science (1984). Graduated from MPEI in 1971. Leading researcher of VNISI named after Vavilov N.I. Senior Scientific Editor of L&E Journal. An expert from the Russian Federation in TC34 IEC "Sources of light and related equipment"

Anatoly Sh. Chernyak,
Engineer. Graduated from MPEI in 1962. Head of the Laboratory of lighting and light devices at the VNISI named after Vavilov N.I.

Alyona B Kuznetsova,
graduated from MPEI NRU in 2011. At present, she is a Senior Research Fellow and postgraduate student at the N.I. Vavilov VNISI LLC

Aleksandra A. Bartseva,
graduated from MPEI NRU in 2013. At present she is an engineer at the N.I. Vavilov VNISI LLC

Light & Engineering
Vol. 28, No. 2, pp. 47–53, 2020

https://doi.org/10.33383/2018–059
Svetotekhnika #6, 2019, pp. 52–57

IMPROVEMENT OF MAJOLICA LIGHTING AT THE KOMSOMOLSKAYA-RADIAL METRO STATION

Alexander E. Guliev

ILEC BL GROUP, Moscow
E-mail: gul.ae@yandex.ru

ABSTRACT

The article describes solving of one of the most important problems of perception of architectural decoration of metro stations: removal of veiling reflections on glazed mosaics and majolica caused by lighting devices.

A number of lighting methods reducing luminance of the veiling reflections is analysed. Their efficiency is exemplified by lighting of the Mine Laying majolica (based on sketches by Eugene Lancer) at the Komsomolskaya station of Moscow Metro.

The content of the article relates not only to metro stations but to any areas with reflective or glazed surfaces.

Keywords: Moscow metro, Komsomolskaya station, lighting devices, light emitting diodes, majolica, glazed surface, veiling reflection, luminance, contrast

1. INTRODUCTION

Veiling reflections are rather common for stations of the Moscow Metro by virtue of rich decorations with various murals, mosaics and frescoes made of polished marble, majolica and smalt mosaic patterns, etc. A veiling reflection is a light spot on a highly illuminated convex or flat glazed surface. It appears as a result of regular reflection or combination of regular and diffuse reflection of radiation of a bright lighting device (LD).

It is well-known that it is virtually impossible to remove veiling reflections on large reflective surfaces illuminated by large number of LDs, which are often also used as decorative elements. Nevertheless, originally the luminance level of veiling reflections at metro stations was significantly less. The problem of veiling reflections is at least not mentioned in literature [1, 2], which is likely to be caused by generally low level of illumination of the early metro stations. It appeared after the first modernisation of lighting conducted in the 60s to increase energy efficiency and the lighting level of certainly dark stations by replacing incandescent lamps (IL) with fluorescent lamps (FL). With that, luminance of LDs largely increased and the veiling reflections appeared on glazed surfaces and began preventing authentic perception of a station and thus nullifying efforts of architects, artists and lighting engineers who had created it. Given that the current level of lighting of the majority of stations does not comply with applicable standards [3], negative effects of veiling reflections on comfortable perception of decorations keep rising.

Human eye is adaptive. Visual perception is influenced by luminance distribution over the field of view [4] and veiling reflections, with their luminance higher than that of surroundings, prevent this perception.

It is obvious that relative position of a spectator and an object and therefore LD illuminating it is one of most important factors of perception of a fresco, mosaic or majolica image, especially when it is illuminated by an artificial light source. With ideal lighting, a spectator's position is usually defined only by the composition of the image, however, LDs often "intervene" in this process creating glaring areas on the viewed surface, and the more

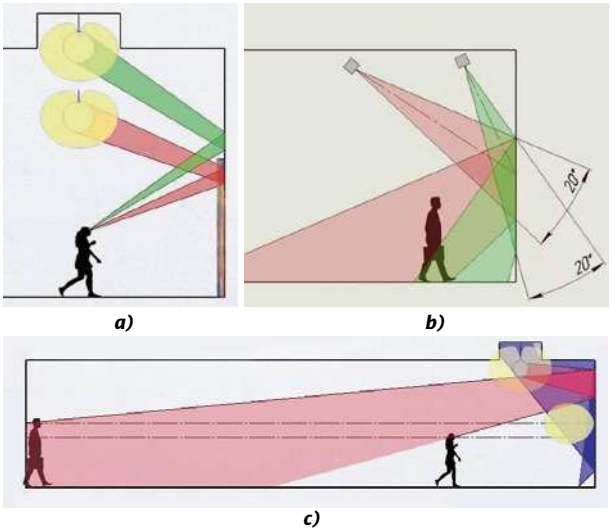

Fig. 1. LD location effect on formation of veiling reflections:
a – lighting at different angles; *b* – height; *c* – illumination from below

there are such areas the less the quality of lighting is. As a result, moving along an art object, a spectator defines the position at which the effect of LD on his/her perception is minimal. That is why it is very important to minimise their effect on perception, which especially applies to large art objects in the case of which it is virtually impossible to fully remove the veiling reflections in the conditions of a metro station. Therefore, alongside with spatial light distribution of LD, the most important characteristics of lighting installations (LI) "responsible" for veiling reflections are geometric relations defining relative position of LD and an object as well as

Fig. 2. Illumination of a mosaic at the Prospekt Mira station of Koltsevaya line

characteristics of the surface of an object reflecting radiation of LD. It is necessary to remember that luminance does not depend on distance; therefore, for instance, if LD is moved at a larger distance from a mural it illuminates, the area of a veiling reflection will reduce but its luminance will remain the same [5].

2. METHODS FOR REMOVAL OF VEILING REFLECTIONS

Reflection diagram of such diffused and glazed surfaces as mosaics and majolica frescos has diffuse and regular components. When lighting such surfaces, it is necessary that a spectator see only the diffuse component. For this purpose, possible specta-

Fig. 3. The northern hall of the Komsomolskaya metro station

Fig. 4. Appearance of the majolica: *a* – the left part with reflections; *b* – the left part without reflections; *c* – the right part with reflections; *d* – the right part without reflections

tor's positions and conditions of his/her perception of a picture or a mosaic, i.e. angle of view at which veiling reflections of a given area and their luminance level, should be defined.

If light distribution curve of LD is narrow, specific for a reflective spotlight LD, the angle of incidence of radiation should be as high as possible; with such method, the reflective component of reflected radiation is directed to the floor and not to a spectator's eyes (Fig. 1, *a*). If LD light distribution curve is wide, specific for diffuse-reflecting optical elements (e.g. frosted diffuser), the height of LD should be increased as much as possible, so that its light is not reflected on a mosaic (Fig. 1, *b*).

As a result of analysis of situations forming veiling reflections, several major methods of their prevention were formulated: 1) the most radical one which completely makes their alignment impossible is changing of beam path by illuminating an object from below; 2) reduction of luminance of veiling reflections; 3) increase of adaptation luminance; 4) changing of position of a veiling reflection relative to an image; 5) reduction of size of a veiling reflection.

The first approach implemented by means of additional luminaires installed underneath [6] (Fig. 1, *c*) provides incidence of the reflective component of a beam on a ceiling whereas the diffuse component reflected by a mural increases its luminance and, subsequently, luminance of adaptation thus making a veiling reflection less visible or completely removing it. Naturally, this method assumes application of LDs with high degree of protection from mechanical damage. Moreover, such allocation of LDs significantly refuses the useful area of a station. Unfortunately, the listed factors do not allow us to use this method (one of the most efficient ones) at metro stations.

The second method may be implemented when light distribution curve of LD illuminating, for instance, a mural is asymmetric, therefore, such LD is a corner reflector [7] or when its luminance at the mural side is lowered.

The third approach may be applied by moving the accent of lighting, for instance, by installing LD inside a column like it is done for lighting of a mosaic at the Prospekt Mira station of the Koltsevaya line (Fig. 2).

The fourth method usually requires changing position of LD relative to a lighted object, which is rather reasonable in some cases.

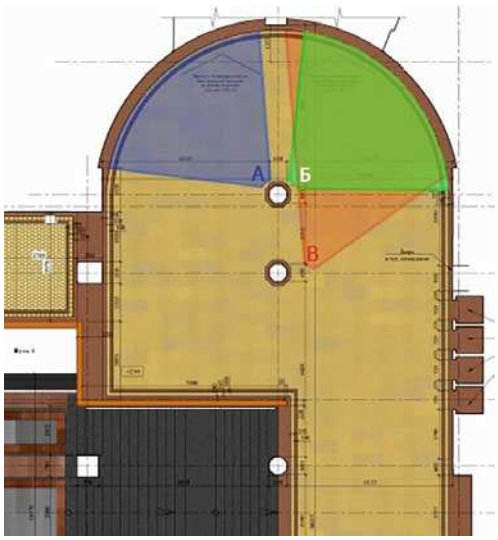

Fig. 5. Characteristic points of view

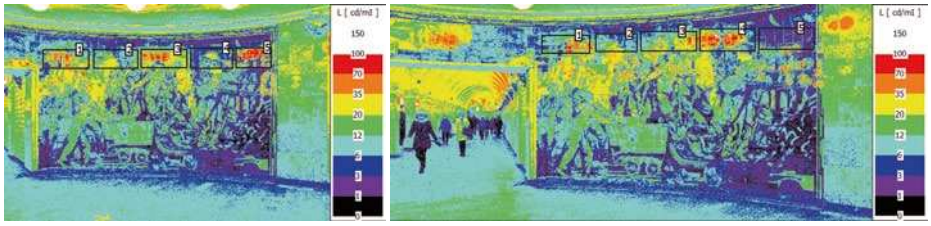

a) *b)*

Fig. 6. Luminance distribution over the right part of the majolica as seen from point B (*a*) and C (*b*)

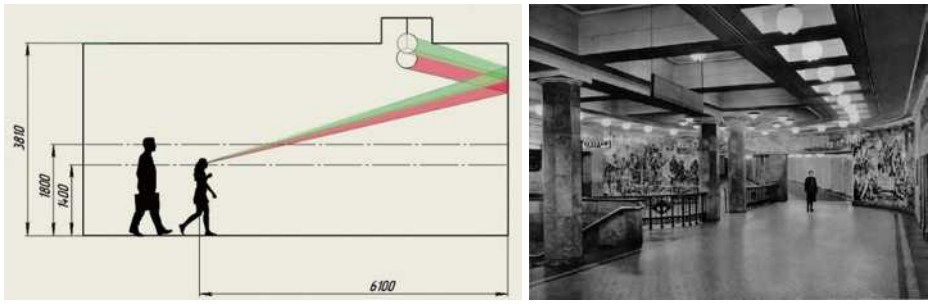

a) *b)*

Fig. 7. The diagram of changing the position and size of a reflection: *a* – dimensions; *b* – the northern hall of the Komsomolskaya station (1935)

Fig. 8. Requirements to position of reflections on the majolica: green and red areas are areas where reflections are acceptable and not acceptable respectively

At last, the fifth approach is implemented by replacing an applied LD with another one of other design or by significantly changing the distance from a lighted object, which is not allowed at cultural heritage objects.

3. GLARE REFLECTIONS REMOVAL OF AT KOMSOMOLSKAYA-RADIAL

Komsomolskaya metro station was the first station where a work of art with a complete composition was used for architectural decoration: the mural about participation of Komsomol in construction of the Metro system based on sketches by Eugene Lancer [8] (four murals had been planned but only one was actually made). The mural is installed on the semi-cylindrical wall of the northern hall. Coloured majolica tiles painted with glaze paint and covered with a layer of transparent glaze, which makes a colour composition glazing and bright after firing, were selected as a material.

Since the surface of majolica is glazed (average reflectance of 0.2, regular reflectance of 0.05), it reflects the light of LDs located in vicinity which forms rather bright veiling reflections on fragments of figures, which makes it impossible to perceive the composition as a whole. Basically removal of these reflections or at least reduction of their effect on perception of majolica (Fig. 3) was the main goal of this work.

Fig. 4 shows the majolica with and without veiling reflections.

At the same time, it is worth noting that current appearance of the station is different from the original one in terms of floor illuminance: illuminance was about 50 lx while currently it is about 150 lx, which still does not comply with applicable requirements (200 lx) [1], just as colour rendering quality does not (R_a < 80), which is caused by use of FL[1]. This is where the main conflict arises: the applicable sanitary standards require higher illumination of the hall floor but it will increase luminance of veiling reflections. Moreover, according to requirements of the metro system, reconstruction should be performed within the framework of heritage preserva-

[1] Besides, the condition of LI requires its new reconstruction at a contemporary level.

Table 1. Specifications of the Luminance Meter

Name	LMK Mobile Advanced
Appearance	
Resolution (effective pixels)	2136×1424
Luminance measurement range, cd/m^2	0.1–10,000
Acceptable relative measurement error, %	± 5
Luminance meter number in National Measuring Equipment Register	55241–13

Table 2. Luminance Measured in Different Areas of the Majolica from Points B and C

Area/Figure		Luminance, cd/m^2		
		minimum	maximum	average
1	Fig. 6, *a*	0.1	131.6	22.6
2		1.1	67.3	13
3		1.1	94.5	26.2
4		0.2	93.6	8.7
5		0	112.8	29.8
1	Fig. 6, *b*	0.2	108.3	19.2
2		0.8	86.5	10.5
3		0.5	93.0	17.7
4		0.2	129.5	28.9
5		0.1	66.8	5.6

tion which means that the station may be illuminated only by LDs similar to original 1935 LDs [10], therefore, only light sources (LS) may be replaced whereas diffusers of LDs should remain the same.

It is obvious that, to solve the said conflicts, it is necessary to develop a brand new LI, which would require conducting experimental studies necessary for calculation of relations between luminance of veiling reflections on majolica and luminance of majolica itself they are aligned on.

4. EXPERIMENTAL STUDIES

The relations between luminance of veiling reflections on majolica and luminance of majolica itself were determined by means of *LMK Mobile Advance* luminance meter [9] based on a *Canon* camera (Table 1). This device also allows us to obtain a graphic image of luminance distribution over the field of view and its software allows the measurement results to process (to determine luminance at a specific point or average luminance of a specific area, to output a pseudo-colour image, etc.). Therefore, just a few pictures may provide all information that we need.

The measurements were performed at characteristic points A, B, and C located near the columns (Fig. 5). The results of the measurements (Fig. 6 and Table 2) demonstrate that luminance of a veiling reflection is 3 to 10 times higher than that of the neighbouring area.

4.1. Removal of Veiling Reflections

Geometric calculations show that increasing of LD height provides positive results (Fig. 7, *a*). It is possible since originally the LDs were installed

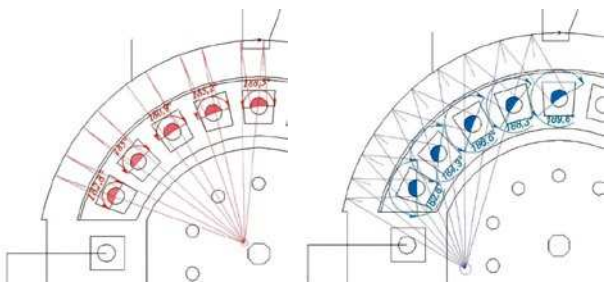

Fig. 9. Geometric calculations for determination of the luminaire segment forming the veiling reflection: *a* – view point 1; *b* – view point 2

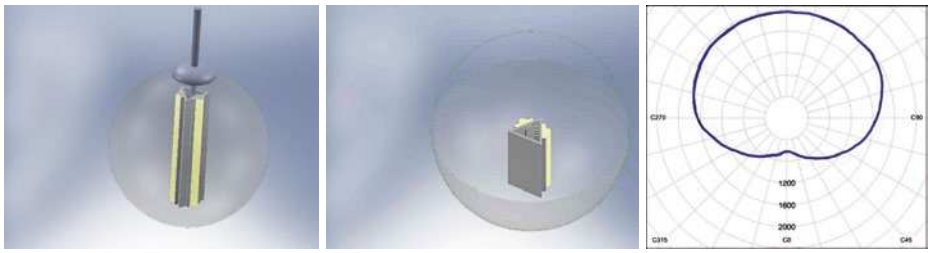

Fig. 10. Modernised LD:
a – structural scheme;
b – horizontal section;
c – horizontal section of the relative photometric body

higher than now (in 1935 [6, 8], LDs were partly located inside the caissons (Fig. 7, *b*)) and their upper parts were obscured by caissons. As a result, the veiling reflection will be reduced by 4 cm and relocated higher by 20 cm and the contours of the caissons will become clearly seen. Relocation of the veiling reflection area has positive effect on perception of the majolica since it is relocated from the narrative area with the metro constructors shown to the less important background area (Figs. 7, *a* and 8, *a*, *b*).

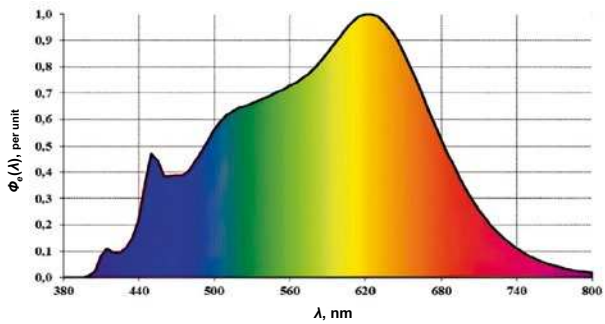

Fig. 11. Relative radiation spectrum of the applied LED models with remote phosphor

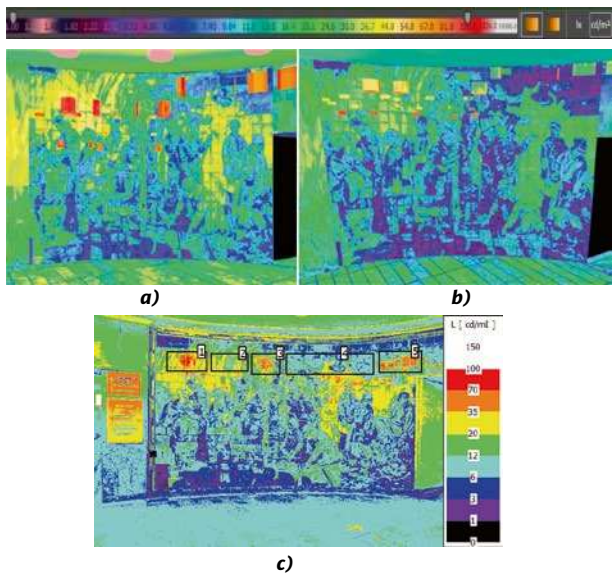

Fig. 12. LI modelling by means of *Dialux Evo 7*:
a – current LI; *b* – new LI; *c* – the results of luminance measurement at point A

4.2. Selection of View Points

As noted above, it is virtually impossible to remove the veiling reflections for all view points since they change their positions depending on a spectator's position, but it is possible to significantly reduce its luminance when viewed from a part of the hall (Fig. 5).

Geometric calculations (Fig. 9) demonstrate that, when watching the majolica at the shown points, reflection of radiation of a segment of LD with width of (180–190) ° can be seen. If we reduce luminance of this part of LD, luminance of the veiling reflection will be significantly lowered.

4.3. Structure of LD

The data obtained allows us to formulate the design principle of the structure of LD (Fig. 10): a triangular-prismatic emitter is installed into a frosted-glass diffuser and LED modules with remote phosphor are installed on two sides of the emitter. The qualitative and quantitative indicators of such modules are high (luminous efficacy of 111.5 lm/W, *R*a > 80, cosine luminous distribution curve (LDC), no peak in the blue region of the spectrum specific for phosphor LEDs (Fig. 11) [11]). With that, one half of the ball diffuser is illuminated by the LED modules and the other one is illuminated only by multiple reflections inside it. The operating principle of such luminaire can be seen in Fig. 10, *a*.

The *Photopia* software [12] calculations demonstrate that LDC of LD with such design would be asymmetric. To test this hypothesis, a current and a modernised LI were simulated by means of *DiaLux Evo 7*. By means of the ray tracing method, luminance distribution over majolica was calculated for both models, which showed that application of LD with asymmetric LDC allows luminance of veil-

Table 3. Luminance Measured in Different Areas of the Majolica from Point A

Area	Luminance, cd/m^2		
	minimum	maximum	average
1	8.4	92.4	33.2
2	4.2	65	18.6
3	1.5	84.7	23.3
4	1.8	49.6	9.8
5	1.5	80	25

ing reflections to halve and "move" them upwards (by increasing the height of LDs) so that they do not prevent perception of composition.

The results of modelling and their comparison with the results of luminance measurement at point A are shown in Fig. 12 and in Table 3.

5. CONCLUSIONS

As a result of studying luminance distribution of majolica, the following was found:

- The sources of veiling reflections are diffusers of LDs which are reflected from the glazed surface of the majolica mural;
- Luminance of the reflections reaches 142 cd/m^2 with average luminance of majolica of (10–15) cd/m^2;
- Depending of the position of a spectator, the veiling reflections are located at height of 2 m to 3.5 m and obscure the narrative part of the composition.

Based on the analysis of the causes of the veiling reflections:

- Requirements to LI allocation and LD design were formulated;
- A model was developed and modelling of luminance distribution over the surface of majolica was performed by means of ray tracing using *Dialux Evo 7* software.

Despite the fact that it was not possible to remove the veiling reflections completely, the designed LI allows luminance and dimensions of the veiling reflections to halve and to move them from the narrative area to the background area, which positively affects perception of the composition.

The conclusion of the article is applicable not only to metro stations but to other areas with reflective or glazed surfaces.

REFERENCES

1. Brodsky, L. Light in the Metro [Svet v metro] // Arkhitekturnaya gazeta, 1935, April 28, p. 3.

2. Brodsky, L. Lighting of Metro Stations [Osveshchenie stantsiy metro] // Arkhitektura SSSR, 1938, Vol. 9, pp. 11–17.

3. SP 2.5.1337–03 The Sanitary Rules of Operation of Metro Systems [Sanitarnyye pravila ekspluatatsii metropolitenov] (as amended on 30.04.2010, No.50).

4. Light Engineering Handbook [Spravochnaya kniga po svetotekhnike] / Edited by J.B. Aizenberg. 3rd Issue, revised and supplemented. Moscow: Znak, 2006, 972 p.

5. Meshkov, V.V. Fundamentals of Light Engineering: Study Guide for Higher Education Institutions. P1 [Osnovy svetotekhniki. Uchebnoye posobiye dlya vuzov]// 2nd Issue, revised and supplemented, Moscow: Energiya, 1979, 368 p.

6. Miras, J.-P., Novakovsky, L.G., Fontoynont, M. Lighting of Mona Lisa: New Lighting Solutions [Osveshcheniye Mony Lizy – noviyye svetoviyye resheniya] // Svetotekhnika, 2005, Vol. 5, pp. 28–33.

7. Meshkov, V.V., Epaneshnikov, M.M. Lighting Installations [Osvetitelniyye ustanovki], Moscow: Energiya, 1973, 360 p.

8. Katsen, I. Moscow Metro [Metro Moskvy], Moscow: Moskovskiy rabochiy, 1947, 178 p.

9. Attachment to Pattern Approval Certificate of Measuring Instruments No. 52728.

10. Gorbachev, N. V., Ratner, E.S. Illumination of the Moscow Metro [Osveshcheniye moskovskogo metro] // Svetotekhnika, 1935, Vol. 1, pp. 2–13.

11. Weinert, J., Spalding, C. LED Lighting Explained: Understanding LED Sources, Fixtures, Applications and Opportunities. Philips Colour Kinetics, 2010, 156 p.

12. URL: http://www.ltioptics.com/en/photopia-general-2017.html (date of reference: 30.04.2019).

13. Shurygina, N.V. Lighting of New Moscow Metro Stations [Osveshcheniye novykh stantsiy moskovskogo metro] // Svetotekhnika, 2015, Vol. 3, pp. 14–21.

Alexander E. Guliev, Master Degree in Electronics and Nanoelectronics, Theoretical and Applied Light Engineering education programme (2019, NIU MEI). At present, he is post-graduate student with NIU MEI (field: Electrical and Heat Engineering) and light engineering specialist with International Light & Engineering Corporation BL GROUP

Light & Engineering
Vol. 28, No. 2, pp. 54–60, 2020

https://doi.org/10.33383/2019-035
Svetotekhnika #6, 2019, pp.31-36

STUDY OF LIGHTING SYSTEMS WITH EXTENDED HOLLOW LIGHT GUIDES

Alexei I. Sterkhov[1], Alexander V. Palagin[1], and Igor Yu. Loshkarev[2]*

[1] Solargy group LLC, Izhevsk
[2] N.I. Vavilov Saratov State Agricultural University, Saratov
** E-mail: igyulo@mail.ru*

ABSTRACT

The article contains comparative results of studying of spectral characteristics of two different light transporting systems: based on *DF2000MA* polymer film (marketed) and based on vacuum-deposited silver coated with silicon and titanium oxides (own development). Studying of *Alanod miro Silver 4270AG*, *Alanod miro Silver 4400AG* and *Alanod miro Silver 4400GP* variants of *Alanod miro Silver* retroreflective material showed that chromaticity of output light of our light guide system is almost the same as that of input natural daylight in visible spectrum. Advantages of optical elements for the light guide system developed by us over those applied in the reference system are demonstrated.

Keywords: light guide, extended hollow light guide, illumination, daylighting, spectrum

1. INTRODUCTION

As known, application of lighting systems based on extended hollow light guides for daylighting of premises is one of the solutions of the problem of reduction of power consumption for lighting. We developed our own lighting system of this type with reflective material based on vacuum-deposited silver, and the goal of this work is to compare it with an existing market analogue with reflective material based on *DF2000MA* polymer film in terms of chromaticity transmission accuracy, integrated transmittance of both the system as a whole and its optical elements as well as technology of manufacturing of reflective tube, system service life, etc.

2. OBJECTS OF RESEARCH

As the subjects of study, the models of a lighting system with a light guide based on *DF2000MA* polymer film and our development *Solarway,* light guide system with the reflective tube based on vacuum-deposited silver coated with silicon and titanium oxides (Fig. 1), have been used.

Elements of the *Solarway* system:

- Light pickup dome: Transparent acrylic sheet with fine texture (*Acryl 92-Z*); made of PMMA *Plexiglass* (by vacuum shaping);
- Thermal barrier: acrylic sheet with thickness of 4mm;

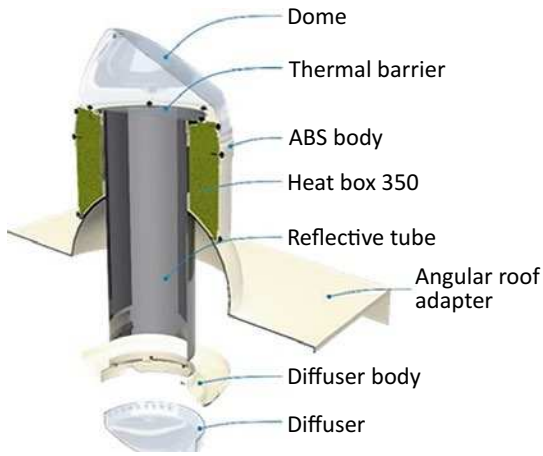

Fig. 1. Scheme of the designed *Solarway* natural lighting system

Fig. 2. Models of the *Solarway* system

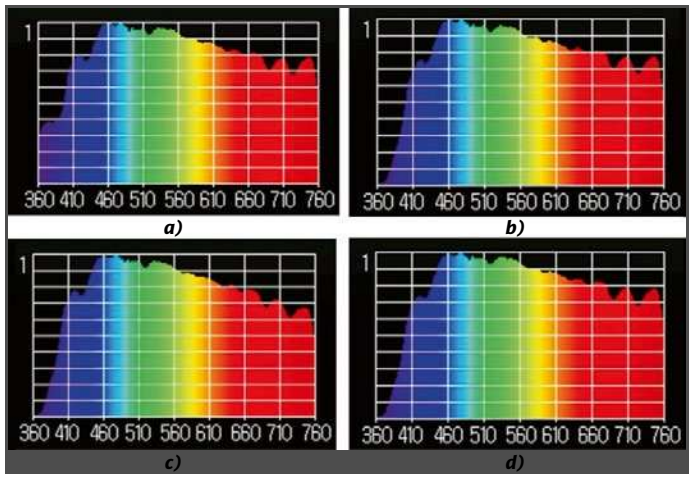

Fig. 3. Relative spectral distribution of radiant energy (as of the moment of measurement): *a*) natural daylight at the moment of measurement, T_{aver} = 5850 K, R_a = 99; *b)* at output of the system with *Alanod miro Silver 4270AG* reflective material; T_{aver} = 5850 K, R_a = 99; *c)* at output of the system with *Alanod miro Silver 4400GP* reflective material, T_{aver} = 5900 K, R_a = 99; *d*) at output of the system with *Alanod miro Silver 4400AG* reflective material, T_{aver} = 5750 K, R_a = 99

• Reflective tube: based on vacuum-deposited silver coated with silicon oxide SiO_2 with low refractive index and titanium oxide TiO_2 with high refractive index;

• Diffuser: transparent acrylic sheet with coarse texture (*Acryl 92-W*) made of PMMA *Plexiglass XT 0A000 Z* (by means of laser cutting).

3. METHOD FOR LIGHT SPECTRAL DISTRIBUTION EVALUATION

The measurements were made:

1. On 01.10.2014, at the latitude of Moscow, at 14:00–14:15 Moscow time, south-easterly, horizon angle of 60°, average illuminance of (5300–5500) lx and cloud cover of about 8 oktas, within the range of λ of (360–760) nm;

2. By means of standard calibrated mobile spectrometer *MK 350* (by *URPtek*, Taiwan); measured parameters: relative spectrum distribution of radiation, correlated colour temperature $T_{cp,}$ and general colour rendering index R_a at input and output of the system; for each object, 5 measurements were made.

The measurements were made for 3 variants of the material of *Solarway* system light guide tube: *Alanod miro Silver 4270AG*; *Alanod miro Silver 4400GP* and *Alanod miro Silver 4400AG.*

The dimensions of the light-guide tube model are as follows: length of 200 mm and diameter of 90 mm (Fig. 2).

Measured values of T_{cp} of natural outdoor lighting varied within the range of

(5750–5900) K and values of T_{cp} at output of the tube of *Alanod miro Silver 4270AG*, *Alanod miro Silver 4400AG* and *Alanod miro Silver 4400GP* were 5850 K, 5750 K and 5900 K respectively.

The study started with measurement of relative spectrum of natural daylight radiation and was continued for three variants of material of the light guide reflective tube at output. The results of this part of the study are presented in Fig. 3 and Table 1.

According to Table 1 and Fig. 4, relative radiation spectrum at output of the light-guide systems is almost equal to that at input.

Fig. 4 demonstrates that, within the λ range of (435–760) nm, relative spectra of radiation of systems with *Alanod miro Silver 4270AG*-based and *Alanod miro Silver 4400AG*-based light guide are equal to relative spectrum of radiation (natural) at input whereas relative spectrum of radiation of the *Alanod miro Silver 4400GP*-based system is slightly lower in the right part of this range.

Table 1. Relative Spectral Distribution of Energy of Daylight Radiation at Input and Output of the Light Guide Systems

Wavelength, nm	Input	Alanod miro Silver 4270AG light guide	Alanod miro Silver 4400GP light guide	Alanod miro Silver 4400AG light guide
385	0.39	0.21	0.23	0.21
390	0.41	0.29	0.31	0.28
400	0.60	0.51	0.56	0.50
410	0.75	0.68	0.72	0.66
420	0.79	0.75	0.77	0.73
430	0.76	0.74	0.75	0.73
440	0.88	0.86	0.86	0.85
450	0.97	0.97	0.96	0.95
460	0.99	0.99	0.99	0.98
470	0.98	0.98	0.98	0.98
480	0.99	0.99	0.99	0.99
490	0.95	0.95	0.95	0.96
500	0.96	0.96	0.96	0.96
510	0.95	0.95	0.95	0.93
520	0.92	0.92	0.92	0.93
530	0.96	0.96	0.96	0.97
540	0.96	0.96	0.95	0.97
550	0.96	0.95	0.94	0.96
560	0.92	0.92	0.91	0.93
570	0.90	0.89	0.89	0.90
580	0.90	0.89	0.89	0.90
590	0.87	0.87	0.86	0.88
600	0.87	0.87	0.86	0.88
610	0.86	0.86	0.85	0.87
620	0.83	0.83	0.82	0.85
630	0.81	0.81	0.80	0.83
640	0.83	0.83	0.81	0.84
650	0.80	0.80	0.78	0.81
660	0.80	0.79	0.77	0.81
670	0.81	0.80	0.78	0.82
680	0.78	0.78	0.75	0.79
690	0.70	0.70	0.67	0.71
700	0.76	0.76	0.71	0.77
710	0.78	0.77	0.71	0.78
720	0.68	0.68	0.62	0.69
730	0.71	0.70	0.63	0.71
740	0.77	0.76	0.67	0.77
750	0.77	0.76	0.66	0.77

Table 2. Spectral Characteristics of Reflective Material of the Light Guide Lighting Systems

Parameters	Technology based on *DF2000MA* polymer film coated by laminating (*Solatube*)	Technology based on *DF2000MA* polymer film coated by laminating (*Solarspot*)	Technology based on vacuum-deposited silver coated with silicon and titanium oxides (*Solarway*)
Integral reflectance of reflective material	99.7 %	99.7 %	Alanod miro Silver 4270AG → 99.8 % Alanod miro Silver 4400AG → 99.8 % Alanod miro Silver 4400GP → 99.8 %

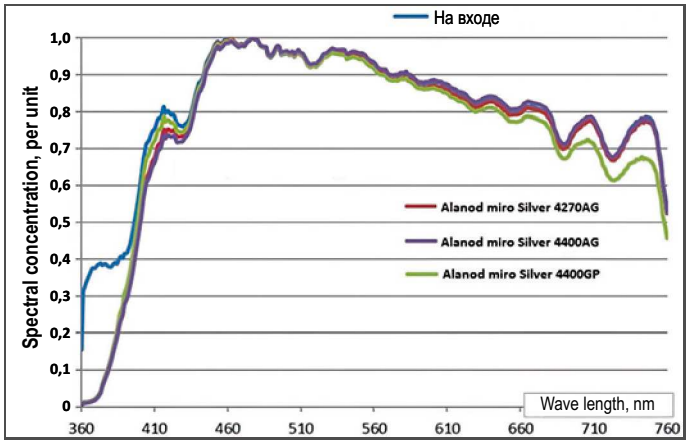

Fig. 4. Graphs of spectra of relative spectral distribution of daylight radiation distributon at input and output of the *Solarway* system with *Alanod miro Silver 4270AG*, *Alanod miro Silver 4400GP* and *Alanod miro Silver 4400AG* variants of light reflecting material

Within the wavelength range (360–410) nm, all these three variants of reflecting material have spectral deviations from the natural daylight radiation due to the fact that acrylic materials contain UV-absorbing photostabilizers protecting acrylic polymer from destructive effect of UV radiation. These spectral differences do not constitute a significant disadvantage since human eye is low sensitive in this range of wavelength. The latter is also proved by the fact that, according to our measurements, all three variants provide maximum possible value of R_a inherent for daylight at output of the system, which is about 99[1].

Integral reflectance of all three variants of reflective material of the *Solarway* system is at the same level as, or higher than, that of microstructure polymer film of the compared light-guide system (Table 2).

Let us consider the differences between manufacturing technologies of these reflecting materials:

Reflective microstructure polymer film is manufactured by depositing dissolved silver and other metals on its base and their further binding by an interferential layer. The film is glued to aluminium base. Application of *DF2000MA* reflective film as a reflective material of light transportation systems [4] is associated with relative risk and special operation conditions: it should not be used as a reflector for sources of radiation without UV-absorbing filter [4]; its operating temperature should be equal to (22–49)°C; when using intensive sources of radiation like light emitting diodes, a protective structure minimising radiant exposure and film heating should be also designed. (Such sources of radiation may cause modification and darkening of its surface.) The basic models showed that first modifications of surface colour begin after reaching the value of radiant exposure of 50 kJ/mm² within the wavelength range (420–500) nm at film temperature of 50 °C.

MiroSilver specular reflective material is produced by depositing vaporized silver on aluminium base and its binding by SiO_2 and TiO_2 oxides. In this case, no glue is used.

Unlike deposited silver, the film material may sometimes be not appropriate due to delamination

[1] If necessary, these differences between natural radiation and output radiation of light guide systems may be slightly reduced by manufacturing the lower diffuser which does not require UV protection of acryl without UV-absorbing additives.

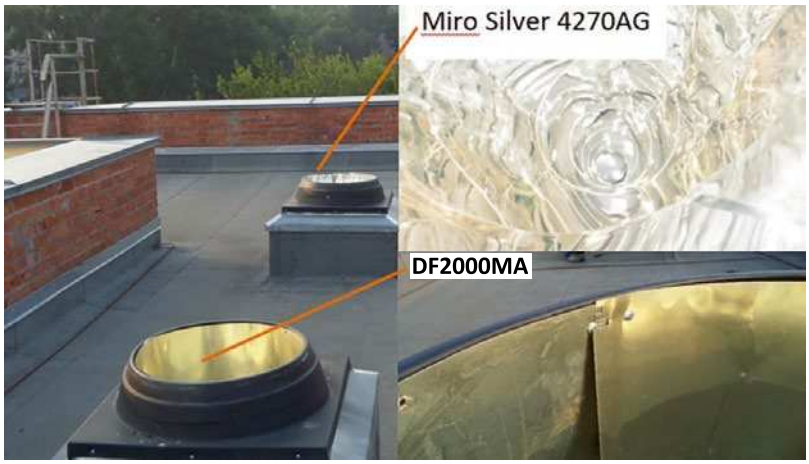

Fig. 5. Appearance of light guides of the two compared systems (2013 variant)

Fig. 6. Appearance of the reflective tube of the light guide based on *DF2000MA* polymer film after a certain period of operation without UV-absorbing filter

of film which lowers characteristics of transmission of natural daylight.

Another one problem of the study was to research the effect of UV radiation on the elements of the *Solarway* system.

In 2016, technical maintenance of the light guides was conducted (4 years after installation). One of them contained *DF2000MA* reflective film material and the other contained the material based on vacuum-deposited silver coated with SiO_2 and TiO_2 oxides (Fig. 5). The domes for both systems were made of PMMA without UV protection. In 4 years, *DF2000MA* reflective material became completely yellow (Fig. 6). However, even yellow material reflects almost the whole spectrum of light with distortions in the yellow, red or green regions of the spectrum but these distortions are not seen but human eye.

PMMA is used for production of light guide domes. This material cuts off most of input UV radiation (at least 72.5 %), however, even a non-significant fraction of this radiation leads to yellowing of reflective material. For additional blocking of this radiation, anti-condensation disc (thermal barrier) also made of PMMA is used in some systems.

Ground UV radiation, mostly within the wavelength range (300–400) nm, getting inside the light guide with *Alanod miro Silver 4400AG*, *Alanod miro Silver 4270AG,* or *Alanod miro Silver 4400GP* reflective materials, does not affect their silver coating adversely since it is almost completely reflected.

Then comparative studies of optical elements of our light guide system *Solarway* (*Solargy SW 250* model, light guide diameter of 250mm) and the light guide system based on *DF2000MA* polymer film (*Solatube 290DS* model, light guide diameter of 350mm) were conducted[2]. The measurements were made by means of *DT-1309* illuminance meter with measurement range of $(1\times10^{-1}–4\times10^{5})$ lx on February 27, 2017 under overcast sky with cloud cover of (8–10) oktas.

Efficiency of the light guide system may be justified based on integrated transmittance τ_o calculated using daylight factor calculation methodology for sidelight systems with different building arrangement schemes in urban development conditions as well as for premises with overhead (by means of lanterns with different designs) and combined (overhead and side) natural lighting systems [11]:

$$\tau_o = \tau_1 \cdot \tau_2 \cdot \tau_3 \cdot \tau_4 \, \tau_5,$$

[2] Length and diameter of light guides make no difference as measurements were made without a reflective tube.

Table 3. Comparative, Declared by the Manufacturer, Characteristics of Optical Elements of Light Guide Lighting Systems Without Reflective Tubes

Characteristics	Technology based on *DF2000MA* polymer film (*Solatube 290 DS*)	Technology based on vacuum-deposited silver coated with silicon and titanium oxides (*Solargy SW 250*)
Light collector and dome manufacturing technology Transmittance τ_1	PC or PMMA, *Plexiglass* casting method (Germany) 0.83 [6] or 0.92	PMMA, vacuum moulding method, *Plexiglass* (Germany) 0.92
Diffuser Transmittance τ_4	*Dual Diffuseur Optiview®* *Dual Diffuseur Vusion®* 0.82 or 0.79	PMMA, *Plexiglass XT 0A000Z* laser cutting (Germany), 0.90
Integrated transmittance τ_0 (τ_2 = 0.9, τ_4 = 0.9, τ_5 = 1.0, taken equal for both systems)	0.55 or 0.58	0.67
Factors	High shock resistance UV radiation integral transmittance of 72.5 %	High shock resistance UV radiation integral transmittance of 72.5 %

Table 4. Comparison of Output Illuminance (lx) of Light Guide Elements (Without Reflective Tube) of *Solargy SW* and *Solatube 290 DS* Systems

System element name	Solatube 290 DS			Solargy SW 250		
	Without element	With element	Element(s) integral transmission	Without element	With element	Element(s) integral transmission
Dome	23,750	15,675	0.66	24,235	23,265	0.96
Thermal barrier	no	no	–	23,563	21,910	0.93
Diffuser	24,255	20,130	0.82	23,900	21,271	0.89
All elements simultaneously and sequentially arranged above each other	21,455	11,753	0.55	21,205	16,498	0.77

where τ_1 is the transmittance of material (system) defined using [11, Table B.7]; τ_2 is the coefficient of light losses at light opening sashes also defined using [11, Table B.7] (light opening dimensions are taken equal to dimensions of sash box based on external measurement); τ_3 is the coefficient of light losses on load bearing structures defined using [11, Table 8] (τ_3 =1 for side lighting); τ_4 is the coefficient of light losses at sunlight-protecting devices defined in accordance with [11, Table B.8]; τ_5 is the coefficient of light losses in protecting net installed above lanterns taken equal to 0.9 [11].

Table 3 demonstrates that the declared values of τ_o without consideration of reflective tube for the compared models *Solargy SW 250* and *Solatube 290 DS* equal to 67 % and 58 % respectively.

It follows from Table 4 that total optical losses amount to 45 % in elements of *Solatube 290 DS* and 23 % in elements of *Solargy SW*. Therefore, in *Solatube 290 DS* major optical losses are associated with its optical elements. This allows a definitive conclusion to draw: the level of light transmission of the elements of the developed system is 1.4 times higher than that of the compared *Solatube* system.

4. CONCLUSION

Comparative study of light guide lighting systems based on *DF2000MA* polymer film and on vacuum-deposited silver coated with silicon and titanium oxides are conducted. Spectral measurements demonstrated slight advantage of the developed *Solarway* system in terms of integral reflective ability of reflective tube reflective material. The *Solarway* system was studied for three variants of *Alanod miro Silver* reflective material. Chromaticity of *Solarway* output light within the λ range of (410–760) nm is absolutely identical to input natural day-

light for two of them, *Alanod miro Silver 4270AG* and *Alanod miro Silver 4400AG* and is close to natural daylight for the third one, *Alanod miro Silver 4400GP*, being slightly less in the far-red region of wavelength (660–760) nm. In the violet range of λ (385–410) nm, all variants of *Alanod miro Silver* cause non-significant optical losses.

In general, according to measurements, the reflective tube with *Alanod miro Silver* transmits natural daylight (within the range of λ (385–750) nm) almost completely and without spectral distortions.

The reflective material of the designed *Solarway* system demonstrated its advantage in terms of service life (without UV radiation protection) over *DF2000MA* film material: 25 years and 10 years respectively. Moreover, unlike multi-polymer film, it is reliable (does not delaminate) in northern climatic areas of the Russian Federation.

Comparison of some light-engineering characteristics of optical elements of the designed system (*Solarway*) and the marketed one (*Solatube*) demonstrated significant advantage of the former.

REFERENCES

1. URL: http://www.solarway.su/ (date of reference: 26.04.2019).

2. Palagin, A.V., Sterkhov, A.I., Korepanov, E.V.. Comparison of Functional and Energy Factors of Natural Daylight Lighting Systems of Buildings [Sravneniye sistem estestvennogo osvachsheniya zdaniy po funktsionalno-energeticheskim faktoram] // Intellektualniye sistemy v proizvodstve, 2014, Vol. 2 (24), pp. 191–194.

3. Solovyov, A.K. Hollow Tube Light Guides and their Application for Natural Lighting of Buildings [Polyiye trubchatyie svetovody i ikh primeneniye dlya estestvennogo osveshcheniya zdaniy] // Promyshlennoye i grazhdanskoye stroitelstvo, 2007, Vol. 2, pp. 53–55.

4. URL: https://multimedia.3m.com/mws/media/982449O/3mtm–specular–film–df2000ma–technical–data–sheet.pdf (date of reference: 26.04.2019).

5. URL: http://www.napcso.hu/my_content/dok/CSTB_Report_2011.pdf (дата обращения: 26.04.2019).

6. URL: http://www.cstb.fr/pdf/atec/GS06–G/AG142204.pdf (date of reference: 26.04.2019).

7. URL: http://www.bibliorossica.com/book.html?currBookId=10063 (date of reference: 26.04.2019).

8. URL: https://solarspot.co.uk/wp–content/uploads/2018/01/BRE–Testing–of–light–tubes.pdf (date of reference: 26.04.2019).

9. URL: http://www.casaportale.com/public/uploads/relazione_ebner.pdf (date of reference: 26.04.2019).

10. URL: http://www.geinnovations.net/solarspot-news_court.html (date of reference: 26.04.2019).

11. SP 23–102–2003 “Design and Construction Regulations. Natural Lighting of Residential and Public Buildings”.

Alexei I. Sterkhov, engineer. Graduated from Izhevsk GTU in 2009. Technical director of Solargy group LLC. Research interests: lighting, energy saving, light guides

Alexander V. Palagin, engineer. Graduated from Izhevsk GTU in 2009. Chief Researcher of Solargy group LLC. Research interests: lighting, energy saving, light guides

Igor Yu. Loshkarev, Ph.D. in Technical Sciences. In 1993, graduated from Saratov M.I. Kalinin Agriculture Mechanisation Institute (winner of the Mark of Honour award). Associate professor of the Engineering Physics, Electric Equipment and Technologies sub-department of N.I. Vavilov Saratov State Agricultural University. Research interests: lighting, energy saving, light guides

Light & Engineering
Vol. 28, No. 2, pp. 61–66, 2020

https://doi.org/10.33383/2019-034
Svetotekhnika #6, 2019, pp. 14–18

CHANGES IN IRRADIANCE AND ILLUMINANCE ON EARTH SURFACE DURING 11-YEAR SOLAR ACTIVITY CYCLE

Alexander V. Leonidov

E-mail: avleonidoff@mail.ru

ABSTRACT

The article formulates the analytic expression approximating the sequence of Gregorian 11-year solar cycles and the expression of solar activity within one cycle. The dependences of effective thermodynamic temperature of the Sun photosphere and the solar constant, and the solar illuminance constant at the upper border of Earth atmosphere on the year number within one solar cycle were obtained. The generalised analytic expression for integral transmittance of atmosphere (within its spectral window) on the Earth surface for the direct and diffuse components of solar radiation and their sums at different solar altitude angles is presented. The analytic expressions of dependences of irradiance and illuminance on the Earth surface within spectral window of atmosphere and within the visible region of solar radiation spectrum on the year number within a certain solar cycle at different solar altitude angles are obtained. The results of calculation of direct and diffuse components of irradiance and illuminance and their sums in the case of clear sky are presented for example. The proposed approach allows similar calculations to conduct for different types of sky cover.

Keywords: 11-year solar cycle, solar constant, solar illuminance constant, solar altitude angle, cyclic changes, direct and diffuse components of irradiance and illuminance, Earth surface

The 11-year solar activity cycle significantly effects energy and light and engineering characteristics of solar radiation (SR) on the Earth surface and defines the nature of all aspects of human activities to a large extent.

The changes of SR in the visible region of spectrum in the spectral window of Earth atmosphere (SWAT) affect daily activity of human neuroendocrine system defining the diurnal rhythms of all biological systems of body. Changes of diurnal rhythms cause changes of daily intellectual activity of human including, in particular, the process of visual perception and building of sensing model of surrounding objects on the basis of it as well as concrete and abstract thinking.

By now, the 11-year cyclic changes in irradiance and illuminance on the Earth surface reaching 30 % and significantly affecting visual perception processes have not been considered in light engineering practice.

This work aims at obtaining analytic expressions describing 11-year cyclic changes in a number of energy (radiometry) and light engineering (photometry) characteristics in different spectral regions of SR at different solar altitude angle[1].

Solar activity is measured by solar activity index characterised by the Wolf number $W = k(10g + s)$, where s is the number of individual spots on the

[1] It was assumed that the obtained results might be:

– Used in studies and forecasts of conscious and unconscious reactions of human body to cyclic changes of solar radiation characteristics including those related to operation of human vision system;

– Taken into account in works for standardization of natural indoor lighting not only for comfortability of visual performance but also for prevention and/or elimination of deviations in human body circadian systems (necessity of such works is demonstrated in the recent review [1]).

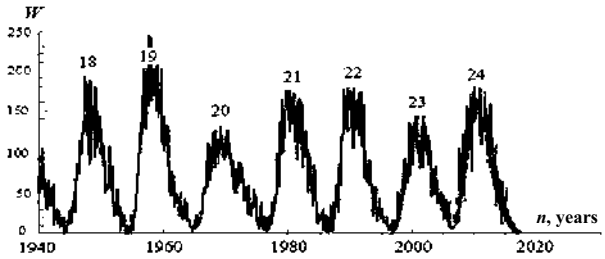

Fig. 1. Wolf number W dependence on the time in Gregorian calendar (numbers 18–24 mark solar cycles from 1940 to 2019 [3–5])

Sun photosphere surface, g is the number of sunspot groups and k is the factor usually taken equal to one [2, 3].

W and its dependence on time characterise the main and the most pronounced 11-year solar cycle, the Schwabe cycle (Fig. 1). Significantly less pronounced cycles (in particular, the 22-year Hale cycle) will not be taken into account.

During minimum solar activity periods, W (= $W_{\min}$) is virtually constant and equals to 0–15. On the contrary, maximum solar activity is characterised by variability of W (= $W_{\max}$) equal to 120–250. For the purposes of this article, the values of $W_{\min}$ = 10 and $W_{\max}$ = 180 averaged over the period from 1940 to 2019 were taken. Moreover, solar activity wave front and fall times were taken equal to each other, which does not cause significant error in the obtained results and allows us to approximate the dependence of W on year number N (with taken assumptions) by means of a sinusoidal function:

$$W(N) = W_{\text{aver}}\left\{1 + 0{,}895 \cdot \sin\left[\frac{2\pi(N-1755)}{11} - \frac{\pi}{2}\right]\right\}, \quad (1)$$

where $W_{\text{aver}} = 0.5(W_{\min} + W_{\max})$, 1755 is the year of minimum solar activity (beginning of the zero cycle) and close to the year of start of regular studying of cyclic changes of solar activity (~1749).

Dependence of W on year number n within a certain 11-year cycle of solar activity has the following form:

$$W(n) = W_{\text{aver}}\left[1 + 0{,}895 \cdot \sin\left(\frac{2\pi n}{11} - \frac{\pi}{2}\right)\right]. \quad (2)$$

The $W(n)$ dependency graph based on the expression (2) is presented in Fig. 2.

Cyclic changes in W lead to cyclic change of the Sun photosphere radiant luminocity M_{eS} [$T_{\text{eff}}(n)$], where T_{eff} is the equilibrium effective thermodynamic temperature of the Sun photosphere radiation. The Planck's radiation model used in the most cases as the model of the Sun photosphere radiation [6, 7] with spectral radiance of m_{eS} (λ, T_{eff}) is expressed as

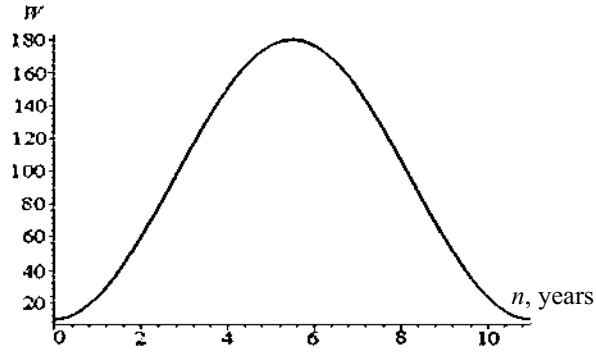

Fig. 2. Changes in Wolf number W within a certain 11-year solar cycle

$$m_{eS}(\lambda, T_{eff}) = C_1 \lambda^{-5}\left(\exp\frac{C_2}{\lambda T_{eff}} - 1\right)^{-1}, \quad (3)$$

where $C_1 \approx 3.742 \cdot 10^{-16}$ Wm^2 and $C_2 \approx 1.439 \cdot 10^{-2}$ mK.

At that:

– Availability of absorption spectral lines in the Sun photosphere radiation spectrum (Fraunhofer lines) [8] and in the Earth atmosphere is significant only for spectroscopy but do not significantly affect results of light engineering calculations;

– It is obvious that T_{eff} is a function of n in (3). Nevertheless, in accordance with the recommendations of the International Radiation commission [9], in (3) and in the integral of m_{eS} (λ, T_{eff}) over λ in the form of M_{eS} (T_{eff}), luminosity of dependence $T_{\text{eff}}(n)$ is not taken into account and the value of T_{eff} is taken equal to a certain constant, which does not allow us to define dependences of energy and light-engineering characteristics of SR on the Earth surface (ES) on n.

As a basis for determination of these dependencies on the Earth surface, the value of solar constant $E_{\text{e.SC}}$ (T_{eff}) in the form

$$E_{e.SC}(T_{eff}) = \int_0^\infty e_{eS}(\lambda, T_{eff})\,d\lambda = \left(\frac{r}{R}\right)^2 \int_0^\infty m_{eS}(\lambda, T_{eff})\,d\lambda, \quad (4)$$

was used, which is the irradiance of an area located on the upper border of Earth atmosphere with nor-

Table 1. Values of Solar Constant in Different Spectral Regions and Solar Illuminance Constant at Minimum and Maximum Solar Activity

Nature of solar activity	$E_{e.SC}$, Wm^{-2}			$E_{v.SC}$, lx
	at $0 \le \lambda \le \infty$ nm	at $300 \le \lambda \le 1200$ nm	at $350 \le \lambda \le 770$ nm	at $350 \le \lambda \le 770$ nm
Minimum	1106.3	838.7	514.0	135110
Maximum	1369.2	1057.4	665.8	173600
Average	1237.7	948.1	589.9	154355

mal incidence of SR. Here, e_{eS} (λ, T_{eff}) is the spectral irradiance on the border of Earth atmosphere, $r = 6.96 \cdot 10^5$ km is the equatorial radius of the Sun, $R = 1.496 \times 10^{12}$ km is the radius of the Earth circular orbit [7].

According to the data of satellite actinometric measurements referring to maximum values of solar cycles 20 and 21, the most probable value of $E_{e \cdot SC}$ (T_{eff}) is 1368–1377 Wm^{-2} provided there are no regular temporal changes, which allows us to use the term "solar constant". The value $E_{e \cdot SC,\ max}(T_{eff}) \approx 1370$ Wm^{-2} taken from the 1956 International Pyrheliometric Scale [7, 9] is taken as a standard value of this indicator. According to (3) and (4), this value corresponds with the value $T_{eff,\ max} = 5780$ K.

Solar illuminance constant $E_{v \cdot SC}$ may be expressed in accordance with (4) as

$$E_{v.SC}\left(T_{eff}\right) = 683 \int_{350}^{770} e_{eS}(\lambda, T_{eff}) V(\lambda) d\lambda = \left(\frac{r}{R}\right)^2 683 \int_{350}^{770} m_{eS}(\lambda, T_{eff}) V(\lambda) d\lambda, \quad (5)$$

and it is the irradiance of an area located on the upper border of Earth atmosphere with normal incidence of SR. In conditions of minimum solar activity, $E_{v.SC} = E_{v.SC,\ min} = 135110$ lx [10, 11], which corresponds with values of $E_{e \cdot SC,\ min}$ of 1106 Wm^{-2} and $T_{eff,\ min}$ of 5480 K. In accordance with (3) and (4), the previously defined value $E_{SC,\ max} \approx 1370$ Wm^{-2} with $T_{eff,\ max} = 5780$ K corresponds to the value $E_{v.SC,\ max} = 173600$ lx.

With known $T_{eff,\ min}$ and $T_{eff,\ max}$, the dependence $T_{eff}(n)$ within a certain 11-year solar cycle is expressed as

$$T_{eff}(n) = T_{eff,\ aver}\left[1 + 0{,}027 \cdot \sin\left(\frac{2\pi n}{11} - \frac{\pi}{2}\right)\right], \quad (6)$$

where $T_{eff,\ aver} = 0.5(T_{eff,\ min} + T_{eff,\ max})$. The chart of this dependence is shown in Fig. 3 and $E_{e.SC,\ min}$ and $E_{e.SC,\ max}$ in different spectral regions are shown in Table 1.

According to (4), with calculated values of $E_{e.SC,\ min}$ and $E_{e.SC,\ max}$ for spectral regions (0–∞) nm, (300–1200) nm (SWAT [7, 12]) and the visible spectrum (350–770) nm in SWAT, dependencies $E_{e.SC}(n)$ have the following form

$$E_{e.SC}(n) = E_{e.SC,\ aver}\left[1 + 0{,}1062 \cdot \sin\left(\frac{2\pi n}{11} - \frac{\pi}{2}\right)\right]$$

at $0\ \text{nm} \le \lambda \le \infty$ nm, (7)

$$E_{e.SC}(n) = E_{e.SC,\ aver}\left[1 + 0{,}1153 \cdot \sin\left(\frac{2\pi n}{11} - \frac{\pi}{2}\right)\right]$$

at $300\ \text{nm} \le \lambda \le 1200$ nm, (8)

$$E_{e.SC}(n) = E_{e.SC,\ aver}\left[1 + 0{,}1287 \cdot \sin\left(\frac{2\pi n}{11} - \frac{\pi}{2}\right)\right]$$

at $350\ \text{nm} \le \lambda \le 770$ nm, (9)

where $E_{e.SC,\ aver} = 0{,}5(E_{e.SC,\ min} + E_{e.SC,\ max})$. The values of $E_{e.SC,\ aver}$ for each spectral region are shown in the last line of Table 1 and the graphs of dependencies (7)–(9) are shown in Fig. 4.

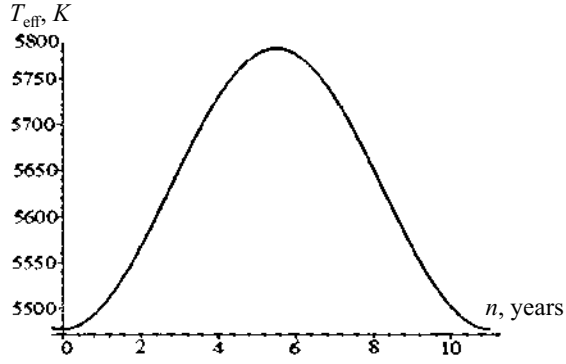

Fig. 3. Changes in effective thermodynamic temperature of Sun photosphere radiation T_{eff} within a certain 11-year solar cycle

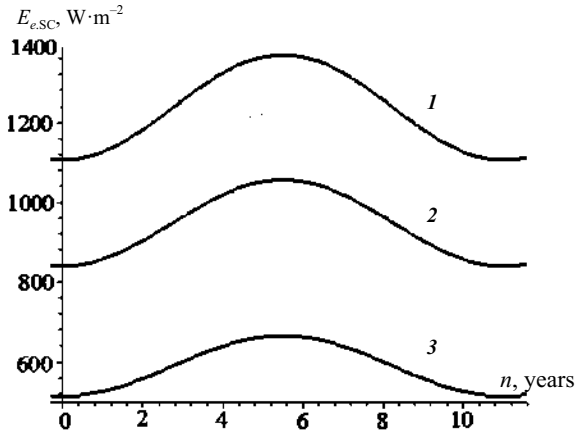

Fig. 4. Changes in solar constant $E_{e.SC}$ in different spectral regions of solar radiation within a certain 11-year solar cycle: (0–∞) nm (*1*), (300–1200) nm (*2*), (350–770) nm (*3*)

According to (5), the dependence $E_{v\cdot SC}(n)$ within a certain 11-year solar cycle has the following form

$$E_{v.SC}(n) = E_{v.SC,aver}\left[1 + 0{,}1247 \cdot \sin\left(\frac{2\pi n}{11} - \frac{\pi}{2}\right)\right], \quad (10)$$

where the value of $E_{v\cdot SC,\,aver}$ is given in the last column of Table 1 and the graph is shown in Fig. 5.

Since SR is distributed in SWAT of (300–1200) nm [7, 12], for determination of irradiance, $E_{e.ES}(n)$, and illuminance, $E_{v.ES}(n)$, on the Earth surface in the visible spectrum of (350–770) nm requires only to take integral transmittance of atmosphere into account.

Since direct solar radiation generates the direct and the diffuse components of SR, let us consider two integral coefficients of atmosphere transmittance corresponding to them, τ_{dir} and τ_{diff}, which depend on solar altitude angle h in a calculated point of Earth surface. Availability of dependencies $\tau_{dir}(h)$ and $\tau_{diff}(h)$ causes availability of corresponding dependencies $T_{eff,\,dir}(h)$ и $T_{eff,\,diff}(h)$, $e_{eS,\,dir}[\lambda, n, T_{eff}(h)]$, $e_{eS,\,diff}[\lambda, n, T_{eff}(h)]$, $E_{e.ES,\,dir}(n, h)$, $E_{e.ES,\,diff}(n, h)$, $E_{v.ES,\,dir}(n, h)$ and $E_{v.ES,\,diff}(n, h)$.

The analysis of data [13] showed that, in different conditions of sky cover (including clear sky) and the surface, the expressions for $E_{e.ES,\,dir}(n, h)$, $E_{e.ES,\,diff}(n, h)$, $E_{v.ES,\,dir}(n, h)$ и $E_{v.ES,\,diff}(n, h)$ with any n of a certain solar cycle (e.g. at n = 0 or 11 corresponding to minimum solar cycle) may be expressed in general form

$$E_{ES}(h) = a\left[1 + \sin(bh - c)\right]. \quad (11)$$

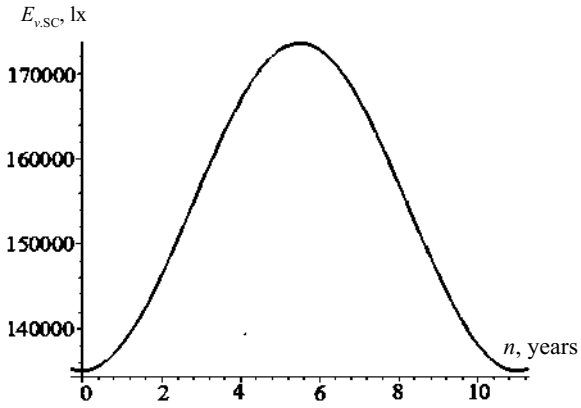

Fig. 5. Changes in solar illuminance constant $E_{e.SC}$ in visible spectrum within a certain 11-year solar cycle

The values of $E_{ES}(90^o)$ for all types of sky cover and for clear sky are defined by approximating data [13] by the expression (11) with further extrapolation up to the value $h = 90^o$.

It is obvious that expressions of dependencies $\tau_{dir}(h)$ and $\tau_{diff}(h)$ have general form

$$\tau(h) = 0{,}5 \cdot \tau(90^o) \cdot \left[1 + \sin(bh - c)\right], \quad (12)$$

where $\tau(90^o)$ is the integral coefficient of atmosphere transmittance for normal incidence of solar radiation on Earth surface in SWAT and visible spectrum at the equatorial latitude during the vernal and autumnal equinoxes and equal to ratios $E_{v.ES,\,min}(90^o) / E_{v.SC,\,min}(90^o)$ or, respectively, $E_{e.ES,\,min}(90^o) / E_{e.SC,\,min}(90^o)$.

With consideration of the expression (11), the values of $E_{e.ES,\,dir}(n, h)$, $E_{e.ES,\,diff}(n, h)$, $E_{v.ES,\,dir}(n, h)$ and $E_{v.ES,\,diff}(n, h)$ for different types of sky cover and different degree of sky cover in visible spectrum are described as

$$E_{e.ES\,i,j}(n,h) = E_{e.SC}(n) \cdot \tau_{i,j}(h), \quad (13)$$

$$E_{v.ES\,i,j}(n,h) = E_{v.SC}(n) \cdot \tau_{i,j}(h), \quad (14)$$

where i and j indices correspond to different types and degrees of sky cover respectively.

As an example, Table 2 contains the values of $E_{e.ES,\,dir}(n)$, $E_{e.ES,\,diff}(n)$, $E_{v.ES,\,dir}(n)$ and $E_{v.ES,\,diff}(n)$ without sky cover in SWAT and in visible region in conditions of minimum and maximum solar activity.

The data shown in Table 2 is obtained using the values $\tau_{dir}(90^o) = 0.729$ and $\tau_{diff}(90^o) = 0.205$ for clear sky after approximation and further extrapolation of data [13].

Table 2. Direct and Diffuse Irradiance and Illuminance on the Earth Surface at Minimum and Maximum Solar Activity without Sky Cover in Spectral Window of Atmosphere Transparency and in Visible Spectrum

Nature of solar activity	At $300 \le \lambda \le 1{,}200$ nm		At $350 \le \lambda \le 770$ nm		At $350 \le \lambda \le 770$ nm	
	$E_{e.ES,\,dir}$, Wm^{-2}	$E_{e.ES,\,diff}$, Wm^{-2}	$E_{e.ES,\,dir}$, Wm^{-2}	$E_{e.ES,\,diff}$, Wm^{-2}	$E_{v.ES,\,dir}$, lx	$E_{v.ES,\,diff}$, lx
Minimum	611.2	172.3	374.6	105.6	98470	27750
Maximum	770.6	217.2	485.2	136.8	126520	35660
Average	690.9	194.7	429.9	121.2	112490	31700

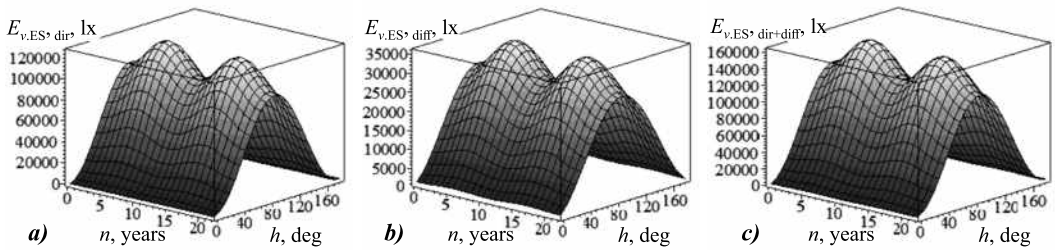

Fig. 6. Dependencies of direct (*a*) and diffuse (*b*) components of illuminance on the Earth surface and their sum (*c*) on solar angle latitude *h* and year number *n* within two 11-year solar cycles

In conditions of clear sky, in SWAT (300–1200) nm, the dependences $E_{e.ES,\,dir}(n,\,h)$, $E_{e.ES,\,diff}(n,\,h)$ and their sum $E_{e.ES,\,dir+diff}(n,\,h)$ have the form

$$E_{e.ES,\,dir}(n,h) = 0{,}5E_{e.ES,\,aver}\left[1+\sin\left(0{,}035h-1{,}473\right)\right]\times \times\left[1+0{,}1153\sin\left(\frac{2\pi n}{11}-\frac{\pi}{2}\right)\right], \quad (15)$$

$$E_{e.ES,\,diff}(n,h) = 0{,}5E_{e.ES,\,aver}\left[1+\sin\left(0{,}030h-1{,}094\right)\right]\times \times\left[1+0{,}1153\sin\left(\frac{2\pi n}{11}-\frac{\pi}{2}\right)\right], \quad (16)$$

$$E_{e.ES,\,dir+diff}(n,h) = E_{e.ES,\,dir}(n,h)+E_{e.ES,\,diff}(n,h). \quad (17)$$

The values of $E_{e.ES,\,aver}$ in (15)–(17) and the following expressions (18)–(23) are shown in the last line of Table 2.

In the spectral region of (350–770) nm for clear sky, the similar dependences and their sum have form

$$E_{e.ES,\,dir}(n,h) = 0{,}5E_{e.ES,\,aver}\left[1+\sin\left(0{,}035h-1{,}473\right)\right]\times \times\left[1+0{,}1287\sin\left(\frac{2\pi n}{11}-\frac{\pi}{2}\right)\right], \quad (18)$$

$$E_{e.ES,\,diff}(n,h) = 0{,}5E_{e.ES,\,aver}\left[1+\sin\left(0{,}030h-1{,}094\right)\right]\times \times\left[1+0{,}1287\sin\left(\frac{2\pi n}{11}-\frac{\pi}{2}\right)\right], \quad (19)$$

$$E_{e.ES,\,dir+diff}(n,h) = E_{e.ES,\,dir}(n,h)+E_{e.ES,\,diff}(n,h). \quad (20)$$

In the spectral region of (350–770) nm for clear sky, the dependences $E_{v.ES,\,dir}(n,\,h)$ and $E_{v.ES,\,diff}(n,\,h)$ have form

$$E_{v.ES,\,dir}(n,h) = 0{,}5E_{v.ES,\,aver}\left[1+\sin\left(0{,}035h-1{,}473\right)\right]\times \times\left[1+0{,}1247\sin\left(\frac{2\pi n}{11}-\frac{\pi}{2}\right)\right], \quad (21)$$

$$E_{v.ES,\,diff}(n,h) = 0{,}5E_{v.ES,\,aver}\left[1+\sin\left(0{,}030h-1{,}094\right)\right]\times \times\left[1+0{,}1247\sin\left(\frac{2\pi n}{11}-\frac{\pi}{2}\right)\right], \quad (22)$$

$$E_{v.ES,\,dir+diff}(n,h) = E_{v.ES,\,dir}(n,h)+E_{v.ES,\,diff}(n,h). \quad (23)$$

As an example, Fig. 6 shows the graphs of dependencies $E_{v.ES}(n,\,h)$ based on expressions (21)–(23) within two cycles of solar activity.

The forms of the graphs of dependencies $E_{e.ES}(n,\,h)$ based on (15)–(20) are similar to the forms of the graphs shown in Fig. 6 but with minimum and maximum values of $E_{e.ES}$ presented in Table 2.

This approach allows us to obtain similar results for nine types of sky cover (A_c, C_b, C_c, C_i, C_s, C_u, N_s, S_c, S_t) and for four values of sky cover degree considered in [13].

The obtained results allow us to clarify changes of energy and light-engineering characteristics of SR on the Earth surface at any date of a certain year within an 11-year solar cycle as well as to increase accuracy of calculations of natural irradiance and illuminance on the Earth surface.

REFERENCES

1. Stanislav Darula "Review of the Current State and Future Development

in Standardizing Natural Lighting in Interiors"// Light & Engineering Journal, 2018, Vol. 26, #4, pp. 5–26.

2. Solar Constant [Solnechnaya postoyannaya] / E.A. Makarova // Fizika kosmosa / Ed. board: R.A. Syunyaev (Ed.-in-chief) et al. 2nd issue. Moscow: Sovetskaya entsiklopediya, 1986, 627 p.

3. Vitinskiy, Yu. I., Kopetskiy, M., Kuklin, G.V. Statistics of Sunspot Generation Activity [Statistika pyatnoobrazovatelnoy deyatelnosti Solntsa]. Moscow: Nauka, 1986.

4. URL: http://www.sidc.be/silso/ssngraphics (SILSO data/image, Royal Observatory of Belgium, Brussels)/ (date of reference: 26.02.2019).

5. URL: http://ciclowiki.org/wiki/11-летний цикл солнечной активности/ (date of reference: 26.02.2019).

6. Meshkov, V.V. Fundamentals of Light Engineering: Study Guide for Higher Education Institutions. P1 [Osnovy svetotekhniki. Uchebnoye posobiye dlya vuzov]. 2nd Issue, revised and supplemented. Moscow: Energiya, 1979, 368 p.

7. Allen, K.U. Astrophysical Magnitudes (Handbook) [Astrofizicheckiye velichiny (Spravochnik)]. Trans. from Eng. Moscow: Mir, 1977, 279 p.

8. Martynov, D. Ya. Course of Practical Astrophysics [Kurs prakticheskoi astrofiziki]. 3rd issue, revised and supplemented. Moscow: Nauka, Chief. ed. board of phys. and mat. lit., 1977, 544 p.

9. Kmito, A.A., Sklyarov, Yu.A. Pyrheliometry [Pirgeliometriya]. Leningrad: Gidrometeoizdat, 1981, 232 p.

10. Solar Constant / Great Soviet Encyclopedia. Vol. 40, 2nd issue / Ed.-in-chief B.A. Vedenskiy. Moscow: Bolshaya sov. entsiklopediya, 1956, p. 25.

11. Zvereva, S.V. Sun as a Source of Light [Solntse kak istochnik sveta]. Leningrad: Gidrometeoizdat, 1988, 160 p.

12. Kononovich, E.V., Moroz, V.I. General Astronomy: Studyguide [Obshchiy kurs astronomii: Uschebnoye posobiye] / Eds. V.V. Ivanov. 2nd issue, revised. Moscow: Editorial URSS, 2004, 544 p.

13. Tables for Calculation of Natural Illuminance and Visibility [Tablitsy dlya raschyota prirodnoy osveshchyonnosti i vidimosti] / Compiled by the Astrophysical lab. Of Leningrad University under supervision of prof. V.V. Sharonov. Moscow – Leningrad: Academy of Sciences of USSR, 1945, 199 p.

Alexander V. Leonidov,
Ph.D. in Technical Science, graduated from MPEI in 1970 by speciality light and engineering and sources of light. Currently, he is a retired freelance researcher

Light & Engineering
Vol. 28, No. 2, pp. 67–76, 2020

https://doi.org/10.33383/2019-030
Svetotekhnika #6, 2019, pp. 23–30

DETERMINATION OF ENERGY CONSUMPTION ACCORDING TO WIRELESS NETWORK TOPOLOGIES IN GRID-FREE LIGHTING SYSTEMS

Musa Çıbuk[1] and Mehmet Sait Cengiz[2]

[1]Department of Computer Engineering, Bitlis Eren University, Turkey
[2]Department of Technical Vocational School, Bitlis Eren University, Turkey
E-mails: mcibuk@beu.edu.tr, msaitcengiz@gmail.com

ABSTRACTS

While Wireless Sensor Networks (WSN) are used in various areas nowadays, they also come in front of us in the remote follow up and management of especially main street, road and city lighting systems and in autonomous applications relating with them.

This study has been conducted with the aim to determine the energy consumed by Wireless Sensor Network (WSN) based monitoring and management systems as per topological sequence of lighting systems with renewable energy sources (RES) in a grid-free environment. In this way it was aimed to maximize the life time of WSN which are formed by minimum energy consumption of lighting elements that store energy with accumulator-battery in grid-free RES lighting systems and which use this energy later on. Physical installation of lighting systems having different topological distributions will show differences with respect to costs, labour force and time. Starting from here on, different topologies for grid-free lighting systems have been created in simulation environment and they have been analyzed and an optimal solution has been searched for. Energy consumptions of each lighting system having linear, random and tree lighting topology have been determined during data exchange. For each topology lighting systems with 25, 50, 100 and 200 armatures have been designed and their energy consumptions for data exchange have been found. It has been seen that data packages were influenced at first degree from node hopping numbers within topology and as being parallel to this, it has been seen that topology consuming most energy was linear lighting and that topology consuming minimum energy was tree lighting.

Keywords: lighting systems, wireless sensor networks, network topology, grid-free lighting

1. INTRODUCTION

Nowadays share of lighting in total energy consumption gets increased day by day. In order to provide sustainable and uninterrupted lighting service, there is need for smart lighting systems. For smart lighting WSNs are frequently used in automation, remote monitoring and remote control systems. Classic WSNs are composed of nodes that have been distributed randomly in an area or which have been previously distributed in a planned way and that have low capacities.

In this study, energy quantity being consumed during data exchange between nodes as per topological distributions in WSNs being needed in lighting systems has been investigated. For this purpose, by comparing energy quantities consumed during data exchange by lighting systems having different topologies in a road lighting have been compared and proposals have been made for optimum topology. In remote monitoring and control system being the subject of this study, nodes (Lighting Node – LN) record various parameters such as lighting level of armature, reduction in light flux as per the

lighting level of first day, fog in the air, moisture ratio, air temperature, whether armature is energized or not, and angular placement of armature as per the ground in their memories and they transmit them to coordinating node (Coordinator Lighting Node – CLN). During data exchange between nodes, energy consumptions per armature change as per topological distribution. For the communication of armatures and to minimize the energy consumed during data exchange, it was tried to determine optimum topology that would increase energy efficiency.

2. WIRELESS SENSOR NETWORKS IN LIGHTING SYSTEMS

Sensor nodes can be generally distributed randomly or in an organized and dense way to a place desired to be observed. When a WSN is created, there is no need to determine location of sensor nodes in advance [1–4].

In literature, in many of the studies being conducted in lighting area, various WSN systems have been used for remote control and a smart system. While in studies being conducted as relating with lighting applications, generally Zigbee and GPRS based systems are preferred, it is seen that Zigbee based systems are more frequently used. Karun et al. (2014) have proposed a smart main street lighting commanding system by using Zigbee Network in the study they conducted [5]. Purpose of this system is to manage the lighting system with no human intervention. In a similar way, Srinath et al (2015), Zigbee have proposed an automatic street lighting control system by using network and sensors having emergency accident warning features [6]. Measurement stations being placed on the main street within the scope of study measure day light of main street and active-passive situations at certain intervals. Purpose is to reduce electrical consumption. Bhargavi et al. (2016), have worked on controlling energy consumption for a more efficient lighting system with remote control with Zigbee [7]. Priti Lahoti et al (2017) have achieved energy consumption of 60 % in the lighting system with remote control which they have proposed [8]. This system is controlled and managed remotely with micro controller and Zigbee. Besides, it was emphasized that it had lower costs when GPRS-GSM was used. It was recommended that it would be more correct to use Zigbee and GPRS-GSM together for remote monitoring-controlled smart road lighting systems with high energy efficiency.

Although usage of Zigbee technology in these studies increase energy efficiency, as Zigbee has low data transmission capacity, it remains to be insufficient in real time applications requiring high data transmission. For example, while Zigbee is sufficient in a system having 25 lighting armatures with respect to data exchange, Zigbee is insufficient in data exchange in long distance lighting systems with much more number of LNs. Since in intense data flow situations much more energy is consumed during communication between LNs and CLN, internal battery in relevant armatures is consumed quickly. Therefore this armature remains outside the system. In lighting, in remote control applications, the method that is used most after Zigbee is GPRS, GSM method. Within this context in various studies in literature in smart lighting system proposals remote control has been made with GPRS-GSM [9–12].

Due to low data transmission ratios of GPRS-GSM and Zigbee technologies and due to disadvantages such as infrastructure costs, in this study, nRF905 Transceiver, having lower cost, being current, having easiness of usage and very low energy consumption during data exchange, has been simulated [13]. Comparison of ZigBee, GPRS-GSM and nRF905 is given in Table 1.

3. WIRELESS SENSOR NETWORKS AND MAINTENANCE FACTOR RELATIONSHIP

Nowadays in smart lighting there is need for automation systems that provide uninterrupted lighting and that require less maintenance. Basic purpose in using WSNs in lighting systems is to create a structure that improves sight comfort and that needs less maintenance and which can be remotely controlled or has an autonomous structure. At this point in electrical facilities with RES feeding without grid connection, it has become a necessity to use WSN topologies having low energy consumption for automation, because in lighting systems with the effect of various negative conditions, maintenance factor gets reduced and energy consumption gets increased. Maintenance Factor (MF), Lamp Lumen Maintenance Factor (LLMF), Lamp Survival Factor (LSF), Luminaire Maintenance Factor (LMF), are composed of total impact of various parameters

Table 1. Comparison of ZigBee, GPRS-GSM and nRF905

	Frequency (MHz)	Modulation	Topology	Energy Consumption	Data Rate	Coverage Radius (m)	Multi-Channel Support
ZigBee	868/915/ 2400	BPSK, OQPSK	Star, P2P, Mesh	Low	250 kbps	10–100	No
nRF905	433/868 / 915	GFSK	–	Very low	250KBps, 1MBps 2MBps	250	Yes
GPRS-GSM	850/900/ 1800/1900	GMSK	P2P, P2M	High	56–114kbps	1000+	No

performance loss in lighting depending on reduction in light flux and optical effect (for LED lamps) [14–22]. Under normal conditions effects originating from WSN technologies and automation are not added to MF. But in lightings being managed with smart city applications or automation systems, when inefficient WSN impacts are added to MF, MF will fall further and it will increase energy consumption. In another way of saying, reduction in MF reduces efficiency and increases lighting costs. MF is used as a multiplier as it can be seen in illuminance level (E) relation in Equation 1 [16, 19, 22–24]. In equation 1, relationship of illuminance level and maintenance factor is seen.

$$E = \frac{I \cdot cos^3 \varepsilon \cdot \Phi \cdot MF}{h^2}, \quad (1)$$

where I is the luminous intensity value (cd), Φ is the luminous flux (lm), MF is the maintenance factor, h is the height of the luminaire from the ground (m), ε is the angle between the light coming from the armature to the surface and the normal of the surface.

4. APPLICATION OF WIRELESS SENSOR NETWORKS TO LIGHTING

WSNs are composed of sensor nodes which have been distributed randomly on an area or previously in a planned way and which have low capacities. Energy limitation of sensor nodes and difficulty in battery replacement are among the most important factors effecting WSN design. Besides development of application specific energy efficient environment access techniques bears significant importance. Energy consumption occurs most during data exchange. Application specific MAC design and studies that would minimize energy consumption in data exchange have been made [1, 2, 25, 26]. In this studies while it is aimed to have anticoincidence environment access, it is targeted to transmit data amount to be sent in minimum and effective way.

Another important design criterion in WSNs is network topology. Network topology is the connective relation between nodes. Basic logic in WSNs is the transmission of data obtained by nodes to coordinator node in some way. Basically connection forms of nodes with each other are divided into two parts such as single-hop and multi-hop as shown in Fig. 1. In lighting applications, lighting armatures which are used as sensor nodes are defined as Lighting Node (LN), and coordinator nodes that are used as management and data collection centres are defined as Coordinator Lighting Node (CLN).

In the connection model with single-hop, LN directly communicates with CLN. In connection model with multi-hop, CLN communicates with LNs within coverage zone of CLN through other LNs within coverage zone. For this reason as it is ap-

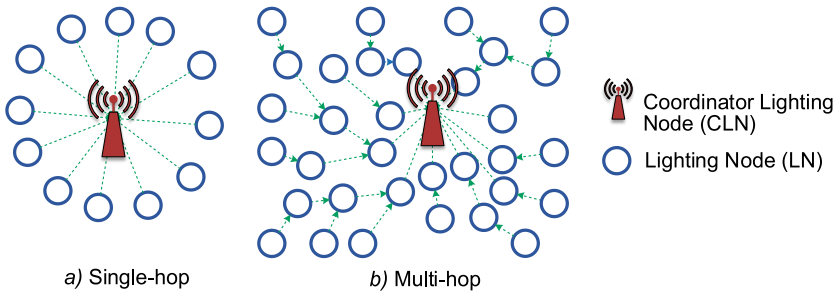

Fig. 1. WSN connection modes

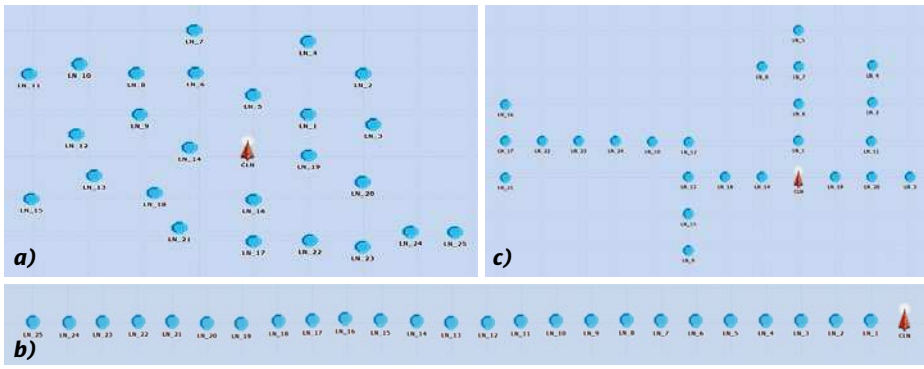

Fig. 2. Lighting topologies: a) random lighting topology; b) linear lighting topology; c) tree lighting topology

proached to CLN in the network, data exchange traffic of LNs gets increased. As being proportionate with this increase, energy consumption also gets increased. Since LNs which are fed with accumulator or battery in this example do not have grid connections, they rapidly consume their energies due to intense data exchange and they split from network.

In multi-hop WSNs, LNs have energy consumptions being different from one another. Because data exchange quantity is different for each LN. Since LNs which are close to CLN undertake the task of directing for LNs that are farther away, data exchange quantity is apparently different from other ones. This situation causes for LNs that are close to CLN to consume more energy. Therefore, when energy of LNs that are close to CLN is rapidly consumed, their communication with WSN is cut. LNs that are farther away as being connected to this LN split from the network even though their energies have not finished. That is meaning the data exchange is cut. In such situations in order for WSN application to be optimum, it is required to prefer method and topologies with which energy will be used efficiently.

5. SELECTION OF OPTIMUM TOPOLOGY

In literature various studies have been made as relating with WSN topologies [3, 4] and as no study has been observed in lighting applications relating with effectiveness of WSN topologies, this has created motivation for this article. In this study, it was aimed to compare the all energy amount consumed by all LNs in WSNs having different topologies. To make analysis, modelling method has been preferred in simulation environment. Physical realization of a real application in WSNs causes for labour loss and costs. In this situation, it is found out that first of all a simulation of application being planned to be designed which would generate results that are close to actual ones is required.

Modelling of developed WSN application was made in Riverbed Modeller simulation environment. Riverbed Modeller is the network simulation software where simulation of all network projects can be made [27]. Monitoring the behaviour of network projects being created provides opportunity to realize various processes such as performance analysis and testing of superiorities. While designing model behaviour, ProtoC language which takes C language as basis and which is specific for software is being used.

Riverbed Modeller enables for simulations with discrete event basis to be made for the analysis of both the behaviour and performance of network model being developed [28].

When WSN is designed, for having an application that is close to actual one, for LNs the features of Nordic platform have been taken as reference. Nordic nRF905 which supports multi-channel communication has been used. In Table 2 technical specifications of nRF905 can be seen [13].

Table 2. The nRF905 Specification

Parameter	Value	Unit
Minimum supply voltage	1.9	V
Maximum transmit output power	10	dBm
Data rate	50	kbps
Supply current in transmit	@ –10	dBm
output power	9	mA
Supply current in receive mode	12.5	mA
Temperature range	–40 to +85	°C
Typical sensitivity	–100	dBm
Supply current in power down mode	2.5	µA
Channel switching time	<650	µs

Table 3. Simulation Parameters for Random, Linear and Tree Topology According to 25, 50 100 and 200 LN Scenario

Scenario	Topology	LN coverage radius (m)	CLN count	Network area (m^2)	Simulation time (s)	Distance between nodes (m)
25 LN	Linear	145	1	2500×100	300	100
	Random	145	1	2000×2000	300	variable
	Tree	145	1	2000×2000	300	100
50 LN	Linear	145	1	5000×100	300	100
	Random	145	1	2000×2000	300	variable
	Tree	145	1	2000×2000	300	100
100 LN	Linear	145	1	10000×100	300	100
	Random	145	1	2000×2000	300	variable
	Tree	145	1	2000×2000	300	100
200 LN	Linear	145	1	20000×100	300	100
	Random	145	1	2000×2000	300	variable
	Tree	145	1	2000×2000	300	100

Table 4. Energy Consumption Values of Nordic Platform

Bandwidth (KHz)	Data rate (bps)	Power consumption type	Power consumption (W)
100	5,95E+05	P_{Tx}	0.0330
		P_{Rx}	0.0366
200	1,19E+06	P_{Tx}	0.0900
		P_{Rx}	0.0384
		P_{Sp}	0.0003
		P_{LPL}	3,75E-05

Two types of nodes are designed in simulation environment and they are CLN for central management point and LN for armatures. For the topological distribution of lighting system, random topology has been designed to represent rural areas, linear topology has been designed to represent road and tunnel lighting, and tree topology has been designed to represent branch-main street-road lighting, Fig. 2.

For each of random, linear and tree topologies, 4 different scenarios being composed of 25, 50, 100 and 200 LN have been created and simulations have been made. Simulation parameters of scenarios being created can be seen in Table 3.

Energy consumptions of Nordic nRF905 radios that are used in node models in simulation environment can be seen in Table 4.

One of the parameters effecting energy consumption is the sizes of data exchange packets that are used in WSNs. In WSNs that are developed within context of this study, 3 different types of packets have been used. Packet types and sizes can be seen in Table 5.

Schedule packets has been used to transmit channel information being assigned by CLN to LNs. Control packets are used by LNs to join the network directly and for the continuity in network. LNs use Relay packets to join the network through other nodes.

6. MATHEMATICAL MODELS

In this study, by adding the energies consumed by *n* pieces of LN and 1 piece of CLN during Sleep Mode, LPL and packet exchange, energy consumption amount is calculated. Here very low power consumptions originating from other parameters, which can cause power consumption have been neglected [1, 2]. Energy amount required for a node to obtain a packet (P_r) is found as per equation (2).

Table 5. Packet Types and Sizes Used in WSN

Packet type	Length (bit)
Schedule packet (Psch)	variable
Control Packet (Pctrl)	32
Relay Packet (Prly)	52

$$P_R = \frac{L_{pkt}}{R_{ch}} * P_{Rx}. \quad (2)$$

Calculation of energy to be used in radio transmission for the transmission of a packet by any LN desiring to send data has been shown in equation (3) [1, 2].

$$P_T = \frac{L_{cp}}{R_{ch}} * P_{Tx}. \quad (3)$$

When number of LN nodes in network is n, consumed energy amount (E_T) that is consumed by $N_C = n.LN+CLN$ pieces of nodes in total is calculated as shown in equation (4) [1, 2].

$$E_T = \sum_{n=1}^{N_C} \left\{ \left(P_R * N_{Rpkt} \right) + \left(P_T * N_{Tpkt} \right) + P_{Sp} + P_{LPL} \right\}. \quad (4)$$

where

P_{Tx} is the transmitter power ;

P_{Rx} is the receivers power;

P_{Sp} is the sleep power;

P_{LPL} is the low sleep power;

E_T is the total energy of nodes;

N_{Rpkt} is the total number of packets received by all nodes;

N_{Tpkt} is the total number of packets transmitted by all nodes

P_R is the power consumption per received Packet;

P_T is the power consumption per transmitted packet;

C_N is the node count;

R_{ch} is the channel data rate (bps);

L_{pkt} is the packet length (bit).

7. RESULTS AND DISCUSSIONS

For WSNs simulation of which has been made within context of this study, node numbers have been determined as 25, 50, 100 and 200. As topology, linear, random and tree distribution have been selected, total energy consumed by all nodes (*n.LN+CLN*) for 3 lighting topologies simulation of which has been made, has been shown. In all graphics it is observed that in the first seconds of simulation energy consumption has rapidly increased because during first participation of LNs in the network, all LNs consume energy together. When LNs are energized for the first time, they use control and relay packets often to join the network. After participation in network is realized, LNs send control and data packages periodically with less frequency. LCN consumes energy for each LN it adds to the network. In the scenario having 25 LN, total energy consumed by 25 LN+CLN is shown in Fig. 3. It can be seen in Fig. 3 that total energy consumptions of 25LN+CLN in simulation environment are respectively 0.114, 0.0827 and 0.0743W in linear, random and tree topologies.

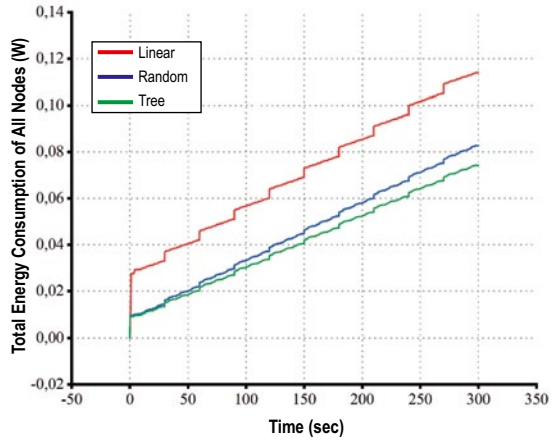

Fig. 3. Consumed total energy by 25LN+CLN

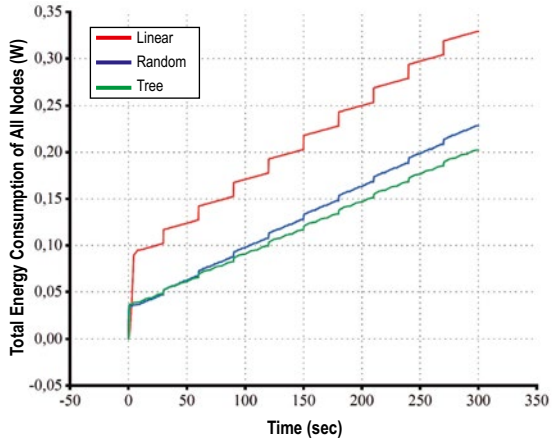

Fig. 4. Consumed total energy by 50LN+CLN

According to this, in an electrical grid having 25 lighting devices, topology that consumes most energy is linear lighting topology with 0.114W. Minimum energy consumption has been observed in tree lighting topology with 0.0743W. In a lighting system with 25LN+CLN, in WSN tree lighting topolo-

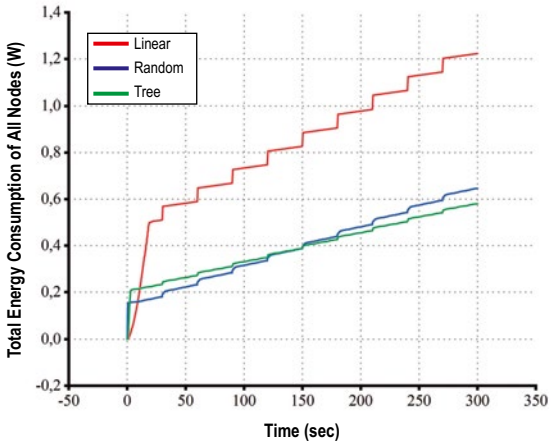

Fig. 5. Consumed total energy by 100LN+CLN

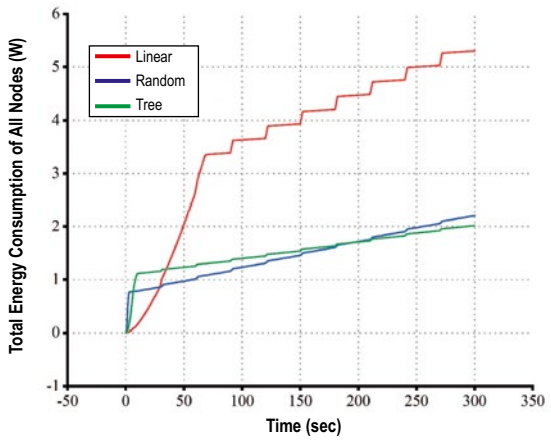

Fig. 6. Consumed total energy by 200LN+CLN

gy consumes 35 % less energy when compared with linear lighting topology. Random topology has consumed 27 % less energy when compared with linear topology. In Fig. 4, total energy consumed by 50LN+CLN is seen.

It can be seen in Fig. 4 that total energy consumptions of 50LN+CLN in simulation environment are 0.3293, 0.2287 and 0.20W respectively for linear, random, and tree topologies. Accordingly, in an electrical grid having 50 lighting devices, topology consuming most energy is linear lighting topology with 0.3293W. Maximum energy consumption has been observed in tree lighting topology with 0.20W. In a lighting system with 50LN+CLN, in WSNs tree lighting topology has consumed 40 % less energy when compared with linear lighting topology. When the number of lamps or fixtures in network gets increase, difference in energy consumption between linear and tree topologies is increasing too. While difference of total energy consumed for linear and tree topologies in WSN with 25LN+CLN is 35 %, in a system with 50LN+CLN total energy difference is 40 %. That is meaning each lighting device included in the system increases energy difference between most appropriate topology and other topologies. In Fig. 5, total energy consumed by 100LN+CLN can be seen.

It can be seen in Fig. 5 that total energy consumptions of 100LN+CLN in simulation are 1.223W, 0.6458W, and 0.58W respectively for linear, random, and tree topologies. Accordingly, in an electrical grid having 100 lighting devices, topology consuming most energy is linear lighting topology with 1.223W. Minimum energy consumption is seen in tree lighting topology with 0.58W. In a lighting system with 100LN+CLN in WSN, tree lighting topology consumes 53 % less energy when compared with linear lighting topology in average. In Fig. 6, total energy consumed by 200LN+CLN can be seen.

It is seen in simulation that total energy consumptions of 200LN+CLN are nearly 5.301W, 2.205 W, and 2.016 W respectively for linear, random and tree topologies. According to this, in an electrical grid having 200 pieces of lighting devices, most energy consuming topology is linear lighting topology with 5.301W. Minimum energy consumption is seen in tree lighting topology with 2.016 W. In a lighting system with 200LN+CLN in WSN, tree lighting topology consumes nearly 62 % less energy when compared with linear lighting topology. For different lighting systems, energy consumptions in WSN and hop-counts can be seen in Table 6.

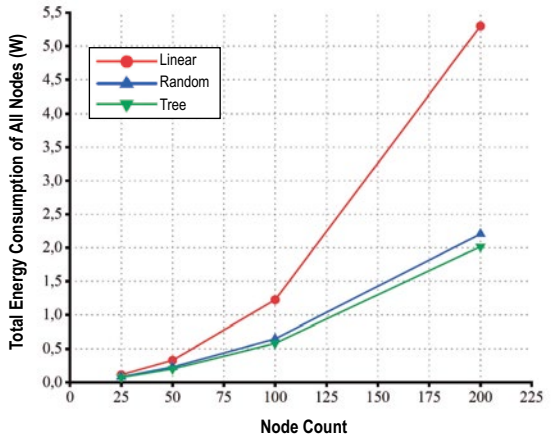

Fig. 7. Total energy consumption due to the increase in LN number for Linear, Random, and Tree topologies

Table 6. Total Energy Consumption in WSNs for Different Lighting Systems

Scenario	Topology	Energy consumption (W)	Advantageous topology (Best / Worst) (%)	Mean hop-count	Max hop-count
25LN+CLN	Linear	0,1140		13	25
	Random	0,0827		1,72	3
	Tree	0,0743	35	1,6	4
50LN+CLN	Linear	0,3293		25,5	50
	Random	0,2287		1,54	4
	Tree	0,2003	40	2,88	7
100LN+CLN	Linear	1,2234		50,5	100
	Random	0,6458		4,19	6
	Tree	0,5801	53	3,49	9
200LN+CLN	Linear	5,3012		100,5	200
	Random	2,2046		7,35	15
	Tree	2,0160	62	4,78	11

Changes in total energy quantities being consumed for the topologies being evaluated in this study are shown in Fig. 7.

As it can be seen in Fig. 7, minimum energy consumption takes place in Tree topology and maximum energy consumption takes place in linear topology. With increasing of the LNs number in network, total energy amount increases exponentially. In the graphic, while very serious differences are not seen between random and tree topologies, in linear topology it is seen that as number of nodes increase, there is very serious level of energy consumption. It is apparent that average hop counts have first degree effect on this outcome. For this reason in simulation studies, besides total energy being consumed, hop counts that are used by LNs to reach CLN for joining network and data transmission have also been investigated. In Table 6, maximum and minimum hop counts have been given for all scenarios and topologies which are used in simulation. As it can be seen in the table, in linear and tree topologies having equal distances between nodes and proper node distribution, energy consumption increases together with hop counts. On the other hand, as there is no proper distribution in random topology, it cannot be stated that average hop counts increase in parallel with increase in node numbers. As being parallel to the increases in node numbers, maximum hop counts also increase and this situation is observed more clearly in linear topology. A LN also transmits data of other LNs to which it serves for relaying besides its own data. Therefore, more number of relaying done by a LN means as much data transmission being made. When each relaying process is considered as a hop for linear topology, hop counts increase, and energy consumed by LNs for data transmission increase in relative degree. To give an example, a LN that is directly connected with CLN can send its own data directly. When the LN, which is connected with CLN through a different node, sends its data, it has to transmit the same data package on the node that functions as relay for it. In transmission of a package with 10 hops, 10 nodes have to transmit the same packet and this requires 10 times the energy that is consumed per packet.

8. CONCLUSIONS

In this study, energy consumptions of lighting system topologies with different scenarios having same number of nodes under same conditions in WSNs have been evaluated. For this purpose, in a scenario being adopted to RES lighting systems, simulation of which has been made, as having linear, random and tree topologies, having no grid connection, energy amounts being consumed during joining network in WSNs and then during data exchange have been measured. According to the being obtained findings, energy consumptions of nodes show variations when topology changes, even if the number of nodes is the same in lighting.

Energy consumption is more during the connection of nodes with network and the reason for this is because at the moment when system is energized,

package traffic takes place which originates from timing, control and relay packages. After package installation is completed, package delivery (data) frequency of relevant lighting node (LN) gets reduced and, depending on this energy quantity being consumed, gets reduced with a fixed slope.

Increase in energy consumption especially attracts attention in an apparent way in linear scenarios. As number of lighting devices increase, energy consumption in WSN has also increased. The reason for this is maximum hop counts in WSN. Minimum energy consumption has occurred in random topology with scenario having 25 nodes and with respect to energy consumption, it is very close to tree lighting topology. It is seen that in general energy consumptions of tree and random topologies are very close to each other and that their energy efficiencies are high. However, with respect to energy consumption fundamental problem is observed in linear topology.

This study has shown that as hop counts in topological distributions increase (especially in networks having linear topologies), there is serious energy consumption during joining network processes. As LN numbers increase, total energy amount being consumed increases exponentially and energy consumption efficiency gets reduced. For this reason, it is required for network joining stages of LNs to be realized specially by using energy efficient methods (or MAC protocols). When the inevitability of Linear topologies in long distance road lighting systems are considered, importance of effective and efficient network joining techniques increases even more. By evaluating this particular in future studies, studies should be conducted on solution methods.

Finally, in the simulation work being done, it was seen that lighting systems having different topologies in WSN consumed energies at different levels.

REFERENCES:

1. Arı, D., Çıbuk, M., Ağgün, F., Effect of Relay Priority Mechanism on Multi hop Wireless Sensor Networks, Bitlis Eren University Journal of Science and Technology, 2017, V7, #2, pp. 145–153.

2. Çıbuk, M., Tek Atlamalı Kablosuz Algılayıcı Ağlarda Yeni Bir Hızlı Ağa Katılım Algoritması, Bitlis Eren Üniversitesi Fen Bilimleri Dergisi, 2018, V7, #1, pp. 72–83.

3. A. Shrestha, L., Xing, A., Performance Comparison of Different Topologies for Wireless Sensor Networks, 2007 IEEE Conf. Technol. Homel. Secur, 2007, pp. 280–285.

4. Q. Mamun, A Qualitative Comparison of Different Logical Topologies for Wireless Sensor Networks Sensors, 2012, V12, #12, pp. 14887–14913.

5. Karun R., Johny M., Street Light Commander System Using Zigbee Network of Devices. 2014, V4, #4, pp. 165–169.

6. Srinath V., Srinivas S., Street Light Automation Controller using Zigbee Network and Sensor with Accident Alert System. International Journal of Current Engineering and Technology, 2015, V5, #4, pp. 2819–2823.

7. Bhargavi, R., Pavitra, B., Development of Automatic Street Light Illumination and Vehicle Speed Controlling System on Arm7 for Roadways, Int J Res Adv Eng. Technol, 2016, V5, #3, pp. 16–22.

8. Journal I, Technology S, Dp T, Prof SOEP, Pune TDPSOE, Remotely Control High Energy Efficient Automatic Street Lighting System. 2015. V1, #11, pp. 43–46.

9. Caponetto, R., Dongola, G., Fortuna, L., Riscica, N., Zufacchi, D., Power consumption reduction in a remote controlled street lighting system. Int Symp Power Electron Electr Drives, Autom Motion, 2008. pp. 428–433.

10. Chen, Y., Liu, Z., Distributed intelligent city street lamp monitoring and control system based on wireless communication chip nRF401. Proc – Int Conf Networks Secur Wirel Commun Trust Comput, 2009. V2, pp. 278–281.

11. Lin J, Jin X, Mao Q, 2009. Wireless monitoring system of street lamps based on ZigBee. Proc – 5th Int Conf Wirel Commun Netw Mob Comput, 2009. pp. 2–4.

12. Jun, L., Cangxu, F., Xuesong, S., Aijun, Y., Street lamp control system based on power carrier wave. Proc-2nd 2008 Int Symp Intel Inf Tech Appl Work IITA 2008, pp. 184–188.

13. Nordic Semiconductor: nRF905 Single chip 433/868/915MHz Transceiver, 2019. http://infocenter.nordicsemi.com/pdf/nRF905_PS_v1.5.pdf (02.02.2019)

14. Özkaya, M., 1994. Aydınlatma Tekniği, Birsen Yayınevi, İstanbul-1994, 91.

15. TSE standard: TS EN13201–2, Road lighting – Part 2: Performance requirements (Effective date: 09.12.2016).

16. Cengiz M.S., A Simulation and Design Study for Interior Zone Luminance in Tunnel Lighting, Light & Engineering. 2019, V27, #2, pp. 42–51.

17. Tetri, E., Chenani, S.B., Rasanen R.S., Advancement in Road Lighting, Light & Engineering, 2018, V26, #1, pp. 99–109.

18. Barua, P., Mazumdar, S., Chakraborty, S., Bhattacharjee, S. 2018. Road Classification Based Energy Efficient Design and its Validation for Indian Roads, Light & Engineering, 2018, V26, #2, pp. 110–121.

19. Cengiz M.S., Cengiz, Ç., Numerical Analysis of Tunnel LED Lighting Maintenance Factor, IIUM Engineering Journal. 2018, V19, #2, pp. 154–163.

20. Iacomussi, Rossi, G., Soardo, P., 2012. Energy Saving and Environmental Compatibility in Road Lighting, Light & Engineering, 2012, V20, #4, pp. 55–63.

21. Van Bommel, W., Van Den Beld, G.,. Van Ooyen M., 2003. Industrial Light and Productivity, Lighting & Engineering, 2003, V11, #1, pp. 14–21.

22. Cengiz M.S., The Relationship Between Maintenance Factor and Lighting Level in Tunnel Lighting, Light & Engineering. 2019, V27, #3.

23. Cengiz M.S., Cengiz, Ç., Numeric Analysis for the Efficiency of LED and Traditional Luminaries used in Tunnel Lighting, International GAP Renewable Energy and Energy Efficiency Congress, 10–12 May 2018, 347–348.

24. Cengiz M.S., Cengiz, Ç., Mamiş, M.S., Contribution of Reflector Design formed by Numeric Calculations to Energy Efficiency, International GAP Renewable Energy and Energy Efficiency Congress, 10–12 May 2018, 349–350.

25. Çıbuk, M., Arı, D., Ağgün, F., Relay Mechanism with Three way Handshake for Wireless Sensor Networks, presented at the 8th International Advanced Technologies Symposium, Elazığ, 2017.

26. Arı, D., Çıbuk, M., Ağgün, F., A New Proxy Based Network Joining Method for Linear Wireless Sensor Networks, presented at the International Engineering and Natural Sciences Conference (IENSC2018), Diyarbakır, 2018.

27. "Riverbed Models, 2018. Available at: https://www.riverbed.com/gb/products/steelcentral /steelcentral-riverbed-modeler.html. (Access date 28-Feb.-2019).

28. Hammoodi, I.S., Stewart, B.G., Kocian, A., McMeekin, S.G., A comprehensive performance study of OPNET modeler for ZigBee wireless sensor networks, 3rd Int. Conf. Next Gener. Mob. Appl. Serv. Technol. 2009, pp. 357–362.

Musa Çıbuk,
received his M. Sc. and Ph. D. degrees from Fırat University, Turkey in 2002 and 2009, respectively. His research interests include WSNs, MAC, Computer Networks, Digital Communication and Image Processing. He worked at the University of Fırat between 2000 and 2010. He is currently working at Bitlis Eren University, in position of Head of Department at Computer Engineering

Mehmet Sait Cengiz
Ph.D. He was Director of Research and Development in period of 2000–2010 years in Turkey Electricity Distribution Company. In 2011, he completed his master degree in the field of Electrical and Electronics Engineering. In 2016, he completed his doctorate degree in Inonu University, Institute of Science and Technology, Electrical and Electronics Engineering and works in the field of applied lighting. He is currently working at Bitlis Eren University

Light & Engineering
Vol. 28, No. 2, pp. 77–84, 2020
https://doi.org/10.33383/2019–030
Svetotekhnika #1, 2020, pp. 48–55

UNCERTAINTY OF DAYLIGHTING PERFORMANCE OF MANUAL SOLAR SHADES AND ITS INFLUENCE ON LIGHTING ENERGY

Jian Yao*, LiYi Chen and Wu Jin

Department of Architecture, Ningbo University, Ningbo, China
**E-Mail: yaojian@nbu.edu.cn*

ABSTRACT

Occupant behaviour significantly influences building energy consumption. This paper is devoted to studies the uncertainty of daylighting performance and lighting energy of manual solar shades on the south facade. A developed stochastic model for manual solar shades was used for co-simulation by BCVTB. Results show that uncertainty of shade action was not suppressed by the shade behaviour model with very weak relationship between different simulation outputs. Uncertainty of daylighting performance is 15.08 % while lighting energy uncertainty is 10.38 %. Although this level of energy uncertainty is not very significant, it influences economic analysis of manual solar shades and therefore, occupant related uncertainty should be taken into consideration when predicting energy performance of manual shades.

Keywords: Building Controls Virtual Test Bed (BCVTB), manual solar shades, uncertainty, daylighting performance, lighting energy

1. INTRODUCTION

Shading devices can be used to control solar gains, adjust daylight levels in the room and eliminate glare and high contrast [1]. Fixed shading devices such as horizontal overhang, vertical fins are widely used in the building envelope to block unwanted solar radiation in summer. However, they also block a significant amount of direct and diffuse daylight in winter and they are not effective under cloudy skies. While for movable shading devices, they can be adjusted to changing outdoor conditions. Thus, movable solar shades have been widely used in buildings either manually controlled or operated by the building automation system. Although automated solar shading system provides a high efficient control of thermal, daylight and glare, its high initial and maintenance costs are still major impediments for its widespread use in hot summer and cold winter zone of China. Therefore, manually operated roller shades are widely used in China, especially in glazed office buildings [2].

Manual solar shades highly rely on occupants' control and thus the prediction of daylighting and energy performance of manual shades should take into account behaviour characteristics, since research works have indicated that building energy consumption is influenced not only by engineering technology, but also by cultural concepts, occupant behaviour, social equity etc. Evidence suggests that occupant behaviour plays a defining role in influencing the total energy consumption [3]. For example, Labat et al [4] carried out numerical estimation and sensitivity analysis of the energy demand for six industrial buildings in France. They found that the computed value of the energy demand for heating and cooling was sensitive to input parameters related to the use of the building rather than to the ones describing the envelope. Building research in recent years has shown differences between the actual and predicted energy performance of buildings. Some of these differences have been attributed to the effect of occupants' behaviour [5]. A study by Haldi et al [6] quantified the impact of occupants' behaviour on building energy demand. Different oc-

Table 1. Characteristics of the Office Room

Parameter	Value
Location	Ningbo city in China, latitude: 30°, longitude: 120°
Room orientation	South
Dimension	Room: (4×4×3) m, Window: (3.8×2.8) m
Window and shading device	Clear double-pane window + manually controlled external shading. A white roller top-down shade with 30 % polyester and 70 % PVC is considered and the visual transmittance is 0.2.
Daylight sensor position	The red point in Fig. 1
Daylighting performance index	Hours of useful daylight illuminance (UDI: (300–2000) lx) [11]
Intensity of radiation	11W/m^2 for daylight illuminance < 300 lx

cupant behaviour models have been integrated within an urban energy modelling tool, called CitySim. The results show that occupants' behaviour has a significant impact (of the order of a factor of two) on buildings' energy demands.

Although a few researches reported the influence of occupant behaviour (manual shades) on energy performance [7, 8], the blind models adopted in these research works were not applicable to manual solar shades with partial shade states (the current studies either consider only two blind states (fully open and fully closed) or are based on unusual shading systems with motorized control. For example, Reinhart [9] simulated building energy performance based on the Lightswitch-2002 model. However, this model can be used only to predict the lighting energy performance, and daylighting performance uncertainty due to occupant behaviour on blinds cannot be simulated by this model. Moreover, the research findings cannot be directly applied in buildings in hot summer and cold winter zone of China due to the differences in shade types and behaviour characteristics.

To analyze the impact of occupant uncertainty of shade control behaviour on building performance, a stochastic model for west-facing facades developed in a previous study [2] based on field measurements was used in this paper. Energy savings compared to regular windows, thermal [10], daylight [11] and visual performance [12] have already been researched. This work is a continuation of the previous study and the focus is the uncertainty of occupant behaviour on solar shades and its influence on daylighting and lighting energy performance.

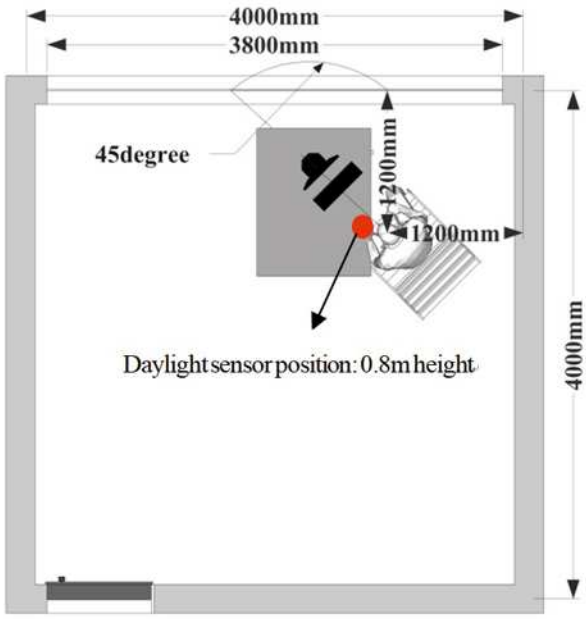

Fig. 1. Room model showing the workplace position (upward direction represents south)

2. METHODOLOGY

2.1 Stochastic Model of Manual Solar Shades

A typical office room model was used in this paper. Its dimension is (4×4×3) m with a (3.8×2.8) m window on the south facade as shown in Fig. 1. The characteristics of the office room including the setting of manually controlled external shading devices and daylighting sensor position are shown in Table 1.

To investigate the uncertainty of daylighting performance of manual solar shades and its influence on lighting energy consumption, the stochastic model developed in a previous study by the author [2] was used in this paper. The model was constructed based on field measurements of a typical high-rise glazing building in hot summer and cold winter zone of China. In this model, the occupants' stochastic behaviour of solar control was divided into 5

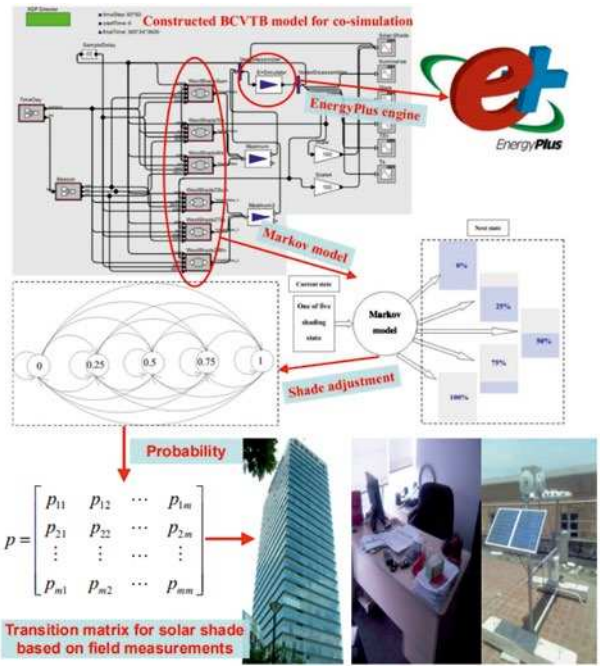

Fig. 2. A graphic illustration of the applied method for co-simulation of daylighting performance of manual solar shades

discrete solar shading positions (fully shaded, 75 % shaded, 50 % shaded, 25 % shaded and fully open). Corresponding values of external shading coefficient (SC) are 0, 0.25, 0.5, 0.75 and 1 respectively. And the adjustment of solar shades was predicted based on the current shade state and solar intensity on the facade (since it is the driving factor according to cumulative odds logit regression) using a first order and discrete-time Markov chain method, which produces Markov chain transition matrix (the probability of solar shade changes from the current state to the next one) for coupling with EnergyPlus. A brief description of how this stochastic model is constructed and the co-simulation is conducted can be seen in Fig. 2. More detailed information of this stochastic model and the co-simulation can be found in the previous paper [2].

2.2. Uncertainty Index

2.2.1. Shade control behaviour

In this paper, uncertainty means the stochastic adjustment of shade devices due to occupant behaviour, which results in the difference of SC value between occupants and thus the resulting building energy difference. The index used to assess how well the relationship between two variables

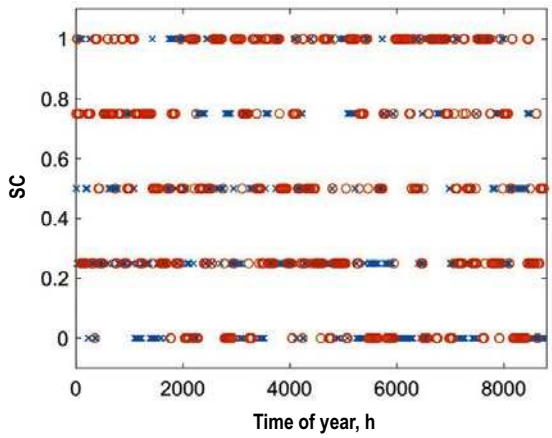

Fig. 3. Hourly SC values of two example simulations during the whole year (o represents simulation N1 and x represents simulation N2)

(here hourly SC values between different simulations) is correlation coefficient, which varies between +1 and –1. A value of +1 indicates a perfect positive correlation between the two variables, –1 represents totally negative correlation and 0 corresponds to an absence of linear correlation. Since SC values in this paper are discrete and ordinal, Spearman rank correlation, a non-parametric test, is used. The Spearman rank correlation test does not carry any assumptions about the distribution of the data and thus is appropriate for correlation analysis for SC values.

2.2.2. Daylighting performance and lighting energy

For uncertainty of daylighting performance and lighting energy, the probability density function (PDF) was used to fit the data. In this paper normal distribution was adopted (since the following analysis confirmed the normal distribution of the data) which uses a two-parameter family of curves. The first parameter, μ, is the mean. The second parameter, σ, is the standard deviation. And the normal PDF of the energy data $f(x)$ can be expressed as:

$$f(x) = \frac{1}{\sigma\sqrt{2\pi}} \exp\left(\frac{-(x-\mu)^2}{2\sigma^2}\right). \quad (1)$$

Using the above fitting analysis, the distribution of hours of useful daylight illuminance (UDI) can be determined and then 95 % confidence interval of daylighting uncertainty (hours of UDI) can be calculated as follows according to the properties of normal distribution:

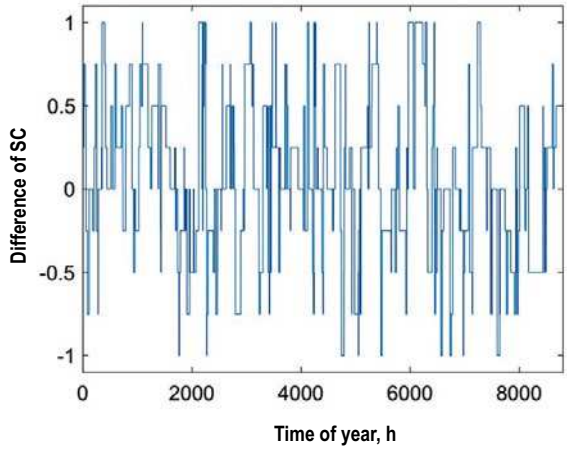

Fig. 4. Hourly difference of SC values of two example simulations during the whole year

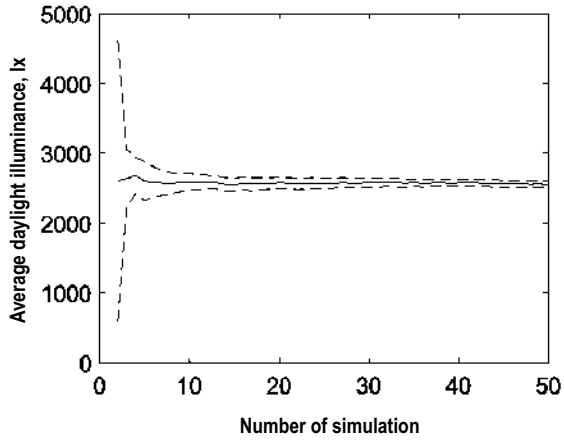

Fig. 5. Convergence of annual average daylight illuminance (the solid line indicates the mean value while the dashed lines indicate 95 % confidence interval)

$$CI = \bar{X} \pm t_{n-1,\alpha/2} \frac{\sigma}{\sqrt{n}}, \quad (2)$$

where $\bar{X}$ is the mean of the output data from the replications, n is the number of replications, $t_{n-1,\alpha/2}$ is the value from Student's t-distribution with (n-1) degree of freedom and a significance level of $\alpha/2$. A significance level (α) of 5 % is selected in this paper. That gives a 95 % probability the value of the true mean lies within the CI interval. To have a percentage value of uncertainty rather than an absolute one, CI was further divided by the mean value.

2.3. Number of Repeated Simulations

Since energy simulation based on the shade behavioural model generates different outputs, repeated simulations are needed to understand the possible distribution of the output parameters. As described in [13], additional simulation time needed for replicates can be considered as a weakness. Thus, this paper calculates the required minimum number of simulations in order to achieve a converged solution according to the graphical method recommended in [14]. The graphical method plots the cumulative mean of the simulation output data and thus, after sufficient replications, the graph will become a flat line with no upward or downward trend. The number of replications required is defined by the point at which the line becomes flat. Based on the above analysis, uncertainty of daylighting performance (hours of UDI since it is an important index in determining daylight performance [11]) as well as lighting energy consumption can be determined.

3. RESULTS AND DISCUSSION

3.1. Uncertainty of Shade Control

3.1.1. Comparison of two example simulations

Two example simulations were given in this section to illustrate the behaviour uncertainty. In each simulation time step, a random number is sampled from a continuous uniform distribution between 0 and 1 and compared with the Markov chain transition matrix (see section 2.1) and thus different hourly SC sequences were generated using the same shade behaviour model as described and shown in Fig. 2. Fig. 3 gives hourly SC values of two example simulations (simulation N1 and simulation N2) during the whole year. It can be seen that SC differs significantly between the two simulations with different fluctuation trends. Fig. 4 further presents the SC differences between these two simulations. Due to the stochastic characteristics of occupant behaviour, the occupant uncertainty can be easily observed with most of times SC difference being not 0 (mainly between about –1 to 1). This difference directly influences final energy performance and therefore, a single simulation run is not capable of capturing energy uncertainty due to occupant behaviour.

3.1.2 Required simulation runs

The minimum number of required simulations for a converged solution is determined based on the graphical method and the results are show in

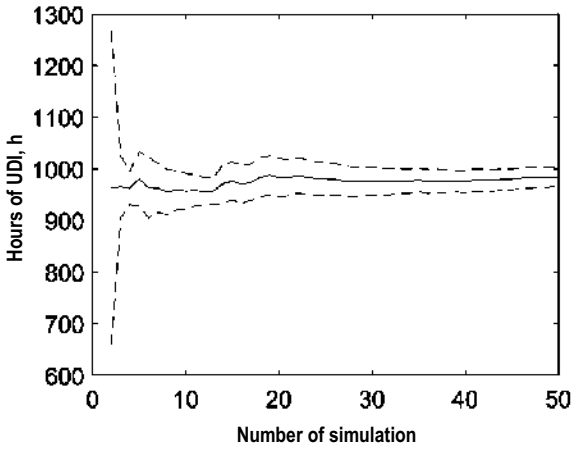

Fig. 6. Convergence of hours of UDI (the solid line indicates the mean value while the dashed lines indicate 95 % confidence interval)

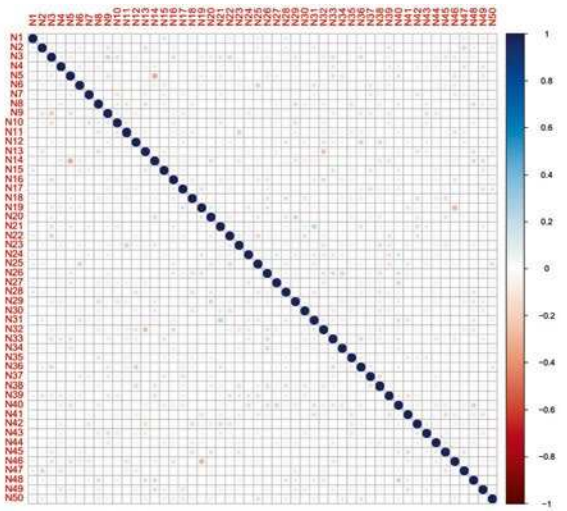

Fig. 7. Correlation coefficient of hourly SC values between each two simulations

Figs. 5, 6. It can be seen that after 20 simulations, annual average daylight illuminance reaches a converged solution while for the hours of UDI it is about 25 simulations. To have a better uncertainty evaluation, 50 simulation runs were selected in this paper. It should be noted that this amount of required simulations is based on the shade behaviour model in this climate region. Other researchers [13] reported a higher number of required simulations when simulating more types of occupant behaviours (a combination of shade adjustment, window opening and thermostat setting etc.). Therefore, generally a smaller number of repeated simulations is required if less types of occupant behaviours are considered. If other shade behaviour models are considered, the number of required simulation runs may be different from this research and it is suggested to be determined by using the graphical method described in section 2.3.

3.1.3 Correlation between repeated simulations

Based on 50 simulation runs, Fig. 7 presents Spearman correlation coefficient of hourly SC values between each two simulations. In this figure, the areas of circles represent the absolute values of corresponding correlation coefficients (a larger area of circles indicates a stronger correlation between simulations). On the principal diagonal line, the areas of circles are the largest with Spearman correlation coefficient of being 1 since the calculation is based on the same simulation. For non-diagonal elements, the distribution of correlation coefficients is illustrated in Fig. 8. It can be seen that correlation coefficients of hourly SC values are close to 0 with only a few values reaching about 0.2 /-0.2, which means

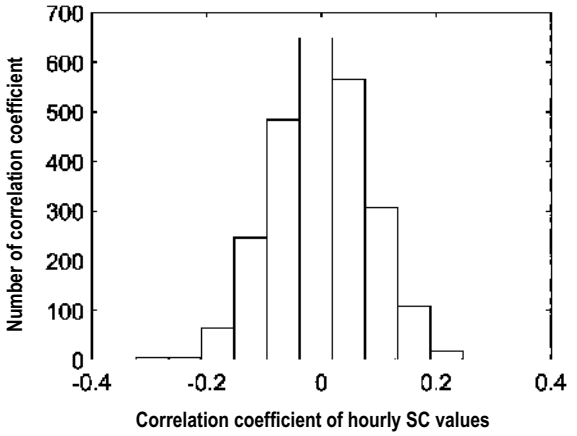

Fig. 8 Distribution of correlation coefficient of hourly SC values between 50 simulations (only non-diagonal elements in Fig. 7 are included in this figure)

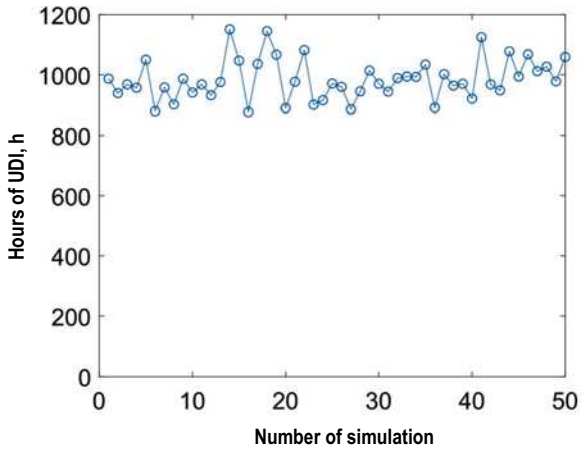

Fig. 9. Hours of UDI for each simulation

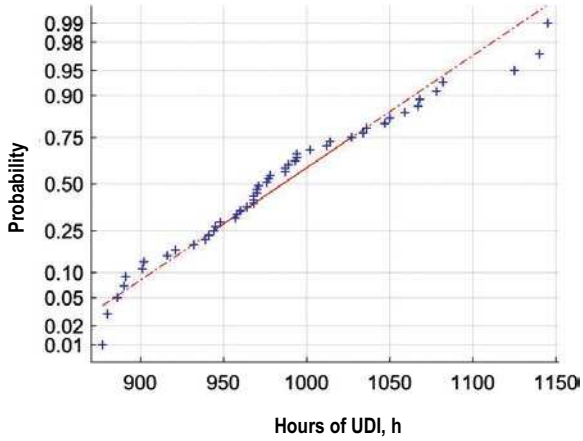

Fig. 10. Normal probability plot of hours of UDI

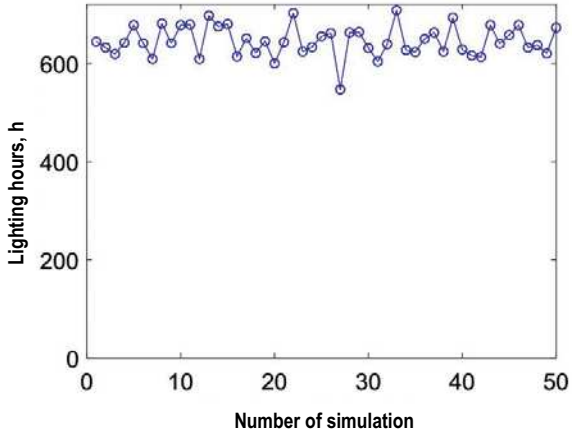

Fig. 11. Lighting hours for each simulation

no or very weak correlation. Therefore, uncertainty of shade action was not suppressed by the shade behaviour model and, thus, this model can be used to conduct uncertainty analysis of daylighting and lighting energy performance.

3.2 Daylight Uncertainty

Fig. 9 gives hours of UDI for each simulation. It can be seen that this value fluctuates among different simulation runs with a variation range of about 800–1200, which means a relatively large uncertainty (about (1200–800)/800×100 % = 50 % for the extreme situations). To further investigate the likely distribution of hours of UDI, a normal probability plot was given in Fig. 10. It can be seen that the data points approximately lie on or near the straight line, indicating a likely normal distribution. Furthermore, a more rigorous statistical test of normality of these energy data was conducted by Shapiro–Wilk test [15]. The test shows that the *p*-value is higher than 0.05 (a threshold value), indicating the null hypothesis cannot be rejected and the data are normally distributed. According to the equations described in section 2.2.2 uncertainty of daylighting performance (hours of UDI) was calculated and its value is 15.08 %, which means an error of about 15 % may exist if occupant behaviour on solar shades is not taken into consideration when predicting daylighting performance.

3.3 Uncertainty of Lighting Energy

Electric lighting is required when daylight illuminance is less than 300 lx according to lighting design standard for office buildings in China. Therefore, lighting energy can be determined according to daylighting performance, and thus the number of lighting hours (hours of daylight illuminance<300 lx) for each simulation is calculated and illustrated in Fig. 11. It can be seen that the number of lighting hours is mainly between 600 and 700. Meanwhile, normal probability plot of lighting hours was also presented in Fig. 12. It can be seen that the data points approximately lie on or near the straight line. Moreover, the Shapiro–Wilk test shows that the *p*-value is higher than 0.05, indicating that the data are normally distributed. Therefore, normal fitting according to the equation (1) was conducted and the percentage uncertainty of lighting energy was calculated according to the equation (2) based on the lighting energy intensity described in Table 1. The result shows that the lighting energy uncertainty is equal to 10.38 %. Although this level of energy uncertainty is not very significant and less than uncertainty of daylighting performance, it influences economic analysis (such as

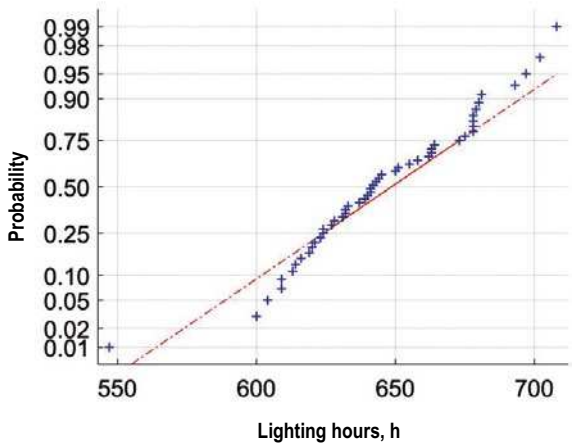

Fig. 12. Normal probability plot of lighting hours

payback period) of manual solar shades and, therefore, occupant related uncertainty should be taken into account when predicting energy performance of manual shades.

Without consideration of occupant behaviour, inappropriate choices may be selected when comparing different energy saving measures (such as clear windows with manual shades vs. low-emitting windows without solar shades). For example, energy simulation is required during building design stage and a predicted energy saving of 50 % must be met according to China's building energy design standards. Even if a simulated building energy saving is only 1 % less than 50 %, better building energy saving measures than those already used in simulated building must be adopted to achieve at least this 1 % improvement in order to meet the mandatory design standards. Therefore, an energy uncertainty of about 10 % can lead to a big difference on the choice of building energy saving measures and there is a need for consideration of energy uncertainty due to occupant behaviour. However, it is challenge for implementation of accurate energy uncertainty analysis in mandatory design standards since existing shade behaviour models are still being developed for research purpose and cannot be directly applied to building design stage. Nevertheless, some improvement strategies may be considered in design standards for better prediction of energy uncertainty instead of assuming simple shade control scenarios (e.g. fully closed or fully open, which is unrealistic occupant behaviour), which typically predict a single deterministic energy performance. For example, using representative SC values (e.g. lower and upper limits of 75 % confidence interval) for simulation according to Fig. 3. This strategy provides the possible intervals of energy performance and the uncertainty level. Besides, more reasonable simulation settings regarding manual solar shades are also required in design standards. However, possible improvements in design standards need to be further investigated and calibrated using more field measurement data in future works.

4. CONCLUSION

This paper gives an uncertainty analysis of daylighting performance and lighting energy of manual solar shades. A stochastic model developed in a previous study was used in this paper for co-simulation. Results show that uncertainty of shade action was not suppressed by the shade behaviour model with very weak relationship between different simulation outputs (SC values). Uncertainty of daylighting performance is 15.08 % while lighting energy uncertainty is 10.38 %. Although this level of energy uncertainty is not very significant, it influences economic analysis of manual solar shades and, therefore, occupant related uncertainty should be taken into consideration when predicting energy performance of manual shades. Otherwise, inappropriate choices may be selected when comparing different energy saving measures.

ACKNOWLEDGEMENT

This work was supported by Natural Science Foundation of Zhejiang Province under Grant No. LY18E080012, National Natural Science Foundation of China under Grant No. 51878358, and National Key Technology R&D Program of the Ministry of Science and Technology under Grant 2013BAJ10B06. The author also would like to thank the K.C. Wong Magna Fund in Ningbo University.

REFERENCES

1. Yao, J. An investigation into the impact of movable solar shades on energy, indoor thermal and visual comfort improvements // Building and Environment. 2014, #1, pp. 24–32.

2. Yao, J. Determining the energy performance of manually controlled solar shades: A stochastic model based co-simulation analysis // Applied Energy. 2014, #8, pp. 64–80.

3. Yan, D., et al. IEA EBC Annex 66: Definition and simulation of occupant behavior in buildings // Energy and Buildings. 2017, #Supplement C, pp. 258–270.

4. Labat, M. and Attonaty, K. Numerical estimation and sensitivity analysis of the energy demand for six industrial buildings in France // Journal of Building Performance Simulation. 2018, #2, pp. 223–240.

5. Guerra-Santin, O., et al. Mixed methods approach to determine occupants' behaviour – Analysis of two case studies // Energy and Buildings. 2016. vol 130, pp. 546–566.

6. Haldi, F. and Robinson, D. The impact of occupants' behaviour on building energy demand // Journal of Building Performance Simulation. 2011 #4, pp. 323–338.

7. Brien, W.O. and Gunay, H.B. Mitigating office performance uncertainty of occupant use of window blinds

and lighting using robust design // Building Simulation. 2015, #6, pp. 621–636.

8. Gilani, S., O'Brien, W. and Gunay, H.B. Simulating occupants' impact on building energy performance at different spatial scales // Building and Environment. 2018. vol 132, pp. 327–337.

9. Reinhart, C.F. Lightswitch-2002: a model for manual and automated control of electric lighting and blinds // Solar Energy. 2004, #1, pp. 15–28.

10. Yao, J., et al. Occupants' impact on indoor thermal comfort: a co-simulation study on stochastic control of solar shades // Journal of building performance simulation. 2016, #3, pp. 272–287.

11. Yao, J. Daylighting performance of manual solar shades // Light & Engineering. 2018, #1, pp. 99–104.

12. Yao, J., Chow, D. and Chi, Y. Impact of Manually Controlled Solar Shades on Indoor Visual Comfort // Sustainability. 2016, #8, article number 727.

13. Chapman, J., Siebers, P. and Robinson, D. On the multi-agent stochastic simulation of occupants in buildings // Journal of Building Performance Simulation. 2018, #5, pp. 604–621.

14. Robinson, S. Simulation: The Practice of Model Development and Use. 2014, UK: Palgrave Macmillan UK.

15. Prada, A., et al. Uncertainty propagation of material properties in energy simulation of existing residential buildings: The role of buildings features // Building Simulation. 2018, #3, pp. 449–464.

Jian Yao,
Ph.D. and Associate Professor at the department of architecture of Ningbo University. Dr. Yao has many years of experience in studying solar shading performance, daylighting and occupant behaviour

LiYi Chen
is a lecturer at the department of architecture of Ningbo University. He has many years of experience in studying architectural design

Wu Jin
is a lecturer at the department of architecture of Ningbo University. He has many years of experience in architectural education and architecture design, including commercial buildings, residential buildings, school buildings, etc.

Light & Engineering
Vol. 28, No. 2, pp. 85–88, 2020

https://doi.org/10.33383/2019-024
Svetotekhnika # 5, 2019, pp. 20–22

DEPENDENCE OF CURRENT HARMONICS OF GREENHOUSE IRRADIATORS ON SUPPLY VOLTAGE

Nadehzda P. Kondratieva[1], Dmitry A. Filatov[2], and Pavel V. Terentiev[2]

[1] Izhevsk State Agricultural Academy, Izhevsk
[2] Nizhny Novgorod State Agricultural Academy, Nizhny Novgorod
E-mail: filatov_da@inbox.ru

ABSTRACT

The article describes the results of the study concerning the effect of the voltage level on current harmonic composition in greenhouses irradiators. It is found that its change affects the level of current harmonics of all types of the studied greenhouse irradiators. With decrease of nominal supply voltage by 10 %, the total harmonic distortion THD_i decreases by 9 % for emitters equipped with high pressure sodium lamps (HPSL), by 10 % for emitters with electrode-less lamps and by 3 % for LED based emitters. With increase of nominal supply voltage by 10 %, THD_i increases by 23 % for lighting devices equipped with HPSL, by 10 % for irradiators with electrode-less lamps and by 3 % for LED based emitters. Therefore, changes of supply voltage cause the least effect on the level of current harmonics of LED based emitters and then the emitters with electrode-less lamps. Change of the level of supply voltage causes the greatest effect on the level of current harmonics of HPSL based irradiators. Mathematical models of dependence of THD_i on the level of supply voltage for greenhouse emitters equipped with LED, electrode-less lamps and HPSL lamps were formulated. These mathematical models may be used for calculations of total current when selecting transformers and supply cable lines for greenhouse lighting devices, for design of new or reconstruction of existing irradiation systems of greenhouse facilities, and for calculation of power losses in power supply networks of greenhouse facilities during feasibility studies for energy saving and energy efficiency increasing projects.

Keywords: greenhouse irradiators, supply voltage, total harmonic distortion of current

1. INTRODUCTION

Application of irradiators equipped with light emitting diodes (LED) and electrode-less fluorescent lamps (EFL) the radiation spectra of which may be defined by content of LED and phosphor respectively is promising for greenhouse horticulture. When growing plants in a photo-culture, there is a capability to monitor and control physiological processes in plants. The analysis of the works by Russian and foreign scientists [1–12] has shown that close data on plant performance may be obtained when using LED and EFL based irradiators with red and blue radiation with installed capacity lower by (30–50)% than that of HPSL based devices for greenhouse facilities and nurseries used currently.

Due to the new prospects, the mutual effect of the prospective emitters and power supply systems as compared to that of existing HPSL based systems is of scientific and practical interest. Greenhouse irradiators are non-linear power consumers generating higher harmonic components of current. The latter may reduce quality of functioning of different devices and electric installations or inflict damage to them, increase additional power losses in power consumers and networks [13]. The studies of the quality of electric power received from a centralised electric network have shown that the range of volt-

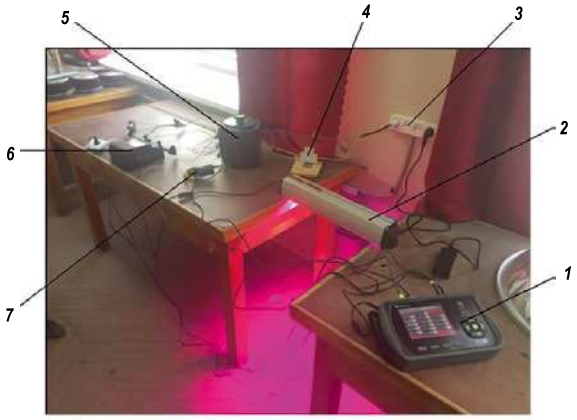

Fig. 1. The electro-technical set for measurement of electric parameters of greenhouse emitters

age level varies within a wide range in many Russian agricultural facilities [14].

The goal of this work is to study the impact of the level of supply voltage on harmonic composition of current in greenhouse emitters.

2. MATERIALS AND METHODOLOGY

The study subjects are ZhSP-series devices equipped with HPSL with a reflector (DNaZ series) manufactured by KETZ LLC, DSO-series LED based emitters manufactured by OKB Luch LLC, and EFL based irradiators manufactured by *S&O*.

The appearance of the measurement electro-technical set is shown in Fig. 1. The measurement electro-technical set includes the following elements: *1 – AR-6* power quality analyser by *Circutor*, *2* – greenhouse irradiator, *3* – ~220V power supply unit, *4* – automatic switch, *5* – RNO-250–2-M voltage controller, *6* – ammeter, *7*–5A current measuring pliers. Adjustment of supply voltage for the light source was performed by means of a line automatic transformer. The electric parameters were

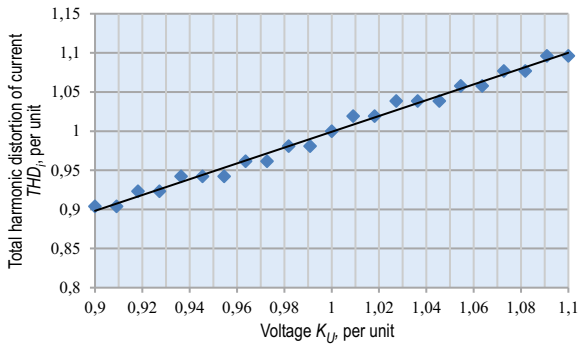

Fig. 3. Dependence of THD_i on K_U for the irradiator with an electrode-less lamp

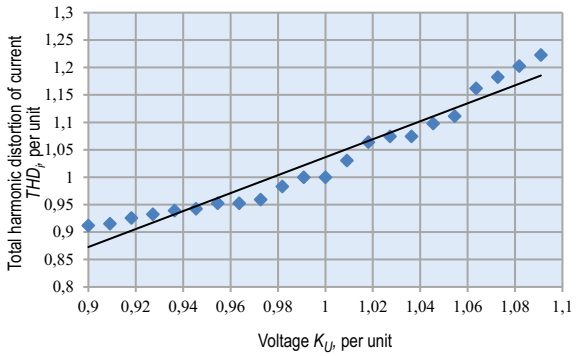

Fig. 2. Dependence of THD_i on K_U for the HPSL based irradiator

read by means of a power quality analyser. The measurements were performed for 2 light sources of each type, 3 measurements were made for each point. Over the first hour after switching on, the emitters were reaching the nominal operation mode, no measurements were made. Then harmonic composition of emitter currents was measured in the nominal operation mode. After it, the harmonics level was measured after changing the level of supply voltage with a step of 2 V.

3. RESULTS

The value of harmonic composition of an alternate current signal which includes harmonic composition of currents is characterised by, in particular, the THD_i[1] ratio.

Fig. 2 shows the results of the studies of the effect of the level of supply voltage (SV) on THD_i of a ZhSP greenhouse emitter equipped with a HPSL. With decrease of nominal SV by 10 %, total harmonic distortion of current decreases by 9 %. With increase of nominal SV by 10 %, total harmonic distortion of current increases by 23 %.

On the basis of the results of the studies, using *MS Excel* software, the mathematical expression of change of *THDi* after change of SV level was obtained:

$$THD_i = THD_{i_{nom}} \cdot (1,6 \cdot K_U - 0,6),$$

$$R^2 = 0.9414,$$

where $THD_{i_{nom}}$ is the nominal THD_i,%; $K_U = U_f / U_{nom}$ is the change of the level of SV, per unit; U_f is

[1] In foreign literature, *THD* stands for *Total Harmonic Distortion*.

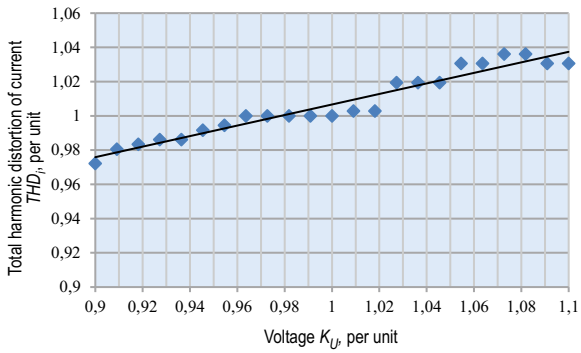

Fig. 4. Dependence of THD_i on K_U for the LED based emitter

the actual SV, V; U_{nom} is the nominal SV, V; R^2 is the determination coefficient, per unit.

Fig. 3 shows the results of the studies of the effect of the SV level on THD_i of a greenhouse irradiator manufactured by *S&O* equipped with EFL. With decrease of nominal SV by 10 %, THD_i decreases by 10 %. With increase of nominal SV by 10 %, THD_i increases by 10 %.

On the basis of the results of the studies, using *MS Excel* software, the mathematical expression of change of THD_i after change of SV level was obtained:

$$THD_i = THD_{i_{nom}} \cdot K_U,$$

$$R^2 = 0.9896.$$

Fig. 4 shows the results of the studies of the effect of the SV level on THD_i of a DSO greenhouse emitter manufactured equipped with LED. With decrease of nominal SV by 10 %, THD_i decreases by 3 %. With increase of nominal SV by 10 %, THD_i increases by 3 %.

On the basis of the results of the studies, using *MS Excel* software, the mathematical expression of change of THD_i after change of SV level was obtained:

$$THD_i = THD_{i_{nom}} \cdot (0,3 \cdot K_U + 0,7),$$

$$R^2 = 0.9435.$$

4. DISCUSSION

The change of SV level affects the level of current harmonics of all types of the studied greenhouse irradiators. For instance, with decrease of nominal supply voltage by 10 %, THD_i decreases by 9 % for emitters equipped with HPSL, by 10 % for emitters with EFL, and by 3 % for LED based irradiators. With increase of nominal SV by 10 %, THD_i increases by 23 % for irradiators equipped with HPSL, by 10 % for systems with EFL and by 3 % for LED based emitters. Therefore, changes of the level of SV cause the least effect on the level of current harmonics in LED based emitters and then on that of EFL based devices. Change of the level of SV causes the greatest effect on the level of current harmonics of HPSL based irradiators.

5. CONCLUSION

Mathematical models of dependence of THD_i on the level of supply voltage for greenhouse lighting devices equipped with LED, EFL and HPSL lamps were formulated; they may be used:

– For calculations of total current when selecting transformers and supply cable lines of greenhouse emitters and for design of new or reconstruction of existing irradiation systems of greenhouse facilities;

– For calculation of power losses in power supply networks of greenhouse facilities during feasibility studies for energy-saving and energy efficiency increasing projects.

REFERENCES

1. Korepanov, D.A., Kondratieva, N.P., Chirkova, N.M. Germinating Capacity of Seeds of Oxycoccus palustris when Using Different Spectra of Photosynthetic Radiation [Vskhozhest semyan klyukvy bolotnoy pri ispolzovanii raznykh spektrov fotosinteticheskoy radiatsii] // Bulletin of Izhevsk State Agricultiral Academy, 2012, Vol. 3, #32, pp. 82–83.

2. Rakutko, S.A., Rakutko, E.N., Vaskin, A.N. Comparative Assessment of Energy-Saving and Environmental Friendliness of Lettuce (Lactuca Sativa L.) Grown under Sodium and Electrodeless Lamps [Sravnitelnaya otsenka energoekologichnosti svetokultury salata (Lactuca Sativa L.) pod natrievymi i induktsyonnymi lampami] / Bulletin of the Saint Petersburg State Agrarian University, 2016, pp. 331–338.

3. Prikupets, L.B., Emelin, A.A., Tarakanov, I.G. LED Phytoemitters: from a Phytotron to a Greenhouse? [Svetodiodnyye fitoobluchateli: iz fitotrona v teplitsu?] / Teplitsy Rossii, 2015, Vol. 2, pp. 52–56.

4. Sokolov, A.V., Yuferev, L. Yu. Energy-saving Lighting System for Protected Ground [Energosberegayushchaya sistema osveshcheniya dlya zashchishchyonnogo grunta] // Innovatsii v selskom hozyaistve, 2014, Vol. 4, #9, pp. 76–69.

5. Johkan M., Shoji K., Goto F., Hahida S., Yoshihara T. Effect of green light wavelength and intensity on photomorphogenesis and photosynthesis in Lactuca sativa// Environmental and Experimental Botany, 2012, Vol. 75, pp. 128–133.

6. Fan X.X., Xu Z.G., Liu X.Y., Tang C.M., Wang L.W., Han X.L. Effects of light intensity on the growth and leaf development of young tomato plants grown under a combination of red and blue light// Scientia Horticulturae, 2013, Vol. 153, pp. 50–55.

7. Lin K.H., Huang M.Y., Huang W.D., Hsu M.H., Yang Z.W., Yang C.M. The effects of red, blue, and white light emitting diodes on the growth, development, and edible quality of hydroponically grown lettuce (Lactuca sativa L. var. capitata) // Scientia Horticulturae, 2013, Vol. 150, pp. 86–91.

8. Pardo G.P., Aguilar C.H., Martínez F.R., Canseco M.M. Effects of light emitting diode high intensity on growth of lettuce (Lactuca sativa L.) and broccoli (Brassica oleracea L.) seedlings // Annual Research & Review in Biology, 2014, Vol. 19, pp. 2983–2994.

9. Sase S., Mito C., Okushima L., Fukuda N., Kanesaka N., Sekiguchi K., Odawara N. Effect of overnight supplemental lighting with different spectral LEDs on the growth of some leafy vegetables // Acta Horticulturae, 2012, Vol. 956, pp. 327–333.

10. Lee J.S., Lim T.G., Kim Y.H. Growth and phytochemicals in lettuce as affected by different ratios of blue to red radiation // Acta Horticulturae, 2014, Vol. 1037, pp. 843–848.

11. Muneer S., Kim E.J., Park J.S., Lee J.H. Influence of green, red and blue light emitting diodes on multiprotein complex proteins and photosynthetic activity under different light intensities in lettuce leaves (Lactuca sativa L.)// International journal of molecular sciences, 2014, Vol. 15, pp. 4657–4670.

12. Report of Testing of DNaT-400 Lamps and 250W M-S and Bi-S Electrodeless Fluorescent Lamps [Otchyot po ispytaniyam lamp DNaT-400 i induktsyonnykh lyuminestsentnykh lamp 250W M-S i Bi-S]. URL: http://growlife.ru/otchet-po-ispytaniyu-lamp-dnat-400-i-indukcionnyx-lyuminescentnyx-lamp-250w-m-s-i-bi-s (date of reference: 23.02.2019).

13. Kondratieva, N.P., Terentiev, P.V., Filatov, D.A. Comparative Experimanetal Analysis of Electromagnetic Compatibility of Discharge and LED Artificial Light Sources for Plant-Growing [Sravnitelnyi experimentalnyi analiz po elektromagnitnoi sovmestimosti razryadnulh i svetodiodnykh iskusstevennykh istochnikov sveta dlya rastenievodstva] // Bulletin of NGIEI, 2018, Vol. 12, #91, pp. 39–49.

14. Filatov, D.A., Terentiev, P.V. Electromagnetic Compatibility of Power Supply Sources and Electric Equipment of Agricultural Facilities with Changes of the Level of Supply Voltage [Elektromagnitnaya sovmestimost sistem elektrosnabzheniya i elektrooborudovaniya selskokhozyaistvennykh predpriyatiy pri izmenenii urovnya pitayushchego napryazheniya] // Bulletin of the Nizhny Novgorod State Agricultural Academy, 2016, Vol. 3, #11, pp. 57–62.

Nadehzda P. Kondratieva, Prof., Dr. of Technical Science, graduated from the Chelyabinsk Institute of mechanization and electrification of agriculture in 1978. At present, she is a Head of the chair of Automated Electric Drive of the Izhevsk State Agricultural Academy. She has its own scientific school in the field of agricultural lighting engineering and is engaged in the development of energy saving lighting technologies for agricultural enterprises, holds the title of Honorary Worker of Higher Professional Education of the Russian Federation

Dmitry A. Filatov**,** Ph.D., graduated from the R.E. Alekseev Nizhny Novgorod State Technical University in 2009. Currently, he is Associated Professor of the Cattle-Breeding Mechanisation and Agriculture Electrification sub-department of the Nizhny Novgorod State Agricultural Academy. His research interests: light sources, electromagnetic compatibility, and electric power quality

Pavel V. Terentiev, Ph.D. in Technical Sciences, graduated from the R.E. Alekseev Nizhny Novgorod State Technical University in 2009. At present, he is the Associate Professor of the Cattle-Breeding Mechanisation and Agriculture Electrification sub-department of the Nizhny Novgorod State Agricultural Academy. His research interests: light sources, electromagnetic compatibility, and electric power quality

Light & Engineering
Vol. 28, No. 2, pp. 89–94, 2020

https://doi.org/10.33383/2019–040
Svetotekhnika #6, 2019, pp. 19–22

POWER LOSSES IN RF INDUCTOR OF FERRITE-FREE CLOSED-LOOP INDUCTIVELY-COUPLED LOW PRESSURE MERCURY LAMPS

Ekaterina V. Lovlya and Oleg A. Popov

National Research University Moscow Power Engineering Institute (NRU MPEI)
E–mail: popovoleg445@yahoo.com

ABSTRACT

RF inductor power losses of ferrite-free electrode-less low pressure mercury inductively-coupled discharges excited in closed-loop dielectric tube were studied. The modelling was made within the framework of low pressure inductive discharge transformer model for discharge lamps with tubes of 16, 25 and 38 mm inner diam. filled with the mixture of mercury vapour (7.5×10^{-3} mm Hg) and argon (0.1, 0.3 and 1.0 mm Hg) at RF frequencies of 1, 7; 3.4 and 5.1 MHz and plasma power of (25–500) W. Discharges were excited with the help of the induction coil of 3, 4 and 6 turns placed along the inner perimeter of the closed-loop tube. It was found that the dependence of coil power losses, P_{coil}, on the discharge plasma power, P_{pl}, had the minimum while P_{coil} decreased with RF frequency, tube diameter and coil number of turns. The modelling results were found in good qualitative agreement with the experimental data; quantitative discrepancies are believed to be due skin-effect and RF electric field radial inhomogeneity that were not included in discharge modelling.

Keywords: inductively-coupled discharge, closed-loop tube, low pressure mercury plasma, induction coil power losses

1. INTRODUCTION

Plasma of ferrite-free inductively-coupled discharges excited in mixture of low pressure (LP) mercury vapour and inert gases in closed-loop quartz tubes are considered as perspectives high efficient sources of UV radiation [1, 2]. Due to the absence of internal electrodes, electrode-less mercury UV lamps can operate at low buffer inert gas pressures of (0.1–0.5) mm Hg that provides maximum efficiency of resonant UV radiation [3].

Since electromagnetic radiation at frequencies of $f < 10$MHz is negligible [4], lamp RF power P_{lamp} is a sum of power absorbed by discharge plasma, P_{pl}, and power losses in coil wire, P_{coil} [5, 6]. Thus, to increase UV lamp efficiency one has to increase coil power efficiency $\eta_{coil} = (1 - P_{coil}/P_{lamp})$ [1], i.e. to minimise P_{coil}.

In the present work, effects of lamp parameters (discharge tube diameter, inert gas pressure, number of coil turns, N, operation frequency, f, and plasma absorbed power, P_{pl}) on coil power losses, P_{coil}, were theoretically studied with the help of transformer model of LP induction discharge [5, 6].

2. DISCHARGE TUBE AND RF INDUCTOR

The lamps studied had length (l_{lamp}) of 406, 426 and 454 mm and width (H_{lamp}) of 106, 126 and 154 mm, respectively. Discharge tube had inner diameter (d_t) of 16, 25 and 38mm and wall thickness (Δ) of 1.0, 1.5 and 2.0 mm, respectively. Induction coils of 3, 4 and 6 turns were made from multiple strand copper wire (Litz wire) with diameter (d_w) of 1.63 mm and resistance per unit length (ρ_w) of 8.5×10^{-4} Ω/cm (at f = (2–5) MHz). The coil turns were placed along the inner perimeter of the lamp that had "long" (l_{per}) length and "short" (H_{per}) length of 370 and 70 mm, respectively (Fig. 1).

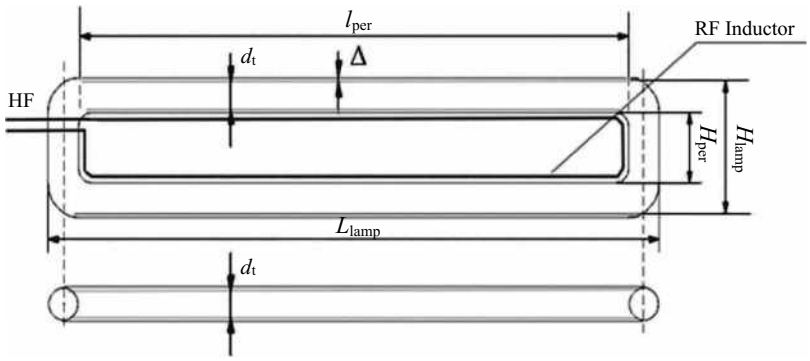

Fig. 1. Diagram of ferrite-free electrode-less inductively-coupled lamp with a closed-loop discharge tube and RF inductor (coil)

Mercury vapour pressure was 7.5×10^{-3} mm Hg (maximum UV radiation flux), inert gas (argon) pressures – 0.1, 0.3 and 1.0 mm Hg. Operation frequencies f are equal to (1,7–5,1) MHz, were chosen to satisfy condition $\omega << \nu_e$ (where $\omega = 2\pi f$ is the circular frequency of RF field, ν_e is the frequency of elastic collisions of electrons with mercury and argon atoms) that allows us to neglect the inductive component of plasma RF electric field. All calculation had been done at plasma powers P_{pl} in range (25–500) W.

3. PLASMA AND COIL PARAMETERS EQUATIONS

For calculation of plasma and coil electric parameters, the transformer model of LP induction discharge [5, 6] was used with assumptions of direct-current analogy [4] and RF electric field, E_{pl}, spatial (radial and azimuth) uniformity, and neglecting of skin-effect.

P_{coil} was calculated as

$$P_{coil} = I_{coil}^2 R_{coil}, \tag{1}$$

where I_{coil} is the RF current in the induction coil and R_{coil} is coil resistance calculated as

$$R_{coil} = \rho_w l_{coil}, \tag{2}$$

where l_{coil} is the length of coil wire defined as

$$l_{coil} = 2(l_{per} + H_{per})N. \tag{3}$$

In accordance with the transformer model of induction discharge, the expression for inductor RF current, I_{coil}, has the following expression [6]

$$I_{coil} = \frac{\bar{E}_{pl} \Lambda_{pl} \sqrt{1+Q_{pl}^2}}{\omega M}, \tag{4}$$

where Λ_{pl} is the length of plasma turn defined as length of centre line of the closed discharge tube, $\bar{E}_{pl}$ is the active component of plasma electric field averaged over cross-section of plasma turn, M is the mutual inductance of the plasma turn and the induction coil [5, 6]:

$$M = k\sqrt{L_{coil} L_{ind}}, \tag{5}$$

where L_{coil} is the inductance of disc shape induction coil ($D_{coil} >> H_{coil}$):

$$L_{coil} = 0,56\mu_o \pi D_{coil} N^2 \tag{6},$$

where $H_{coil} \approx d_w$ is the coil height, $D_{coil} = (4S_{coil}/\pi)^{1/2}$ is the coil equivalent diameter; k is the coupling coefficient of the plasma turn and the induction coil calculated as the ratio of the area encircled by the coil turn S_{coil} to the area encircled by the plasma turn S_{pl} [5, 6]:

$$k = \frac{S_{coil}}{S_{pl}},$$

where Q_{pl} is the plasma turn quality-factor that is defined as

$$Q_{pl} = \frac{\omega L_{ind}}{R_{pl}},$$

where $R_{pl} = P_{pl}/I_{pl}^2$ is the plasma turn resistance, I_{pl} *is* the discharge current, L_{ind} is the geometric inductance of plasma turn [7]:

$$L_{ind} = 2\pi D_{pl}\left[\ln\left(\frac{4D_{pl}}{0,39d_{pl}}\right) - 2\right]\cdot 10^{-9},$$

where $d_{pl} \approx 0,75d_t$ is the diameter of cross-section of plasma turn, $D_{pl} = (4S_{pl}/\pi)^{1/2}$ is the equivalent diameter of the area encircled by plasma turn, S_{pl} [8].

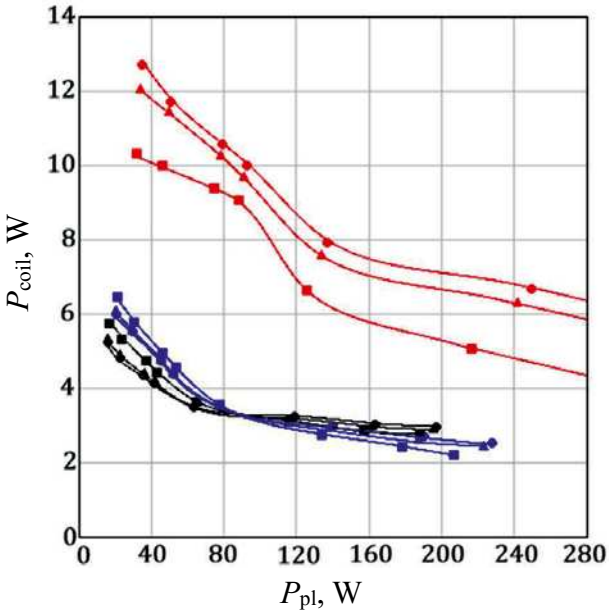

Fig. 2. Dependence of coil power losses, P_{coil}, on plasma power P_{pl}, tube diameter d_t, mm: 16 (red), 25 (blue), 38 (black); argon pressure p_{Ar}, mmHg: ● – 0.1; ▲– 0.3; ■ – 1.0; number of coil turns $N = 4$; RF frequency $f = 3.4$MHz

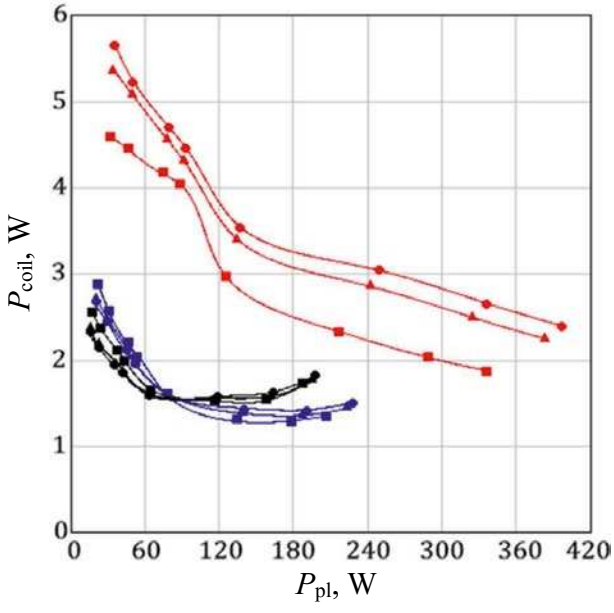

Fig. 3. Dependence of P_{coil} on P_{pl}, d_t, mm: 16 (red), 25 (blue), 38 (black); p_{Ar}, mmHg: ● – 0.1; ▲– 0.3; ■ – 1.0; $N = 4$; $f = 5.1$MHz

The equation that connects coil power losses, P_{coil}, with induction coil and discharge plasma parameters could be obtained from (1, 4):

$$P_{coil} = \frac{\left(\bar{E}_{pl}\Lambda_{pl}\right)^2 (1+Q_{pl}^2)\rho_w l_{coil}}{(\omega M)^2} . \qquad (7)$$

And using (3), (5), (6) and (7) one can get an expression that could be used for P_{coil} calculation:

$$P_{coil} = \frac{\left(\bar{E}_{pl}\Lambda_{pl}\right)^2 (1+Q_{pl}^2)\rho_w (l_{per}+H_{per})}{0,28\mu_o \pi D_{coil} N (k\omega)^2 L_{ind}}. \qquad (8)$$

With the approximation of direct-current analogy, we used values of electric field, E_{pl}, in the plasma positive column of argon-mercury discharge with the same tube diameter and fill pressure and operated at the same plasma power but at low frequency of 50 Hz [9].

4. CALCULATIONS RESULTS AND DISCUSSION

The dependencies of P_{coil} on P_{pl} calculated for lamps with various discharge tube and RF inductor parameters are shown in Fig. 2–5. It is seen that at relatively low values of P_{pl} values of P_{coil} in all lamps decrease considerably with P_{pl} increase. As P_{pl} grows the decrease of P_{coil} "slows down" and at a certain plasma power value, $P_{pl} = P_{pl,\,min}$, coil power losses reach their minimum value, $P_{coil,\,min}$, and then slightly increases with P_{pl}. The larger tube diameter, d_t, the lower value of $P_{pl,\,min}$ at which coil power losses reach their minimum value, $P_{coil,\,min}$.

The increase of RF frequency f causes the decrease of P_{coil} and shifts value of $P_{pl,\,min}$ to smaller values of P_{pl}. The effect of RF frequency on coil power losses can be explained by the transformer model of induction discharge excited at RF frequencies, $\omega << \nu_e$, which do not affect plasma power balance [4]. Therefore, $\bar{E}_{pl}$ and, hence, plasma turn RF voltage, U_{pl} (= $\bar{E}_{pl}\Lambda_{pl}$), do not depend from RF frequency ω. Note that in accordance with the induction discharge transformer model, coil RF voltage, U_{coil}, is related to U_{pl} as $U_{coil} \approx U_{pl}N/k^{1/2}$ [2, 6].

At the same time, coil inductive resistance, ωL_{coil} (here L_{coil} is coil conductance), increases linearly with the increase of RF frequency, $\omega = 2\pi f$. Since coil inductive resistance, $\omega L_{coil} >> R_{coil}$, the induction coil impedance has inductive character so RF coil current, I_{coil}, could be determined as, $I_{coil} \approx U_{coil}/(\omega L_{coil})$. Thus, I_{coil} is inversely proportional to ω while coil power losses, $P_{coil} \sim I_{coil}^2$ (see Eq. (1)) are inversely proportional to f^2. This is justified by the results of calculation of P_{coil} made at two RF frequencies, $f = 3{,}4$ and 5,1 MHz, for induction lamps with identical lamp parameters (Figs. 2,3).

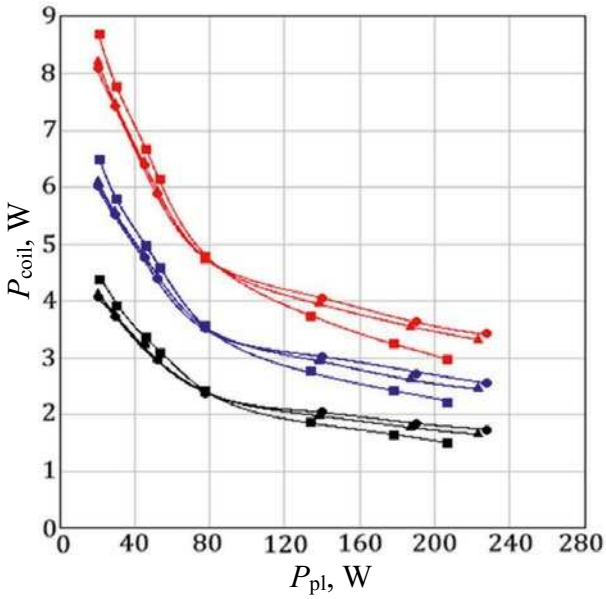

Fig. 4. Dependence of P_{coil} on P_{pl}; d_t = 25mm; N: 3 (red), 4 (blue), 6 (black); p_{Ar}, mmHg: ● – 0.1; ▲– 0.3; ■ – 1.0; f = 3.4MHz

It can be also seen from Figs. 2 and 3 that at relatively high values of P_{pl} in the lamp with d_t = 38 mm, P_{coil} could be higher than that in the lamp with d_t = 25mm. The higher f, the lower value of P_{pl} at which the curves P_{coil} (P_{pl}) calculated for lamps with different diameter "cross".

In low temperature low pressure (LP) plasmas, the increase of plasma power (actually, plasma electron density, n_e) causes the transition of ionization mechanism from electron-atom single collision to two-step ionisation process and, hence, to reduction of RF electric field in plasma, E_{pl} [4]. In non-ferrite LP induction discharges excited with the help of induction coil at frequencies of $\omega << \nu_e$, lowering of $\bar{E}_{pl}$ causes in accordance with (7) and (8) the decrease of P_{coil}.

Reducing lamp tube diameter, d_t, from 16 mm to 25mm leads to the decrease of plasma electric field, $\bar{E}_{pl}$, [2, 9] that in its turn causes significantly, in accordance with (8), decrease coil power losses, P_{coil} (Figs. 2 and 3) and k (due to the increase of S_{pl}) but results in the increase of Λ_{pl} and Q_{pl}. As it follows from (8) and is shown in Figs. 2 and 3, the dependence of P_{coil} on d_t turn out to be very complex and has its minimum at relatively high values of P_{pl} and f.

Increase of buffer gas (argon) pressure from 0.1 to 1.0 mmHg causes insignificant decrease of E_{pl} [9] and, in accordance with (7) and (8), slight decrease of P_{coil} (Figs. 2 and 3).

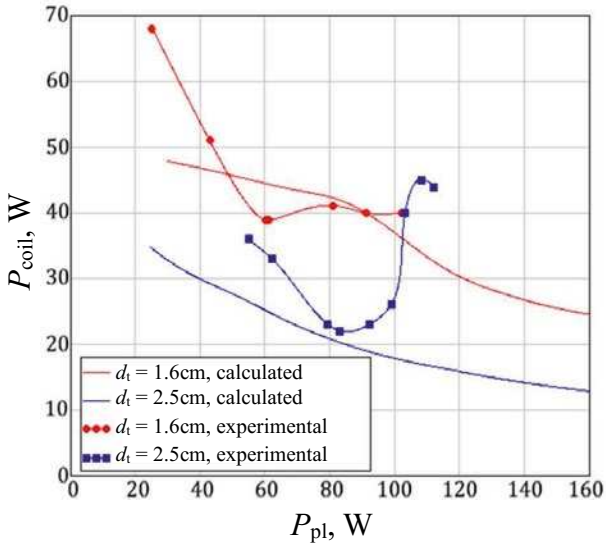

Fig. 5. Dependence of P_{coil} on P_{pl}; d_t = 16mm and 25mm; p_{Ar} = 1.0mmHg; N = 3; f = 1.7MHz

Increase of P_{pl} (and, therefore, I_{pl} and n_e) is accompanied by the decrease of R_{pl}, that (with a reasonable assumption of independence of L_{ind} on I_{pl}) causes the growth of plasma quality factor, Q_{pl} (= $\omega L_{ind}/R_{pl}$). At low values of P_{pl}, when R_{pl} is high, plasma quality factor, Q_{pl}, is very low (<0.1) and in accordance with (7) and (8) does not affect P_{coil}. The further increase of P_{pl} and d_t causes the decrease of R_{pl} and, hence, the growth of Q_{pl} that increasingly affects P_{coil} and the character of the dependence of P_{coil} on P_{pl} that changes from "negative" to positive" one forming the minimum at $P_{pl, min}$ (Fig. 3). Similar dependences of P_{coil} on P_{pl}, with the their minimums shifted with increase of f and d_t to lower values of P_{pl}, were experimentally observed in linear ferrite-free electrode-less lamps excited with the help of induction coil at f = 6–12 MHz [10].

The effect of the number of coil turns, N, on coil power losses, P_{coil}, is shown in Fig. 4. It is seen that in accordance with (8), P_{coil} is inversely proportional to N.

5. COMPARISON OF CALCULATION RESULTS WITH THE EXPERIMENT

The experimental data of P_{coil} measured in two inductive lamps with tube diameter 16 and 25 mm excited at RF frequency of 1,7 MHz are presented in Fig. 5 as functions of P_{pl}. The dependencies of P_{coil} on P_{pl} calculated for the same lamps are plotted in Fig. 5. It is seen that the experimental dependence

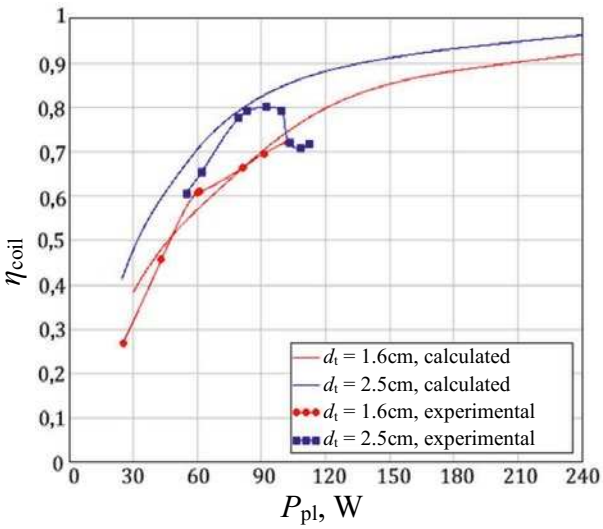

Fig. 6. Dependence of RF inductor (coil) power efficiency, η_{coil}, on P_{pl}. d_t = 16 mm and 25 mm; p_{Ar} = 1.0 mmHg; N = 3; f = 1.7MHz

of P_{coil} on P_{pl} of the lamp with smaller tube diameter (16 mm) has shallow minimum at $P_{pl,\,min}$= 60W while the experimental dependence of P_{coil} on P_{pl} of the lamp with larger tube diameter (25 mm) has deep minimum at $P_{pl,\,min}$ = 85W. It should be noted that the calculated values of P_{coil} of the lamp with d_t = 16 mm are in good agreement with the calculated data of P_{coil} of the lamp with the tube of larger diameter (25 mm) considerably exceed the experimental ones at $P_{pl,\,min}$ > 90 W.

It is from Fig. 5 that both minimums in dependencies $P_{coil}(P_{pl})$ are at plasma powers, $P_{pl,\,min}$, which are much smaller than those caused by coil power losses increase due to the growth of plasma quality factor, Q_{pl} > 0,3, see (8). It is believed that the minimums in Fig. 5 and further growth of P_{coil} observed in the experimental dependencies of P_{coil} on P_{pl} are related to skin effect pronounced in induction discharges at f = 1–5MHz and plasma densities, $n_e > 10^{11}$cm^{-3} [4, 10, 11].

Indeed, skin effect that "pushes" RF electric field to discharge tube walls where coil wire is located, thereby, increases $\bar{E}_{pl}$ [4, 11] and thus causes the increase P_{coil}. The observed discrepancy between calculated and experimental data seems to be caused by not taking into account skin effect in inductive discharge model.

It could be seen in Fig. 6 that in both lamps, at relatively low values of P_{pl}, η_{coil} rapidly increases with P_{pl} and at high values of P_{pl} asymptotically approaches to 1. The discrepancy between experimental and calculated dependencies of η_{coil} on P_{pl} in the lamp with d_t = 25mm observed at P_{pl} > 85W are believed to be due to non-considering skin effect in LP inductive discharge model.

6. CONCLUSION

- With the use of the transformer model, the analytic expression for induction coil power losses, P_{coil}, in LP inductively-coupled discharges excited at frequencies of $\omega << \nu_e$ in ferrite-free closed-loop tube with the mixture of mercury vapour and argon were derived.
- It was found that the dependence of P_{coil} on plasma power, P_{pl}, has the minimum that shifts to lower values of P_{pl} as the discharge tube diameter, d_t, and RF frequency, f, increase.
- It was shown that discharge tube diameter, d_t, affects coil power losses, P_{coil}, via RF electric field, plasma turn length, Λ_{pl}, and quality factor, Q_{pl}, and plasma turn and induction coil coupling coefficient, k.
- It is found that P_{coil} is inversely proportional to coil turns number, N, and slightly decreases as argon pressures grows from 0.1 mm Hg to 1.0 mm Hg.
- The results of calculation of coil power losses, P_{coil}, and coil power efficiency, Q_{coil}, made for the ferrite-free electrode-less lamp with discharge tube diameter, d_t = 16mm, were found in satisfactory qualitative agreement with the experiment. Discrepancy between calculated and experimental obtained P_{coil} and Q_{coil} in lamp with tube diameter of 25mm at $P_{pl} \geq$ 80W is supposedly due to not taking into account skin effect in the transformer model of LP inductively-coupled discharge.
- The results obtained could be used for optimisation of RF frequency, induction coil number of turns, and length, and diameter of discharge closed-loop tube of ferrite-free electrode-less LP mercury UV lamps.

REFERENCES

1. Pavel V. Starshinov, Oleg A. Popov, Igor V. Irkhin, Vladimir A. Levchenko, and Vasina Victoria N. Electrodeless UV Lamp on the Basis of Low-Pressure Mercury Discharge in a Closed Non-Ferrite Tube// Light & Engineering, 2019, Vol. 27, # 6, pp. 133–136.

2. Starshinov, P.V., Popov O.A., Irkhin, I.V., Vasina, V.N., Levchenko, V.A. Electric and Radiation Characteristics of Ferrite-free Electrodeless Inductively-coupled

UV Lamps in Closed-loop Tubes [Elektricheskie i izluchatelnyiye kharakteristiki induktivnykh besferritnykh rtutnykh UF lamp v zamknutykh trubkakh] // Bulletin of MEI, 2019, #. 3, pp. 87–97.

3. Vladimir A. Levchenko, Oleg A. Popov, Sergei A. Svitnev, and Starshinov Pavel V.

Electric and Radiation Characteristics of a Transformer Type Lamp with a Discharge Tube of 16.6 mm Diameter// Light & Engineering, 2016, Vol. 24, #2, pp. 77–81.

4. Raiser, Yu.P. Physics of Gas Discharges [Fizika gazovogo razryada]. Moscow: Nauka, 1987, 591 p.

5. Piejak, R.B., Godyak, V.A., Alexandrovich, B.M. A Simple Analyses of an Inductive RF Discharge // Plasma Sources Sci.Technol. 1992, № 1, pp. 179–185.

6. Popov, O.A., Chandler, R.T. Ferrite-free High Power Electrodeless Fluorescent Lamp Operated at a Frequency of 160–1000 kHz // Plasma Sources Science and Technology, 2002, # 11, pp. 218–227.

7. Gudmundsson, J.T. and Lieberman, M.A. Magnetic Induction and Plasma Impedance in a Cylindrical Inductive Discharge// Plasma Sources Sci. Tech. 1997, Vol. 6, № 4, pp. 540–550.

8. Popov, O.A., Starshinov, P.V., Vasina, V.N. Study of Characteristics of Electrodeless Ferrite-free Low Pressure Mercury Discharge in a Closed-loop Tube [Issledovanie kharakteristik induktsionnogo besferritnogo rtutnogo razryada nizkogo davleniya v zamknutoi trubket] // Bulletin of MEI, 2018, Vol. 4, pp. 89–96.

6. Rokhlin, G.N. Discharge light sources [Razryadnyie istochniki sveta]. Moscow: Energoatomizdat, 1991, 720 p.

10. Svitnev, S.A., Popov, O.A., Levchenko, V.A., Starshinov, P.V. Characteristics of Low-Pressure Ferrite-free Induction Discharge. Part 1. Electrical Parameters of Induction Coil [Kharakteristiki besferritnogo induktsionnogo razryada nizkogo davleniya. Chast 1. Elektricheskiye parametry katushki] // Uspekhi prikladnoi fiziki, 2016, Vol. 2, pp. 139–149.

11. Nikiforova, V.A., Popov, O.A. Effect of RF Field Frequency and Discharge Current on Radial Distribution of Parameters of Plasma of Ferrite-free Inductively-coupled Discharge in Closed-loop Tube [Vliyanie chastoty VCh polya i razryadnogo toka na radialnoye raspredeleniye parameterov plazmy induktsionnogo besferritnogo razryada v zamknutoi trubke] // Bulletin of MEI, 2012, Vol. 1, pp. 108–114.

Ekaterina V. Lovlya,
student of the Light Engineering department,
NIU MEI

Oleg A. Popov,
Prof., Doctor of Technical Sciences, graduated from Moscow Power Engineering Institute (MEI) in 1965. Currently, he is a Professor of Light Engineering department, NIU MEI, Member of the Russian Academy of Electric Engineering

Light & Engineering
Vol. 28, No. 2, pp. 95–105, 2020

https://doi.org/10.33383/2019-021
Svetotekhnika #4, 2019, pp. 29–34

MAGNETIC FIELD IMPLEMENTING INTO THE ELECTROLUMINESCENCE OF OLED DEVICES DOPED WITH $CoFe_2O_4$ NANOPARTICLES

Selin Pıravadılı Mucur[1], Betül Canımkurbey[2], and Ayşe Demir Korkmaz[3]

[1]*The Scientific and Technological Research Council of Turkey (TÜBİTAK) Marmara Research Centre (MAM), Materials Institute, Kocaeli, Turkey*
[2]*Amasya University, Faculty of Arts and Sciences, Department of Physics, Amasya, Turkey*
[3]*Istanbul Medeniyet University, Faculty of Science, Department of Chemistry, Istanbul, Turkey*
E-mail: selin.piravadili@tubitak.gov.tr

ABSTRACT

Cobalt ferrite magnetic nanoparticles ($CoFe_2O_4$ MNPs) were successfully prepared by citric acid-assisted sol-gel auto combustion method and used in emissive layer of organic light emitting diode (OLED). Dimensional, structural and magnetic properties of $CoFe_2O_4$ nanoparticles (NPs) were recearched and compared by using X-ray diffraction (XRD), scanning electron microscopy (SEM), and vibrating sample magnetometer (VSM). $CoFe_2O_4$ MNPs were utilized at various concentrations (0.5 wt%, 1.0 wt% and 2.0 wt%) in the emissive layer of the OLEDs. The luminance, current efficiency and the electroluminescence characteristics of the devices with and without $CoFe_2O_4$ MNPs were investigated. An external magnetic field, B_{ext}, has also been applied to the OLEDs doped with MNPs while under operation. Effects of MNPs on OLED characteristics under B_{ext} were studied thoroughly. In the tailored device architecture, poly (3,4-ethylenedioxythiophene): poly polystyrene sulphonate (PEDOT: PSS) and poly(2-methoxy-5-(2-ethylhexyloxy))-1,4-phenylene vinylene (MEH-PPV) were used as a hole transport layer (HTL) and an emissive layer respectively with ITO/PEDOT: PSS/MEH-PPV: $CoFe_2O_4$/*Ca*/*Al* device architecture. The obtained results of the fabricated OLEDs were enhanced in the presence of $CoFe_2O_4$ NPs under B_{ext} due to providing density of states in the polymer matrices. The turn-on voltage was diminished slightly in the device doped with 0.5 % wt MNP compared to the devices with other concentrations of MNPs.

Keywords: magnetic field, OLED, electroluminescence, magnetic nano particles

1. INTRODUCTION

The field of organic devices that are based on π-conjugated organic materials has improved rapidly. At the moment, display and solid state lighting technology based on organic light emitting diodes (OLEDs) are the most immanent and developing field [1–3]. Although important progress has been achieved on the performance of OLEDs, further development is still needed for gaining a place in the market. Imbalanced charge injection, recombination and low fraction of singlet excitons limit the performances of devices [4, 5]. Using different charge injection and transport layers that have proper energy level or doping the charge transport and emissive layers are the recipe of controlling and balancing the carriers [4–8]. Device engineering and using nanomaterials are some examples to enhance OLED performance since radiative singlet excitons have a maximum value of 25 %, which is a restriction on efficiency of the device [5, 9–14]. Thus, there are various serious constraints for the development of OLEDs. Recently, experimental and theoretical studies have been performed which claim that the electron-hole recombination is spin de-

pendent [10, 15–21]. In particular, the recombination ratio is raised by the heavy atoms embedded in polymers [22]. Poly (*p*-phenylene vinylene) (PPV), polyfluorene (PFO), and their derivatives are the most frequently used polymers in device technology, but they have no heavy atoms in their backbone and 75 % triplet electron hole pair seriously limit the device efficiency. Therefore, the electroluminescence (EL) efficiency is enhanced by triplet electron hole pair conversion to the singlet exciton. Hu *et al.* used *CoPt* ferromagnetic nanowires in MEH-PPV and iridium complex *Ir* (ppy) to investigate the exciton formation [11]. When an external magnetic field is applied, *CoPt* nanowires increase the singlet-to-triplet exciton ratio in organic semiconductors that increase the singlet-to-triplet ratio. The doping of magnetic nanomaterials in OLEDs based on conjugated polymers has enhanced the performances [11, 14, 23]. Sun *et al.* doped $Co_{70}Fe_{30}$ MNPs in the emissive layer of OLEDs [23]. The EL of the device was enhanced with doping, and it was further enhanced when an external magnetic field was applied to the device. The increment in the fraction of singlet excitons and new trapping sites by magnetic field enhanced the generation of excitons. The pioneering studies were done in the discovery of magnetic field effects in organic semiconductors in 1960s [24–27]. Recently, the effects of magnetic field on tris (8-hydroxyquinoline) aluminum (III) (Alq_3) – based devices were searched by various groups [28–32]. The effect of magnetic field on organic semiconductors is explained by excitonic [33, 34] and bipolaron systems [35]. In the excitonic model, magnetic field changes intersystem conversion rates and traps the carriers in triplet state [33, 34]. In the bipolaron model, polarons were hopping and bipolarons were generated under magnetic fields [35].

Cobalt ferrite ($CoFe_2O_4$) is a kind of ferromagnetic materials. Recently, many academic and industrial studies have been done due to the magnetostrictive of $CoFe_2O_4$. Magnetostriction of a materials causes to change their shape or dimensions during the magnetization. This property has enabled applications in the surfaces on the wings of airplanes, sensors, corrosion in pipes. In this study, we reported and discussed the effects of $CoFe_2O_4$ MNPs doping in MEH-PPV. The hole transport studies in the MEH-PPV and MEH-PPV: $CoFe_2O_4$ MNPs composite have been carried out in ITO/PEDOT: PSS/MEH-PPV: $CoFe_2O_4$ MNPs/*Ca*/*Al* device configuration. Interesting results including applied B_{ext} have been found in these investigations. The doping of cobalt ferrite MNPs in MEH-PPV reduces the hole mobility by way of providing density of states (DOS), new trap sites and opened the way for balanced injection and radiative recombination of the charge carriers to realize improved performance of OLEDs. These results were reported and discussed in this study.

2. EXPERIMENT

2.1. Materials and Synthesis

All analytical grade chemicals for the synthesis, such as ferric nitrate nonahydrate ($(Fe(NO_3)_3 \cdot 9H_2O)$), cobalt nitrate tetrahydrate ($Co(NO_3)_2 \cdot 4H_2O$), citric acid and ammonia solution (30 %), were used without further purification. $CoFe_2O_4$ MNPs were synthesized as reported in the literature. Stoichiometric amounts of ferric nitrate and cobalt nitrate were dissolved in deionized water and poured into a crucible, in a molar ratio of 2:1. While this solution was being stirred, 2 g of citric acid to facilitate the distribution of the metal salts homogeneously and segregation of the metal ions was added [36]. Then, the pH was adjusted to 7.5 by adding ammonia to the solution in the crucible drop by drop. The solution was heated firstly to form a viscous gel and when the temperature reached to around 150 °C, a self-propagating combustion process occurred and a grey-black powder was obtained.

2.2. Instrumentation

The ITO-coated glass substrates (ITO thickness 120nm, 10 ohms/sq.) were purchased from KINTEC Systems Ltd. Aluminum (*Al*) pellets and *Ca* (99.99 % pure) was purchased from Kurt J. Lesker Company. PEDOT: PSS and MEH-PPV (Mn~40.000–70.000) were purchased from Heraeus Clevios GmbH and Sigma-Aldrich respectively. PEDOT: PSS was filtered through a 0.45 μm membrane PVDF filter. The MEH-PPV solution was prepared in toluene:1.2-dichlorobenzene (3:1) mixture with 8 mg/cm^3 concentration and filtered through a 0.45 μm PTFE membrane filter. $CoFe_2O_4$ powder was distributed in butyl benzoate at 8 mg/ml and the mixture was stirred for 2 hours by using ultrasonication. Patterned ITO-coated glass substrates were cleaned ultrasonically in acetone, detergent solution

(PCC-54 2 % wt dispersed in H_2O) and finally with deionized water and isopropyl alcohol respectively. Except for HTL, all device layers were deposited in a glove-box system.

Hamamatsu PMA-12 C10027 Photonic Multichannel analyzer and digital multimeter (2427-C3A Keithley) were used to measure electroluminescence, current efficiency, brightness and current-voltage relation of the devices with various MNPs concentration. All devices were measured in a dark sample chamber to get away any influence of ambient light. A stylus profiler (KLA Tencor P-6) was used to determine the thickness of organic layers. The optical transmission spectra were recorded using FS5 spectrofluorometer (Edinburg Inst, wavelength range of (300–800) nm. SEM images were acquired by a Philips XL 30 SFEG. Elemental distribution and associated spectra were obtained by EDAX Energy Dispersive X-ray Spectroscopy (EDS). Electron Spin Resonance spectrum was measured by Bruker ELEXSYS E580. The magnetic characterization was performed at room temperature by using a vibrating sample magnetometer (LDJ Electronics Inc., Model 9600) in an external field up to 15 kOe. The crystalline structure of the MNPs was determined with X-ray diffraction (XRD) measurements by using a Bruker D8 DISCOVER with DAVINCI design using *Cu Kα* radiation in the 2θ range of 20°–70°. Spin casting of the emissive layer was done within a controlled N2 environment in the glove-box system. All the devices of this study were exposed to air after the encapsulation with epoxy under UV light for 3 minutes.

2.3. Device Fabrication

PEDOT: PSS was used as for the holes injection layer (HIL). A layer of PEDOT: PSS (thickness ~ 60 nm) was spin-coated onto the pre-cleaned ITO-coated glass at 4000 rpm for 30 s and then baked at 120 °C for 20 min. This procedure flattens the ITO-coated glass slides, gets rid of humidity from surface and avoids short circuits. $CoFe_2O_4$ MNPs: MEH-PPV blend was prepared in the concentration of 0.5 % wt, 1.0 % wt and 2.0 % wt. This blend was deposited (thickness ~ 100 nm) on top of the holes injection layer by spin coating at 1000 rpm for 40 s then baked at under its T_g for 20 min in N_2 environment to evaporate the solvents. Finally, calcium as an electron injection layer (~15 nm) and cathode layer of aluminium (~120 nm) were deposited by vacuum evaporation (5 x 10^{-6} mbar) technique. The active emission area was 9.0 mm^2. The thickness of evaporated layers was measured by a quartz crystal monitor. The devices with ITO/PEDOT: PSS/MNPs: MEH-PPV/*Ca*/*Al* structure were fabricated.

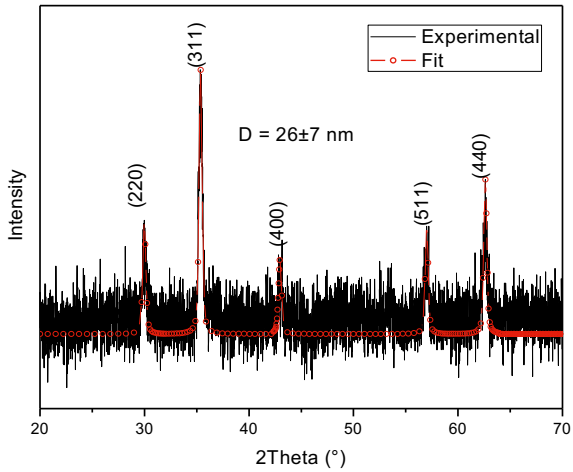

Fig. 1. XRD powder pattern of $CoFe_2O_4$ MNPs.

3. RESULTS AND DISCUSSION

3.1. XRD Analysis of $CoFe_2O_4$ MNPs

The structure and phase purity of $CoFe_2O_4$ MNPs were confirmed by investigating their X-ray diffraction pattern as seen in Fig. 1. All the observed XRD peaks could be assigned to cubic spinel lattice indicating the single phase cubic spinel structure of $CoFe_2O_4$ MNPs. The broadening of the peaks was due to the small crystallite size. The line profile fitting technique stated in Wejrzanowski *et al.* [37, 38] was applied by fitting five observed peaks of the XRD powder pattern with the following miller indices: (220), (311), (400), (511) and (440) to calculate the mean size of the crystallites. The peaks matched very well with the Powder Diffraction File (PDF) card number 00–022–1086. The line profile fitting method revealed that the mean crystallite size was 26±7 nm.

3.2. SEM Analysis of $CoFe_2O_4$ NPs

The particle morphologies of the $CoFe_2O_4$ MNPs were investigated using SEM micrographs. The surface of the $CoFe_2O_4$ MNPs composed of platelets as seen in Fig 2b. The platelet like structure was also observed in a study by Venkatesan *et al.*

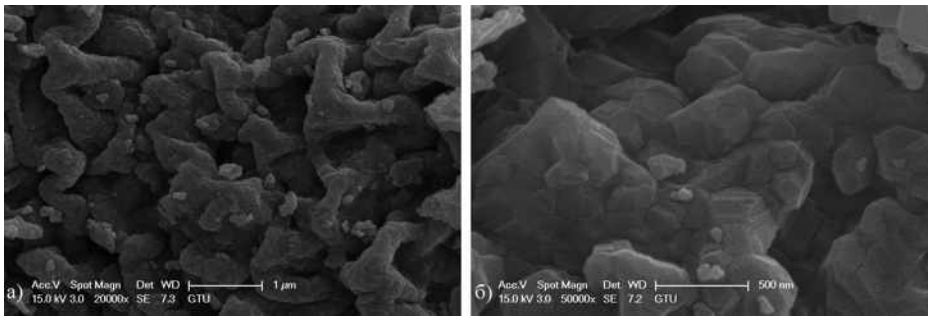

Fig. 2. SEM analysis of $CoFe_2O_4$ MNPs

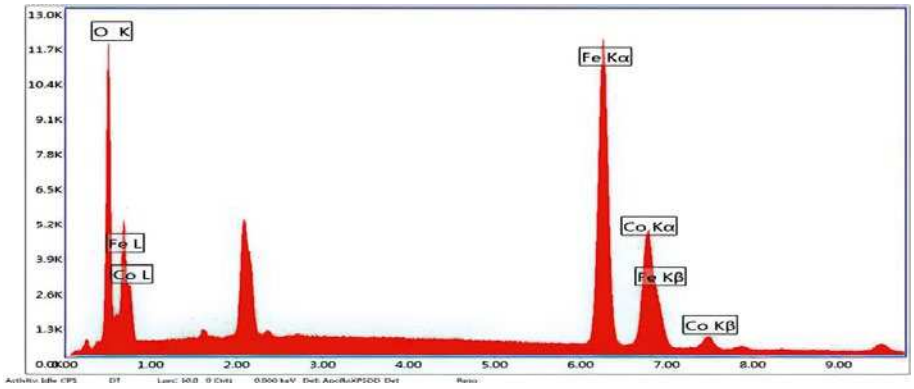

Fig. 3. Elemental distribution and associated spectra were obtained by EDAX Energy Dispersive X-ray Spectroscopy (EDS) of $CoFe_2O_4$ MNPs coated with gold

where $CoFe_2O_4$ MNPs were synthesized by solution combustion method. They suggested that the formation of agglomerated particles was due to less gas being released during the combustion process [39]. The SEM analysis showed the agglomeration of particles which might also be due to the magnetic attraction of nanoparticles to each other.

In order to confirm the presence and the composition of cobalt ferrite nanoparticles, the final product was characterized by energy dispersive spectroscopy (EDS) coupled with SEM unit. EDS scan supported the presence of $CoFe_2O_4$ with the inclusion of cobalt, oxygen, cobalt, and iron respectively. No impurity was detected in the synthesized $CoFe_2O_4$ MNPs. A profile of these four elements was shown in Fig. 3.

3.3. VSM Analysis of $CoFe_2O_4$ NPs

The magnetization of the $CoFe_2O_4$ MNPs has been studied as a function of the applied magnetic field using a variable sample magnetometer (VSM) at 300 K and the behaviour was shown in Fig. 4. The hysteresis loop of magnetization indicated the ferromagnetic behaviour of $CoFe_2O_4$ MNPs. The field dependent magnetization (M-H) curve of $CoFe_2O_4$ MNPs was recorded at room temperature by varying the externally applied field up to ±15 kOe. The saturation magnetization (σ_s) value was determined

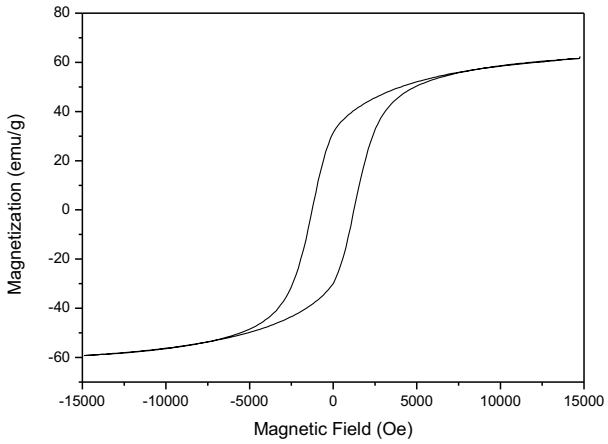

Fig. 4. The magnetization of the $CoFe_2O_4$ MNPs as a function of the applied magnetic field using a variable sample magnetometer (VSM) at 300 K

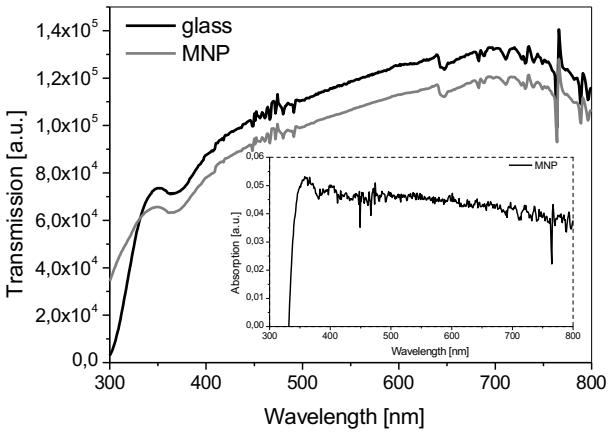

Fig. 5. Transmission and absorption properties of the MNP thin film

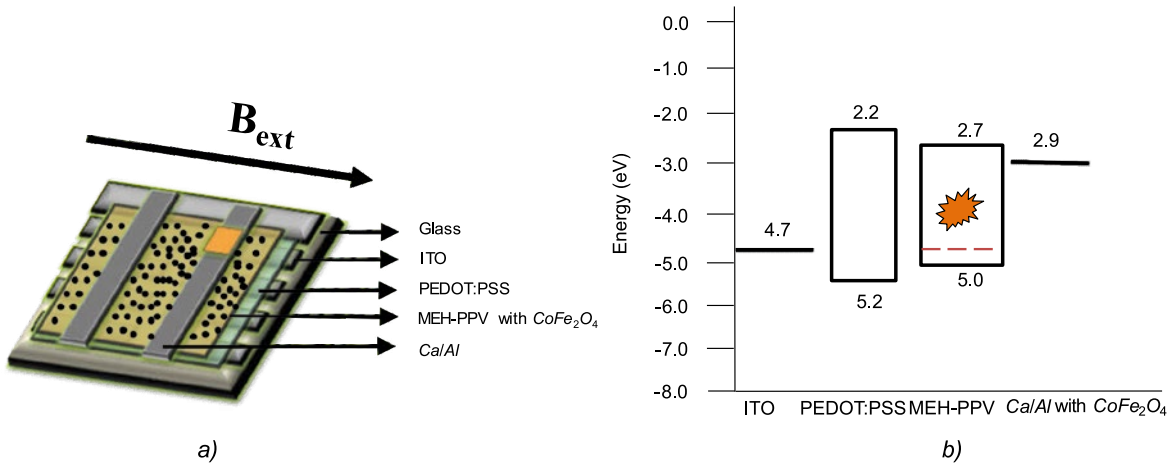

Fig. 6. Schematic cross-sectional structure of OLED and chemical structure of polymer used in this study – a; energy diagram of the OLED: the highest occupied molecular orbital (HOMO) and lowest unoccupied molecular orbital (LUMO) band energies – b

by the law of as approaching saturation, which is also known as the Stoner-Wohlfarth (S-W) model by extrapolating the plot of σ (magnetization) vs $1/H^2$ to, where $1/H^2$ approaches zero [40]. The S-W model accounts for single-domain and non-interacting particles carrying randomly oriented uniaxial anisotropy directions [41]. Based on the S-W model mentioned above, the maximum saturation magnetization value (M_s) was determined as 60.78 emu·g^{-1} lower than the 80.8 emu·g^{-1} value M_s for bulk $CoFe_2O_4$ [42]. The remnant magnetization (Mr) was found as 30.69 emu·g^{-1} and the coercivity (Hc) was determined as 1246 Oe, which was somewhat smaller than that of bulk $CoFe_2O_4$ with a room-temperature coercivity of 5.4 kOe [43]. These results might be arising from a spin-glass shell formed as the magnetically dead or inert layer on the surface of cobalt ferrite nanoparticles [42, 43].

The remanence (M_r) to saturation (M_s) magnetization ratio (M_r/M_s) was found to be 0.50 which was expected for a system with non-interacting single-domain particles with uniaxial anisotropy directions [44, 45].

3.4. Photophysical Properties of $CoFe_2O_4$ NPs

The photo-physical properties of $CoFe_2O_4$ MNPs in butyl benzoate thin film, which were spin coated on glass substrates, were investigated by UV–VIS absorption, Fig. 5. A little absorption behaviour was observed and correspondingly, transmission values were nearly the same with glass substrates. This high transmission characteristics allow the use of MNPs in OLED devices.

3.5. Electroluminescence Properties

Fabricated OLED device structure could be seen from Fig. 6a. Fabrication procedure was discussed in detailed in experimental section. It was clearly seen from Fig. 6b that the HOMO energy level of MEH-PPV polymer matched with the PEDOT: PSS HOMO energy level, thus the transportation of holes from ITO to emissive layer becomes easier. MEH-PPV has also suitable lowest unoccupied molecular orbital (LUMO) energy level (–2.75 eV), which is high enough to transport of electrons from the cathode, thus this improved the luminance efficiency by efficient recombination of electrons and holes in the emissive layer. The Fermi level of the doped $CoFe_2O_4$ MNPs was ~0.3 eV lower than the HOMO of MEH-PPV. Similar to the doping of single wall carbon nano-tubes in polymers [11, 14], it might be derived that in this case, also the holes may get injected into MNPs and transport via internal hopping through MNPs. To investigate the effect of the concentration of $CoFe_2O_4$ MNPs on the OLED device performances, the emissive layer was doped with $CoFe_2O_4$ MNPs in various concentrations: 0.5 % wt, 1.0 % wt and 2.0 % wt.

All the devices exhibited the same luminance values, Fig. 7a, while the device doped with 0.5 % MNPs had maximum luminous efficiency and EQE, 0.83 cd/A and 0.43 % respectively, Fig. 7b and Fig. 7d. The device characteristics were enhanced upon varied concentrations of MNPs as summarized in Table 1. **Fig. 7c** showed the experimental I–V characteristics of the devices at different MNP concentrations. The turn-on voltage values of the de-

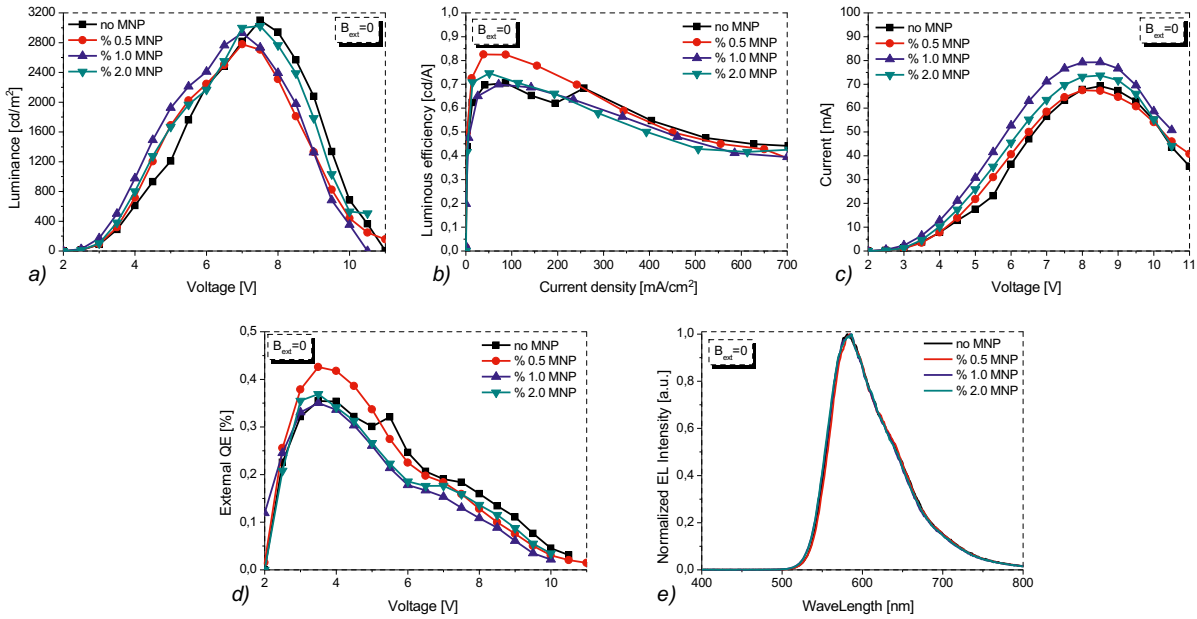

Fig. 7. OLED characteristics for different MNPs concentration: a) luminance–voltage, b) luminous efficiency–current density, c) current–voltage, d) EQE- voltage, e) normalized EL intensity

vices were slightly different. The conductance and charge hopping mechanism of the devices including MNPs were expected to increase their charge carrying mobility and resulted in lower turn-on voltages. In this study, the devices with doped MNPs showed lower turn-on voltage compared with the device without MNPs. The device turn-on voltage for the emission of photons is associated with the minority carrier injection. At low voltages, I–V characteristics showed Ohmic behaviour. At higher voltages, I–V behaviour was found to be governed by space charge limited conduction (SCLC). In the SCLC, current has directly proportional with the density of states (DOS).

As it could be seen in the Fig. 7c, the current of the devices with MNPs were higher than the device without MNPs, therefore doping concentration could increase the DOS. However, due to the small size and low concentration of the particles in the present case, the MNPs did not form local conducting channels as in the case of nano-rods. Further, as the MNPs were distributed homogenously throughout the MEH-PPV layer, the probability of internal hopping through the particles was negligible. Therefore, the most probable way was each nanoparticle served as a trap for the holes. Therefore, the trap density was being enhanced by the doping of MNPs in MEH-PPV. Note that the enhancement in the net trap density in the blend did not exactly correspond to the nanoparticle density. The increment in the trapping sites was more than the density of the MNPs in the present case. In general, the traps were created in a system by the doping/impurities and the structural/interfacial defects [42]. When MNPs were doped in emissive layer interface defect states at the MEH-PPV–MNPs interface were also created, which could serve as trapping sites; therefore, the number of trapping sites increased more than the density of the MNPs. It was also important to note that because of low doping and good dispersion of MNPs, we have ruled out the possibility of formation of conducting channels and particle–particle interaction in the present case. However, particle–particle interaction can play an important role in the determination of device performance. Bakuzis *et al*. [43] investigated particle–particle interaction in magnetic fluids containing MNPs. The interaction of the particles depends on their concentration. The higher the particle concentration the lower the particle–particle distance, which increases the interaction among the nanoparticles.

The EL spectra of the fabricated OLEDs were shown in Fig. 7e. EL spectrum exhibited peak is about 594 nm wavelength. All devices had EL emission peak at the same wavelength, namely MNPs did not affect the morphology and dominant wavelength of the emitted light from OLEDs.

These *J-V* curves were described by a power law of $J \sim V^{m+1}$ and, in logarithmic scale (Fig. 8) to determine the mechanisms of electrical conductivi-

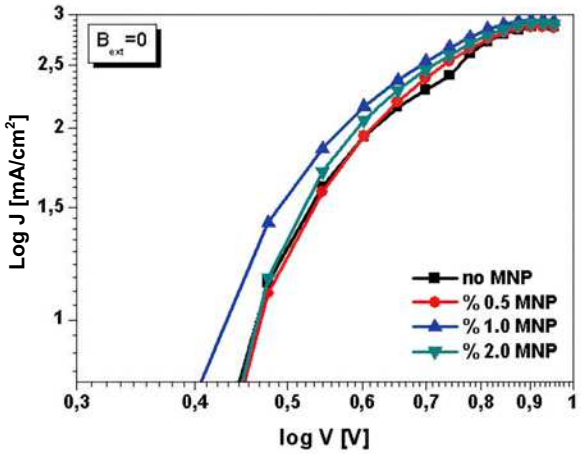

Fig. 8. Logarithmic dependencies of current density-voltage curves

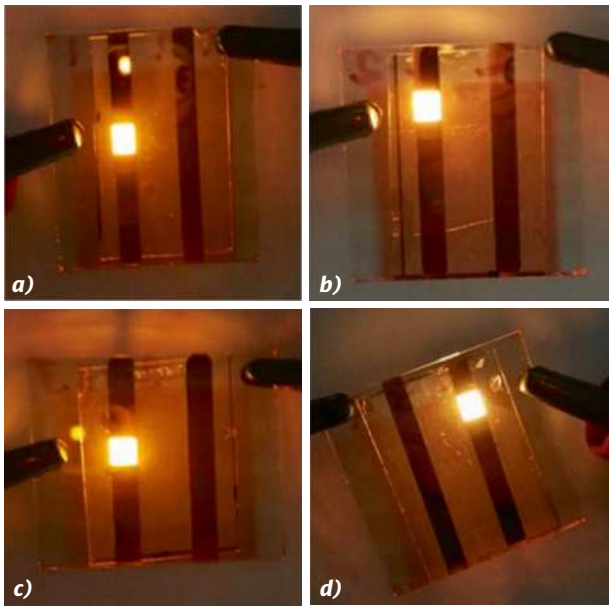

Fig. 9.The light output at 6 V of OLEDs with a) no MNP, b) 0.5 % wt, c) 1.0 % wt, d) 2.0 % wt

ty of the devices. At the low voltage area, the conduction mechanism is given by m = 1 in all devices, therefore, this behaviour can show the hole current contribution as a space charge limited conduction (SCLC) mode with no traps, given by:

$$J=9/8(\varepsilon_0\varepsilon_r)\mu V^2L^{-3},$$

where μ is the carrier mobility, $\varepsilon_0\varepsilon_r$ is the permittivity of MEH-PPV and L is the thickness of the sample. At the high voltage area, decrease of the current density can be observed suggesting a trap distribution where the electrons were trapped mainly by the MNP, which were filled during the charge injection in the OLEDs. In the absence of oxidizing mechanism on the surfaces, the MNP should favoured the hole injection inducing the lowering of the critical voltage because the Fermi level of MNP was between that of the ITO and the HOMO level of the emission layer.

In Fig. 9, the light output images of the OLEDs with varied MNPs concentration could be seen under applied voltage 6 V. In Fig. 10, the performanc-

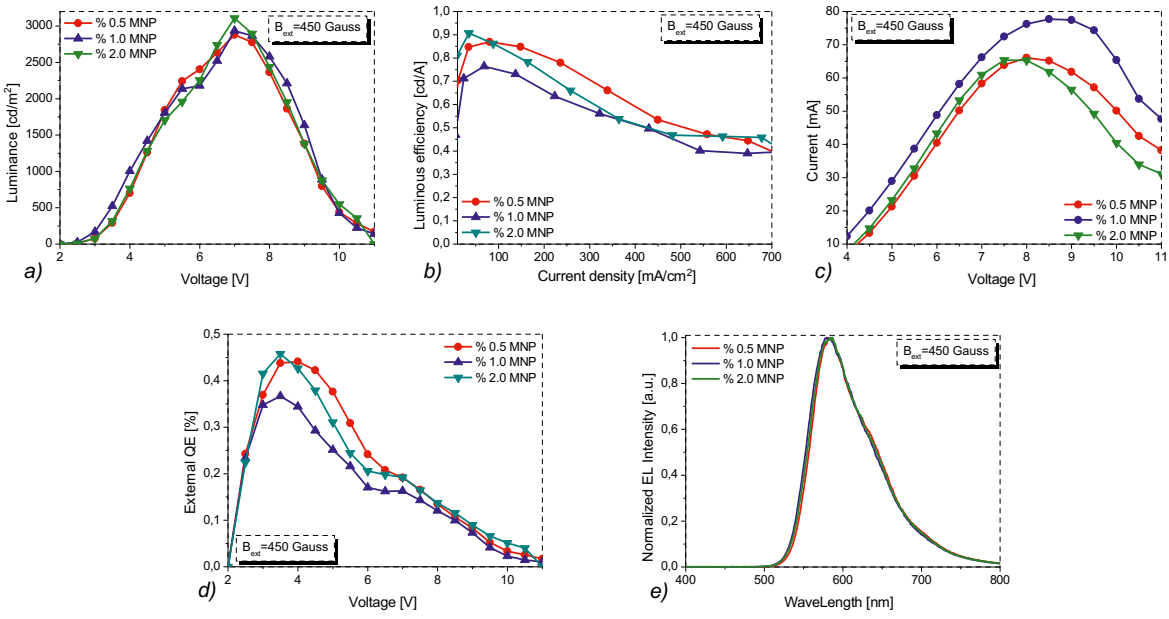

Fig. 10. The performances of the devices with MNPs under B_{ext}: a) luminance–voltage, b) luminous efficiency–voltage, c) current–voltage, d) EQE- voltage, e) normalized EL intensity

Table 1. Device Performances of OLEDs Depending on MNP Concentrations in the Emissive Layer with / without Applied Magnetic Field (B_{ext})

Device Configuration	Turn on Voltage* [V]	Max. Luminance [cd/m^2]	Max.Luminous Efficiency [cd/A]	EQE [%]
B_{ext}=0				
No MNP	2.05	3101	0.71	0.35
0.5 % wt MNP	2.04	2279±2.5	0.83±0.03	0.43±0.01
1.0 % wt MNP	2.01	2931±5.7	0.70±0.01	0.35±0.04
2.0 % wt MNP	2.04	3023±6.3	0.75±0.07	0.37±0.04
$B_{ext}\neq0$				
0.5 % wt MNP	1.72	2879±0.5	0.87±0.02	0.44±0.03
1.0 % wt MNP	2.02	2935±5.7	0.76±0.09	0.37±0.08
2.0 % wt MNP	2.06	3108±8.8	0.91±0.10	0.47±0.04

*Turn on voltage is defined as the applied voltages when the luminance is 1 cd/m^2.
Each error was found between the pixels of the same device.

es of the devices with MNPs could be seen under B_{ext}. In our study, a 45 mT (450 Gauss) homogenous magnetic field was applied to the doped devices under operation. The values were also summarized at the Table 1. As seen in the Table 1**,** the performances of all MNPs doped devices under B_{ext} were enhanced. As an example, the luminance of the device doped with 0.5 % MNPs increased from 2279 cd/m^2 up to 2879 cd/m^2 while luminous efficiency increased from 0.83 cd/A to 0.87 cd/A respectively. This device had also the lowest turn-on voltage among all devices (Fig. 7). These investigations could be applied for other MNP-doped devices. Early studies demonstrated that magnetic fields can influence the triplet-triplet annihilation process in organic materials and can change the intensity of the resulting delayed fluorescence signal. Additionally, it was found that magnetic fields also have an effect on the photoconductivity of organic films. Finally, a broad interest in magnetic phenomena in organics started to arise when the magnetic field effect on device current and electroluminescent properties of OLED devices was discovered [48–50]. In 2003, Kalinowski *et al.* discovered that in tri-(8-hydroxyquinoline)-aluminium (Alq_3) based devices with non-magnetic electrode materials the application of a magnetic field of 500 mT increases the current flow through the devices as well as their light output by up to 3 % [29]. This novel phenomenon started to receive increasing attention one year later when Francis et al. demonstrated that a large change in the resistance of more than 10 % can be succeeded in polyfluorene based OLEDs at room temperature and weak magnetic fields in the order of 10 mT [31]. This publication introduced the term "organic magnetoresistance effect" (OMR effect) and triggered several studies in the following years. Mermer et al. showed that the OMR effect is a general phenomenon and can be observed in both polymeric and small-molecule materials [32, 50, 51]. Therefore, the enhancement in the device performances might be attributed to the delayed fluorescence phenomenon because of triplet-triplet annihilation, so the singlet state is formed in the system. The EL spectra of the fabricated OLEDs were shown in Fig. 10 e. EL spectrum exhibited a peak at ~ 594 nm, the same as with B_{ext} = 0. Therefore, the application of B_{ext} did not have an influence on the emitted light characteristics but enhanced the performance of the devices. Desai *et al.* have been observed that low magnetic field can increase the triplet concentration due to an increase in the rate of intersystem crossing from photo-generated singlet to triplet state [44]. When the number of triplet excitons increase, due to longer lifetime of triplet excitons compared to that of the singlet excitons in bulk materials, dissociated charge carriers can increase. Applied magnetic field increases the intersystem crossing rate leading to an increase in the triplet population, which in turn increases the efficiency.

4. CONCLUSION

In this work, we presented the effect of concentration of MNPs on the performance of OLEDs under B_{ext}. In conclusion, $CoFe_2O_4$ MNPs were doped in MEH-PPV and device characteristics were carried out at different concentrations under applied magnetic field. Doping of MNPs in MEH-PPV had no effect on EL characteristics but increased DOS. Device performances with MNPs were enhanced under applied B_{ext} when the device was under operation. This was an important fundamental and applied finding that could help in achieving balanced radiative recombination of the charge carriers and hence improved performances in OLEDs.

5. REFERENCES

1. A. Köhler, J.S. Wilson, R.H. Friend, Fluorescence and phosphorescence in organic materials// Advanced Engineering Materials, 2002, Vol. 4, #7, 453p.

2. B.W. D'Andrade, S.R. Forrest, White organic light emitting devices for solid state lighting// Advanced Materials, 2004, Vol. 16, #18, pp. 1585–1595.

3. J. Feng, T. Okamoto, R. Naraoka, S. Kawata, Enhancement of surface plasmon-mediated radiative energy transfer through a corrugated metal cathode in organic light-emitting devices// Applied Physics Letters, 2008, Vol. 93, #5, 051106.

4. T. Ahn, H. Lee, S.-H. Han, Effect of annealing of polythiophene derivative for polymer light-emitting diodes// Applied physics letters, Vol. 80, #3, pp. 392–394.

5. A. Misra, P. Kumar, M. Kamalasanan, S. Chandra, White organic LEDs and their recent advancements// Semiconductor science and Technology, 2006, Vol 21, #7, R35.

6. S.-M. Seo, J.H. Kim, J.-Y. Park, H.H. Lee, Coordination-complex polymer as an organic conductor for organic light-emitting diodes// Applied Physics Letters, Vol. 87, #18,183503.

7. S.Y. Kim, J.M. Baik, H.K. Yu, K.Y. Kim, Y.-H. Tak, J.-L. Lee, Rhodium-oxide-coated indium tin oxide for enhancement of hole injection in organic light emitting diodes// Applied Physics Letters, 2005, Vol. 87, #7, 072105.

8. J.-H. Li, J. Huang, Y. Yang, Improved hole-injection contact for top-emitting polymeric diodes// Applied physics letters,2007, Vol. 90, #17, 173505.

9. M. Suzuki, S. Tokito, F. Sato, T. Igarashi, K. Kondo, T. Koyama, T. Yamaguchi, Highly efficient polymer light-emitting devices using ambipolar phosphorescent polymers// Applied Physics Letters, 2005, Vol. 86, #10, 103507.

10. M. Baldo, D. O'brien, M. Thompson, S. Forrest, Excitonic singlet-triplet ratio in a semiconducting organic thin film// 1999, Physical Review B, Vol. 60, #20, 14422.

11. B. Hu, Y. Wu, Z. Zhang, S. Dai, J. Shen, Effects of ferromagnetic nanowires on singlet and triplet exciton fractions in fluorescent and phosphorescent organic semiconductors// Applied physics letters, Vol. 88, #2, 022114.

12. P.P. Ruden, D.L. Smith, Theory of spin injection into conjugated organic semiconductors// Journal of applied physics, 2004, Vol. 95, #9, pp. 4898–4904.

13. P. Blom, M. De Jong, S. Breedijk, Temperature dependent electron-hole recombination in polymer light-emitting diodes// Applied Physics Letters,1997, Vol. 71, #7, pp. 930–932.

14. Z. Xu, Y. Wu, B. Hu, I.N. Ivanov, D.B. Geohegan, Carbon nanotube effects on electroluminescence and photovoltaic response in conjugated polymers// Applied Physics Letters, 2005, Vol. 87, #26, 263118.

15. Y. Cao, I.D. Parker, G. Yu, C. Zhang, A.J. Heeger, Improved quantum efficiency for electroluminescence in semiconducting polymers// Nature,1999, Vol. 397, #6718, pp. 414–417.

16. P.K. Ho, J.-S. Kim, J.H. Burroughes, H. Becker, S.F. Li, T.M. Brown, F. Cacialli, R.H. Friend, Molecular-scale interface engineering for polymer light-emitting diodes// Nature, 2000, Vol. 404, #6777, pp. 481–484.

17. M. Wohlgenannt, K. Tandon, S. Mazumdar, S. Ramasesha, Z. Vardeny, Formation cross-sections of singlet and triplet excitons in π-conjugated polymers// Nature, 2001, Vol. 409, #6819, pp. 494–497.

18. J. Wilson, A. Dhoot, A. Seeley, M. Khan, A. Köhler, R. Friend, Spin-dependent exciton formation in π-conjugated compounds// Nature, 2001, Vol. 413, #6858, pp. 828–831.

19. Z. Shuai, D. Beljonne, R. Silbey, J.-L. Brédas, Singlet and triplet exciton formation rates in conjugated polymer light-emitting diodes// Physical review letters, 2000, Vol. 84, #1, 131.

20. M.N. Kobrak, E.R. Bittner, Quantum molecular dynamics study of polaron recombination in conjugated polymers// Physical Review B, 2000, Vol. 62, #17, 11473.

21. T.-M. Hong, Meng H.-F. Spin-dependent recombination and electroluminescence quantum yield in conjugated polymers// Physical Review B, 2001, Vol. 63, #7, 075206.

22. V. Cleave, G. Yahioglu, P.L. Barny, R.H. Friend, Tessler N. Harvesting singlet and triplet energy in polymer LEDs// Advanced Materials, 1999, Vol. 11, #4, pp. 285–288.

23. C.-J. Sun, Y. Wu, Z. Xu, B. Hu, J. Bai, J.-P. Wang, Shen J. Enhancement of quantum efficiency of organic light emitting devices by doping magnetic nanoparticles// Applied physics letters, 2007, Vol. 90, #23, 232110.

24. E.L. Frankevich, Balabanov E.L. New effect of increasing the photoconductivity of organic semiconductors in a weak magnetic field// ZhETF Pisma Redaktsiiu, 1965, Vol. 1, #6, pp. 33–37.

25. E. Frankevich, The nature of a new effect of a change in the photoconductivity of organic semiconductors in a magnetic field, Soviet Physics JETP// 1966, Vol. 23, #5, pp. 1226–1234.

26. E.L. Frankevich, E.L. Balabanov, Changes in photoconductivity of an anthracene single crystal in amagnetic field// Solid State Physics, 1966, Vol. 8, #3, pp. 855–889.

27. E. Frankevich, E.L. Balabanov, G.V. Vselyubskaya, Investigation of change in photoconductivity of organic semiconductors in a magnetic field//Solid State Physics, 1966, Vol. 8, pp. 1970–1973.

28. J. Kalinowski, J. Szmytkowski, Stampor W. Magnetic hyperfine modulation of charge photogeneration in solid films of Alq 3// Chemical physics letters, 2003, Vol. 378, #3, pp. 380–387.

29. J. Kalinowski, M. Cocchi, D. Virgili, P. Di Marco, Fattori V. Magnetic field effects on emission and current in Alq 3-based electroluminescent diodes// Chemical Physics Letters, 2003, Vol. 380, #5, pp. 710–715.

30. A.H. Davis, Bussmann K. Large magnetic field effects in organic light emitting diodes based on tris (8-hydroxyquinoline aluminum)(Alq 3)/N, N′-Di (naphthalen-1-yl)-N, N′ diphenyl-benzidine (NPB) bilayers// Journal of Vacuum Science & Technology A: Vacuum, Surfaces, and Films, 2004, Vol. 22, #4, pp. 1885–1891.

31. T. Francis, Ö. Mermer, G. Veeraraghavan, Wohlgenannt M. Large magnetoresistance at room temperature in semiconducting polymer sandwich devices// New Journal of Physics, 2004, Vol. 6, #1, 185.

32. Ö. Mermer, G. Veeraraghavan, T. Francis, Y. Sheng, D. Nguyen, M. Wohlgenannt, A. Köhler, M.K. Al-Suti, Khan M., Large magnetoresistance in nonmagnetic π-conjugated semiconductor thin film devices// Physical Review B, 2005, Vol. 72, #20, 205202.

33. V. Prigodin, J. Bergeson, D. Lincoln, Epstein A. Anomalous room temperature magnetoresistance in organic semiconductors// Synthetic Metals,2006, Vol. 156, #9, pp. 757–761.

34. P. Desai, P. Shakya, T. Kreouzis, W. Gillin, N. Morley, Gibbs M. Magnetoresistance and efficiency measurements of Al q 3-based OLEDs// Physical Review B, Vol. 75, #9, 094423.

35. P. Bobbert, T. Nguyen, F. Van Oost, V.B. Koopmans, Wohlgenannt M. Bipolaron mechanism for organic magnetoresistance// Physical Review Letters, 2007, Vol. 99, #21216801.

36. H. Kavas, A. Baykal, A. Demir, M.S. Toprak, Aktaş B. ZnxCu (1– x) Fe_2O_4 Nanoferrites by Sol–Gel Auto Combustion Route: Cation Distribution and Microwave Absorption Properties// Journal of Inorganic and Organometallic Polymers and Materials, 2014, Vol. 24, #6, pp. 963–970.

37. Pielaszek R. Analytical expression for diffraction line profile for polydispersive powders, Applied Crystallography// Proceedings of the XIX Conference, World Scientific, Singapore, 2004, pp. 43–50.

38. T. Wejrzanowski, R. Pielaszek, A. Opalińska, H. Matysiak, W. Łojkowski, Kurzydłowski K. Quantitative methods for nanopowders characterization// Applied Surface Science, 2006, Vol. 253, #1, pp. 204–208.

39. K. Venkatesan, D.R. Babu, M.P.K. Bai, R. Supriya, R. Vidya, S. Madeswaran, P. Anandan, M. Arivanandhan, Hayakawa Y. Structural and magnetic properties of cobalt-doped iron oxide nanoparticles prepared by solution combustion method for biomedical applications// International journal of nanomedicine, 2015, Vol. 10, Suppl 1, 189.

40. S. Asiri, S. Güner, A. Demir, A. Yildiz, A. Manikandan, Baykal A. Synthesis and Magnetic Characterization of Cu Substituted Barium Hexaferrites// Journal of Inorganic and Organometallic Polymers and Materials, 2018, Vol. 28, #3, pp. 1065–1071.

41. Kojima H. Fundamental properties of hexagonal ferrites with magnetoplumbite structure// Handbook of Ferromagnetic Materials, 1982, 3, pp. 305–391.

42. K.C. Kao, Hwang W., Electrical transport in solids, wuth particular reference to orgainc semiconductorys// Pergamon Press, 1981.

43. A. Bakuzis, A. Pereira, J. Santos, Morais P. Superexchange coupling on oleylsarcosine-coated magnetite nanoparticles// Journal of Applied Physics, 2006, Vol. 99, #8, 08C301.

44. P. Desai, P. Shakya, T. Kreouzis, Gillin W.P. The role of magnetic fields on the transport and efficiency of aluminum tris(8-hydroxyquinoline) based organic light emitting diodes// Journal of Applied Physics, 2007, Vol. 102, #7, 073710.

Selin Piravadili Mucur
after completing her primary and secondary education in Bandırma completed her graduate and Master of Science education at Hacettepe University in Physics Engineering Department in period 2000–2007. In 2011, she began experimental studies as a student in the Photonics, Electronics and Sensors Laboratory TÜBİTAK UME and started her Ph.D. program in the Institute of Engineering and Science, Physics Department at Gebze Technichal University and finished it in 2015. Her Ph.D. subject was "Effect of Metal and Semiconductor Nanoparticles on the Performance of Organic Lıght Emitting Diodes Based on Conjugated Polymers". Since 2013, she has been working as a researcher in the Photonics Technologies Group at Marmara Research Centre, TUBITAK. Her scientific field interests are optoelectronic devices, organic field effect transistors, thin films, organic light emitting devices, and organic photovoltaic devices

Betül Canimkurbey
has graduated from Gebze Technical University with Ph.D. degree in 2017. At present, she is an Assistant Professor and the Assistant Director of the central research laboratory at Amasya University. Her scientific field interests are: optoelectronic devices, organic field effect transistors, thin films, organic light emitting devices, and organic photovoltaic devices

Ayse Demir Korkmaz
received her Ph.D. degree in chemistry from Fatih University in Istanbul, Turkey in 2015. She has been working as a research assistant in Istanbul Medeniyet University since 2012 where she conducts research activities in the areas of magnetic nanoparticles, inorganic nanomaterials, and their biomedical applications

Light & Engineering
Vol. 28, No. 2, pp. 106–112, 2020

https//doi.org./10.33383/2019-015
Svetotekhnika #4, 2019, pp. 79–83

CALCULATION OF LIGHT DISTRIBUTION OF A CONVENTIONALLY POINT LIGHT SOURCE IN AN ARBITRARILY ORIENTED COORDINATE SYSTEM

Sergei V. Prytkov* and Alexei O. Syromyasov

National Research University – N.P. Ogaryov Mordovia State University, Saransk
** E-mail: sergeyvladi88@gmail.com*

ABSTRACT

The article reviews calculation of total light distribution of several light sources (LS), which are differently oriented in space with their locations conventionally [1] being the same. It is proposed that luminous intensity curves (photometric body) of LSs are described in *IESNA* format (or in the format of tables, which is basically the same). Two methods of solving the problem are proposed. The first one is related to preliminary trigonometric interpolation of luminous intensity curves for each LS performed by means of discrete Fourier transformation (DFT). The second one is based on piecewise-linear interpolation of this curves using Delaunay triangulation. Both methods may be implemented by means of popular mathematic software (such as *Wolfram Mathematica* or *Octave*) and their applicability is confirmed experimentally.

Keywords: luminous intensity angular distribution, total luminous intensity distribution, photometric data, trigonometric interpolation, discrete Fourier transformation, piecewise-linear interpolation, Delaunay triangulation, coordinate system rotation, coordinate transformation

1. INTRODUCTION

Recently, the interest in the idea of design of lighting devices (LD) with units or tens of light emitting diodes (LED) or LED modules with secondary optic devices which are differently oriented in space has become evident in scientific publications [1–4]. Such approach has two advantages. First, it allows us to create an LD with a photometric body (PB) of any complexity using secondary optics with simple geometry. Second, by providing capability of rotation of specific LEDs (LED modules) in the structure of a LED based LD, it is possible to optimise its luminous intensity distribution depending on lighting conditions.

However, over the last decade, the range of secondary optics for LED based outdoor lighting luminaires has significantly increased, therefore, the said approach to development of luminaires of this category, in point of fact, has lost its necessity. At the same time, it is our opinion that it is still necessary, for instance, for development of crossbar luminaires for railroad lighting and lighting of production premises as well as luminaires for architectural lighting of buildings and structures. Accordingly, the studies for calculation of total angular distribution of luminous intensity (spatial light distribution) of a system of differently oriented LSs with known PB (or, which is the same, luminous intensity curves) are still necessary.

Solution of the problem is significantly complicated by the fact that PBs of initial LSs are three-dimensional. Even one of the recent studies on mathematical modelling of LED modules [5] reviews the dependence of light distribution on one vectorial angle, i.e., in fact, a two-dimensional problem is solved.

[1] Conventionally concentrated at a large distance from a photoelectric receiver

Nowadays, there is a method developed by S.G. Ashurkov and A.A. Bartsev [1] which allows us to solve a three-dimensional problem provided the initial PBs of LSs are axially symmetric. This article proposes two ways of solving this problem but without the said limitation, i.e. with non-symmetric initial PBs of LSs.

2. STATEMENT OF THE PROBLEM OF CALCULATION OF TOTAL LIGHT DISTRIBUTION

It is known that PB of a point LS is a function $I(\vec{e})$ expressing dependence of the values of luminous intensity I in direction $\vec{e}$. The latter may be defined by two angles in one of the systems: (A,α), (B,β) or (C,γ) [6]. In terms of mathematics, PB is a surface in a spherical coordinate system where I acts as a radius and angular coordinates depend on selection of the photometric system.

Usually PB is found by measurement data of a goniophotometer output in *IESNA* format [7]: in point of fact, in the form of a table where the values of angular coordinates are given with a specific increment and the values of luminous intensity correspond with each pair of such coordinate values.

Let us designate angular coordinates in a given spherical system as Θ and Φ (Fig. 1), $\Theta\in[0°, 180°]$ and $\Phi\in[0°, 360°]$ and let us perform measurements of the first angle with increment of $\Delta\Theta$ and of the second angle with increment of $\Delta\Phi$. Introducing the following designations:

$$\Theta_k = k\Delta\Theta,\ \Phi_l = l\Delta\Phi, \tag{1}$$

where $k = 0–N_\Theta$, $l = 0–N_\Phi$, $N_\Theta = 180°/\Delta\Theta$ and $N_\Phi = 360°/\Delta\Phi$, we will get that the following values of luminous intensity are known

$$i_{kl} = I(\Theta_k,\Phi_l). \tag{2}$$

Then let us consider several LSs located at one point with PB of each one known and expressed by (1) and (2). All PBs are described in the same photometry system, for instance, (C,γ), with the role of γ angle is played by Θ and the role of Φ is played by C. (It is evident to consider that measurement increments $\Delta\Theta$ and $\Delta\Phi$ are common for all LSs though this consideration is not crucial.)

The LSs are differently oriented in space and light distribution of each of them is described in its *own* coordinate system rigidly bound to data of a specific LS. At the same time, relative positions of LSs are known, i.e. the sequence of rotations allowing own coordinate systems to combine is known.

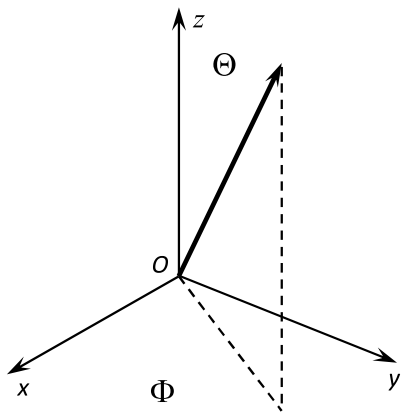

Fig. 1. Angular coordinates in a spherical system

The problem is as follows: total light distribution of the above described conventionally point LSs should be found.

Due to misalignment of their own coordinate systems, it is impossible to directly sum up the values of i_{kl} of different LSs in relevant nodes of the mesh. It is necessary to select some *common* coordinate system, to recalculate the $I(\vec{e})$ functions for each LS in it, and only then to sum up. To reduce calculations, the own coordinate system of one of the LSs may be selected as the common system or some other one may be selected.

Below, two methods of solving the stated problem are presented and the experimental set, by means of which the input data for verification of theoretical computations was performed and the methods were compared, is described.

3. USE OF TRIGONOMETRIC INTERPOLATION

Let us know the analytic expression for each LS:

$$I_j = I_j(\Theta,\Phi),\ j = 1–N, \tag{3}$$

where N is total number of LSs, the j index is used for their numbering, and the Θ and Φ angles correspond with the own coordinate system of the j-th LS.

As the transformation formulae combining own coordinate systems of different LSs are known, we may find the dependence between the angular coordinates in the own system and its coordinates Θ and φ in the common system (where PBs of LSs will be

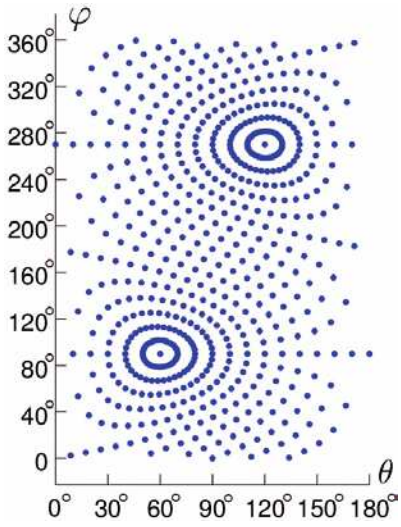

Fig. 2. Distortion of a regular mesh after 60° rotation around the *Oy* axis

summed up). The said dependence will have the following form for the *j*-th LS

$$\Theta = T_j(\theta,\varphi),\ \Phi = F_j(\theta,\varphi). \tag{4}$$

According to expressions (3) and (4), total light distribution of *N* LSs in the said common coordinate system will be expressed as

$$I(\theta,\varphi) = I_1(T_1(\theta,\varphi),F_1(\theta,\varphi)) + ... \\ ... + I_N(T_N(\theta,\varphi),F_N(\theta,\varphi)). \tag{5}$$

The said approach is detailed in [8] and in this work, model examples of its application are built.

To implement the said approach, it is necessary to recover the functions (3) by means of input data (1, 2).

Previous attempts to solve this problem are described in [9]. PB was expanded in degree of *cos θ*. Disadvantages of such solution are taking of only one angular variable into account (i.e. transition from space to plane) and low number of summands in the expanding (just 4). In their recent work [5], the authors increased accuracy of such expanding by multiplying the number of summands and advancing the methods of coefficient definition in such sums, however, the problem of transition from plane to space was not solved by them.

Possible approaches to solve the said problem different in terms of accuracy and complexity are described in [3, 10]. When interpolating photometric data, it is necessary to take PB (3) argument periodicity into account: it is obvious that Θ period of function I_j should be equal to 180° and that of Φ should be equal to 360°. Therefore, it is reasonable to calculate these functions in the form of double trigonometric series by Θ and Φ.

The data set in the form of equations (1,2) is finite, therefore, substantially the case in hand is trigonometric polynomial with $(N_\Theta + 1)\ N_\Phi$ summands; the coefficients of these polynomials are subject to definition:

$$I(\Theta,\Phi) = \sum_m \cos m\Theta \sum_n (a_{mn}\cos(n\Phi) + \\ + b_{mn}\sin(n\Phi)). \tag{6}$$

In real photometric experiments, increments $\Delta\Theta$ and $\Delta\Phi$ are small, therefore, the number of unknown variables is rather high: for instance, with $\Delta\Theta = 1°$ and $\Delta\Phi = 5°$, it is equal to 13,032. That is why this brings up the question of the fastest and the most accurate method of trigonometric interpolation.

As shown in [4], such method is the method of discrete Fourier transformation (DFT). In its simplest variant, it allows to roughly recover the periodic function by its known values. For array $\{x_k\}$ with period of *N*, DFT is defined by the formula

$$X_n = \sum_{k=0}^{N-1} x_k \exp(-i\frac{2\pi nk}{N});$$

then the continuous function

$$x(t) = \frac{1}{N}\sum_{n=0}^{N-1} X_n \exp\left(i\frac{2\pi nt}{N\Delta t}\right)$$

is periodic, and $\{x_k\}$ are its values obtained at values of *t* taken with increment of Δt [11].

The said transformation generalised for the periodic function by two its variables should be applied to the data set (2) after which it is necessary to define the real part in the obtained expression and then to reduce the number of summands excluding all expressions with coefficients a_{mn} and b_{mn} less than some previously defined value (it is defined with consideration of the desired accuracy) out of the sum.

So, according to the first algorithm of calculation of total light distribution of several LSs based on the results of photometric experiments, it is necessary to:

- Define light distribution (3) of each LS in its own coordinate system applying DFT to data (1)–(2);
- Define concretely the transformations (4) relating angular variables in own coordinate systems

of LSs and in the common one to each other knowing relative positions of LSs;

• Calculate total luminous intensity distributions (common PB) in the common coordinate system using formula (5).

As a result of these actions, some formula (rather cumbersome) expressing the required function $I(\theta,\varphi)$ will be obtained. It may seem inconvenient but it may be used to compile the table of values in the form (2) and to obtain the expression in the form (6) in the common coordinate system by it.

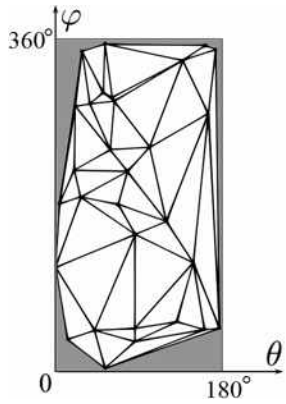

Fig. 3. Non-full covering of the region [0°; 180°]× × [0°; 360°] by the non-regular mesh

4. USE OF PIECEWISE-LINEAR INTERPOLATION

If PB (3) of each specific LS is not of interest, it is possible to try to avoid application of DFT. In this case, it is necessary to transfer to the common coordinate system from the beginning. The angular coordinates which the measured values of luminous intensity i_{kl} correspond with after this transition may be defined by the system (4) defined by θ and φ:

$$\theta = t_j(\Theta,\Phi),\ \varphi = f_j(\Theta,\Phi),\ j = 1\text{–}N. \qquad (7)$$

After substituting the values of Θ_k and Φ_l for all N LSs into (2) and (7), the table of values of luminous intensity will be obtained in the following form

$$i_{kl} = I_j(\Theta_k,\Phi_l), \qquad (8)$$

where, according to (7), $\theta_k = t_j(\Theta_k,\Phi_l)$ and $\varphi_l = f_j(\Theta_k,\Phi_l)$.

Since different functions t_j and f_j correspond with different LSs, after transformation of coordinates, the same angles Θ_k and Φ_l transform into different angles θ_k and φ_l. As a result, summing up of i_{kl} related to different LSs is impossible right after rotation. This problem did not arise using the analytic expressions (3) as they allow at any point to define I_j. Therefore, interpolation should be performed for all rotated LSs to define luminous intensity of different LSs at the same points.

$$\theta_p = p\Delta\Theta,\ \varphi_q = q\Delta\Phi, \qquad (9)$$

where it is convenient to select corresponding increments of modification of angular variables in own coordinate systems and in the common one.

After rotation, the mesh Θ_k, Φ_l covering the interval [0°; 180°]×[0°; 360°] ceases to be regular (Fig. 2).

Among the methods applicable to such meshes, piecewise-linear interpolation is the simplest one as it provides acceptable accuracy with sufficient number of mesh nodes. That is why this method is used hereafter. For its implementation, it is necessary to perform triangulation of the region by the nodes of the obtained non-regular mesh, to define which of the triangles a specific point (9) gets into and to define I_j at this point knowing i_{kl} at apexes of the triangle.

Absolute error of such interpolation is known [3]: within each triangle, it does not exceed $M{\cdot}h^2/6$ where M is the largest value of second derivatives of the approximated function, h is the diameter of

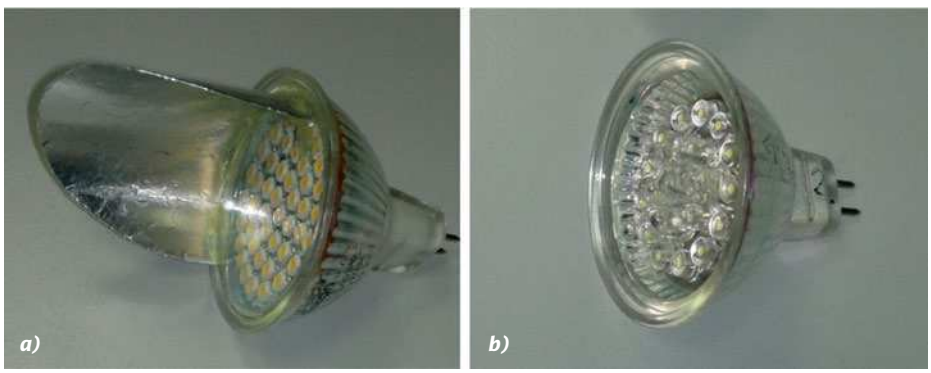

Fig. 4. Light sources used in the photometry experiment:
a – LS1; *b* – LS2

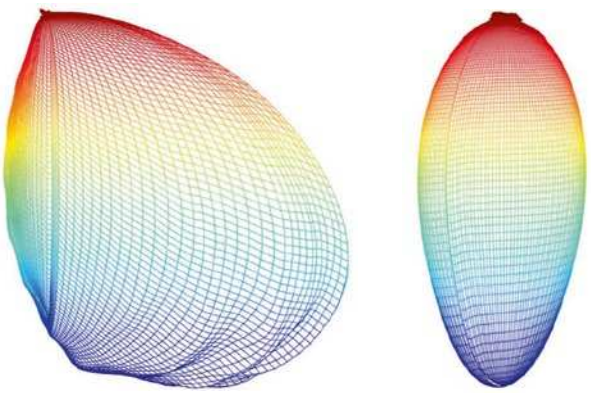

Fig. 5. Experimentally acquired photometric bodies of LS1 and LS2

the escribed circle of the triangle. To reduce the error, h should be minimised. For this purpose, fragmentation of the said region is performed by means of Delaunay triangulation for minimisation of the error [12]. With such approach, none of the mesh nodes gets into the escribed circle of any triangle. Delaunay triangulation is distinctive with minimal sum of radii of the escribed circles of all triangles. Therefore, it is this approach which "averagely" provides the least error.

The advantage of this algorithm is that it is supported by many mathematical software packages, e.g. *Mathematica* [13] or *Octave* and does not require additional programming.

Ultimately, the second algorithm of calculation of total light distribution consists of the following steps:

- Transfer to the common coordinate system using formulae (7) and (8);
- Fragmenting of the computational region by means of Delaunay triangulation;
- Piecewise-linear interpolation of photometric data of all LS's at the same points (9);
- Summing up of the values of luminous intensity of different LS's at points (9).

The result of implementation of this algorithm is the table of total values of luminous intensities.

Implementation of this plan is related to a number of complications.

First, in the own coordinate systems, the results of photometry at $\Theta = 0°$ provide different values of luminous intensity at different Φ angles although, based on introduction of the spherical coordinate system, these values should be equal (Fig. 1). The similar statement is correct at $\Theta = 180°$. This effect may be explained both by vibrations of the goniophotometer during measurements and by the fact that a luminaire may emit more or less light at different moments whereas photometric measurement is not performed in a moment.

When DFT is used, this phenomenon is not crucial because regularity of positions of points (Θ_k, Φ_l) is of key importance; with piecewise-linear interpolation it plays negative role. Consequently, the luminous intensity of each LS at one point has several values, which makes interpolation impossible.

In order to solve this problem, the angle $\Theta = 0°$ is replaced by the angle $\Delta\Theta/100$ in photometric tables and the angle $\Theta = 180°$ is replaced by $(180° - \Delta\Theta/100)$. As a result, different values of luminous intensity in the neighbourhood of $\Theta = 0°$ and 180° correspond to different (though closely positioned) points of space.

Second, while the initial mesh (1) in the own coordinate system of a specific LS covers the whole region [0°; 180°]×[0°; 360°], the non-regular mesh in the common system obtained by means of transformations (7) "backs out" of its edges (Fig. 3).

It is necessary to apply extrapolation instead of interpolation in regions not covered by the mesh, which leads to high errors.

In order to solve this problem, the initial (regular) mesh is widened and periodicity of functions $I_j(\Theta, \Phi)$ by both variables and their parity relative to Θ are used. For instance, instead of the range [0°, 360°], the change range of angle Φ is considered: from $10\Delta\Phi$ to $360° + 10\Delta\Phi$. Experience has proven that the described widening is sufficient for full covering of the region [0°; 180°]×[0°; 360°] by the non-regular mesh in the common coordinate system.

5. EXPERIMENT DESCRIPTION

The actual data required to perform comparative analysis of the methods described above was obtained in the course of the goniophotometer experiment. The LED based LSs used in the experiment are presented in Fig. 4. The first one (LS1) is an oblique luminaire on a basis of a *Feron 3602 LB-24 MR16* LED lamp and the second one (LS2) is a LED lamp for accent lighting with axially symmetric light distribution with power comparable to that of LS1.

Luminous intensity was measured in standard conditions by means of a *GO2000A* goniophotometer set containing: *GO2000A* goniometer (range of rotation in horizontal and vertical planes: ±180°, ac-

curacy of rotation angle setting: 0.1°); *ID-1000* photometer based on a silicone photodiode adjusted for the function $V(\lambda)$, accuracy class *L*; *DPS1060* power supply unit.

All photometric data used in the further calculations is the arithmetic mean of the results of 5 measurements.

Photometry was performed in the system (C, γ). Measurement interval was 5° for plane C and 1° for plane γ. The experimental PBs of each LS are presented in Fig. 5.

For measurement of total light distribution of the said sources (Fig. 6), LS1 was installed so that its geometrical axis was parallel to the axis of photometry and orientation of LS2 was defined by the sequence of rotations of its geometrical axis: by 46° around the axis *Ox* and by 190° around the axis *Oz*. The common coordinate system was affixed to LS1.

5. COMPARISON OF CALCULATION METHODS

The comparison criteria of the calculation methods included simplicity of algorithm implementation, speed of their work, and accuracy.

Both methods were implemented by means of *Wolfram Mathematica*. The input photometric data was imported from the *XLS* file by means of embedded functions of this mathematical software. Both DFT and piecewise-linear interpolation in a non-regular mesh are standard functions of this software and *Mathematica* uses the Delaunay triangulation for this interpolation. With consideration of these circumstances, complexity of programming using this software as basically the same for both methods.

The same may be said about their processing speed. The calculations were performed using a laptop with 2,400GHz *Intel Core i7–4500U Haswell* CPU with 6Gb of RAM and powered by *Win 8.1×64*. In both cases, the computation required (15–20) minutes and the total light distribution values calculated using both methods were rather close to those experimentally discovered (Fig. 7).

The accuracy criterion was relative error of calculation of the values of total luminous intensity of two LSs as compared to its experimental (measured) values I_{pq} at points (9). Comparison of the calculated and experimental data was performed only within the region $I_{pq} \geq I_{max} / 2$ where I_{max} is the largest measured value of total luminous intensity. Such limitation allows us to ignore the regions which are not illuminated by the LSs [3]. On the other hand, it is these regions not interesting from technical point of view where relative error may drastically increase due to smallness of the measured values.

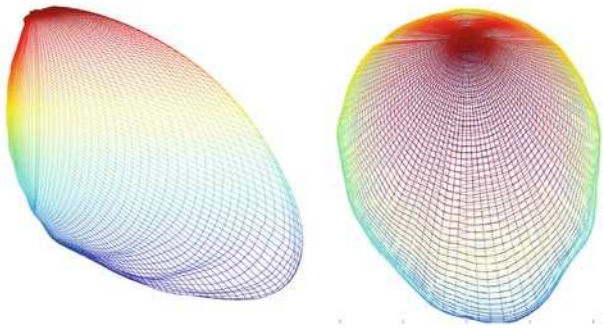

Fig. 6. Total photometric bodies acquired experimentally

In the selected region, maximum value of error was less than 4 % for trigonometric interpolation and about 6.5 % for piecewise-linear interpolation.

6. CONCLUSION

The article proposes and analyses two methods of calculation of total luminous intensity distribution of several LSs with different spatial orientation with their positions being conventionally the same. The first one is related to trigonometric interpolation of photometric data, the second one is related to its piecewise-linear interpolation.

During the numerical experiment with use of real photometric data, trigonometric interpolation

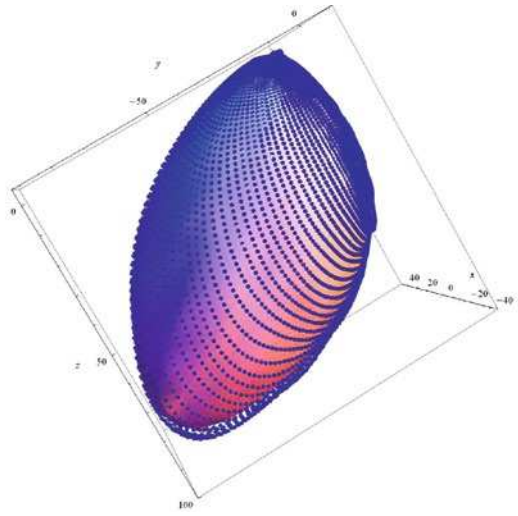

Fig. 7. Total luminous intensity distribution obtained by means of trigonometric interpolation (the points stand for experimental data, the solid surface stands for the results of calculation)

proved to be more accurate. With that, its error is partially related to exclusion of small summands out of expressions (6). That is why it may be also reduced by using a larger number of summands; however, this would impair processing speed of the method.

With the defined data set (2), there are no reserves for increase of accuracy of the method of piecewise-linear interpolation.

It is worth noting that PB's described by means of formulae of the form (3) and defined by means of trigonometric interpolation may be of inherent value. Being defined once, they may be used for different calculations, e.g. for transformation of photometric systems.

REFERENCES

1. Ashurkov, S.G., Bartsev, A.A. Method of Calculation of a Light Distribution Solid of Emitters with LEDs of Different Spatial Orientation [Metod raschyota fotometricheskogo tela izluchateley so svetodiodami raznoy prostranstvennoy orientatsii] // Svetotekhnika, 2007. #. 1, pp. 43–44.

2. Kovalenko, O. Yu., Zakharzhevskiy, O.A., Afonin, V.V. Modelling of a LED Module Based on the Defined Light Distribution Curve [Modelirovaniye svetodiodnogo modulya po zadannoy krivoy sily sveta] / CAD/CAM/CAE/PDM Design, Modelling, Production Preparation and Project Management Systems: II International Scientific and Practical Conference: Collected Papers. Penza: ANOO Privolzhskiy Dom Znaniy, 2008, pp. 30–33.

3. Syromyasov, A.O., Prytkov, S.V. Approximation of Photometric Data by One-Variable Trigonometric Polynomials [Approksimatsiya fotometricheskikh dannykh trigonometricheskimi polinomami odnoy peremennoy] // Almanac of Contemporary Science and Education [Almanakh sovremennoy nauki i obrazovaniya], 2014, Vol. 5–6 (84), pp. 117–122.

4. Syromyasov, A.O. Calculation of Light Distribution of Point Light Sources by Means of Discrete Fourier Transformation [Raschyot svetoraspredeleniya tochechnykh istochnikov s pomoshchyu diskretnogo preobrazovaniya Fourier] // Almanac of Contemporary Science and Education [Almanakh sovremennoy nauki i obrazovaniya], 2014, Vol. 9 (87), pp. 127–131.

5. Kaljun D., Novak T., Žerovnik J. Improved approximation of spatial light distribution // PLos ONE. 2017. N12(4): e0176252. URL: https://doi.org/10.1371/journal.pone.0176252 (reference date: 22.04.2019).

6. GOST R54350–2015 Light devices. Light requirements and test methods.

7. IESNA LM-63–95 "IESNA Recommended Standard File Format for Electronic Transfer of Photometric Data".

8. Ashryatov, A.A., Prytkov, S.V., Syromyasov, A.O. Method of Calculation of Spatical Light Distribution of a System of Differently Oriented LED Emitters [Metod raschyota prostranstvennogo svetoraspredeleniya sistemy raznoorientirovannykh svetodiodnykh izluchateley] // Kompyuternyye issledovaniya i modelirovaniye, 2014, Vol. 6, Issue 4, pp. 577–584.

9. Sapozhnikov, R.A. Theoretical Photometry [Teoreticheskaya fotometriya]. – 3rd ed., reviewed and supplemented. Moscow: Energiya, 1977, 264 p.

10. Syromyasov, A.O., Prytkov, S.V. On Methods of Interpolation on the Basis of Photometric Data in Plane [O metodakh interpolyatsii na osnove foto*me*tricheskikh dannykh na ploskosti] / Proceeds of the XI International Scientific and Practical Conference Integration of Science and Practice as a Mechanism of Efficient Development of Modern Society, Moscow, 2014, pp. 13–17.

11. Sergienko, A.B. Digital Processing of Signals [Tsyfrovaya obrabotka signalov], Saint Petersburg: Piter, 2002, 608 p.

12. Skvortsov, A.V. Delaunay Triangulation and Its Use. [Triangulyatsiya Delaunay i eyo primeneniye], Tomsk: Tomsk University Press, 2002, 128 p.

13. Dyakonov, V.P. Mathematica 5/6/7. Full Guide [Mathematica 5/6/7. Polnoye rukovodstvo], Moscow: DMK Press, 2010, 624 p.

Sergei V. Prytkov,
Eng. D. He graduated from the N.P. Ogaryov Mordovia State University in 2010. At present, he is the Assistant Professor of the Faculty for Lighting Engineering at the National Research University – the N.P. Ogaryov Mordovia State University. His research interest is the lighting design

Alexei V. Syromyasov,
Ph.D. in Physical and Mathematical Sciences, Associate Professor, graduated from the N.P. Ogaryov Mordovia State University in 2004. At present, he is the Associate Professor of the Applied Mathematics, Differential Equations and Theoretical Mechanics sub-department of the N.P. Ogaryov Mordovia State University. His research interests are mathematical and computer models of physical and technical processes

Light & Engineering
Vol. 28, No. 2, pp. 113–119, 2020

https://doi.org/10.33383/2019
Svetotekhnika #5, 2019, pp.29–34

DESIGN OF AN EDGE-LIT BACKLIGHT MODULE FOR AN AUTOSTEREOSCOPIC DISPLAY

Chien-Min Hun, King-Lien Lee*, Che-Yen Lin, Mei-Wen Chen, and Jin-Jei Wu

Department of Electro-Optical Engineering, National Taipei University of Technology, Taipei, Taiwan
**E-mail: kllee@ntut.edu.tw*

ABSTRACT

Study focuses on optimization of an edge-lit backlight module for a three-dimensional liquid crystal mobile phone display. The module is designed with microstructures on the top and bottom surfaces of the light-guide plate to offer time-multiplexed projection of light into a viewer's eyes. We simulated the module by optical software (TracePro) and liquid crystal software (LCDMaster 2D). The results effectively eliminate the need for prism sheets and satisfy three main performance metrics, namely a direction light-emission angle, uniformity of illumination, and crosstalk elimination.

Keywords: geometrical optics, optics in computer engineering, design and manufacture of optics, physical optics

1. INTRODUCTION

With the gradual popularization of 3D images in daily life, people enjoy the 3D image brought about the sensory stimulation. Autostereoscopic displays work by emitting two lights at different angles for a viewer's left and right eyes, thereby producing a stereoscopic view [1, 2]. This method is called multiplexed-2D, that is to use 2D screen to produce 3D images, and this way can be divided into two main types: spatial-multiplexed and time-multiplexed types. The current technique of spatial-multiplexed type for an autostereoscopic display requires the periodic striped shelter, a prism sheet or lenticular lenses to produce the right eye and left eye of the two groups of signals at the same time, not only the brightness and resolution will be declined, but also the energy is a great loss [3–6]. The technique of time-multiplexed type intermittently generates a left image and a right image projecting the left and right eyes, respectively. The frequency of this signal is greater than the frequency of visual persistence that allows the audience to produce stereoscopic vision [7–15]. An edge-lit backlight module can reduce costs if it can be designed to produce light for left and right eyes only, by using a light-guide plate (LGP). In this study, an edge-lit backlight for a time-multiplexed stereoscopic display is proposed for use in mobile phones.

The viewer's left and right eyes are perpendicular to the light emission. The angles of light emission for viewer's eyes are at about ±10°, as shown in Fig. 1. An LGP can provide directional brightness and uniformity of the output light [16–19].

We design a 5.0-inch time-multiplexed LGP to generate two highly directional lights based on optimized micro-structural plates. When the left- and right-side light sources are active, the LGP can emit light directly into the viewer's right and left eyes, respectively.

Through cooperation between the sequentially switching light sources and the liquid crystal, the left and right eyes can acquire two signals to achieve a stereoscopic effect. Optical software TracePro™ is used to simulate the illuminance, direction, uniformity, and crosstalk of the output lights. It is shown that our proposed LGPs with v-cut and curved microstructures have ideal efficiencies in terms of orientation angle, uniformity, and crosstalk of the output light.

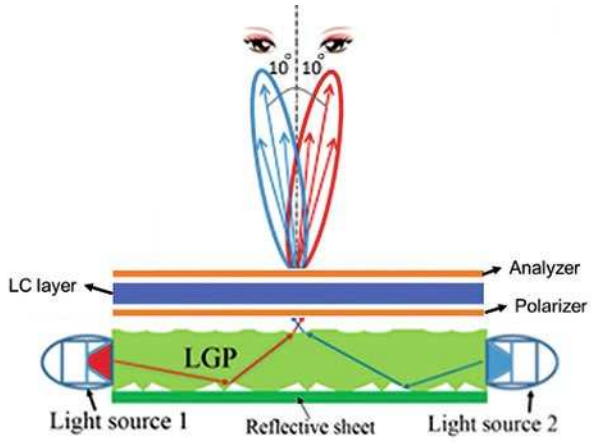

Fig. 1. Edge-lit Backlight Module in Autostereoscopic Display

2. DEVICE STRUCTURE

Fig. 2(a) depicts the structure of the backlight module including the LGP, reflective sheet, observation plane, and left- and right-side light sources. Each light source comprises twelve light emitting diodes (LEDs) placed along the z-axis. The LGP is made of Polymethyl methacrylate (PMMA); its index of refraction is 1.49, its area is 110 mm×65 mm, and its thickness is 3 mm. Structural parameters of the Siemens LWT676 LED are shown in Table 1. The surface of the reflective sheet is diffusely white. The observation plane is 1 mm above the LGP and can detect the distribution of the illuminance of the output light.

Three types of LGP microstructures are compared with one another, as shown in Figs. 2 (b), (c), and (d). Type 1 has v-cut microstructures on its bottom surface. Setting the median of the LGP as the plane of symmetry, the v-cut microstructures are described by a one-dimensional linear equation according to a previous study [20], as shown in Eq. (1).

$$S = aT - b, \tag{1}$$

Table 1. Parameters of the Siemens LWT676 LED Light Source

Source type	Flux
Luminous flux	0.051 m
Wavelength	0.5461 um
Angular distribution	Lambertian
Total rays	240000

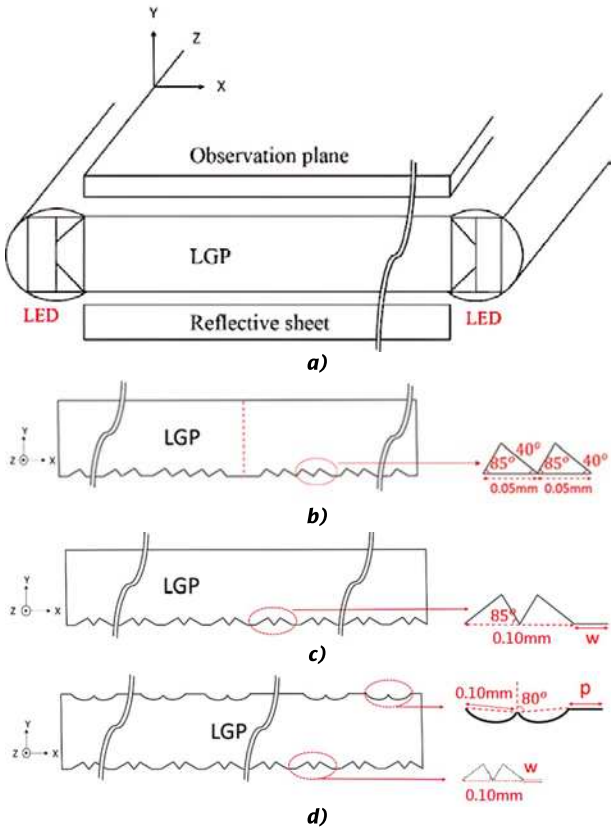

Fig. 2. Structure of the backlight module - (a), Type 1 - (b), Type II - (c), and Type III - (d)

where, S is the interval with v-cut corrugation and T is the interval without v-cut corrugation and are adjustment parameters. The T interval is needed to uniformly distribute the light power across the whole LGP area. Without a T interval, the light rays will be distributed intensely in the area near the light source. Microstructures are placed along the x-axis but in two opposite directions on the bottom surface of the LGP. As shown in Fig. 2(b), the left and right halves of the LGP have microstructures described by one-dimensional linear equations along the +x and –x axes respectively. Each groove of the v-cut microstructure has a 55° vertex angle and base angles of 40° and 85°. There is a 0.05-mm space between each groove climax.

The Type II LGP has a symmetric v-cut microstructure of fixed spacing w, which is uniformly arranged on its bottom surface. The microstructure is created by two oppositely placed Type I microstructures, each with a width of 0.10 mm as shown in Fig. 2(c).

Type III combines the Type II design with another micro-structure uniformly arranged on the top surface of the LGP. This other microstructure is symmetrically curved, with a fixed spacing p. The

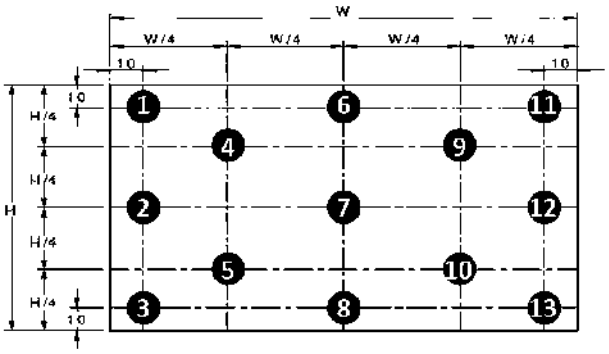

Fig. 3. Illuminance in the 13 points at the observation plane

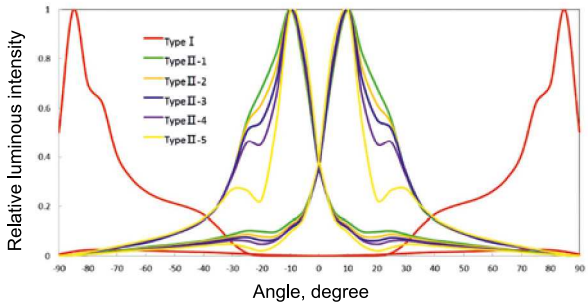

Fig. 4. Rectangular relative luminous intensity distribution plot

curved microstructure consists of two circular arcs, each of width 0.10 mm, and the tilt degree of each curved surface is ±10° as shown in Fig. 2(d).

The crosstalk between the right view and left view for the central observer is determined the following equation [14]:

$$Crosstalk = \frac{1}{2}\left(\frac{I_L(\theta_R)}{I_R(\theta_R)} + \frac{I_R(\theta_L)}{I_L(\theta_L)}\right), \qquad (2)$$

where I_R and I_L are the measured maximum intensity for the right and left views at the viewing angles θ_R and θ_L respectively. In this experiment, we found that leakage and signal ratio is similar at 10˚ and –10˚ in the left eye and the right eye. A definition of crosstalk is present in this study as follow [21]:

$$Crosstalk = leakage / signal \times 100\%, \qquad (3)$$

where leakage is defined as the maximum luminance of light that leaks from the unintended channel into the intended one, whereas the signal is defined as the maximum luminance of the intended

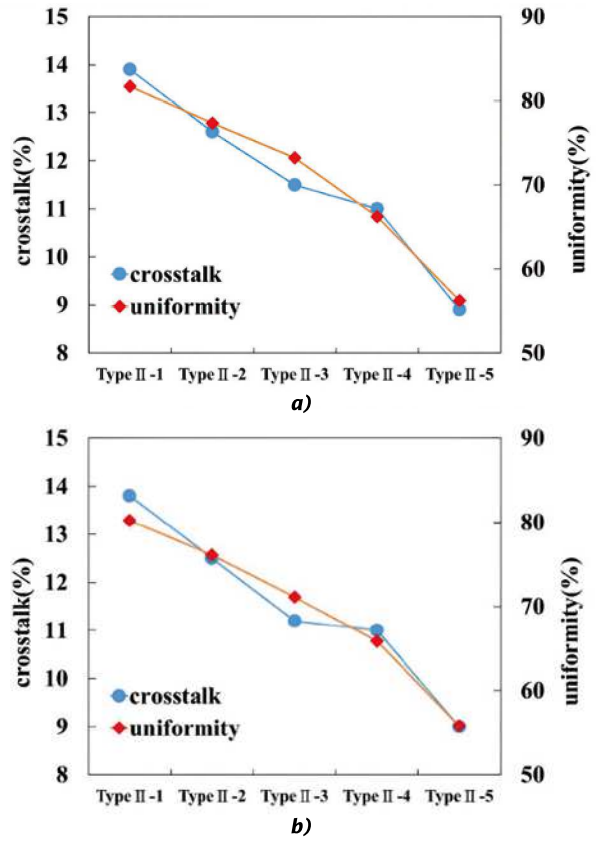

Fig. 5. Comparison of uniformity and crosstalk: (a) – left light source, (b) – right light source

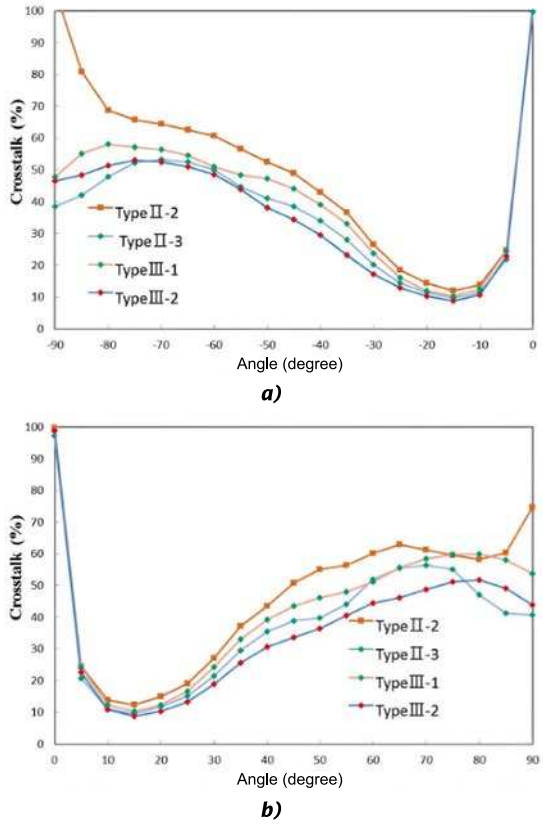

Fig. 6. Crosstalk: (a) – crosstalk when the right side light source emits; (b) – crosstalk when the left side light source emits

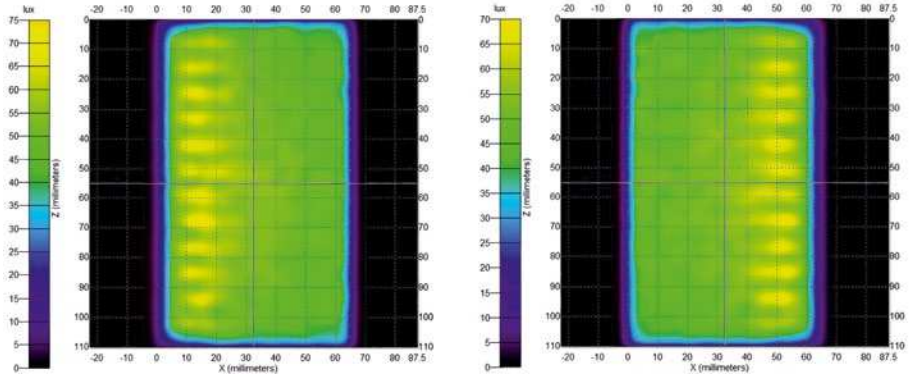

Fig. 7. Illuminance map of Type III-2 LGP: (a) – the uniformity is 76.1 % when the left side light source emits; (b) – the uniformity is 75.9 % when the right side light source emits

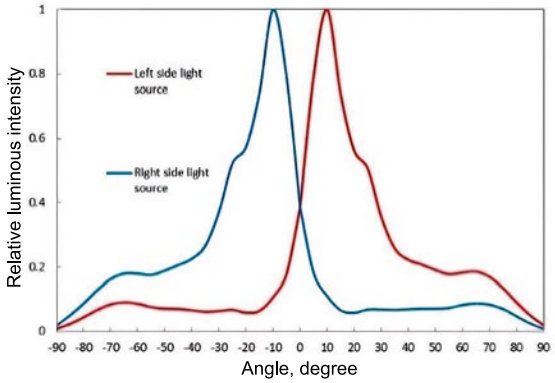

Fig. 8. Restangular luminous intensity distribution plot of Type111-2 LGP when both light sources emit

channel that is detected at an angle of maximum light emission. In this study, we aim to reduce crosstalk. In the right-eye channel, the ratio of the measured luminance of the right-side light source (leakage) to that of the left-side light source (signal) should be lower. Conversely, the ratio should be lower in the left-eye channel too.

In addition to testing the crosstalk of a directional light source, uniformity is considered a metric for evaluating the performance of the backlight module in an autostereoscopic display. Fig. 3 shows the uniformity of the output light. The ratio of minimum illuminance (I_{min}) to maximum illuminance (I_{max}) at 13 points on the observation plane can be expressed as Eq. (4).

$$Uniformity = \left(I_{min} / I_{max}\right) \times 100\%. \quad (4)$$

The optical conversion efficiency of the output light is well-defined as the ratio of the illuminance (I_o) on the observation plane to the emitted illuminance (I_e) of the light sources, and is evaluated as Eq. (5).

$$Opical\ conversion\ efficiency = \left(I_o / I_e\right) \times 100\ . \quad (5)$$

3. RESULTS AND DISCUSSION

Six models of LGP microstructures are compared with one another in terms of uniformity, angle of maximum light emission, and crosstalk, as shown in Table 2. For the Type LGP, the v-cut microstructure on the bottom surface is described by *S=T-10(T≥13),* with a = 1 and b = 10. For the Type II-1, II-2, II-3, II-4, and II-5 LGPs, w (the interval on the bottom surface) is set to 1.5 mm, 1.2 mm, 1.0 mm, 0.8 mm, and 0.8 mm respectively.

In the results all measurements from viewer's left and right eyes are going on in perpendicular direction to the light emission. The maximum light emission of the Type I LGP is concentrated on the source side, and the maximum light-emission angles are 85° and –85°; those of the Type II-4 and Type II-5 LGPs are 9° and –9°, whereas those of all other LGPs are 10° and –10°. These results show that the maximum light-emission angles of the Type II designs are more suitable than those of the Type I design for use in a backlight module, as shown in Figs. 4 and 5.

Comparing the uniformity and crosstalk in Fig. 5, we observe that lower values of w produce lower crosstalk and uniformity, whereas higher values produce higher crosstalk and uniformity. Because the major parameters for evaluating the performance of backlighting modules for time-multiplexed autostereoscopic displays have higher uniformity, lower crosstalk, and maximum light emission, we select the Type II-2 and II-3 designs for use, as their uniformity is higher than 70 %, crosstalk is less than 13 %, and light-emission angles are at 10° and –10°.

To reduce crosstalk in the left- and right-eye channels, we add curved microstructures to the tops of the Type II-2 and Type II-3 LGPs, forming

Table 2. The LGP with V–Cut Microstructures on the Bottom Surface

Type	Uniformity	Light emitting angle [a]	Crosstalk (%) [b]
Type 1, S=T-10(T≥13)	10.3 %	–85° and 85°	
Type 11–1, w =1.5 mm	81.7 %	–10° and 10°	13.8 and 13.9
Type 11–2, w =1.2 mm	77.3 %	–10° and 10°	12.5 and 12.6
Type 11–3, w =1.0 mm	73.2 %	–10° and 10°	11.2 and 11.5
Type 11–4, w =0.8 mm	66.2 %	–9° and 9°	11.1 and 11.0
Type 11–5, w =0.5 mm	56.2 %	–9° and 9°	9.0 and 8.9

a left and right angle of the maximum emitting light
b crosstalk at left and right eye channel (%)

Table 3. Results of Uniformity, Optical Conversion Efficiency and Crosstalk of Emitting Lights

Type	Fixed spacing of *w* and *p*	Uniformity	Efficiency, % [c]		Crosstalk, % [b]	
11–2	*w* = 1.2 mm	77.3 %	49.7 49.9		12.5	12.0
11–3	*w* = 1.0 mm	73.2 %	53.0 53.1		12.6	12.3
11–1	*w* = 1.2 mm, *p*=1.1 mm	77.3 %	56.0 56.0		11.2	10.7
11–2	*w* = 1.0 mm, *p* = 1.1 mm	73.2 %	57.9 57.9		11.5	10.9

c optical conversion efficiency of left and right light
b crosstalk at left and right eye channel

Type III-1 and Type III-2 designs respectively, similar to Fig. 2(d). The curved micro-structures are symmetrically arranged with a regular interval of p = 1.1 mm. When the left and right sources are active, the results of uniformity and optical conversion efficiency are detected in the observation plane and those of crosstalk are detected at the maximum light-emission angles of –10° and 10°, as summarized in Table 3.

For the sight range of the human eye from ±7.5° to ±20°, we observe that the Type III-2 design has the best quality in terms of time-multiplexed projection into eyes for an autostereoscopic display, and that the optical conversion efficiencies of the Type III-1 and Type III-2 designs are higher than those of the Type III-2 and Type II-3 ones. Figs. 6(a) and (b) show the crosstalk detected on the observation plane when the right and left sources emit light into the left- and right-eye channels respectively. The illuminance maps of the Type III-2 design are shown in Figs. 7(a) and (b). Fig. 8 provides a rectangular candela-distribution plot of the Type III-2 LGP.

By liquid crystal software (LCD master 2D), the simulated results of the Type III-2 design are shown in Fig. 9. As an example in Fig. 1, we simulate the illumination property of a twist nematic (TN) cell. We set the polarizer thickness is 10 μm and angle is 45˚, the analyzer thickness is 10μm and angle is 135˚ in Fig. 1, the alignment directions of the upper and lower substrates are parallel to the polarizer and analyzer respectively. There are added the liquid crystal that parameters are has elastic constants k11= 16.7pN, k22=1pN, k33=18.1pN, Δn = 0.083 and $\Delta\varepsilon$ = –4.2. The liquid crystal cell gap is 10μm. The simulated results are shown in Fig. 10.

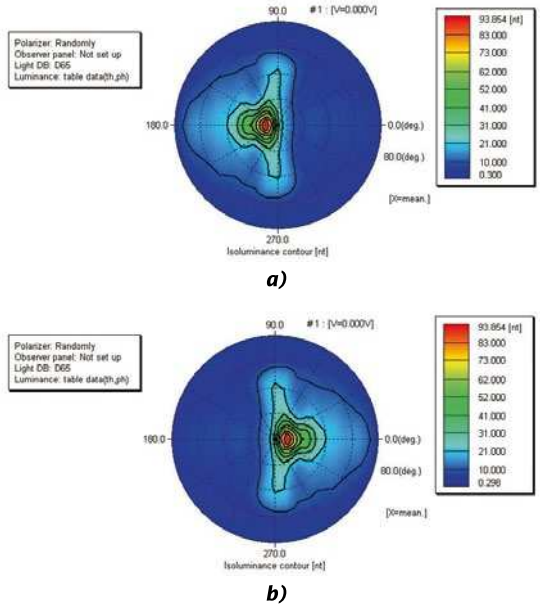

Fig. 9. Illumination: (a) – right side light source; (b) – left side light source

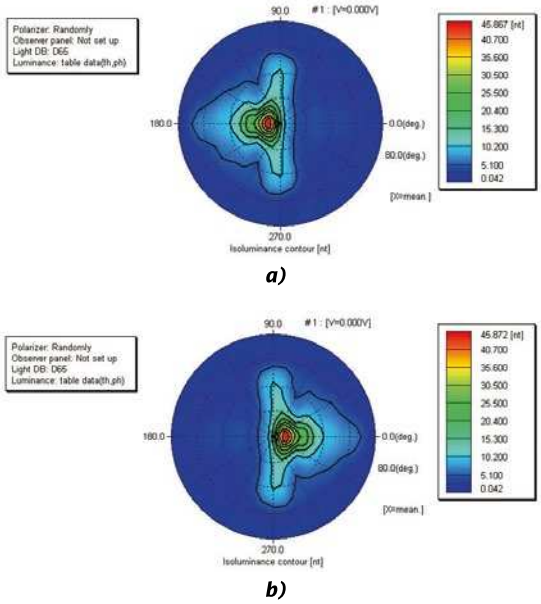

Fig. 10. Illumination through liquid crystal: (a) – right side light source; (b) – left side light source

Checking the Fig. 10 against the Fig. 9, we find almost the same each other about a direction light-emission angle, uniformity of illumination, and crosstalk elimination.

5. CONCLUSION

It was observed that the Type III-2 LGP design offers the largest luminance at ±10° for human eyes. This design exhibits an average uniformity of above 75 %, an average crosstalk ratio of below 10.8 %, and an optical con-version efficiency of above 57.9 %. Our successful results effectively eliminate the need for a prism sheet and satisfy three main performance parameters, including a direct angle of light emission, uniformity of illumination, and elimination of crosstalk.

REFERENCES

1. A. Yuukia, M. Agaria, N. Iwsakia, T. Sasagawaa, S. Tahataa, T. Satakea, O. Murakamia, K. Odaa, A. ltob and S. Miyakeb, "A new field sequential stereoscopic LCDs by use of dual-directional-backlight," Journal of Information Display, 2004, #**5**, pp. 6–9.

2. B. Lee, "Three-dimensional displays, past and present," Phys. Today, 2013, #**66**, pp. 36–41.

3. X. Xiao, B. Javidi, M. Martinez-Corral, and A. Stern, "Advances in three-dimensional integral imaging: sensing, display, and applications," Appl. Opt. 2013, #**52**, pp. 546–560.

4. W. Maphepo, Y.P. Huang, and H. P.D. Shieh, "Enhancing the brightness of parallax barrier based 3D flat panel mobile displays without compromising power consumption," J. Disp. Technol. 2010, #**6**, pp. 60–64.

5. C. H. Chen, Y.P. Huang, S.C. Chuang, C.L. Wu, H.P. Shieh, W. Mphepö, C.T. Hsieh, and S.C. Hsu, "Liquid crystal panel for high efficiency barrier type autostereoscopic displays," Appl. Opt. 2009, #**48**, pp. 3446–3454.

6. Y. Inoue, S. Sakamoto, K. Takahashi, C. Kanai, Y. Imai, and Y. Shimpuku, "A novel parallax liquid crystal barrier for temporally interlaced autostereoscopic 3D displays," SID Digest 2012, #**43**, pp. 221–224.

7. Y. P. Huang, C.W. Chen, T.C. Shen, and J.F. Huang,"Autostereoscopic 3D display with scanning multi-electrode driven liquid crystal (MeD-LC) lens," J. 3D Res. 2010, #**1**, pp. 39–42.

8. C. W. Chen, M. Cho, Y.P. Huang, and B. Javidi, "Improved viewing zones for projection type integral imaging display using adaptive liquid crystal prism array," J. Disp. Technol. 2014, #**10**, pp. 198–203.

9. B. Lee and J.H. Park, "Overview of 3D/2D switchable liquid crystal display technologies," Proc. SPIE, 2010, #**7618**, 761806.

10. Y. P. Huang, L.Y. Liao, and C.W. Chen, "2-D/3-D switchable autostereoscopic display with multi-electrically driven liquid-crystal(MeD-LC) lenses," J. Soc. Inf. Disp. 2010, #**18**, pp. 642–646.

11. Y. C. Chang, T.H. Jen, C.H. Ting, and Y.P. Huang, "High-resistance liquid-crystal lens array for rotatable 2D/3D autostereoscopic display," Opt. Express 2014, #**22**, pp. 2714–2724.

12. T. H. Jen, Y.C. Chang, C.H. Ting, H.P. Shieh, and Y.P. Huang, "Locally controllable liquid crystal lens array for partially switchable 2D/3D display," J. Disp. Technol. 2015, #**11**, pp. 839–844.

13. R. Brott and J. Schultz, "Directional backlight guide considerations for full resolution autostereoscopic 3D displays," SID Digest, 2010, #**41**, pp. 218–221.

14. C.H. Ting, Y.C. Chang, C.H. Chen, Y.P. Huang, and H.W. Tsai, "Multi-user 3D film on a time-multiplexed side-emission backlight system", Applied Optics, 2016, #**55**, pp. 7922–7928.

15. K.W. Chien and H.P.D. Shieh, "Time-multiplexed three-dimensional displays based on directional backlights with fast-switching liquid-crystal displays," Applied Optics, 2006, #**45**, pp. 3106–3110.

16. C.F. Chen and S.H. Kuo, "A Highly Directional Light Guide Plate Based on V-grooves Microstructure Group," Journal of Display Technology, 2014, #**10**, pp. 1030–1035.

17. J.W. Chen, K.L. Lee∗, J.J. Wu, C.Y. Lin, "Design a backlight system to a LCD of vertical-field-switching bluephase," Optik, 2014, #**125**, pp. 6713–6715.

18. K.L. Lee and K.Y. He, "Effect of Micro-Structural Light Guide Plate on Source of Linearly Polarized Light," Journal of Lightwave Technology 2011, #**29**, pp. 3327–3330.

19. J.R. Yan, Q.H. Wang, D.H. Li, and J.D. Zhang, "Edge-Lighting Light Guide Plate Based on Micro-Prism for Liquid Crystal Display," Journal of Display Technology **5**, 355–357(2009).

20. C.Y. Lin, K.L. Lee, P.Y. Tsai and J.W. Chen, "Design of Directional Light Source for Blue Phase LCD," Proc. SPIE, 2014, **9272**, 927205.

21. A.J. Woods, "How are crosstalk and ghosting defined in the stereoscopic literature," Proc. SPIE, 2011,**7863**, 78630Z.

Chien-Min Hun
received his M.S. degree in electrical engineering and computer science from National Taipei University of Technology in 2011. He is currently working toward the Ph.D. degree at the electro-optical engineering, National Taipei University of Technology. His current research interest includes backlight module design and industry trend analysis and innovations of new prototype design

King-Lien Lee
received the M.S. degree in physics from National Taiwan Normal University (NTNU) in 1980 and received the Ph.D. degree in Graduate Institute of Science Education from NTNU in 1999. He is a Professor of Electro-Optical Engineering at National Taipei University of Technology. His research interests are backlight system, industry trend analysis and innovations of new prototype design

Che-Yen Lin
received the M.S. degree in electro-optical engineering, from National Taipei University of Technology in 2015.
His research interest includes backlight module design and structure optimization

Mei-Wen Chen
received her M.S. degree in electro-optical engineering from National Taipei University of Technology in 2018. Her current research interest includes backlight module design and structure optimization

Jin-Jei Wu
received his M.S. degree in Industrial engineering from National Chiao Tung University (NCTU) in 1980 and received the Ph.D. degree in Department of Electronics Engineering from NCTU in 1989. He is a Professor of Electro-Optical Engineering at National Taipei University of Technology. He has more than 20 years experience in liquid crystal display improvement

CONTENTS

VOLUME 28 **NUMBER 3** **2020**

LIGHT & ENGINEERING
(SVETOTEKHNIKA)

New Publications March 2020

CIE238:2020 Characterization of AC-Driven LEDs for SSL Applications

This Technical Report provides guidance for optical measurements of AC LEDs, performed at testing laboratories with emphasis on reproducibility and small measurement uncertainties by accurately setting and controlling the junction temperature. The report includes measurement methods, instrumentation, and procedures. The measurement methods and procedures used for optical measurement of AC LEDs are based on a specified junction temperature using either single AC cycle operation or continuous AC operation.

The publication is written in English, with a short summary in French and German. It consists of 25 pages with 15 figures and is readily available from the CIE Webshop or from the National Committees of the CIE.

The price of this publication is EUR84,-

CIE239:2020 Goniospectrodariometry of Optical Radiation Sources

This Technical Report provides basic measurement principles and practical guidance in goniospectroradiometry of optical radiation sources (i.e. measurement of the spectral distribution as a function of the emission angle of the source). Specifically, it includes measurement principles of the angular distribution of spectral, radiometric, photometric and colorimetric quantities of optical radiation sources, the related scanning method and a practical guide to determine sampling interval, uncertainty aspects and calibration.

The publication is written in English, with a short summary in French and German. It consists of 22 pages with 10 figures and is readily available from the CIE Webshop or from the National Committees of the CIE.

The price of this publication is EUR84,-

Note that when making a purchase from the Webshop, Members of a National Committee of the CIE receive a 66,7 % discount on these prices. Please approach your NC or ANC for information on accessing this discount.

Joining CIE Technical Committees

CIE has over 70 TCs working on new reports and international standards. If you have expertise to contribute to any of these or the new ones highlighted below, then simply fill out the CIE TC Membership form and CIE Copyright Agreement form and email them to the relevant TC Chair, with copy to CIE Central Bureau.

Call for Experts for CIE Technical Committees

TC4–62: Adaptive Road Lighting

The purpose of this TC is to analyze needs, specify recommendations, develop methodology and promote application of adaptive road lighting based on various conditions and input data from field sensors and interconnected systems with respect and tailored to specific requirements of different user groups and user patterns.

Chair: Thomas Baenziger

TC2–93: Revision of ISO 23539:2005(E)/CIE S010/E:2004 Photometry – The CIE system of physical photometry

The purpose of this TC is to revise ISO 23539:2005(E)/CIE S010/E:2004 Photometry – The CIE system of physical photometry considering the comments raised at the systematic review of this international standard.

Chair: Anders Thorseth

PARTNERS OF LIGHT & ENGINEERING JOURNAL

Editorial Board with big gratitude would like to inform international lighting community about the Journal Partners Institute establishment. The list with our partners and their Logo see below. The description of partner's collaboration you can found at journal site *www.sveto-tekhnika.ru*

BL Group
International Lighting Engineering Corporation
BOOS LIGHTING GROUP

ВНИСИ

REFLUX
HID Lighting systems

interlight RUSSIA | intelligent building RUSSIA